Some Structural and Photochemical Studies in Triterpenoids

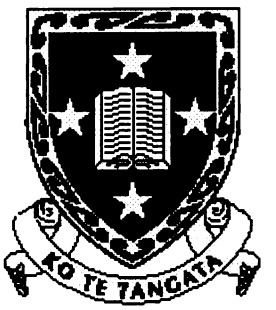

A thesis submitted in fulfilment of the requirements

for the Degree of

Doctor of Philosophy

in Chemistry

at

The University of Waikato

by

Julie Hehui Zhu

Hamilton, New Zealand

2000

To

Mum and Dad

and

Myself

ABSTRACT

This thesis describes the photochemical behaviour of 22-hydroxyhopan-7-one, hop-22(29)-en-7-one, 22-hydroxyhopan-15-one, hop-21-en-15-one, hop-22(29)-en-15-one, hopan-15-one and 21α-H-hopan-15-one in different solvents, and the isolation and structural elucidation of a new stictane and a new flavicane triterpene from the New Zealand lichen *Pseudocyphellaria colensoi*.

Photolysis of 22-hydroxyhopan-7-one in benzene-methanol was reinvestigated and confirmed to afford methyl 22-hydroxy-7,8-secohopan-7-oate. The photochemical behaviour of 22-hydroxyhopan-7-one and hop-22(29)-en-7-one in the presence of benzene alone, and in benzene-isopropanol, were also investigated.

Photolysis of hop-22(29)-en-7-one in benzene-methanol afforded methyl 7,8-secohop-22(29)-en-7-oate while photolysis of 22-hydroxyhopan-7-one in methanol-isopropanol afforded isopropyl 22-hydroxy-7,8-secohopan-7-oate. Photolysis of 22-hydroxy-hopan-7-one in benzene alone afforded mainly unreacted starting material and some minor products, one of which was believed to be 22-hydroxy-7,8-secohop-8(26)-en-7-al.

The stereochemistry at C-8 for these compounds was determined by analyses of ROESY or NOESY NMR spectral data which showed the C-8 methyl group to be β-oriented, and indicated that photochemical rearrangement reactions proceeded with retention of configuration at C-8. Modelling analyses indicated the 8β-methyl secoesters to have lower energy than the corresponding 8α-methyl isomers.

Complete assignments of the ^{1}H and ^{13}C NMR signals of methyl 22-hydroxy-7,8-secohopan-7-oate, isopropyl 22-hydroxy-7,8-secohopan-7-oate and methyl 7,8-secohop-22(29)-en-7-oate, were achieved using a combination of one- and two-dimensional NMR techniques.

The three products obtained on photolysis of 22-hydroxyhopan-15-one, in benzene-methanol, benzene-isopropanol, or benzene alone, were identified as 14,15-seco-15,22-*O*-*abeo*hop-14(27)-en-15α-ol, 14,15-seco-15,22-*O*-*abeo*hop-14(27)-en-15-one, and 14,15-seco-15,22-*O*-*abeo*hopa-14(27),15-diene, respectively. These products can be envisaged as arising from

participation of the 22-hydroxyl group in the photoreaction pathway, after the initial formation of a 14,15-secoaldehyde.

Photolysis of hop-21-en-15-one in benzene-methanol afforded 14,15-secohopa-14(27),21-dien-15-al as the major product, while photolysis of hop-22(29)-en-15-one gave a complex mixture of products which was not further investigated. Photolysis of hopan-15-one yielded two products which were identified as the isomeric alcohols, 14,15-seco-15,22-*abeo*hop-14(27)-en-15α-ol and 14,15-seco-15,22-*abeo*hop-14(27)-en-15β-ol. Photolysis of 21α-H-hopan-15-one afforded two products, which were identified as methyl 14α,21α-H-14,15-secohopan-15-oate and methyl 21α-H-14,15-secohopan-15-oate.

Complete assignments of the ^{1}H and ^{13}C NMR signals of the foregoing series of 15-oxohopanoid photoreaction products, and where appropriate the stereochemistry at C-14 and/or C-15, were achieved using a combination of one- and two-dimensional ROESY, NOESY, COSY, HMBC, and HSQC NMR spectral data, and molecular modelling results.

The results of the series of 15-oxohopanoid photoreactions can be interpreted indicating that in the presence of an α-oriented side chain (ie 22-hydroxyisopropyl group or isopropyl group) at C-21, the photoreaction proceeds with hydrogen transfer *via* an eight-membered transition state to afford a secoaldehyde or 14,15-secohop-14(27)-en-15-al which then affords 14,15-seco-15,22-*O*-*abeo*hop-14(27)-en-15α-ol *via* participation of the 22-hydroxyl group and related analogues. Similarly the isomeric alcohols, 14,15-seco-15,22-*abeo*hop-14(27)-en-15α-ol and 14,15-seco-15,22-*abeo*hop-14(27)-en-15β-ol, obtained on photolysis of hopan-15-one can be viewed as 22-H participation products. On the other hand photolysis of a 15-oxohopanoid possessing a β-oriented side chain at C-21 was found to proceed with hydrogen transfer *via* a six-membered transition state to afford a pair of epimeric 14,15-secoesters.

A new stictane triterpene, and a new flavicane triterpene were isolated from extracts of the New Zealand lichen *Pseudocyphellaria colensoi*, and identified by analyses of mass spectral and one- and two-dimensional NMR spectral data to be 3α,6β,22α-triacetoxystictane and 22-hydroxyflavicano-25,3β-lactone, respectively. Complete assignments of the ^{1}H and ^{13}C NMR signals of the new triterpenes, and revisions to previously reported ^{13}C NMR signal assignments for 22α-hydroxystictano-25,3β-lactone are reported.

ACKNOWLEDGEMENTS

I wish to express my sincere thanks to all supervisors, colleagues and friends, at the Department of Chemistry of the University of Waikato, who in numerous ways have contributed to this study.

Special thanks to:

Professor Alistair Wilkins, my supervisor, for introducing and guiding me to this interesting research and exciting NMR experiments. Your enthusiasm, invaluable guidance, encouragement and critical expertise will never be forgotten. I do enjoy working with you.

Professor Brian Nicholson, Chairperson of the Department of Chemistry, and Associate Professor Lyndsay Main, former Chairperson of the Department, for your support and encouragement. Professor Brian Nicholson, specially, for your help and guidance when I attempted to grow crystals. Associate Professor Lyndsay Main, my second supervisor, I sincerely thank you for your continuing support and help, to enable me to carry on and concentrate on the research.

Mrs Jannine Sims, for assistance in training in GC/MS and the analyses of samples. In particular your friendship and smile were of great support to me.

Dr. Ralph Thomson, for your technical advice in the high field NMR spectrometer. I truly appreciated your help and support.

Everyone else in the Department of Chemistry, for your assistance and friendship, and for making me feel at home. My time here is always pleasant and unforgettable.

Mr Keith Williams, for proofreading my thesis and valuable and interesting comments.

I am deeply indebted to all of my friends: Dr Tao Xie (for his academic advice), Xi Fong, Chunmei Feng and Qibo Hou, Helen Whua, Joy Wong (for his computer assistance), Dr Bo Han, Dr Dawei Deng, Marleen and Sam Tsai, Dr Fengming Tian, Dr Deliang Zhang, Jason and Catharine Wu, Charolyne Huang, Lillian Geng, Charlie Luo and Yun Liu, Biao Yao, Mark Q. Li, Zailu Yang, Jiamin Ji and Fang Chen, as well as Judith and Bob Haworth. Your love, friendship, support, encouragement and accompany greatly help me.

Finally, I am particularly indebted to my parents and other family members for their love and support, for being always 'together' with me.

TABLE OF CONTENTS

LIST OF TABLES

LIST OF FIGURES

LIST OF SCHEMES

ABREVIATIONS

%	percent
α	alpha face, or lower face
β	beta face, or upper face
δ	chemical shift
^1J	one bond NMR coupling constant
^2J	two bond NMR coupling constant
^3J	three bond NMR coupling constant
^4J	four bond NMR coupling constant
1D	one-dimensional
2D	two-dimensional
Ac	acetyl
br	broad
°C	degree Celsius
ca.	*circa* (approximately)
$CDCl_3$	deuterochloroform
C_5D_5N	deuteropyridine
COSY	homonuclear (^{1}H-^{1}H) correlated spectroscopy
d	doublet NMR signal
D1	repetition delay
Da	dalton
DEPT	distortionless enhancement by polarisation transfer
Dr	Doctor
eg	*exempli gratia* (for example)
et al.	e*t alii* (and others)
eV	electron volts
F1	frequency dimension one
F2	frequency dimension two
FID	free induction decay

FT	Fourier transformation
g	gram(s)
GC	gas chromatography
GC/MS	gas chromatography/mass spectrometry
h	hour(s)
HMBC	heteronuclear multiple bond correlation
HMQC	heteronuclear multiple quantum coherence
HSQC	heteronuclear single quantum coherence
Hz	hertz
id	internal diameter
ie	id est (that is)
J	coupling constant
L	litre
LAH	lithium aluminum hydride
LB	line broadening
lit.	literature
M^+	molecular ion (positive ion detection)
m	multiplet NMR signal
MC	magnitude calculation (NMR transform mode)
Me	methyl group
mg	milligram(s)
MHz	megahertz
min	minute(s)
mL	millilitre
m.p.	melting point
m/z	mass/charge ratio
MS	mass spectrometer
ms	millisecond(s)
MWt	molecular weight
NMR	nuclear magnetic resonance
NOE	nuclear Overhauser enhancement

NOESY	nuclear Overhauser enhancement spectroscopy
P	power mode (NMR transform mode)
P.	*Pseudocyphellaria*
PLC	preparative layer chromatography
ppm	parts per million
Prof	Professor
q	quartet NMR signal
R_f	rate of flow
SW	sweep width
s	singlet NMR signal
s	second(s)
T	temperature
t	triplet NMR signal
TIC	total ion chromatogram
TLC	thin layer chromatography
TMS	tetramethylsilane
UV	ultra violet
V	volts
W	phase-sensitive mode (NMR transform mode)
WDW1, WDW2	window type (1st and 2nd dimensions)
Wt.	weight

Chapter One

Introduction

In this thesis the results of a series of photochemical reactions of some 7-oxo and 15-oxo hopane triterpenoids, and the structural elucidation of a new stictane and a new flavicane triterpene from the New Zealand lichen *Pseudocyphellaria colensoi* are reported. Aspects of the photochemistry of terpenoid compounds, and the distribution of triterpenes in New Zealand *Pseudocyphellaria* lichens are reviewed in this Chapter.

1.1 Photochemistry of Triterpenoids

Photochemistry is one of the most rapidly expanding fields in organic chemistry. Until the early 1950's, light-induced organic reactions were not well understood because of the unexpected and diversified reactivities displayed by excited molecules. However, this situation has changed dramatically in subsequent years due to developments in theory and in experimental techniques. Applications of organic photochemistry to natural product synthesis have been extensively studied for about thirty years, because they provide important synthetic methods for preparing unusual compounds.

1.1.1 Photochemical Reaction of Cyclic Ketones

The photochemistry of cyclic ketones is among the most documented of chemical reactions. These investigations have spanned more than ninety years since the first discovery in the early twentieth century by Ciamician (1907) (the father of organic photochemistry) that irradiation of menthone in the presence of water afforded the corresponding secoacid (see Scheme 1-1).

It is now well established that photo-irradiation of cyclic ketones results in α-cleavage (also known as a Norrish Type I process) (Bamford & Norrish, 1938; DePuy & Chapman, 1972; Horspool, 1976, 1994; Cowan & Drisko, 1976). This term is used to denote the cleavage of a carbon-carbon bond α to a carbonyl group to give a biradical.

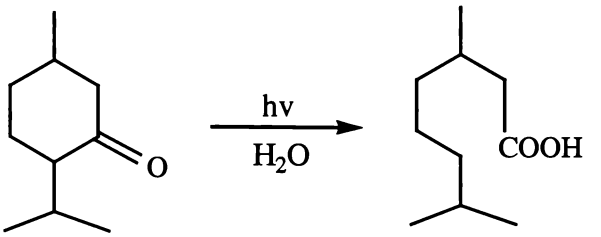

Scheme 1-1. Photochemical transformation of menthone to afford a secoacid.

This cleavage shows a tendency to produce the most substituted radical species. It undoubtedly arises from the ability of the α-substituents to stabilise the alkyl portion of the biradical and thus to enhance the rate of the cleavage. The resulting biradical can then react according to the pathways depicted in Scheme 1-2.

Intramolecular hydrogen abstraction in biradical (I) can give either unsaturated aldehydes (II) and (III), or an intermediate ketene (IV), which is formed by the migration of a hydrogen atom from the position adjacent to acyl radical to alkyl radical site. The intermediate ketene (IV) then gives rise to a secoacid (V) in the presence of water, or to a secoester (VI) in the presence of an alcohol (ROH) (see Scheme 1-2).

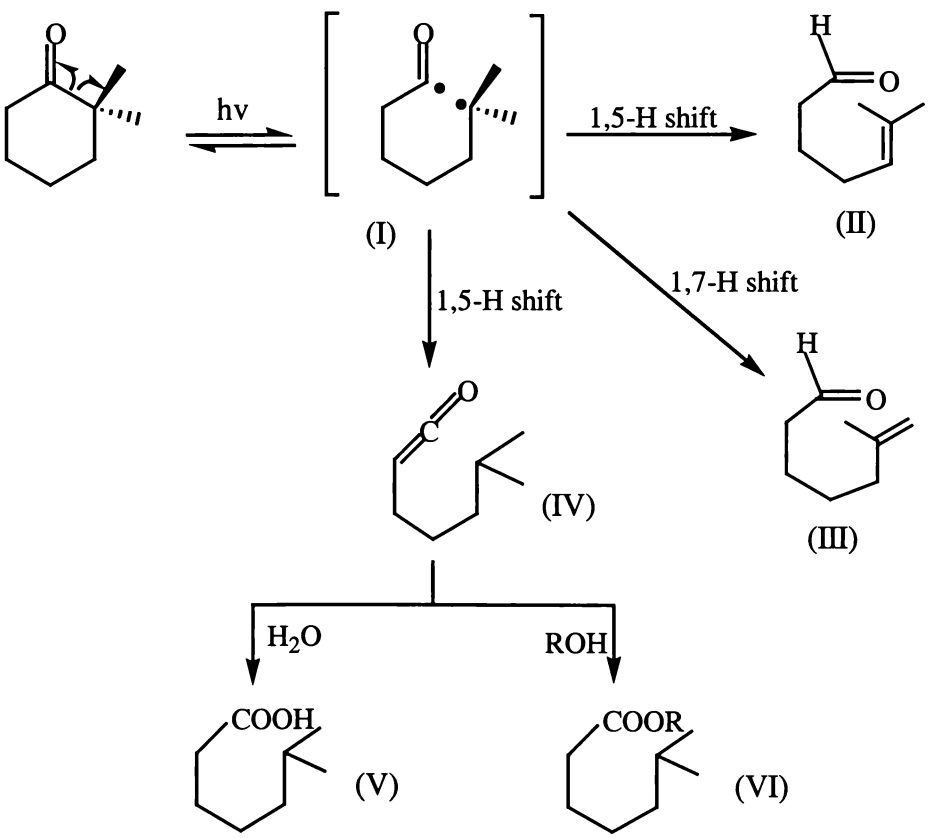

Scheme 1-2. Photoreaction pathways for 2,2-dimethylhexanone (a cyclic ketone).

1.1.2 Photochemistry of Some Natural Products

The photochemistry of a wide variety of natural products, including triterpenoid ketones and steroid ketones, has been reported (Bladon *et al.*, 1963; Dreyers & Rigod, 1974; Goh, 1981; Hunter, 1993; Okogun *et al.* 1998).

Upon irradiation these compounds typically undergo a Norrish Type I process (α-cleavage) to give biradicals. Subsequently intramolecular hydrogen abstraction, *via* five-, six- and even eight-membered transition states, can lead to the formation of different intermediate ketenes, which react with alcohols or water to afford photoreaction products.

Bladon *et al.* (1963) has reported that irradiation of a solution of hecogenin acetate (**1-1**) in dioxane initially afforded 3β-acetoxy-12,13-seco-5α,25D-spirost-13-en-12-al (**1-2**) in 80% yield (Scheme 1-3). More prolonged irradiation afforded 3β-acetoxy-12α,14α-epoxy-5α,25D-spirostane (photohecogenin acetate) (**1-3**).

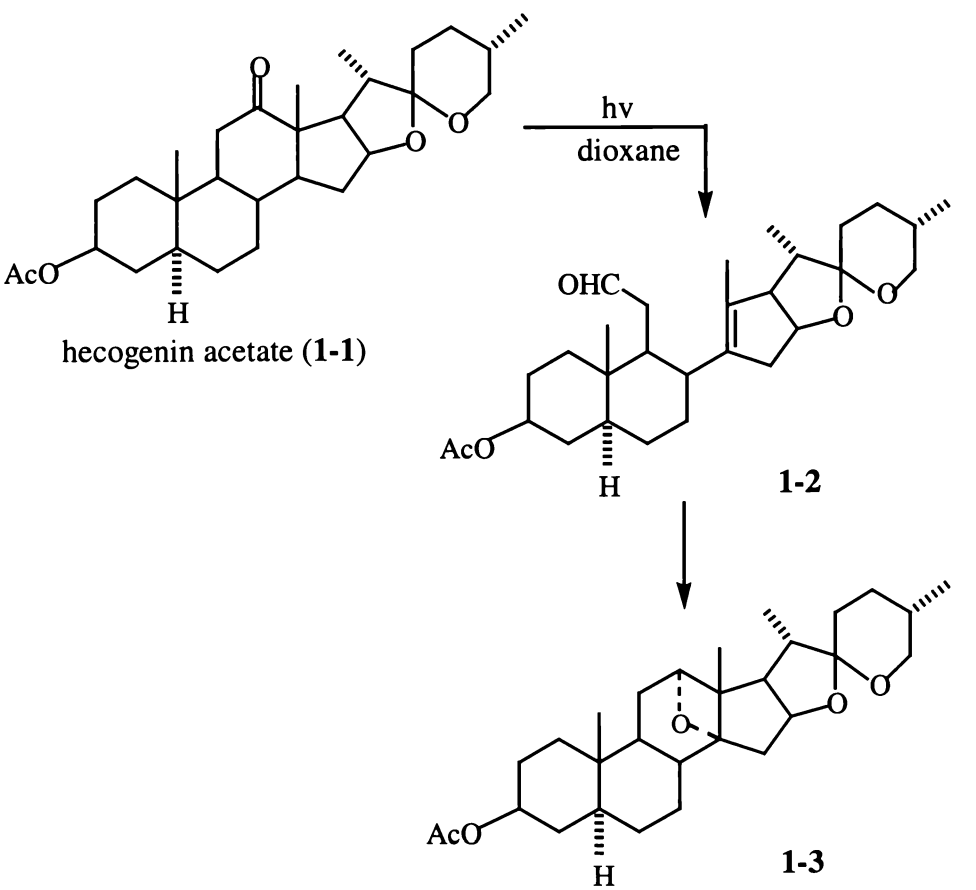

Scheme 1-3. Photolysis products (**1-2**) and (**1-3**) of hecogenin acetate (**1-1**).

The photolysis of some steroidal β-epoxyketones has been reported by Chambers & Marples (1972). Irradiation of the 9α,10α-epoxyketone (**1-4**) in methanol afforded the methyl secoester (**1-5**) in 73% yield, whereas irradiation in diethyl ether and in an atmosphere of nitrogen resulted in rapid decarbonylation and formation of the unsaturated epoxide (**1-6**) in 20% yield, and several other minor products (Scheme 1-4).

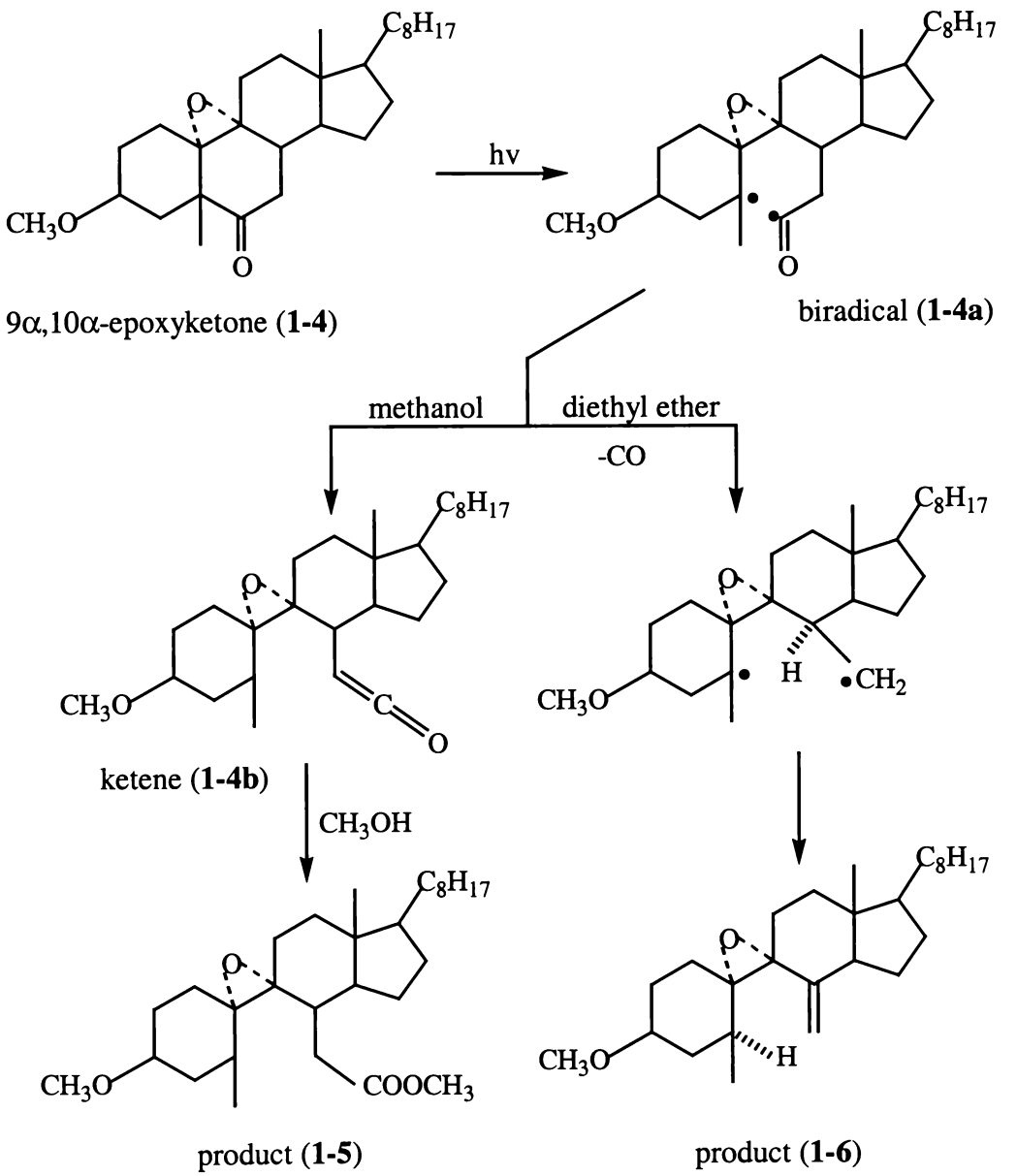

Scheme 1-4. Photolysis products of the 9α,10α-epoxyketone (**1-4**) in methanol, and in diethyl ether.

Investigations of the photochemical behaviour of the pentacyclic triterpene ketone, friedelin (**1-7**) have been reported (Kohen & Stevenson, 1966; Kohen *et al.*, 1969;

Takai *et al.*, 1970; Aoyagi *et al.*, 1970; Stevenson *et al.*, 1971; Aoyagi *et al.*, 1973). Irradiation of friedelin, which possesses an α-methylcyclohexanone ring-A system, afforded several structurally interesting products (Scheme 1-5).

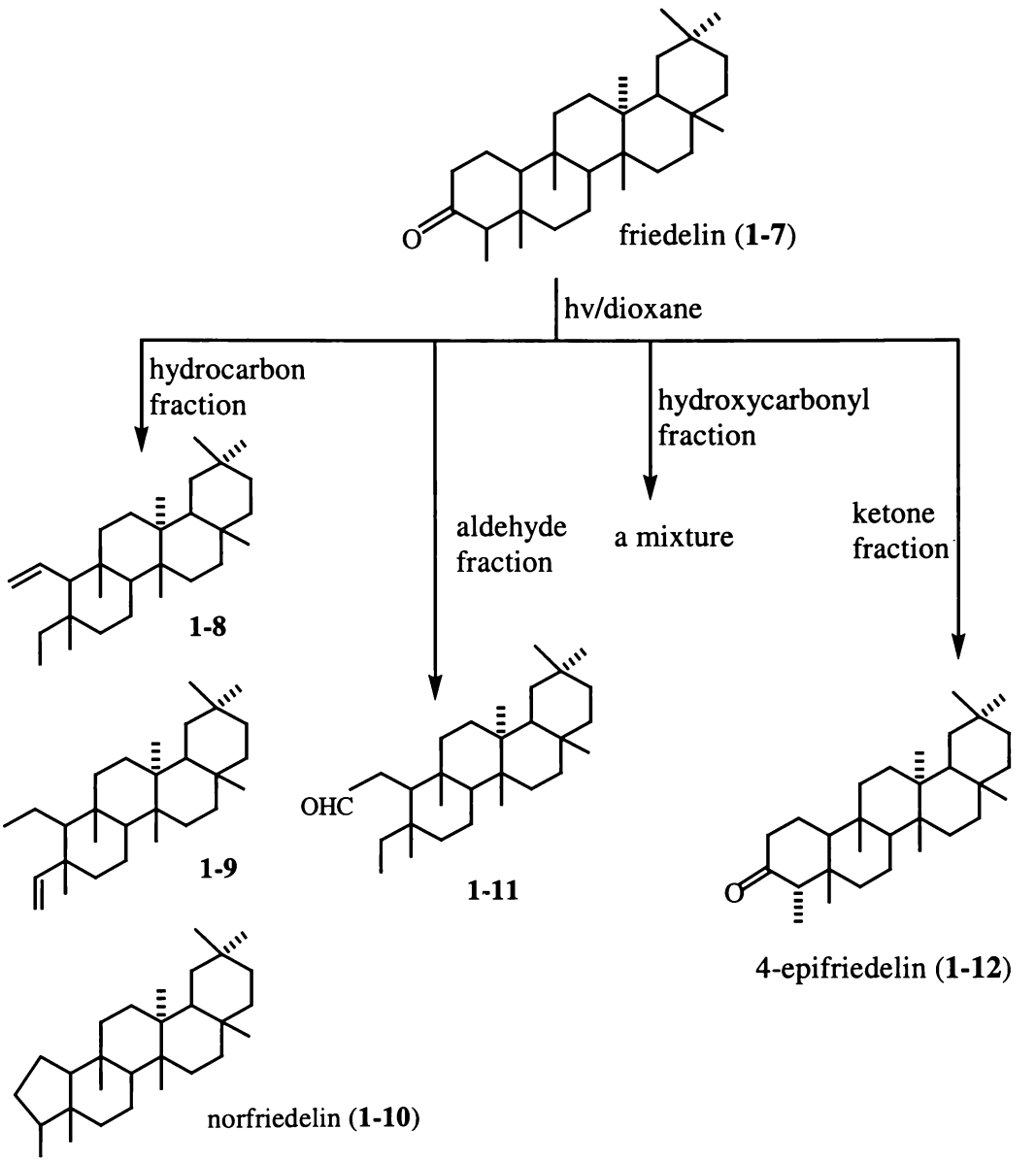

Scheme 1-5. Products from the photochemical reaction of friedelin (**1-7**) in dioxane.

For example, irradiation of friedelin (**1-7**) in dioxane afforded hydrocarbon, aldehyde, ketone and hydroxycarbonyl fractions which were separated by column chromatography on alumina (Kohen *et al.*, 1969). The hydrocarbon fraction consisted mainly of products (**1-8**), (**1-9**) and norfriedelin (**1-10**) (Scheme 1-5). The major component of the aldehyde fraction, which consisted of at least two compounds, was

believed to be 3-nor-3,4-secofriedelin-2-al (**1-11**) (Scheme 1-5). It was subsequently shown to also be the major photoproduct of **1-7** in diethyl ether (Stevenson *et al.*, 1971). The ketone fraction was comprised mainly of 4-epifriedelin (**1-12**). No components of the hydroxycarbonyl fraction, which consisted of at least three constituents, were isolated in a pure form.

Photolysis reactions of limonin (**1-13**), a C_{26} tetranortriterpene (Dreyers & Rigod, 1974) responsible for bitterness in processed citrus products, are of interest due to the possibility that the products they might be exploited as debittering agents.

Irradiation of limonin (**1-13**) in dioxane or methylene chloride afforded two major photoproducts, a ring B secoaldehyde named as photolimonin (**1-14**) and a ring reclosure product (**1-15**), which was identified as the C-8 epimer of limonin (**1-13**). Some other further minor products were detected by TLC, but could not be separated (see Scheme 1-6).

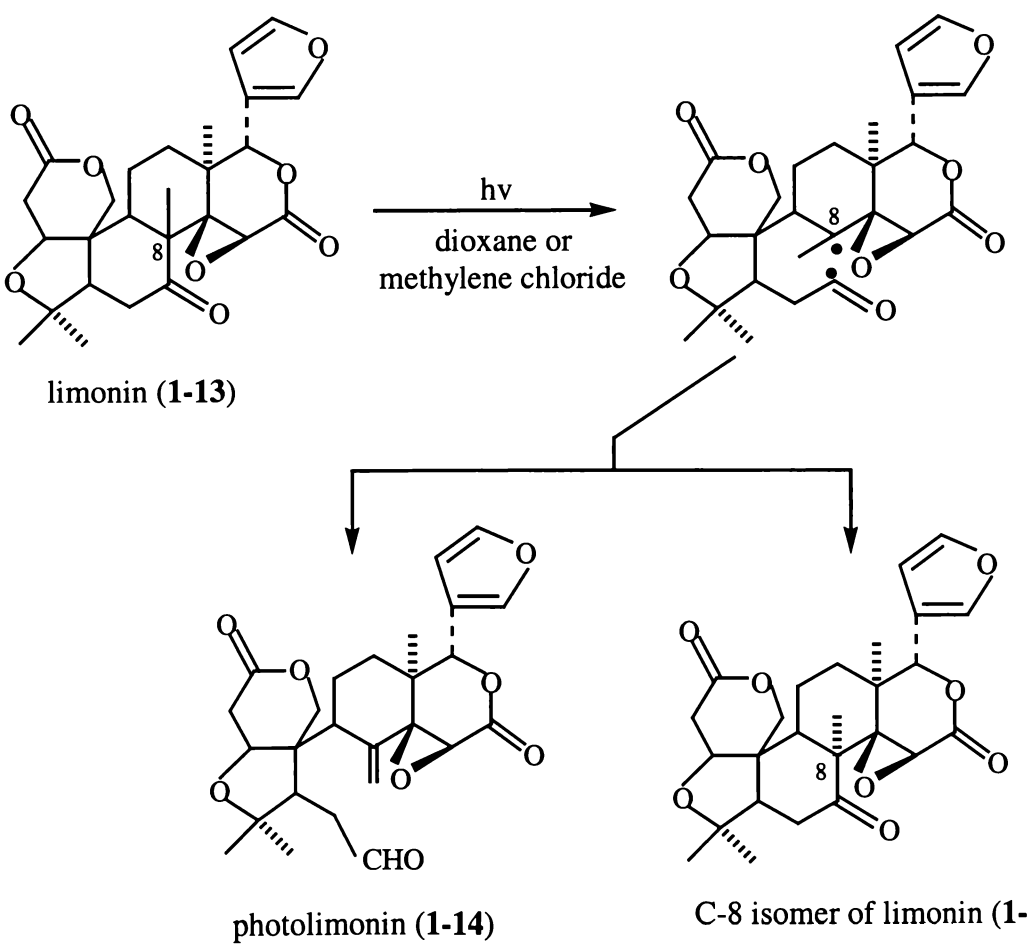

limonin (**1-13**)

photolimonin (**1-14**)

C-8 isomer of limonin (**1-15**)

Scheme 1-6. The structures of major products obtained on photolysis of limonin (**1-13**) in the presence of dioxane or methylene chloride.

Okogun *et al.* (1998) has reported the photochemical behaviour of 7-deacetoxy-7-oxokhivorin (**1-16**) in methanol. The major product was identified as 3-deoxo-1α,3α-diacetoxy-1,2,2,2,8,30-hexahydro-18β-H-andirobin (**1-17**) (see Scheme 1-7). It is of note that, as in the case of **1-13,** photolysis of **1-16** proceeded with inversion of the configuration at C-8.

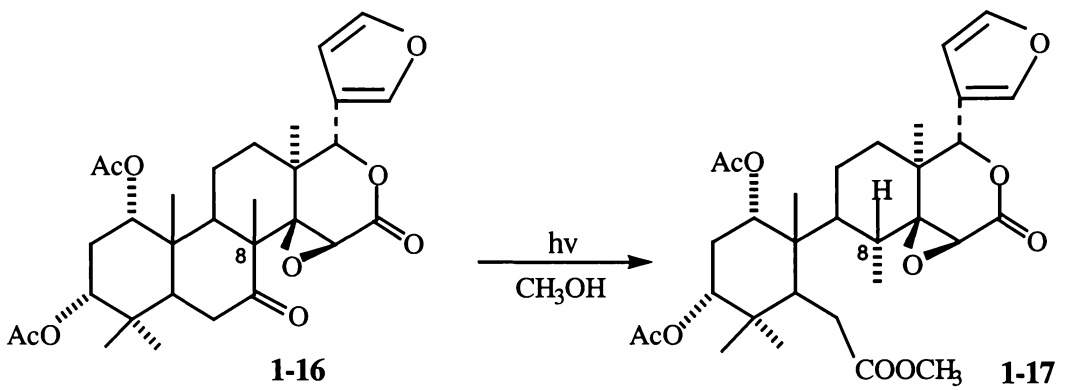

1-16 **1-17**

Scheme 1-7. Photolysis of 7-deacetoxy-7-oxokhivorin (**1-16**) to afford (**1-17**).

It is apparent from the review of Goh (1981) that the photolysis of 3-oxo-4,4-dimethyl triterpenes typically proceeded *via* six-membered transition states (ie transfer of a hydrogen atom from C-2 to C-4) (Nakanishi *et al.*, 1975) to afford saturated ketenes, which then reacted with water or alcohols to give either 3,4-secoacids or 3,4-secoesters (see Table 1-1).

Goh (1981) also reported that the photochemical reaction of 22α-hydroxystictan-3-one (a boat ring B triterpene) (**1-24**) in methanol proceeded to afford methyl 22-hydroxy-3,4-secostictan-3-oate (**1-25**) as the major product, or 22-hydroxy-3,4-secostictan-3-oic acid (**1-26**) in the presence of water (Scheme 1-8).

Photochemical reactions performed using deuterium-labelled compounds have verified the shift of a hydrogen atom from C-2 to C-4 (Quannes & Beugelmans, 1972; Aoyagi *et al.*, 1973; Goh, 1981). For example, upon irradiation of 2,2-$^2D_2$-22α-hydroxystictan-3-one (**1-24**), rearrangement of the initially formed biradical *via* a six-membered transition state with deuterium transfer from C-2 to C-4 afforded an intermediate ketene which then reacted with methanol to give a 4-^{2}D-3,4-secoester (Goh, 1981) (see Scheme 1-9).

Table 1-1. Photolysis products from some 3-oxo-4,4-dimethyl triterpenoids.

compound	photolysis condition	photoproducts	refs.
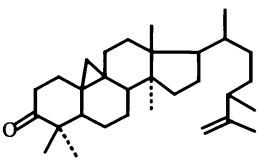 cyclolaudenone (**1-18**)	H_2O/dioxane	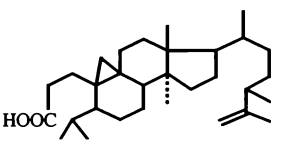	Quannes & Beugelmans (1972)
	methanol	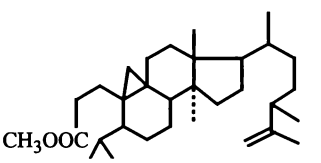	
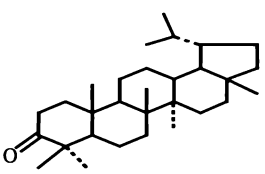 lupan-3-one (**1-19**)	*n*-hexane	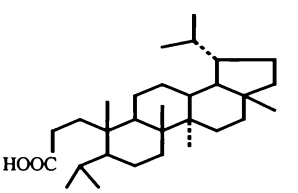	Hirota *et al*, (1974)
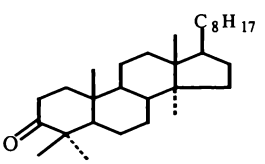 lanostanone (**1-20**)	acetic acid-H_2O (9:1)	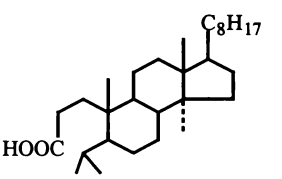	Arigoni *et al*, (1959)
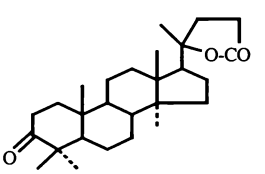 γ-lactone (**1-21**)	acetic acid-H_2O (9:1)	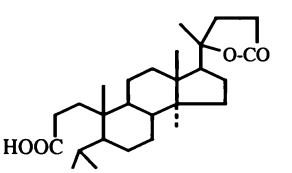	Arigoni *et al* (1959)
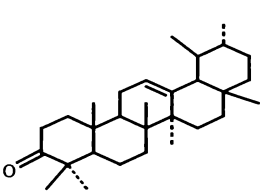 α-amyrone (**1-22**)	acetic acid-H_2O (9:1)	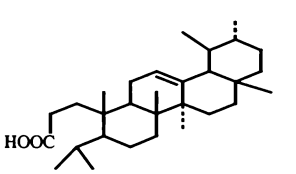	Arigoni *et al* (1959)
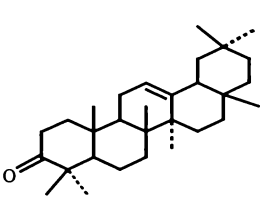 β-amyrone (**1-23**)	acetic acid-H_2O (9:1)	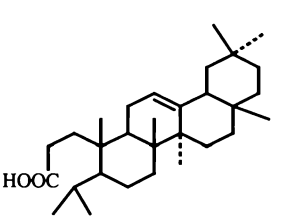	Arigoni *et al* (1959)

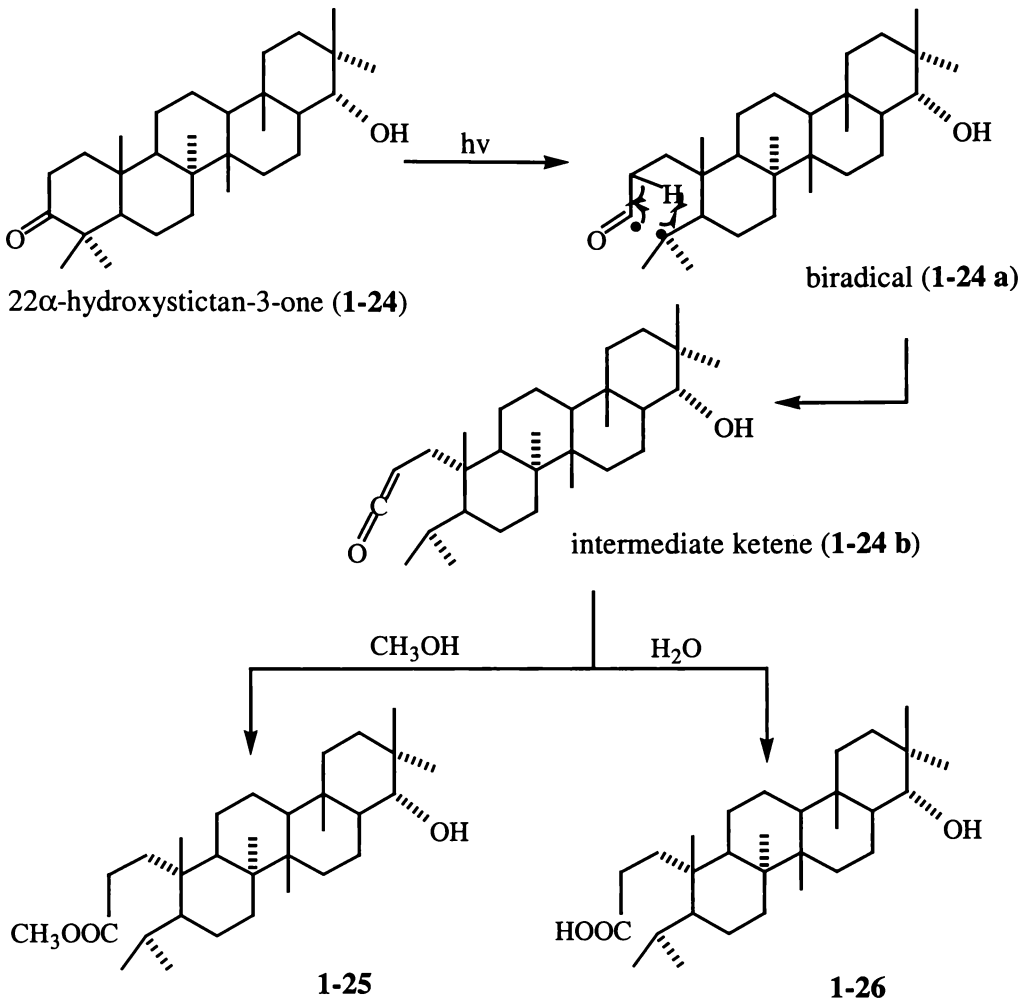

Scheme 1-8. Photolysis products of 22α-hydroxystictan-3-one (**1-24**) in the presence of methanol or water.

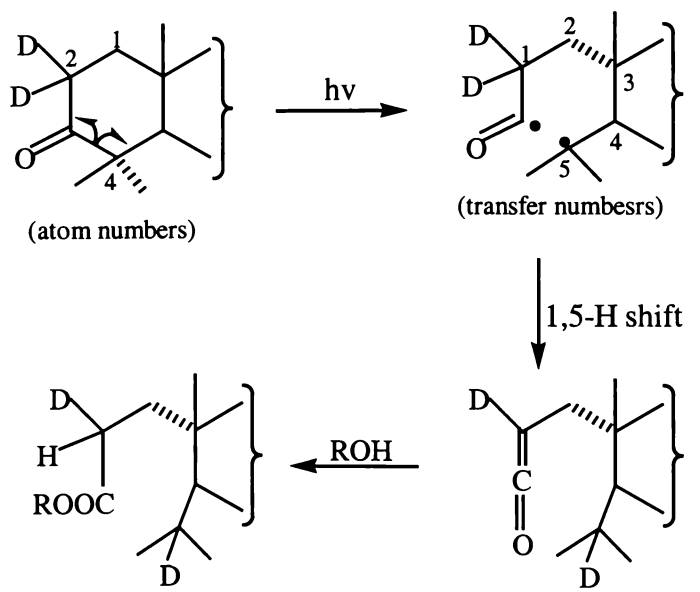

Scheme 1-9. Photochemical rearrangement of 2,2-$^2D_2$-22α-hydroxystictan-3-one (**1-24**).

Hunter (1993) has investigated the photochemical behaviour of 22-hydroxyhopan-7-one (**2-1**) in benzene-methanol and identified methyl 22-hydroxy-7,8-secohopan-7-oate (**2-2**) as the major product (Scheme 1-10).

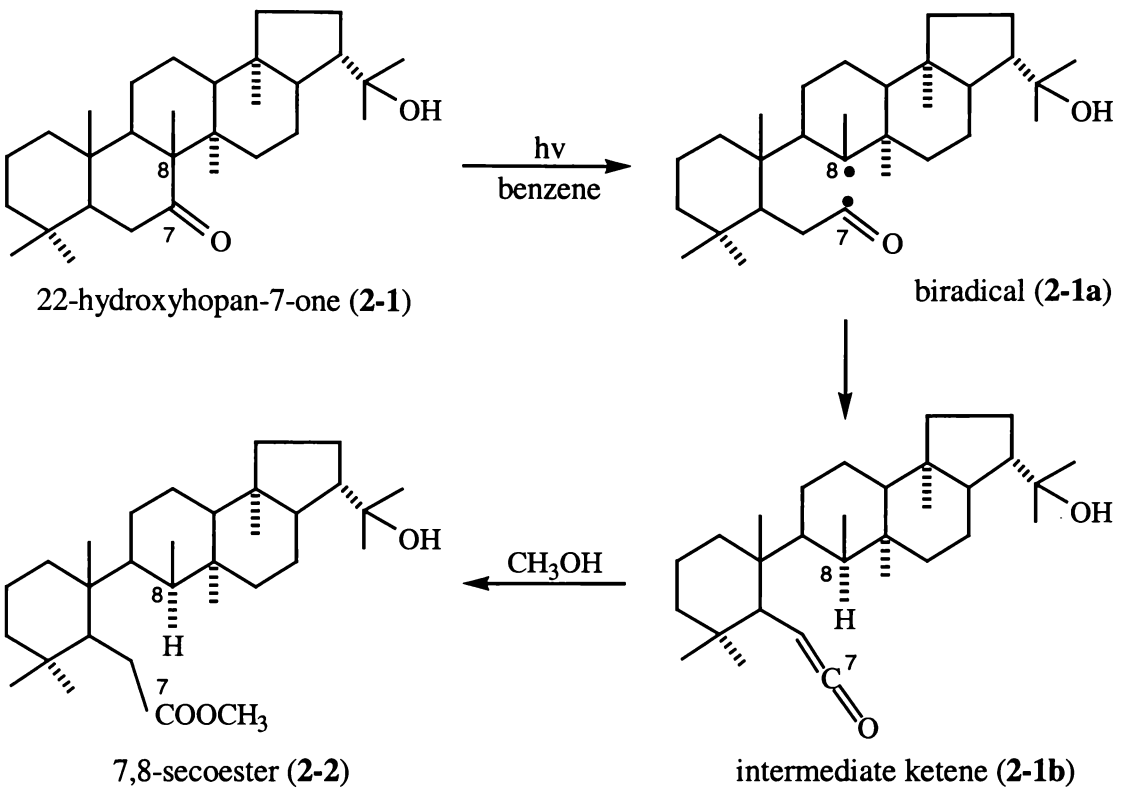

Scheme 1-10. Photoreaction of 22-hydroxyhopan-7-one (**2-1**) to afford methyl 22-hydroxy-7,8-secohopan-7-oate (**2-2**).

Hunter (1993) also found that photolysis of 22-hydroxyhopan-15-one (**3-1**) afforded a mixture of products which appeared to include participation products with the 22-hydroxyl group (see Chapter Three). However only GC/MS evidence was obtained in support of this proposal. The occurrence in some of the products of a strong *m/z* 164 ion was believed to be associated with formation of 15,22-*O-abeo* ring (see Section **3.3**). Further supporting evidence, eg., NMR spectral data, was not obtained due to difficulties encountered in the separation of the reaction mixture.

There is an interest in the availability of the 7,8- or 14,15-secohopanoids, both as synthetic substrates and authentic standards, in connection with investigations concerned with the biogenic transformations of hopanoids in fossil fuels.

1.2 Distribution of Triterpenoids in New Zealand Lichens

1.2.1 Lichens

Lichens are defined to be a mutualistic symbiotic association between a fungal partner and a population of unicellular or filamentous algal or cyanobacterial cells. Briefly, they are symbiotic organisms consisting of algae and fungi, and renowned for their wide and diverse range of metabolic products, which are of considerable chemotaxonomic importance and have been studied by many organic chemists since the beginning of the 19th century. For example, some lichen depsidones are known to chelate strongly to metal ions and are thought to be able supply the producer lichen with essential minerals from the substrate the lichen is growing on (Purvis & Elix, 1987; 1990). They can also be used as environmental indicators for pollution monitoring (Ballarindenti *et al.*, 1998) around cities and factories.

Lichens are also being examined for new pharmaceuticals (Gonzaleztejero *et al.*, 1995; Marcano *et al.*, 1999; Smriga & Saito, 2000) and agrochemicals, as well as commercially valuable enzymes for use in biosensors, biotransformation reactions and diagnostic kits. Recent work has identified compounds with marked anti-tumour properties (terpenes) (Back & Chappell, 1996), anti-amoeba activity (fatty acids), nematocidal activity (Stevens, 1998), and anti-microbial, allelopathic and anti-feedant activities (Huneck & Yoshimura, 1996). It has been reported that a crude extract from New Zealand lichen *Pseudocyphellaria coronata* significantly prolonged the life span of mice previously inoculated with an acute lymphocytic leukaemia (Burton & Cain, 1959; Cain, 1961).

Lichens are taxonomically divided into a variety of genera and species, and there are now more than 20,000 species of lichens distributed in most of the environmental habitats of the world. New Zealand has a richly diverse and well-developed lichen flora. Chemical substance distributions in New Zealand lichens have been summarised by Galloway (1985) and subsequently updated by Walker & Lintott (1997). The substances are mainly amino acids, polyols and sugar, triterpenoids, steroids, depsides, depsidones and aromatic pigments (Elix *et al.*, 1984; 1987).

1.2.2 Distribution of Triterpenoids in New Zealand *Pseudocyphellaria* Lichens

New Zealand lichens have proved to be a prolific source of triterpenoids. More than 50 species of New Zealand lichens have been reported to contain hopane, stictane, fernene and/or lupane triterpenes (Galloway, 1985; Walker & Lintott, 1997). Triterpenoids are especially prolific in New Zealand *Pseudocyphellaria* species.

Detailed structural and synthetic investigations of triterpenoids isolated from New Zealand *Pseudocyphellaria* species have been carried out at Otago University (Chin *et al.*, 1973; Corbett & Wilkins, 1977a; 1977b; Corbett *et al.*, 1985), and at Waikato University (Ronaldson & Wilkins, 1978; Goh *et al.*, 1978; Holland & Wilkins, 1979; Ronaldson & Wilkins, 1979; Corbett *et al.*, 1982, 1987; Wilkins & Goh, 1988; Wilkins *et al.*, 1989; Wilkins & Elix, 1990).

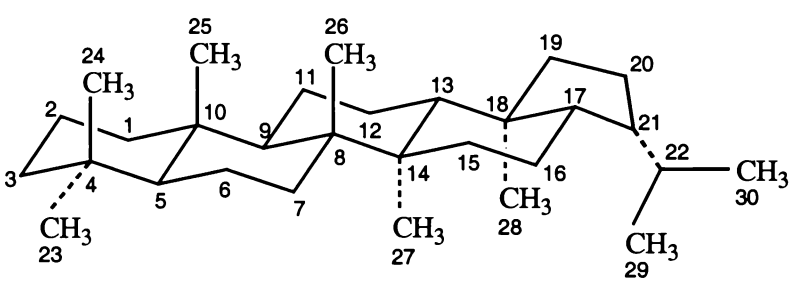

Figure 1-1. Hopane skeleton and its numbering system.

Triterpenoids which have been identified in New Zealand *Pseudocyphellaria* lichen species are listed in Table 1-2. The *Stictiacae* includes *Pseudocyphellaria* and *Lobaria* species, however *Lobaria* species generally do not contain triterpenoids. Fernene and stictane triterpenoids have however been isolated from a Himalayan collection of *Lobaria retigera* (Corbett & Wilkins, 1976c; Rao & Seshadri, 1968), a Norwegian collection of *Cetraria nivalis* (Wilkins, 1977a; 1977b) and South American collection of *Xanthoria resendei* (Gonzalez *et al.*, 1974), as well as from *Pseudocyphellaria* species (Chin *et al.*, 1972; Corbett & Heng, 1973; Goh *et al.*, 1978; Wilkins & Elix, 1990). *L. retigera* also occurs in New Zealand, however the isolation of fernene triterpenoids from a New Zealand collection of this species has not been reported.

Table 1-2. Triterpenoid distributions in some New Zealand lichen species.

lichen species		triterpenoids isolated
Lobaria retigera		stictane-3β,22α-diol, retigeranic acid
Nephroma	*N. helveticum*	7β-acetoxyhopan-22-ol, hopane-7β,22-diol
	N. rufum	7β-acetoxyhopan-22-ol, hopane-7β,22-diol
***Peltigera** dolichorhiza*		7β-acetoxyhopan-22-ol, hopane-7β,22-diol, 15α-acetoxyhopan-22-ol hopane-15α,22-diol, hopane-6α,22-diol (zeorin)
Physica	*P. aipolia*	hopane-6α,22-diol (zeorin)
	P. caesia	hopane-6α,22-diol (zeorin), hopane-6α,16β,22-triol (leucotylin)
	P. stellaris	hopane-6α,22-diol (zeorin), hopane-6α,16β,22-triol (leucotylin)
	P. tenuisecta	hopane-6α,22-diol (zeorin)
	P. trabacioides	hopane-6α,22-diol (zeorin), hopane-6α,16β,22-triol (leucotylin)
Pseudocyphellaria	*P. allanii*	7β-acetoxyhopan-22-ol, hopane-15α,22-diol
	P. ardesiaca	2α-acetoxystictane-3β,22α-diol, 3β-acetoxystictane-2α,22α-diol 2α,3β-diacetoxystictan-22α-ol, stictane-2α,3β,22α-triol, 2α,3β,22α-triacetoxystictane
	P. billardierei	6α-acetoxyhopane-7β,22-diol 7β-acetoxyhopan-22-ol, hopane-15α,22-diol
	P. carpoloma	6α-acetoxyhopane-7β,22-diol, 7β-acetoxyhopane-6α,22-ol, hopane-7β,22-diol
	P. chloroleuca	7β-acetoxyhopan-22-ol, hopane-15α,22-diol
	P. cinnamomea	7β-acetoxyhopan-22-ol, hopane-15α,22-diol
	P. colensoi	2α-acetoxystictane-3β,22α-diol, 3β-acetoxystictane-2α,22α-diol 2α,3β-diacetoxystictan-22α-ol, 22α-hydroxystictan-3-one, stictane-3β,2α-diol, stictane-2α,3β,22α-triol, 2α,3β,22α-triacetoxystictane
	P. coriacea	7β-acetoxyhopan-22-ol, hopane-15α,22-diol, hopane-7β,22-diol,
	P. coronata	2α-acetoxystictane-3β,22α-diol, 3β-acetoxystictane-2α,22α-diol 2α,3β-diacetoxystictan-22α-ol, 22α-hydroxystictan-3-one, stictane-3β,22α-diol stictane-2α,3β,22α-triol, 2α,3β,22α-triacetoxystictane
	P. crassa	hopane-6α,7β,22-triol
	P. degelii	3-acetoxy-3,4-secostict-4(23)-en-3-ol, 22α-hydroxy-3,4-secostict-4(23)-en-3-oic acid, 22α-hydroxy-3,4-secostict-4(23)-en-3-al, stictane-3β,22α-diol
	P. dissimilis	7β-acetoxyhopan-22-ol, hopane-15α,22-diol
	P. durietzii	hopane-6α,7β,22-triol
	P. episticta	7β-acetoxyhopan-22-ol, 15α-acetoxy-22-hydroxyhopan-24-oic acid 15α,22-dihydroxy-24-hopanoic acid, hopane-15α,22-diol
	P. faveolata	hopane-6α,7β,22-triol
	P. fimbriata	7β-acetoxyhopan-22-ol, hopane-15α,22-diol, hopane-7β,22-diol
	P. fimbriatoides	7β-acetoxyhopan-22-ol, hopane-15α,22-diol, hopane-7β,22-diol
	P. glabra	7β-acetoxyhopan-22-ol, hopane-15α,22-diol, hopane-7β,22-diol
	P. granulata	hopane-6α,7β,22-triol

Table 1-2 (continued)

Pseudocyphellaria	*P. homoeophylla*	7β-acetoxyhopan-22-ol, hopane-15α,22-diol, hopane-7β,22-diol
	P. hookeri	hopane-6α,7β,22-triol
	P. initricata	7β-acetoxyhopan-22-ol, hopane-15α,22-diol, hopane-7β,22-diol,
	P. knightii	7β-acetoxyhopan-22-ol, hopane-15α,22-diol
	P. lividofusca	15α-acetoxy-22-hydroxyhopan-22-oic acid, 7β-acetoxyhopan-22-ol 15α,22-dihydroxy-24-hopanoic acid, hopane-15α,22-diol
	P. maculata	hopane-6α,22-diol,
	P. margaretiae	hopane-15α,22-diol, hopane-6α,7β,22-triol
	P. montagnei	hopane-6α,7β,22-triol
	P. multifida	7β-acetoxyhopan-22-ol, hopane-15α,22-diol, hopane-7β,22-diol
	P. murrayi	7β-acetoxyhopan-22-ol, hopane-15α,22-diol
	P. neglecta	6α-acetoxyhopane-7β,22-diol, 7β-acetoxyhopane-6α,22-diol hopane-6α,7β,22-triol, hopane-7β,22-diol
	P. pickeringii	3β-acetoxystictan-22-ol, 2α-acetoxystictane-3β,22α-diol 3β-acetoxystictane-2α,22α-diol, 2α,3β-diacetoxystictan-22-one 2α,3β-diacetoxystictan-22α-ol, 3β,22α-diacetoxystictane, stictane-3β,22α-diol, stictane-2α,3β,22α-triol, 2α,3β,22α-triacetoxystictane
	P. pubescens	hopane-15α,22-diol, hopane-6α,7β,22-triol
	P. rufovirescens	7β-acetoxyhopan-22-ol, hopane-6α,7β,22-triol, hopane-15α,22-diol
	P. sericeofulva	6α-acetoxyhopane-7β,22-diol, 7β-acetoxyhopan-22-ol hopane-6α,7β,22-triol, hopane-7β,22-diol,

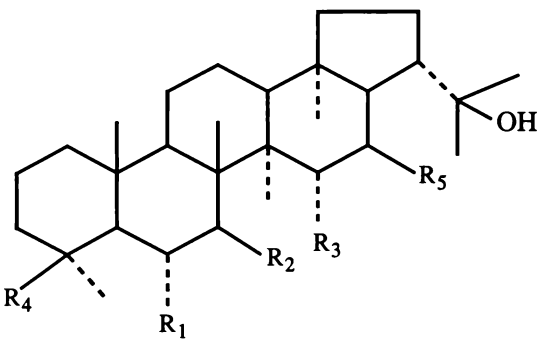

(1-27) R_1=R_3=R_5 =H, R_2=OAc, R_4=Me
(1-28) R_1=R_2=R_5 =H, R_3=OH, R_4=Me
(1-29) R_1=R_3=R_5 =H, R_4=Me, R_2=OH
(1-30) R_1=R_2=R_3=R_5=H, R_4=Me
(1-31) R_1=R_2=R_5=H, R_3=OAc, R_4=COOH
(1-32) R_1=OH, R_2=R_3=R_5=H, R_4=Me,
(1-33) R_1= R_2=OH, R_3=R_5=H, R_4=Me,
(1-34) R_1=OAc, R_2=OH, R_3=R_5=H, R_4=Me
(1-35) R_1=OH, R_2=OAc, R_3=R_5 H, R_4=Me

Figure 1-2. Structures of some hopanoid triterpenes isolated from New Zealand *Pseudocyphellaria* lichens.

The first reported isolation of triterpenoids from a New Zealand *Pseudocyphellaria* species occurred when Corbett & Young (1966a, 1966b) identified 7β-acetoxyhopan-22-ol (**1-27**) and hopane-15α,22-diol (**1-28**) from the extractives of collections originally identified as *P. billardierei*, but now referred to *P. rufovirescens* (Galloway, 1985). Minor compounds which accompany these substances are hopane-7β,22-diol (**1-29**) and hopan-22-ol (**1-30**). The level of hopane-7β,22-diol in lichen collections is such that it can sometimes be detected by thin layer chromatography (TLC) analysis (Wilkins & James, 1979; Galloway, 1985), while that of hopan-22-ol (**1-30**) is generally not sufficient for TLC characterisation. These triterpenoids also occur in a number of other species including *P. initricata*, and *P. multifida* (see Table 1-2).

Although 15α-acetylation activity is lacking in *P. rufovirescens* and related species, it is observed in *P. episticta* and *P. lividofusca* species. The major constituent of these lichens is 15α-acetoxy-22-hydroxyhopan-24-oic acid (**1-31**) (amphistictinic acid) (Ronaldson & Wilkins, 1978). Hopane-6α,22-diol (zeorin) (**1-32**) appears to be confined to a single New Zealand *Pseudocyphellaria* species (Galloway, 1985). This species, identified by Galloway (1985) as *P. billardierei*, has the code B chemistry of Wilkins & James (1979).

The major accessory substances which also occur in collections of this lichen appear to be 6α,16β,22-trisubstituted hopane triterpenoids present in *Parmelia entotheiochroa* (Yosioka *et al.*, 1966). The trisubstituted triterpenoid, hopane-6α,7β,22-triol (**1-33**), is widely distributed in white medulla New Zealand *Pseudocyphellaria* species, and also occurs in some *Nephroma* species (Wilkins, 1980).

Yellow medulla New Zealand *Pseudocyphellaria* lichens are the only significant source of stictane triterpenoids. Ten stictane triterpenoids (**1-36**)~(**1-45**) (Figure 1-3 and 1-4) have been isolated from collections of *P. colensoi, P. coronata*, and *P. pickeringii* (at the time referred to as *P. flavicans*) (Chin *et al.*, 1973; Wilkins, 1977b), while three 3,4-secostictane triterpenoids (**1-46**), (**1-47**), (**1-48**) (Figure 1-5) and stictane-3β,22α-diol (**1-42**) were isolated from *P. degelii* (Goh *et al.*, 1978).

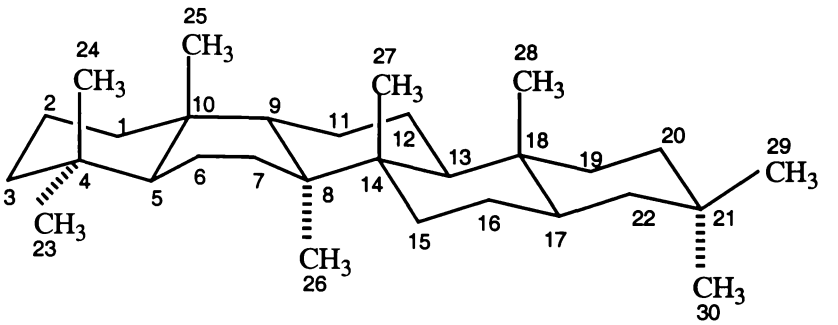

Figure 1-3. The stictane skeleton, showing the B ring boat conformation.

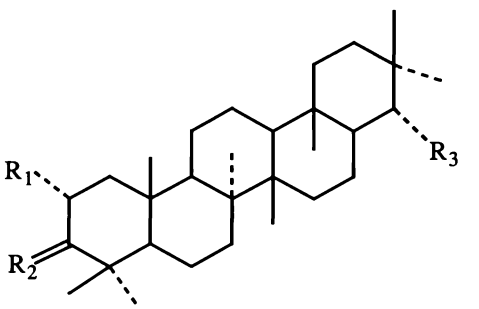

(**1-36**) R_1=OH, R_2=H, β-OH, R_3=OH	stictane-2α,3β,22α-triol
(**1-37**) R_1=OAc, R_2=H, β-OAc, R_3=OAc	2α,3β,22α-triacetoxystictane
(**1-38**) R_1=OAc, R_2=H, β-OAc, R_3=OH	2α,3β-diacetoxystictan-22α-ol
(**1-39**) R_1=OAc, R_2=H, β-OH, R_3=OH	2α-acetoxystictane-3β,22α-diol
(**1-40**) R_1=OH, R_2=H, β-OAc, R_3=OH	3β-acetoxystictane-2α,22α-diol
(**1-41**) R_1=OAc, R_2=H, β-OAc, R_3=O	2α,3β-diacetoxystictan-22-one
(**1-42**) R_1=H, R_2=H, β-OH, R_3=OH	stictane-3β,22α-diol
(**1-43**) R_1=H, R_2=H, β-OAc, R_3=OAc	3β,22α-diacetoxystictane
(**1-44**) R_1=H, R_2=H, β-OAc, R_3=OH	3β-acetoxystictan-22α-ol
(**1-45**) R_1=H, R_2=O, R_3=OH	22α-hydroxystictan-3-one

Figure 1-4. Structures of stictane triterpenes isolated from New Zealand collections of *P. colensoi, P. coronata* and *P. pickeringii*.

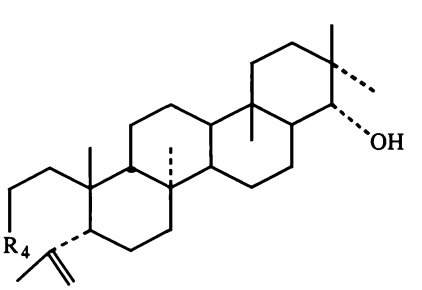

(**1-46**) R_4=CHO
(**1-47**) R_4=COOH
(**1-48**) R_4=CH_2OAc

Figure 1-5. Structures of 3,4-secostictane triterpenoids isolated from New Zealand collections of *P. degelii*.

Stictane triterpenoids have a very limited distribution in nature. Other than yellow medulla *Pseudocyphellaria* species, stictane triterpenoids have only been isolated from Himalayan *collections* of *L. retigera* (Corbett & Wilkins, 1976c) and a Norwegian collection of *C. nivalis* (Wilkins, 1977a).

A group of fernene triterpenoids, which can be viewed as migrated hopanes, (**1-49**), (**1-50**) and (**1-51**) (see Figure 1-6) have been isolated from the collections of *P. aurata* (Wilkins & Elix, 1990). Prior to the isolation of these compounds, Wilkins & James (1979) noted the presence in collections of *P. aurata* of unknown substances, possibly triterpenoids or sterols.

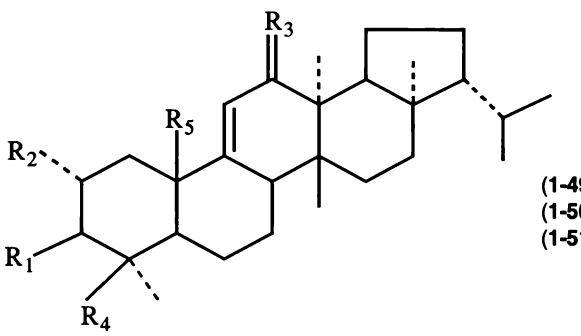

(**1-49**) R_1=OAc; R_2=H; R_3=O; R_4=R_5=Me
(**1-50**) R_1=OAc; R_2=H; R_3=H,β-OH; R_4=R_5=Me
(**1-51**) R_1=OAc; R_2=H; R_3=H,β-OAc; R_4=R_5=Me

Figure 1-6. Structures of fernene triterpenoids isolated from *P. aurata.*

Corbett *et al.* (1985, 1987) have demonstrated that *P. rubella* (a yellow medulla species) contains a complex array of lupane, norlupane and trisnorlupane triterpenoids, variously substituted at C-3, C-20, and or C-29, including (**1-52**)-(**1-57**) (Figure 1-7). Two of the substances isolated from the extractives were shown to be lupeol acetate (**1-58**) and 3β-acetoxy-20,29-epoxylupane (**1-59**) (Figure 1-8). Lupane triterpenes have a different primary biosynthetic pathway from hopane, fernene and stictane triterpenoids.

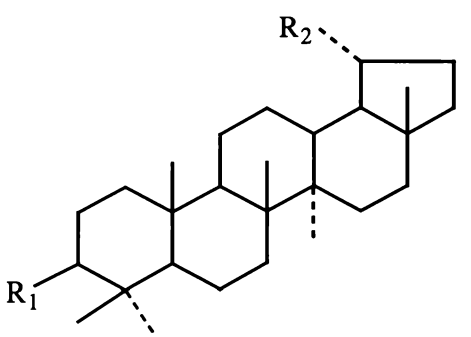

(**1-52**) R_1=OAc, R_2=OH
(**1-53**) R_1=OAc, R_2=$CH(CH_3)OH$
(**1-54**) R_1=OAc, R_2=$CH(CH_3)CHO$
(**1-55**) R_1=OAc, R_2=$CH(CH_3)CH_2OH$
(**1-56**) R_1=OAc, R_2=CH(CH3)COOH
(**1-57**) R_1=OAc, R_2=$C(CH_3):CH_2$

Figure 1-7. Structures of lupane triterpenoids isolated from *P. rubella.*

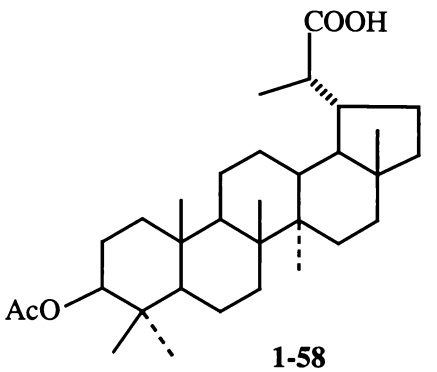

1-58

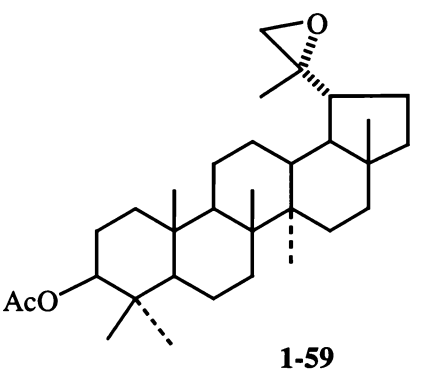

1-59

Figure 1-8. Structures of lupeol acetate (**1-58**) and 3β-acetoxy-20,29-epoxylupane (**1-59**) isolated from *P. rubella*.

1.2.3 Structure Relationships in *Pseudocyphellaria* Triterpenoids

The interesting aspect in the structures of hopane hydrocarbons and substituted hopanoids such as hopane-7β,22-diol (**1-29**) and hopane-15α,22-diol (**1-28**) is that there exists a local two fold rotational (C_2) symmetry axis about ring C, if rings A and E are ignored. This symmetry is exemplified by the ^{13}C NMR chemical shifts established for some saturated and unsaturated hopane hydrocarbons and equivalently substituted C-7 and C-15 compounds (Wilkins *et al*, 1987a, 1987b, 1989).

Stictane triterpenoids are unusual in that they possess a boat ring B system (Chin *et al.*, 1973; Corbett *et al*, 1982; Wilkins & Goh, 1988). The boat ring B conformation was originally deduced from an analysis of ^1H NMR spectral data determined for some hop-17(21)-ene triterpenes and for some flavic-17(21)-ene triterpenes, which were prepared by dehydration and ring contraction of 22α-hydroxylated stictane triterpenes (Corbett & Wilkins, 1976a, 1976b).

Rings C, D and E of the respective groups of triterpenes are antipodally related (see Figure 1-9). Subsequently the structures of the stictane and secostictane triterpenoids were confirmed by X-ray crystallographic analyses (Corbett *et al.*, 1982; Wilkins & Goh, 1988). A later NMR study resulted in the isolation and the structural elucidation of a new stictane lactone (**1-60**) (Figure 1-10), a minor constituent of *P. pickeringii* (Wilkins *et al.*, 1989).

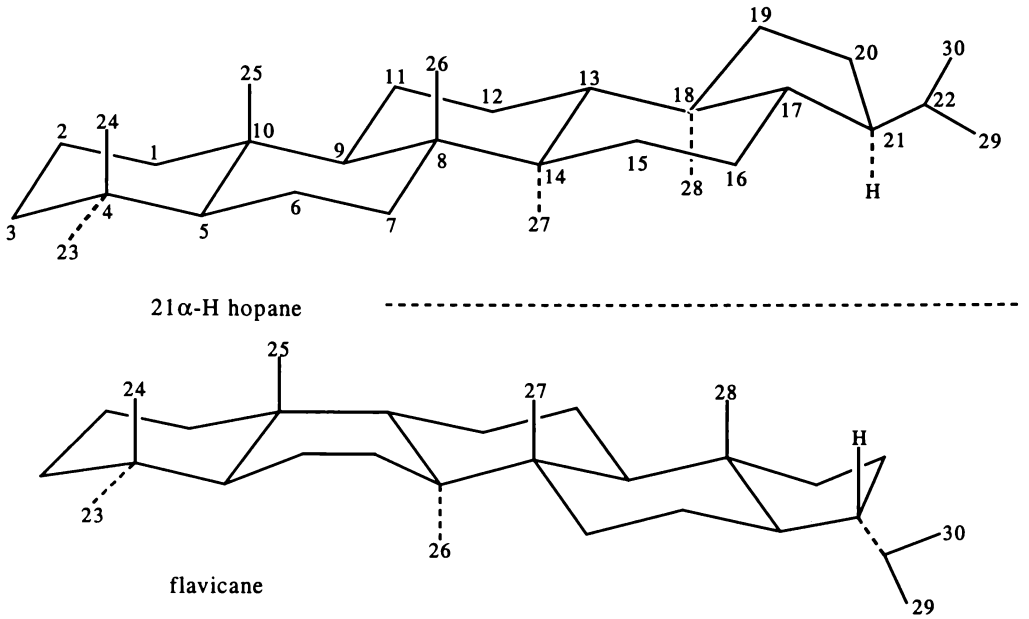

Figure 1-9. The antipodal relation between rings C, D and E of 21α-H-hopane and flavicane.

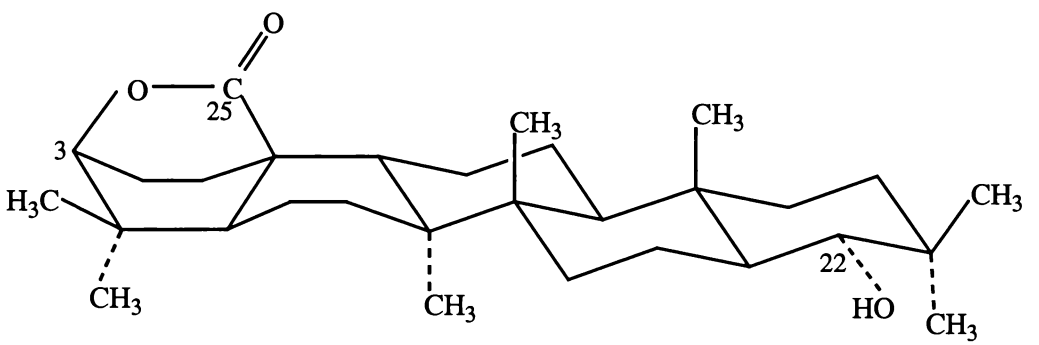

Figure 1-10. Structure of a stictane triterpene lactone (**1-60**) isolated from *P. pickeringii*.

1.3 Aims of the Present Study

Hitherto Hunter (1993) has investigated the photochemistry of two hopane triterpenoids, 22-hydroxyhopan-7-one (**2-1**) and 22-hydroxyhopan-15-one (**3-1**). Photolysis of the former proceeded to afford the expected product (Scheme 1-9), while the latter appeared to give the products of uncertain structures, possibly arising from participation of the 22-hydroxyl group. His investigations were however curtailed by the failure of the UV lamp. Significant levels of 22-hydroxyhopan-15-one (**3-1**) were, for example, still present after 212 hours.

The structures of the dominant hopane, stictane, lupane and fernene triperpenoids occurring in New Zealand lichen *Pseudocyphellaria* species are well known. There are, however, a number of unknown minor triterpenoids in the extracts.

The aims of this study were:

(i) A reinvesitigation of the photochemical reactions of 7-oxo and 15-oxohopanoids, including the structure analyses of photo products prepared from 15-oxohopanoids, and the identification of factors which contribute to the formation of 22-hydroxyl group participation products.

(ii) Isolation and structural elucidation of new minor triterpenoids present in extracts of *P. colensoi.*

A further objective of the work was the complete assignments, using a combination of one- and two-dimensional NMR techniques, of the ^{13}C and ^{1}H NMR signals of the hopane, stictane and flavicane triterpenoids (synthetic and natural) prepared or isolated during the study.

Chapter Two

Photochemical Reactions of 22-Hydroxyhopan-7-one and Hop-22(29)-en-7-one

2.1 Introduction

Hunter (1993) has previously identified methyl 22-hydroxy-7,8-secohopan-7-oate (**2-2**) as the major photolysis product of 22-hydroxyhopan-7-one (**2-1**) when a mixture of benzene and methanol was used as the reaction solvent. The formation of the 7,8-secoester (**2-2**) was consistent with the proposal of Goh (1988) and others (Kohen *et al.*, 1969; Stevenson *et al.*, 1971), that the photolysis of **2-1** involved biradical formation, followed by hydrogen transfer from C-6 to C-8 *via* a six-membered transition state, to give an intermediate ketene, which then reacted with methanol to afford the 7,8-secoester as the major product (see Section **2.6**).

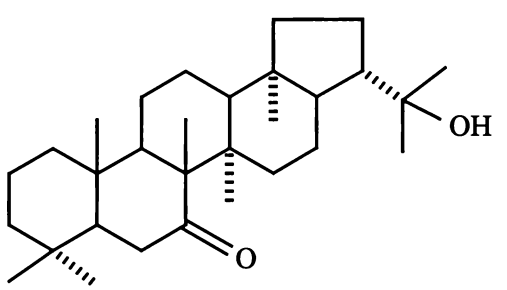

2-1

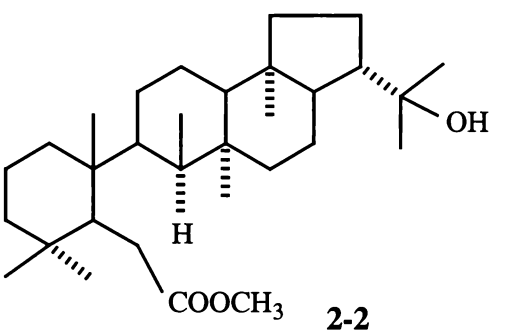

2-2

Figure 2-1. The structures of 22-hydroxyhopan-7-one (**2-1**) and the photolysis product methyl 22-hydroxy-7,8-secohopan-7-oate (**2-2**).

Hunter (1993) concluded that the C-8 stereochemistry was *probably* that with an α-orientation for H-8, and a β-orientation for the 8-methyl group, as in the starting material (**2-1**). It was anticipated that the availability of a higher field NMR instrument (400 MHz) than was the case when Hunter's investigation was performed, would enable

the C-8 stereochemistry to be *unequivocally* established. At the outset of these investigations it was also of interest to ascertain if the currently available UV lamp (a different design and source type from that used by Hunter) afforded photolysis products which corresponded to those obtained by Hunter (1993).

In the present study, the photochemical behaviour of 22-hydroxyhopan-7-one (**2-1**) and its olefinic analogue, hop-22(29)-en-7-one (**2-3**), in the presence of benzene alone, and in a mixture of benzene and isopropanol, was also investigated since it was anticipated that in the benzene only reaction, the inability of an intermediate ketene to react with methanol, or the replacement of methanol by isopropanol (a more bulky alcohol), might influence the product outcome(s) of these reactions (see Sections **2.3** and **2.4** respectively).

Additionally, because of other outcomes observed for 15-oxohopanoids in Chapter Three, the photochemical behaviour of hop-22(29)-en-7-one (**2-3**) (a substrate lacking a 22-hydroxyl group) was also investigated (see Section **2.5**).

22-Hydroxyhopan-7-one (**2-1**) and hop-22(29)-en-7-one (**2-3**) were prepared using standard methods (Corbett & Young, 1966a), from 7β-acetoxyhopan-22-ol (**2-4**) which was isolated from the lichen *Pseudocyphellaria homoeophylla* (see Scheme 2-1).

Reduction of 7β-acetoxy-22-hydroxyhopane (**2-4**) with lithium aluminum hydride (LAH) in refluxing diethyl ether afforded hopane-7β,22-diol (**2-5**). Oxidation of hopane-7β,22-diol (**2-5**) with CrO_3 in pyridine, as described by Corbett & Young (1966a), afforded 22-hydroxyhopan-7-one (**2-1**).

Dehydration of 22-hydroxyhopan-7-one (**2-1**) with $POCl_3$ in pyridine afforded a mixture of hop-21-en-7-one and hop-22(29)-en-7-one (**2-3**), which were separated using a silver nitrate impregnated alumina column and mixtures of light petroleum and diethyl ether as eluents. Synthetic details are reported in Section **6.2** of Chapter Six.

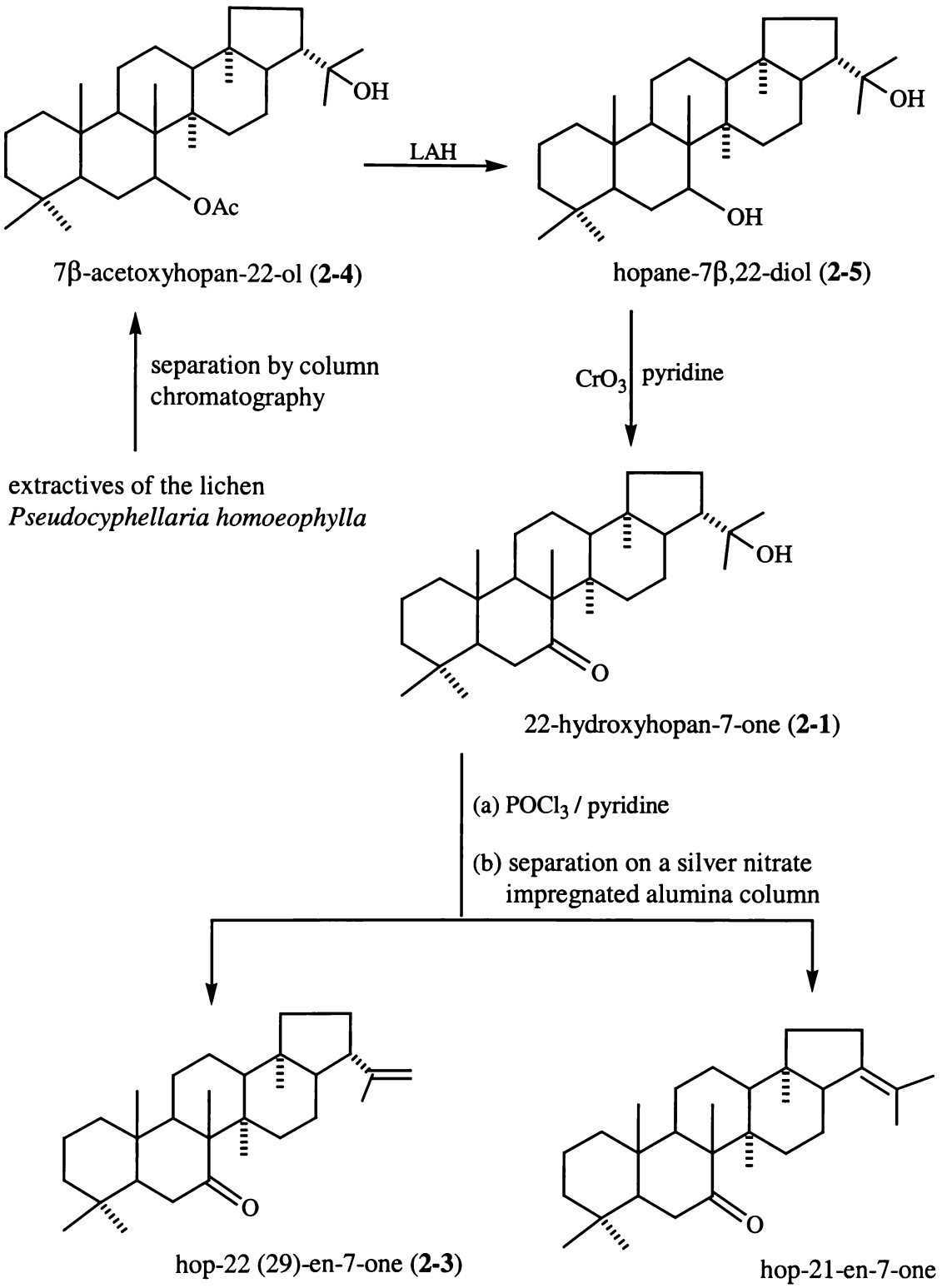

Scheme 2-1. The reaction sequence used to prepare (**2-1**) and (**2-3**) from 7β-acetoxyhopane-22-ol (**2-4**).

2.2 Photolysis of 22-Hydroxyhopan-7-one in Benzene-Methanol

2.2.1 Photolysis of 22-Hydroxyhopan-7-one (2-1)

Photolysis of 22-hydroxyhopan-7-one (**2-1**) in benzene-methanol (1:1) for 4 h afforded product material, which was purified by radial chromatography on silica gel using mixtures of light petroleum and diethyl ether as eluents. This gave methyl 22-hydroxy-7,8-secohopan-7-oate (**2-2**), identical (^{1}H and ^{13}C NMR, MS) to a specimen of this compound prepared by Hunter (1993). A more extensive MS and NMR characterisation of **2-2** than that undertaken by Hunter (1993), including the elucidation of the C-8 configuration, is reported below.

2.2.2 Structural Elucidation of Methyl 22-hydroxy-7,8-secohopan-7-oate (2-2)

2.2.2.1 Mass Spectral Analysis of Methyl 22-hydroxy-7,8-secohopan-7-oate (2-2)

The highest observed ion in the mass spectrum of **2-2** occurred at *m/z* 456, corresponding to the loss of water from an expected molecular ion of *m/z* 474 ($C_{31}H_{54}O_3$). This feature of the mass spectrum of **2-2** is in accordance with the observation that many 22-hydroxyhopanoids show only weak molecular ions, together with more intense M-H_2O fragment ions (Corbett & Young, 1966a; Schmidt & Huneck, 1979).

The strong *m/z* 259 and *m/z* 197 fragment ions observed in the mass spectrum of **2-2** can be attributed to the cleavage across the C-9-C-10 bond, while the *m/z* 123 fragment ion can be envisaged as arising from the *m/z* 197 ion by loss of a CH_3COOCH_3 molecule (74 mass units) (see Scheme 2-2). The relative intensities of these, and some other fragment ions observed in the mass spectrum of **2-2** are listed in Table 2-1.

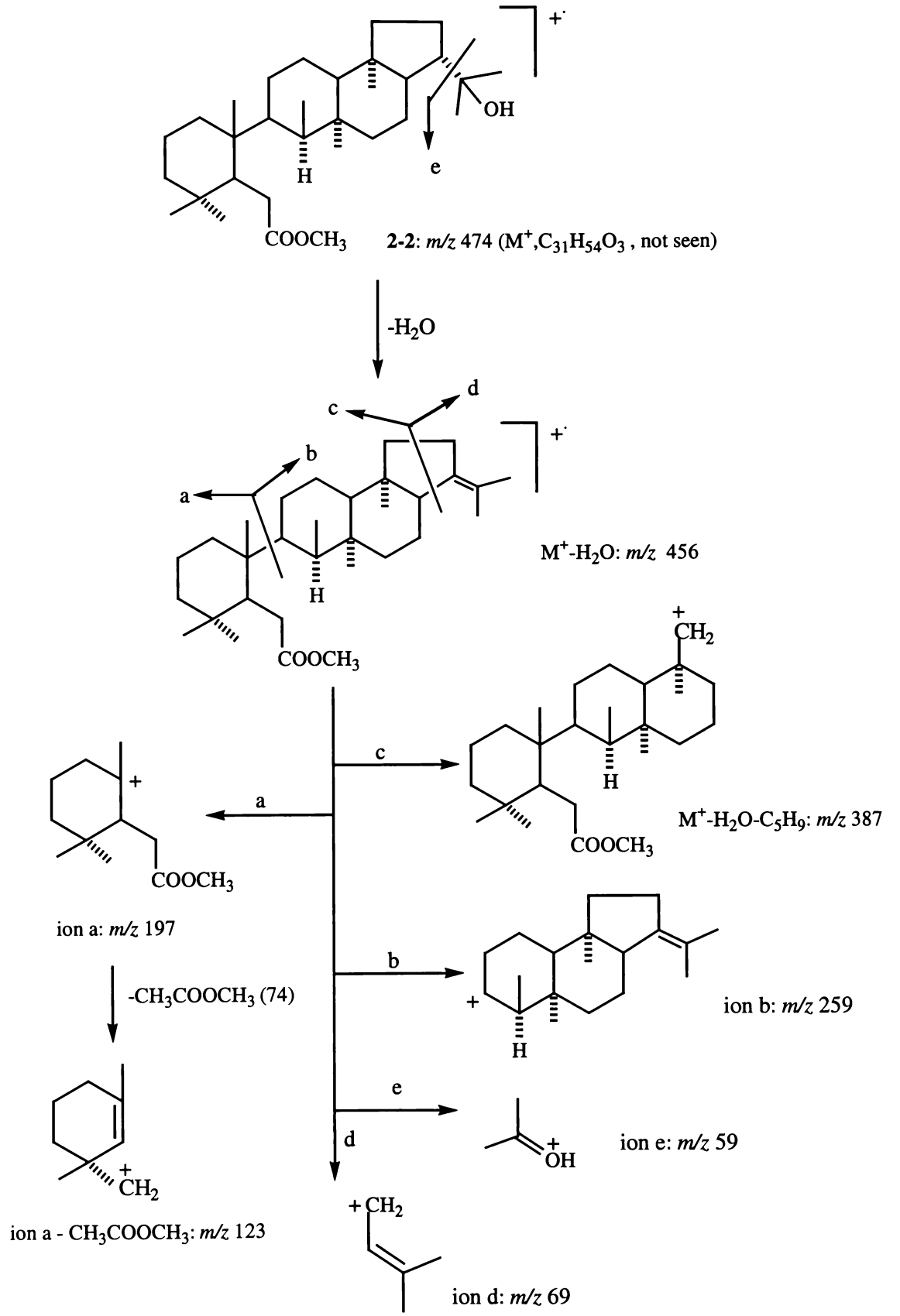

Scheme 2-2. Proposed mass spectral fragmentation pathways for methyl 22-hydroxy-7,8-secohopan-7-oate (**2-2**).

Table 2-1. Selected mass spectral fragment ions observed for methyl 22-hydroxy-7,8-secohopan-7-oate (**2-2**).

ions	*m/z* (% relative intensities)
M^+	474 (not seen)
M^+-H_2O	456 (37)
M^+-H_2O-CH_3	441 (11)
M^+-H_2O-C_3H_7	413 (39)
M^+-H_2O-C_5H_9 (ion c)	387 (8)
M^+-H_2O -C_3H_7 -C_3H_6	345 (21)
$C_{19}H_{31}^+$(ion b)	259 (32)
$C_{12}H_{21}O_2^+$ (ion a)	197 (100)
$C_9H_{15}^+$ (ion a-CH_3COOCH_3)	123 (84)
$C_9H_{13}^+$	121 (66)
$C_5H_9^+$ (ion d)	69 (45)
$C_3H_7O^+$ (ion e)	59 (34)

2.2.2.2 NMR Spectral Analyses of Methyl 22-hydroxy-7,8-secohopan-7-oate (2-2)

Complete assignments of the ^{13}C and ^1H NMR signals of methyl 22-hydroxy-7,8-secohopan-7-oate (**2-2**), and its LAH reduction product 7,8-secohopane-7,22-diol (**2-6**) (see Section **2.2.3**) are presented in Table 2-2. These assignments can be compared with those proposed by Hunter (1993) for 22-hydroxyhopan-7-one (**2-1**).

^1H NMR Spectrum of Methyl Secoester (2-2)

The ^1H NMR spectrum of **2-2** included signals attributable to seven tertiary methyl groups in the region 0.70~1.25 ppm, a secondary methyl group at 0.84 ppm (d, J = 6.9 Hz), and an ester methoxyl group signal at 3.70 ppm.

Methyl group assignments of **2-2** were established (see Table 2-2) by comparisons with assignments reported by Hunter (1993) for **2-1**, and those which he proposed for **2-2**. Correlations observed in the HMBC, HSQC, COSY and ROESY spectra determined in the present study for **2-2** verified these assignments.

Processing of the ^{1}H NMR spectrum of **2-2** with resolution enhancement revealed that the 14α-methyl (0.94 ppm) and 18α-methyl (0.72 ppm) proton signals could be resolved into finely coupled doublets (J = 0.77 and 0.72 Hz respectively). The COSY spectrum of **2-2** showed that these couplings originated from the adjacent coplanar methylene protons H-15β (1.54 ppm) and H-19β (0.97 ppm) respectively (Figure 2-2).

Table 2-2. ^{13}C and ^{1}H NMR signals (δ ppm in $CDCl_3$) observed for 22-hydroxyhopan-7-one (**2-1**), methyl 22-hydroxy-7,8-secohopan-7-oate (**2-2**) and 7,8-secohopane-7,22-diol (**2-6**).

atom	22-hydroxyhopan-7-one (2-1)			Methyl 22-hydroxy-7,8-seco-hopan-7-oate (2-2)			7,8-secohopane-7,22-diol (2-6)		
	^{13}C	$^1H_\alpha$	$^1H_\beta$	^{13}C	$^1H_\alpha$	$^1H_\beta$	^{13}C	$^1H_\alpha$	$^1H_\beta$
1	40.3 t	0.82 t	1.75 d	34.2 t	1.34 t	1.54 d	34.1 t	1.21 t	1.48 d
2	18.4 t	1.42 d	1.60 q	18.6 t	1.37 d	1.53 t	18.6 t	1.31 d	1.52 q
3	41.6 t	1.14 t	1.40 d	41.7 t	1.18 t	1.40 d	41.9 t	1.03 t	1.35 d
4	33.3 s			35.1 s			35.1 s		
5	53.9 d	1.11 d		46.5 d	2.01 t		46.6 d	0.94 s (br)	
6	37.8 t	2.10 d	2.48 t	32.6 t	2.24 t		31.6 t	1.51 q	
7	215.2 s			175.5 s			65.8 t	3.57 t (J = 8.0 Hz)	
8	58.3 s			44.1 d	1.40 d		44.2 d	1.42 d	
9	52.9 d	1.61 d		40.7 d	1.56 q		39.6 d	1.77 d	
10	37.5 s			40.0 s			40.0 s		
11	20.6 t	1.63 t	1.33 q	22.1 t	1.68 d	1.29 t	21.9 t	1.45 d	1.32 m
12	24.6 t	1.42 q	1.42 d	25.0 t	1.30 t	1.44 d	24.9 t	1.33 d	1.41 t
13	51.4 d		1.19 d	49.8 d		1.10 d	49.8 d		1.09 d
14	42.5 s			39.3 s			39.3 s		
15	35.7 t	2.57 d	1.33 t	39.2 t	1.12 d	1.54 t	39.1 t	1.11 d	1.55 q
16	22.2 t	1.61 q	1.89 d	22.2 t	1.66 t	1.94 d	22.1 t	1.65 q	1.92 d
17	54.0 d		1.44 t	54.7 d		1.49 t	54.7 d		1.46 t
18	44.5 s			44.1 s			44.1 s		
19	41.3 t	1.50 t	0.92 q	40.8 t	1.55 q	0.97 q	40.7 t	1.52 t	0.94 q
20	26.2 t	1.47 t	1.71 q	26.6 t	1.52 q	1.78 q	26.6 t	1.50 q	1.75 q
21	51.1 d		2.19 q	51.1 d		2.23 q	51.0 d		2.20 q
22	73.6 s			74.0 s			74.0 s		
23	32.5 q	0.80 s		34.0 q	0.85 s		34.6 q	0.85 s	
24	20.9 q	0.77 s		22.8 q	0.91 s		22.6 q	0.94 s	
25	15.6 q	0.96 s		17.8 q	0.87 s		17.4 q	0.87 s	
26	15.8 q	1.16 s		10.8 q	0.84 d (J = 6.9 Hz)		10.7 q	0.83 d (J = 6.9 Hz)	
27	19.8 q	1.01 s		25.2 q	0.94 s		25.3 q	1.02 s	
28	16.0 q	0.72 s		16.2 q	0.72 d (J = 0.77 Hz)		16.2 q	0.74 s	
29	29.0 q	1.14 s		28.9 q	1.18 s		28.8 q	1.17 s	
30	30.7 q	1.18 s		30.9 q	1.21 s		30.8 q	1.21 s	
31				51.6 q	3.70 s				

COSY Spectrum of Methyl Secoester (2-2)

The ^1H-^1H COSY spectrum of **2-2** included correlations (cross peaks) arising from long-range (^4J) couplings between axially oriented methyl groups (including those which could not be resolved in finely coupled doublets when the spectrum was processed with resolution enhancement) and 1,2-*trans* diaxially oriented methylene (and occasionally methine) protons. For example, the 10β-methyl group showed ^4J correlations to H-1α and H-5α respectively (see Figure 2-2 and Table 2-3).

The COSY spectrum of **2-2** (δ 0.5 to 2.5 ppm region) showed some of the ^4J correlations exhibited by the methyl group protons (see Table 2-3).

Table 2-3. Selected ^1H-^1H COSY correlations (δ ppm in $CDCl_3$) observed for methyl 22-hydroxy-7,8-secohopan-7-oate (**2-2**).

^1H NMR signals	correlated ^1H signals
2.24 t (H-6a/b)	2.01 t (H-5α)
2.23 q (H-21β)	1.52 q/1.78 q (H-20α/β), 1.49 t (H-17β)
2.01 t (H-5α)	2.24 t (H-6a/b)
1.94 d (H-16β)	1.66 t (H-16α), 1.49 t (H-17β), 1.12 d /1.54 t (H-15α/β)
1.78 q (H-20β)	2.23 q (H-21β), 1.52 q (H-20α), 0.97 q (H-19β)
1.68 d (H-11α)	1.56 q (H-9α), 1.30 t/1.44 d (H-12α/β), 1.29 t (H-11β)
1.54 t (H-15β)	1.94 d (H-16β), 1.12 d (H-15α)
1.52 q (H-20α)	1.78 q (H-20β), 0.97 q (H-19β)
1.49 t (H-17β)	2.23 q (H-21β), 1.94 d (H-16β)
1.34 t (H-1α)	1.54 d (H-1β), 0.87 s (H-10β-Me)*
1.29 t (H-11β)	1.68 d (H-11α), 1.44 d (H-12β), 1.10 d (H-13β)
1.18 t (H-3α)	1.40 d (H-3β), 1.37 d (H-2α), 0.91 s (4β-Me)*
1.12 d (H-15α)	1.66 t/1.94 d (H-16α/β), 1.54 t (H-15β)
1.10 d (H-13β)	1.30 t/1.44 d (H-12α/β), 1.29 t (H-11β)*
0.97 t (H-19β)	1.55 q (H-19α), 1.52 q/1.78 q (H-20α/β)
0.94 s (14α-Me)*	1.54 t (H-15β)*
0.91 s (4β-Me)*	1.18 t (H-3α)*, 0.85 s (4α-Me)*
0.87 s (10β-Me)*	1.34 t (H-1α)*, 2.01 t (H-5α)*
0.84 d (8β-Me)	1.40 d (H-8α)
0.72 s (18α-Me)*	0.97 q (H-19β)*

* ^4J coupling

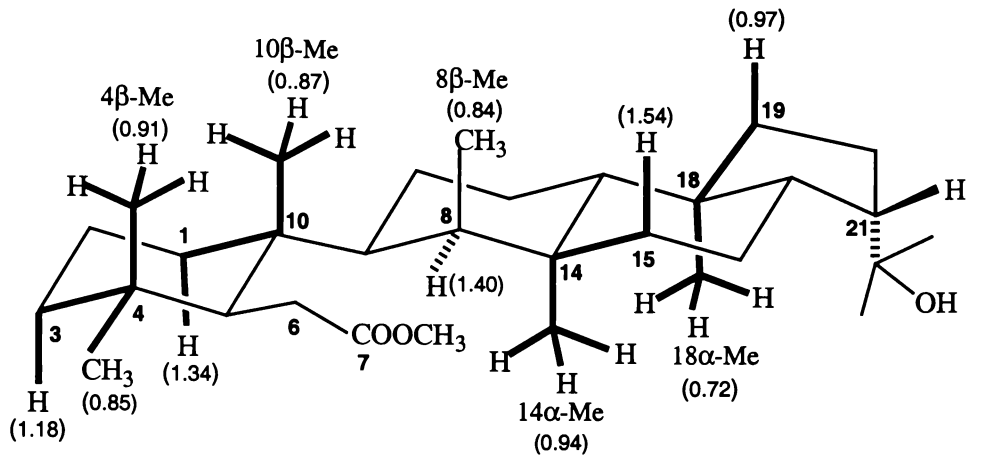

Figure 2-2. Selected ^4J COSY correlations (bold bonds) observed for some of the methyl groups of methyl 22-hydroxy-7,8-secohopan-7-oate (**2-2**).

^{13}C and DEPT135 NMR Spectra of Methyl Secoester (2-2)

The ^{13}C NMR spectrum of methyl 22-hydroxy-7,8-secohopan-7-oate (**2-2**) showed the presence of thirty-one carbon resonances, which were characterised by a DEPT135 NMR spectrum to arise from nine quartet (CH_3), ten triplet (CH_2), six doublet (CH) and six singlet (C) carbons. Two of the resonances were attributable to an ester carbonyl carbon (175.5 ppm) and a methoxyl carbon (51.6 ppm).

The resonances of the majority of the ring D and E carbon atoms of **2-2** corresponded closely to those determined for **2-1** (see Table 2-2), however there were significant differences in the resonances of some of the ring A, B and C carbons (see Table 2-2) in close proximity to C-7. For example, C-1 (34.2 ppm) and C-9 (40.7 ppm) exhibited the upfield shifts, while C-15 (39.2 ppm), C-25 (17.8 ppm) and C-27 (25.2 ppm) showed downfield shifts.

HSQC and HMBC Spectra of Methyl Secoester (2-2)

Methyl group assignments

The HSQC spectrum of **2-2** showed that the secondary 8β-methyl group signal (0.84 ppm) correlated to the carbon resonance which occurred at 10.8 ppm (C-26). In the HMBC spectrum (see Figure 2-3) the protons of this methyl group exhibited long-range correlations with C-8 (44.1 ppm, s), C-9 (40.7 ppm, d) and C-14 (39.3 ppm, s) (see

Table 2-4). The protons of each of the 4α- and 4β-methyl groups exhibited correlations to C-3 (41.7 ppm), C-4 (35.1 ppm), and C-5 (46.5 ppm), while each of the C-22 methyl groups exhibited correlations to C-21 (51.1 ppm) and C-22 (74.0 ppm). The HSQC and HMBC correlations exhibited by these and other methyl groups of **2-2** are presented in Table 2-4 (see Figure 2-3 and 2-4).

Table 2-4. ^{1}J, ^{2}J and ^{3}J heteronuclear ^{1}H-^{13}C correlations (δ ppm in $CDCl_3$) observed for methyl 22-hydroxy-7,8-secohopan-7-oate (**2-2**).

^{1}H signal	^{1}J correlated ^{13}C signal	^{2}J and ^{3}J correlated ^{13}C signals
0.85 s (4α-Me)	34.0 (C-23)	46.5 (C-5), 41.7 (C-3), 35.1 (C-4), 22.8 (C-24)
0.91 s (4β-Me)	22.8 (C-24)	46.5 (C-5), 41.7 (C-3), 35.1 (C-4), 34.0 (C-23)
0.87 s (10β-Me)	17.8 (C-25)	46.5 (C-5), 40.7 (C-9), 40.0 (C-10), 34.2 (C-1)
0.84 d (8β-Me)	10.8 (C-26)	44.1 (C-8), 40.7 (C-9), 39.3 (C-14)
0.94 s (14α-Me)	25.2 (C-27)	49.8 (C-13), 44.1 (C-8), 39.3 (C-14), 39.2 (C-15)
0.72 s (18α-Me)	16.2 (C-28)	54.7 (C-17), 49.8 (C-13), 44.1 (C-18), 40.8 (C-19)
1.18 s (22a-Me)	28.9 (C-29)	74.0 (C-22), 51.1 (C-21), 30.9 (C-30)
1.21 s (22b-Me)	30.9 (C-30)	74.0 (C-22), 51.1 (C-21), 28.9 (C-29)
3.70 s ($COOCH_3$)	51.6 ($COOCH_3$)	175.5 (C-7)
2.24 t (H-6a/b)	32.6 (C-6)	175.5 (C-7), 46.5 (C-5), 40.0 (C-10), 35.1 (C-4)
2.01 t (H-5α)	46.5 (C-5)	175.5 (C-7), 40.7 (C-9), 40.0 (C-10), 34.0 (C-23), 35.1 (C-4) 34.2 (C-1), 32.6 (C-6), 22.8 (C-24), 17.8 (C-25)
1.66 t/1.95 d (H-16α/β)	22.2 (C-16)	54.7 (C-17), 51.1 (C-21), 44.1 (C-18), 39.3 (C-14), 39.2 (C-15)
1.49 d (H-17β)	54.7 (C-17)	74.0 (C-22), 51.1 (C-21), 44.1 (C-18), 40.8 (C-19),39.2 (C-15) 26.6 (C-20), 22.2 (C-16)*, 16.2 (C-28)

* ^{4}J coupling

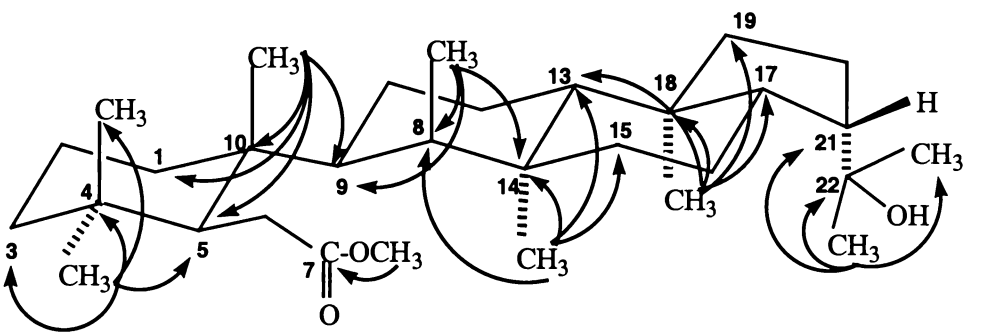

Figure 2-3. Selected HMBC correlations observed for the methyl groups of methyl 22-hydroxy-7,8-secohopan-7-oate (**2-2**).

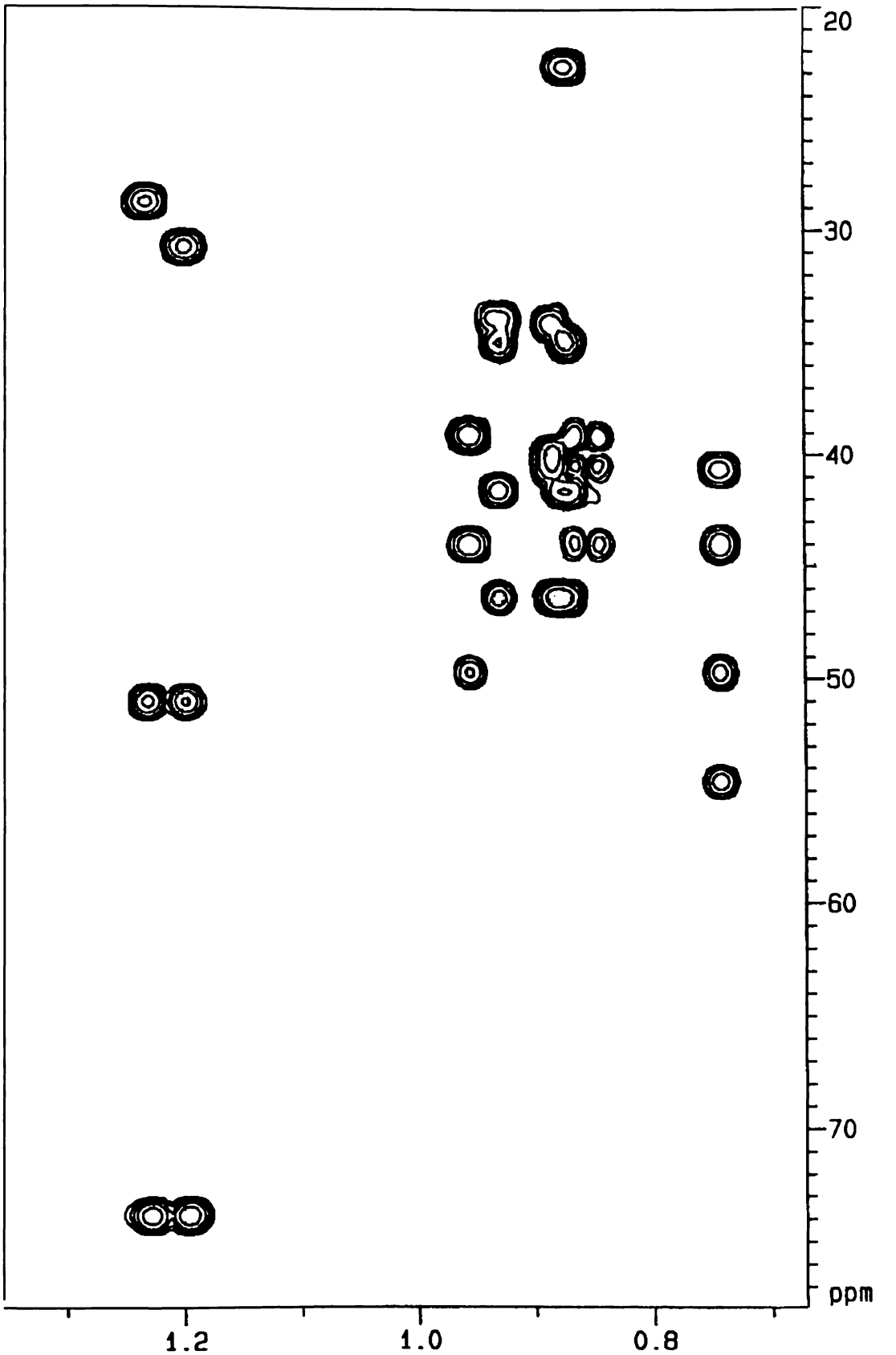

Figure 2-4. Selected HMBC correlations (the methyl group region) observed for methyl 22-hydroxy-7,8-secohopan-7-oate (**2-2**).

Methine signal assignments

The HSQC spectrum of **2-2** established that the methine carbon resonances which occurred at 46.5, 44.1, 40.7, 49.8, 54.7 and 51.1 ppm correlated with the proton resonances which occurred at 2.01, 1.40, 1.56, 1.10, 1.49 and 2.23 ppm, respectively.

The C-17 (54.7 ppm) and C-21 (51.1 ppm) resonances of **2-2** corresponded closely to those determined by Hunter (1993) for **2-1**, as did the H-17β (1.49 ppm) and H-21β (2.23 ppm) resonances, while the H-8 (1.40 ppm) resonance was recognised *via* the correlation which this signal exhibited in the COSY spectrum with that of secondary C-8 methyl group. The C-8 resonance (44.1 ppm) was in turn elucidated by the corresponding HSQC correlation.

C-5 (46.5 ppm) exhibited HMBC correlations with the 4α-, 4β- and 10β-methyl groups. C-9 (40.7 ppm) exhibited HMBC correlations with the 10β- and the secondary 8β-methyl groups, while C-13 (49.8 ppm) exhibited correlations to the 14α- and 18α-methyl groups (see Table 2-4). The resonances of H-5α, H-9α and H-13β were thus established to be 2.01, 1.56 and 1.10 ppm respectively, *via* the HSQC correlations which these methine signals exhibited with the corresponding carbon resonances (see Table 2-2 and Table 2-4).

The identification of these methine proton resonances was of paramount importance in defining the C-8 stereochemistry of **2-2** *via* correlations observed for the secondary C-8 methyl group in the ROESY spectrum of **2-2** (see below).

Methylene signal assignments

Many of the methylene carbon assignments (eg the C-1, C-3, C-15 and C-19 resonances), could be readily achieved from analyses of HMBC correlations exhibited by the methyl groups (see Table 2-4), while some assignments (eg C-2, C-11, C-12, C-16 and C-20), were elucidated by HMBC correlations arising from other downfield signals (eg methine protons) which occurred in region 1.50~ 4.0 ppm (see Table 2-4).

In the most cases, the orientation (α- or β-) of individual methylene protons could be identified by splitting patterns observed in the phase sensitive HSQC spectrum. The resolution of the HSQC spectrum was such that large $^2J_{geminal}$ and $^3J_{ax\text{-}ax}$ couplings of the order 10~16 Hz were resolved, whereas $^3J_{eq\text{-}eq}$ or $^3J_{ax\text{-}eq}$ couplings of the order 3~5 Hz were not resolved. This information, in combination with COSY and HMBC data, was used to assign the resonances of the majority of axial and equatorial methylene protons.

For example, the resonances of the two C-1 methylene protons (H-1α, 1.34 ppm, ~t, and H-1β, 1.54 ppm, ~d), were differentiated on the basis that H-1α (in an axial position) would be expected to exhibit a triplet-like correlation pattern, due to the large $^2J_{H\text{-}1\alpha\text{-}H\text{-}1\beta}$ and $^3J_{H\text{-}1\alpha\text{-}H\text{-}2\beta}$ couplings with H-1β and the axially oriented H-2β protons, respectively, while H-1β (in an equatorial position) would be like to exhibit a doublet correlation pattern arising from a large $^2J_{H\text{-}1\beta\text{-}H\text{-}1\alpha}$ coupling with H-1α, and unresolved couplings to H-2β and H-2α.

This approach was extensively used to assign the resonances of ring A, B, C and D methylene protons of **2-2**, its reduction product (**2-6**) (see Section **2.4**) and other photolysis reaction products (see Chapter Three) and the new triterpenes isolated during the present investigation (see Chapter Four and Chapter Five).

It is also well known that, in a cyclohexane system with a chair conformation, axial protons normally experience larger shieldings than is the case for equatorial protons, and that the chemical shift of axial protons is typically 0.2~0.5 ppm less than that of equatorial positions (Zhao, 1983).

ROESY Spectrum and Molecular Modelling Analysis of Methyl Secoester (2-2)

Originally, Hunter (1993) was not able to unequivocally define the stereochemistry at C-8 due to the inability, at the time, to selectively irradiate (excite) the secondary C-8 methyl group, or suitably oriented methine protons, due to their occurrence in a crowded region of the ^{1}H NMR spectrum. This difficulty can be overcome in NOESY, or ROESY spectra, where conventional NOE, or rotating framework ROE, responses

are detected in two-dimensional analogues of the COSY, or TOCSY experiments. NOESY, or ROESY experiments utilise of a series of suitable phased cycled, non-selective, hard pulses and a mixing time (with spin locking in ROESY experiments) during which NOE (or ROE) correlations are developed and subsequently detected. The availability of a higher field spectrometer (400 MHz) than that which was accessible to Hunter (1993) also facilitated the analyses of 2D-NOESY and ROESY spectra.

Close inspection of the ROESY spectrum of **2-2** revealed that the secondary 8β-methyl group exhibited correlations with the methine proton resonance occurred at 1.10 ppm, and one or more of the methylene proton resonances which occurred at 1.54 ppm.

HSQC and HMBC NMR spectral data identified this methine signal as that attributable to H-13β (see Tables 2-2 and 2-4), while a ^4J COSY correlation which the methylene signal at 1.54 ppm exhibited with the 14α-methyl group identified it as H-15β. The multiplicity of the HSQC correlation pattern observed for this signal (~t) (see Table 2-2) was consistent with the methylene proton being axially orientated. It therefore follows that the C-8 methyl group is axially (β-) oriented, and that photolysis of **2-1** has proceeded with retention of configuration at C-8.

Other ROESY Correlations Observed for Methyl Secoester (2-2)

Other structurally significant ROESY correlations observed for **2-2** are given in Table 2-5. Correlations were observed between the 4β- and 10β-methyl groups, and between the 14α- and 18α-methyl groups, and suitable oriented adjacent protons in close proximity to these methyl groups.

The analyses of ROESY and NOESY spectral data were facilitated by the results of a molecular modelling investigation, performed using MacroModel and Chem3D Plus software (see Chapter Six). The global minimium was recognised using MacroModel software. Atom positions and graphic representations were further refined using Chem3D software.

Molecular modelling investigation indicated that the preferred conformation of methyl 22-hydroxy-7,8-secohopan-7-oate (**2-2**) was likely to be that in which ring A was

rotated about the C-9–C-10 bond by *ca.* 90° (see model B in Figure 2-5), thereby relieving the steric compression between the 8β- and 10β-methyl groups. Model B exhibited a lower steric energy (E = 90.6 KCal) than that determined for 'unrotated' model A (E = 94.8 KCal).

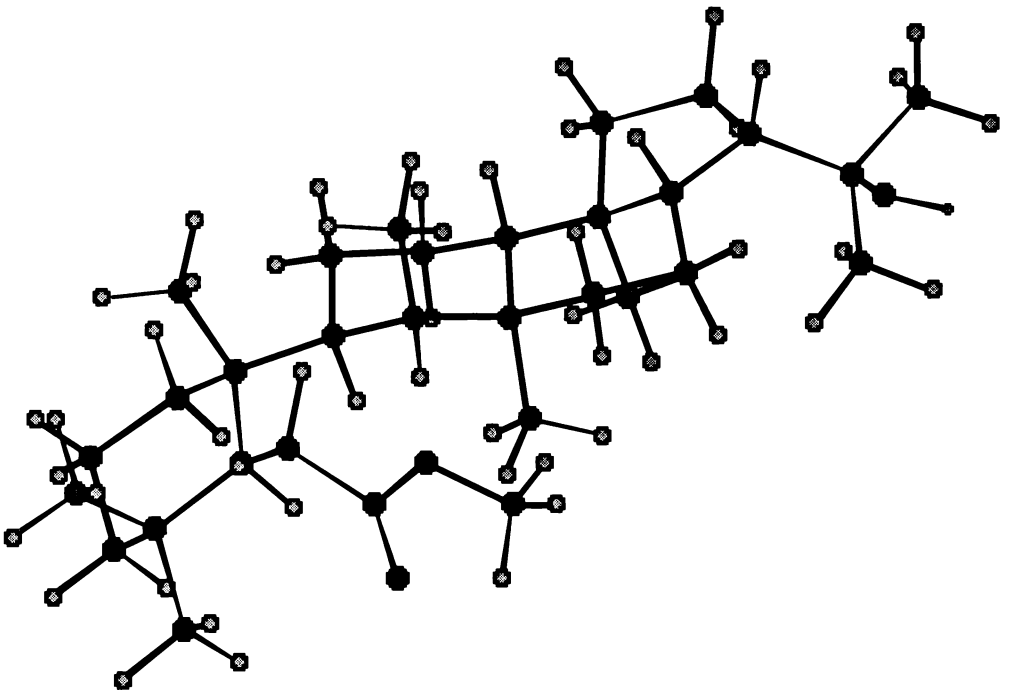

Model A: Refined without rotation about the C-9–C-10 bond.

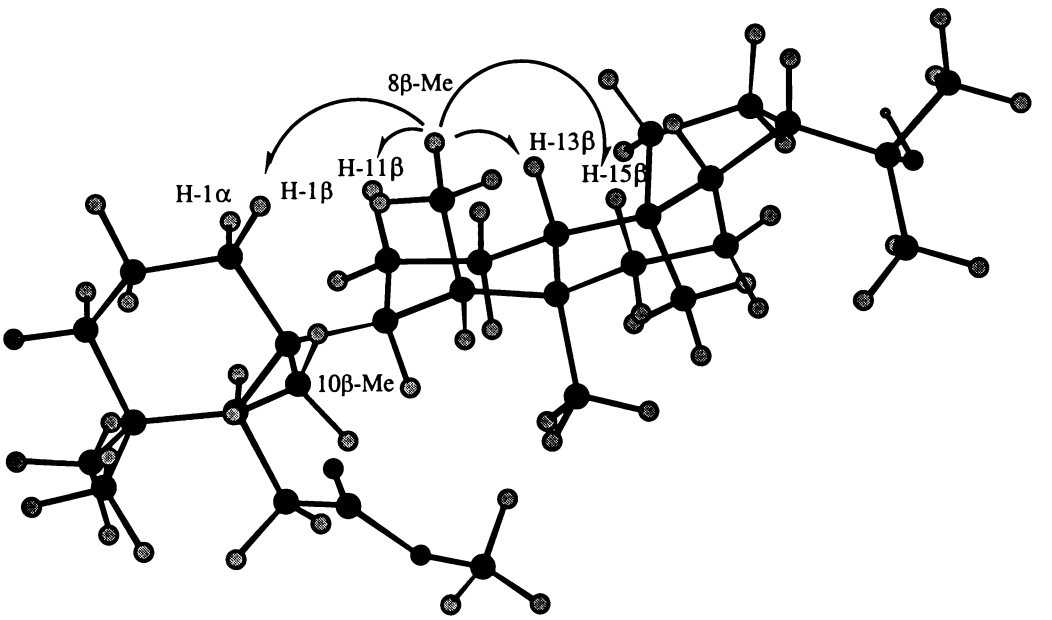

Model B: Refined after *ca.* 90° rotation about the C-9–C-10 bond.

Figure 2-5. MM2 modelled conformations determined for **2-2** without rotation (model A) and with rotation about the C-9-C-10 bond (model B).

The calculated inter-nuclear distance between 8β- and 10β-methyl groups (2.19 Å) in model B, suggested the existence of a ROESY (or NOESY) correlation between these methyl groups, however the close proximity of ^{1}H NMR signal resonances of 8β-methyl (0.84 ppm) and 10β-methyl (0.87 ppm) groups prevented the detection of this correlation.

The ROESY correlations which the 8β-methyl group exhibited with the methylene signals at 1.54 ppm (H-1β and H-15β) (see Figure 2-5) were consistent with the conclusion that model B best represented the preferred solution conformation of **2-2**, since in model A H-1β is too distance from the 8β-methyl group for a NOE or ROESY correlation to be observed.

The ROESY correlation which H-5α (2.01 ppm) exhibited with H-11α (1.68 ppm) (see Table 2-5) was also consistent with the rotation about the C-9-C-10 bond in model B (Figure 2-5), whereas in model A (Figure 2-5), and in **2-1**, H-11α is too distant from H-5α for this ROSEY correlation to be observed.

Table 2-5. Selected ^{1}H-^{1}H ROESY correlations (δ ppm in $CDCl_3$) observed for methyl 22-hydroxy-7,8-secohopan-7-oate (**2-2**).

^{1}H NMR signals	correlated ^{1}H signals
2.24 t (H-6a/b)	1.68 d (H-11α), 1.56 q (H-9α), 0.91 s (4β-Me), 0.87 s (10β-Me)
2.23 q (H-21β)	1.52 q (H-20α), 1.18 s/1.21 s (22a/b-Me)
2.01 t (H-5α)	1.68 d (H-11α), 1.56 q (H-9α), 1.18 t (H-3α), 0.85 s (4α-Me)
1.94 d (H-16β)	1.49 t (H-17β), 1.18 s/1.21 s (22a/b-Me), 1.12 d (H-15α)
1.18 s /1.21 s (22a/b-Me)	2.23 q (H-21β), 1.66 t /1.94 d (H-16α/β), 1.52 q (H-20α) 0.97 q (H-19β), 0.72 d (18β-Me)
0.94 s (14α-Me)	1.66 t (H-16α), 1.55 q (H-19α), 1.40 d (H-8α), 0.72 d (18β-Me)
0.91 s (4β-Me)	0.87 s (10β-Me), 0.85 s (4α-Me) 2.24 t (H-6a/b), 1.53 t (H-2β), 1.29 t (H-11β)
0.87 s (10β-Me)	2.24 t (H-6a/b), ~1.54 {H-1β, H-2β}, 0.91 s (4β-Me)
0.85 s (4α-Me)	2.01 t (H-5α), 1.37 d (H-2α), 1.18 t (H-3α), 0.91 s (4β-Me)
0.84 d (8β-Me)	~1.54 {H-15β, H-1β}, 1.29 t (H-11β), 1.10 d (H-13β)
0.72 d (18α-Me)	1.66 t (H-16α), 1.52 q (H-20α), 1.30 t (H-12α) 1.18 s /1.21 s (22a/b-Me), 0.94 s (14β-Me)

2.2.3 Preparation of 7,8-Secohopane-7,22-diol (2-6)

Reduction of methyl 22-hydroxy-7,8-secohopan-7-oate (**2-2**) with LAH in refluxing dioxane afforded 7,8-secohopane-7,22-diol (**2-6**). The mass spectral and NMR spectral features of this compound corresponded closely with those determined for **2-2**.

2.2.3.1 Mass Spectral Analysis of 7,8-Secohopane-7,22-diol (2-6)

Structurally significant fragment ions observed in the mass spectrum of **2-6** are listed in Table 2-6. The highest observed ion (*m/z* 428) corresponded to the loss of water from the expected molecular ion of *m/z* 446 ($C_{30}H_{54}O_2$). Replacement of the 7-$COOCH_3$ group of **2-2** by a 7-CH_2OH group afforded a *m/z* 169 fragment (ion a), analogous to the *m/z* 197 ion observed for **2-2**. Loss of ethanol from this ion would afford a *m/z* 123 fragment ion, while rupture cleavage across the C-9–C-10 bond can be envisaged as leading to a *m/z* 259 ion, as is also the case for **2-2**.

Table 2-6. Selected mass spectral fragment ions observed for 7,8-secohopane-7,22-diol (**2-6**).

ions	*m/z* (% relative intensities)
M^+	446 (not seen)
M^+-H_2O	428 (4)
M^+-H_2O-CH_3	413 (10)
M^+-H_2O-C_3H_7	385 (6)
M^+-H_2O- C_5H_9	359 (9)
M^+-H_2O- C_5H_9- C_3H_6 (42)	317 (5)
$C_{19}H_{31}^+$ (ion b)	259 (25)
ion b-C_3H_6 (42)	217 (20)
$C_{11}H_{21}O^+$ (ion a)	169 (21)
ion a - H_2O	151 35)
$C_9H_{15}^+$ (ion a - CH_3CH_2OH)	123 (23)
$C_9H_{13}^+$	121 (38.5)
$C_5H_9^+$ (ion d)	69 (100)
$C_3H_7O^+$ (ion e)	59 (11)

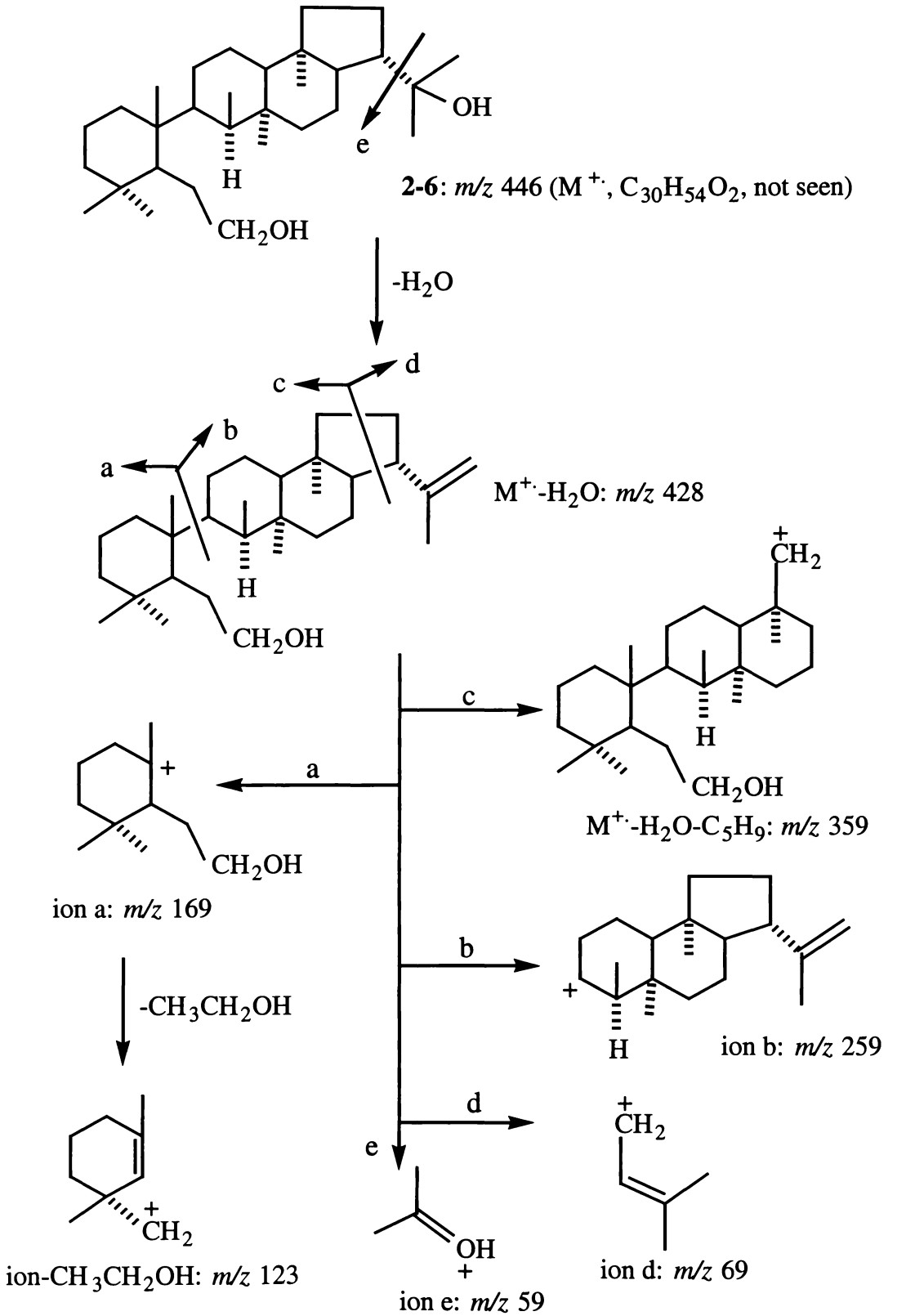

Scheme 2-3. Proposed mass spectral fragmentation pathways for 7,8-secohopane-7,22-diol (**2-6**).

2.2.3.2 NMR Spectral Analyses of 7,8-Secohopane-7,22-diol (2-6)

A complete assignment of the ^{13}C and ^{1}H NMR signals of **2-6**, which was elucidated in a manner similar to that described above for **2-2**, is presented in Table 2-2.

^{1}H NMR Spectrum of 7,8-Secohopane-7,22-diol (2-6)

The ^{1}H NMR spectrum of **2-6** included signals attributable to seven tertiary methyl groups in the region 0.70 ~1.25 ppm, a secondary methyl group signal at 0.83 ppm (d, J = 6.9 Hz), and a two proton signal at 3.57 ppm (t, J = 8.0 Hz) assignable to the 7-CH_2OH group.

The majority of the methyl group resonances corresponded closely to those observed for **2-2**. These assignments, and those of the protons to which these signals exhibited long range couplings in the COSY spectrum, are shown in Figure 2-6.

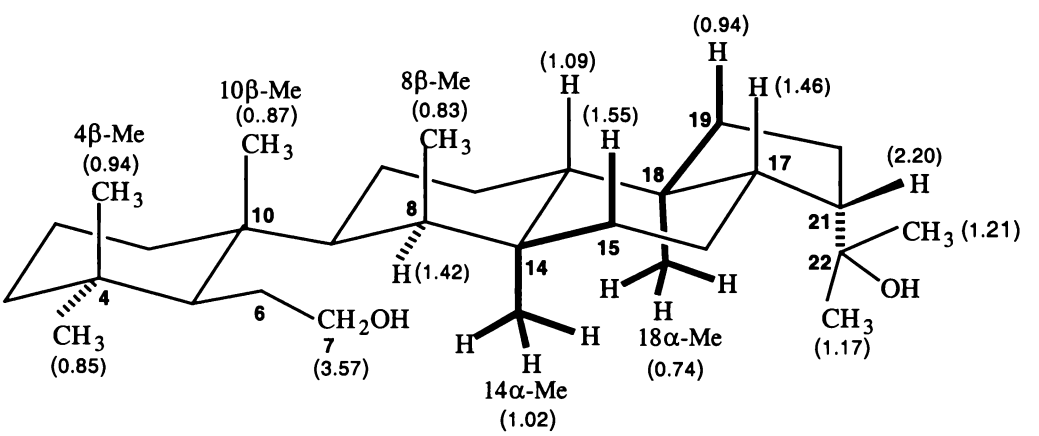

Figure 2-6. Selected ^{1}H NMR signals and ^{4}J correlations (bold bonds) observed for 7,8-secohopane-7,22-diol (**2-6**).

COSY Spectrum of 7,8-Secohopane-7,22-diol (2-6)

The COSY spectrum of **2-6** included correlations between H-7a/b (3.57 ppm) and the adjacent H-6a/b (1.51 ppm) protons, H-21β (2.20 ppm) and H-17β (1.46 ppm), H-20α (1.75 ppm) and H-20β (1.50 ppm), and H-8α (1.42 ppm) and the secondary 8β-methyl group (0.83 ppm, J = 6.9 Hz). Other structurally significant COSY correlations observed for **2-6**, including ^{4}J correlations exhibited by some of the methyl groups (see Figure 2-6), are presented in Table 2-7.

Table 2-7. Selected ^{1}H-^{1}H COSY correlations (δ ppm in $CDCl_3$) observed for 7,8-secohopane-7,22-diol (**2-6**).

^{1}H NMR signals	correlated ^{1}H signals
3.57 t (H-7a/b)	1.51 q (H-6a/b)
2.20 q (H-21β)	1.50 q /1.75 q (H-20α/β), 1.46 t (H-17β)
1.92 d (H-16β)	1.65 q (H-16α), 1.46 t (H-17β), 1.11 d/1.55 q (H-15α/β)
1.75 q (H-20β)	2.21 q (H-21β), 1.52 t/ 0.94 q (H-19α/β), 1.50 q (H-20α)
1.65 q (H-16α)	1.92 d (H-16β), 1.11 d (H-15α)
1.52 t (H-19α)	1.50 q/1.75 q (H-20α/β), 0.94 q (H-19β)
1.46 t (H-17β)	2.20 q (H-21β), 1.92 d (H-16β), 1.75 q (H-20β)
1.11 d (H-15α)	1.65 q/1.92 d (H-16α/β), 1.55 q (H-15β)
1.09 d (H-13β)	1.33 d/1.41 t (H-12α/β)
1.03 t (H-3α)	1.35 d (H-3β)
1.02 s (14α-Me)	1.55 q (H-15β)*
0.83 d (8β-Me)	1.42 d (H-8α)
0.74 s (18α-Me)	0.94 t (H-19β)*

*^{4}J coupling

^{13}C and DEPT135 NMR Spectra of 7,8-Secohopane-7,22-diol (2-6)

The ^{13}C NMR spectra of **2-6** showed the presence of thirty carbon signals, which were characterised by a DEPT135 NMR spectrum to arise from eight quartet (CH_3), ten triplet (CH_2), six doublet (CH) and six singlet (C) carbons, rather than the 31 carbon signals observed for **2-2**.

Only the C-6 (31.6 ppm) and C-7 (65.8 ppm) resonances of **2-6** differed significantly from those determined for **2-2** (see Table 2-2). The C-7 chemical shift was consistent with the presence in **2-6** of a primary hydroxyl group (Breitmaier & Voelter, 1987).

HSQC and HMBC Spectra of 7,8-Secohopane-7,22-diol (2-6)

HSQC and HMBC correlations observed for the methyl groups, and some other protons of **2-6** are presented in Table 2-8. These assignments, and those established for the methylene protons of **2-6,** corresponded closely to those determined for **2-2**.

Amongst the methine protons, however the resonance of H-5α (0.94 ppm) differed appreciably from that observed for **2-2** (2.01 ppm). This difference can be attributed to the absence in **2-6** of the deshielding influence of the C-7 ester carbonyl group of **2-2**.

Table 2-8. ^{1}J, ^{2}J and ^{3}J heteronuclear ^{1}H-^{13}C correlations (δ ppm in $CDCl_3$) observed for 7,8-secohopane-7,22-diol (**2-6**).

^{1}H signal	^{1}J correlated ^{13}C signal	^{2}J and ^{3}J correlated ^{13}C signals
0.85 s (4α-Me)	34.6 (C-23)	46.6 (C-5), 41.9 (C-3), 35.1 (C-4), 22.6 (C-24)
0.94 s (4β-Me)	22.6 (C-24)	46.6 (C-5), 41.9 (C-3), 35.1 (C-4), 34.6 (C-23)
0.87 s (10β-Me)	17.4 (C-25)	46.6 (C-5), 39.6 (C-9), 40.0 (C-10), 34.1 (C-1)
0.83 d (8β-Me)	10.7 (C-26)	44.2 (C-8), 39.6 (C-9), 39.3 (C-14)
1.02 s (14α-Me)	25.3 (C-27)	49.8 (C-13), 44.2 (C-8), 39.3 (C-14), 39.1 (C-15)
0.74 s (18α-Me)	16.2 (C-28)	54.7 (C-17), 49.8 (C-13), 44.1 (C-18), 40.7 (C-19)
1.17 s (22a-Me)	28.8 (C-29)	74.0 (C-22), 51.0 (C-21), 30.8 (C-30)
1.21 s (22b-Me)	30.8 (C-30)	74.0 (C-22), 51.0 (C-21), 28.8 (C-29)
3.57 t (H-7a/b)	65.8 (C-7)	46.6 (C-5), 31.6 (C-6)
2.20 q (H-21β)	51.0 (C-21)	74.0 (C-22), 54.7 (C-17), 44.1 (C-18), 30.8 (C-30) 28.8 (C-29), 26.6 (C-20)
1.92 d (H-16β)	22.1 (C-16)	54.7 (C-17), 44.1 (C-18), 39.3 (C-14), 39.1 (C-15)
1.50 q/1.75 q (H-20α/β)	26.6 (C-20)	74.0 (C-22)*, 51.0 (C-21), 54.7 (C-17) 44.1 (C-18), 40.7 (C-19)
1.51 q (H-6a/b)	31.6 (C-6)	65.8 (C-7), 46.6 (C-5), 40.0 (C-10), 35.1 (C-4)

* ^{4}J coupling

NOESY Spectrum of 7,8-Secohopane-7,22-diol (2-6)

The NOESY spectrum of **2-6** included correlations (see Table 2-9) which validated the methyl group assignments presented in Tables 2-2 and 2-8.

The secondary 8β-methyl group signal (0.83, d, J = 6.9 Hz) exhibited correlations to H-8α (1.42 ppm), H-13β (1.09 ppm), H-11β (1.32 ppm) and H-15β (1.55 ppm), but 10β-methyl group. This observation was consistent with the 8-methyl group being β-oriented.

NOSEY correlations exhibited by the 10β-methyl group signal (0.87 ppm) to H-9α (1.77 ppm, d) and H-8α (1.42 ppm, d) were also in agreement with the conclusion that cleavage of the C-7-C-8 bond led to **2-6** adopting preferred solution analogous to that proposed for **2-2** (see model B in Figure 2-5).

Table 2-9. Selected ^{1}H-^{1}H NOESY correlations (δ ppm in $CDCl_3$) observed for 7,8-secohopane-7,22-diol (**2-6**).

^{1}H NMR signals	correlated ^{1}H signals
3.57 t (H-7a/b)	1.77 d (H-9α), 1.51 q (H-6a/b), 1.42 d (H-8α), 1.33 d (H-12α), 1.02 s (14α-Me) 0.94 br s (H-5α), 0.85 s/0.94 s (4α/β-Me)
2.20 q (H-21β)	1.75 q (H-20β), 1.46 t (H-17β), 1.17 s/ 1.21 s (22a/b-Me)
1.92 d (H-16β)	1.65 q (H-16α), 1.46 t (H-17β), 1.11 d/ 1.55 q (H-15α/β) 1.17 s/ 1.21 s (22a/b-Me)
1.17 s (22a-Me)	0.74 s (18α-Me), 2.20 q (H-21β), 1.92 d (H-16β), 1.50 q (H-20α)
1.21 s (22b-Me)	0.74 s (18α-Me), 2.20 q (H-21β), 1.65 q/1.92 d (H-16α/β), 1.50 q (H-20α)
1.02 s (14α-Me)	0.74 s (18α-Me), 3.57 t (H-7a/b), 1.77 d (H-9α), 1.65 q (H-16α) 1.42 d (H-8α), 1.33 d (H-12α)
0.94 s (4β-Me)	0.87 s (10β-Me), 0.85 s (4α-Me), 3.57 t (H-7a/b), 1.77 d (H-9α) 1.51 q (H-6a/b), 1.35 d (H-3β)
0.87 s (10β-Me)	0.94 s (4β-Me), 1.77 d (H-9α), 1.50 t (H-2β),1.42 d (H-8α)
0.85 s (4α-Me)	0.94 s (4β-Me), 3.57 t (H-7a/b), 1.51 q (H-6a/b), 1.31 d (H-2α),1.04 t (H-3α)
0.83 d (8β-Me)	1.55 q (H-15β), 1.51 q (H-6a/b), 1.42 d (H-8α), 1.31 t (H-11β), 1.09 d (H-13β)
0.74 s (18α-Me)	1.02 s (14α-Me), 1.17 s/ 1.21 s (22a/b-Me) 1.65 q (H-16α), 1.50 q (H-20α), 1.42 d (H-8α), 1.33 d/1.41 t (H-12α/β)

2.3 Photolysis of 22-Hydroxyhopan-7-one in Benzene

In the course of investigations of the photochemical reactions of 22-hydroxyhopan-15-one (**3-1**) in benzene, benzene-methanol, or benzene-isopropanol as described in Chapter Three, it emerged that the dominant products were derived *via* the intramolecular cyclisation of an initial secoaldehyde with the 22-hydroxyl group, to afford products such as the 14,15-seco-15,22-*O*-*abeo*hopanes (**3-3**), (**3-5**) and (**3-6**) (see Section **3.3**).

It was therefore of interest to determine, if in the absence of methanol (ie in benzene alone), photolysis of 22-hydroxyhopan-7-one (**2-1**) proceeded *via* an intermediate ketene, followed by intermolecular reaction with the 22-hydroxyl group of a second hydroxyketene molecule, to give a dimeric product of the type depicted in Figure 2-7, or if other products corresponding (for example) to the secoaldehyde obtained on photolysis of freidelone in benzene (Stevenson *et al.*, 1971), were formed.

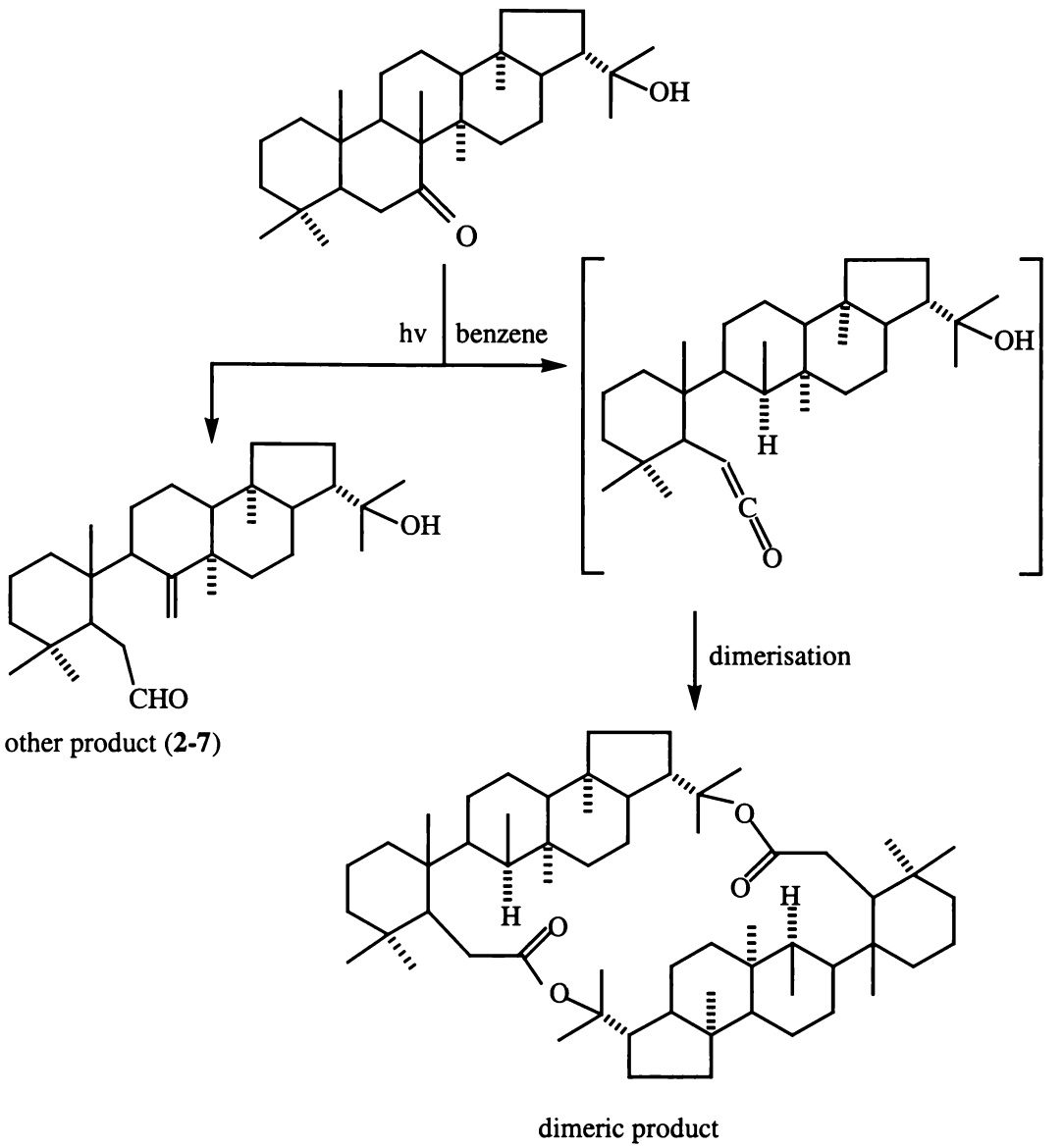

Figure 2-7. Possible photoreaction products of **2-1** in the absence of alcohol.

Photolysis of a specimen of **2-1** in benzene for 9 h, and again for 16 h afforded product material which was shown by GC/MS analyses to be comprised mainly of starting material (**2-1**), two minor products (products 1 and 2), and a number of other components believed to be dehydrated analogues of the starting material (**2-1**) (see Figure 2-8).

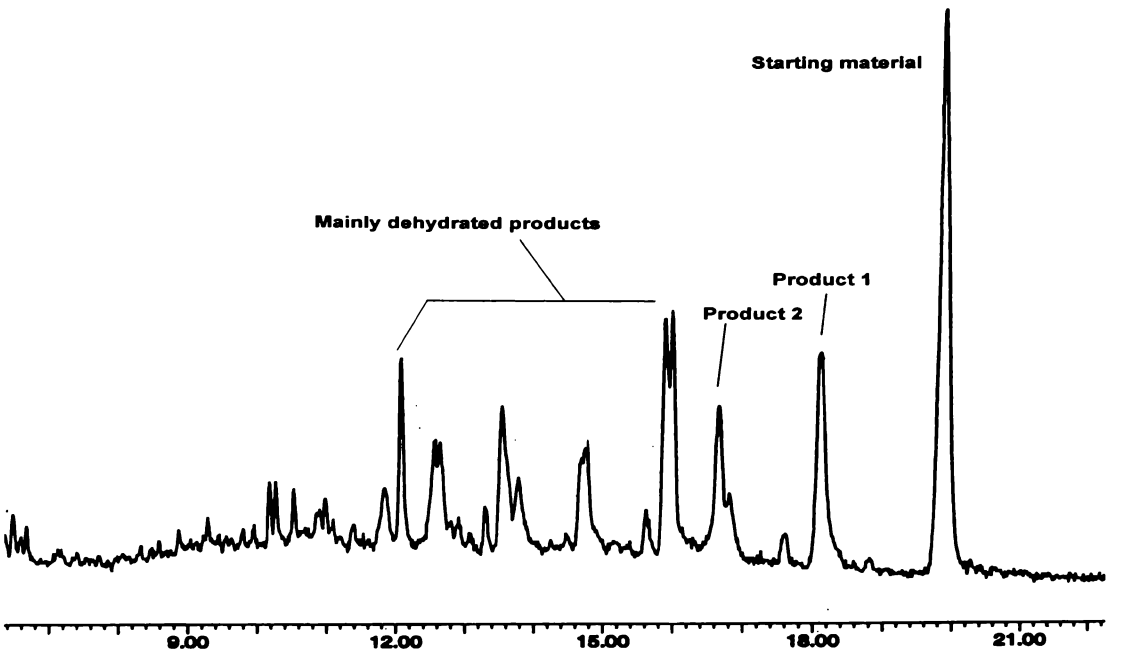

Figure 2-8. GC/MS profile of the reaction mixture obtained on photolysis of **2-1**.

2.3.1 GC/MS Investigation of the Reaction Mixture

The mass spectrum of the starting material (**2-1**) and products 1 and 2 each included a strong *m/z* 59 ion attributable to a $CH(CH_3)_2OH^+$ ion, as would be expected for a 22-hydroxyl group. The presence in the mass spectrum of product 2 of a moderate *m/z* 257 ion suggested it was a 7,8-secohopanoid, possibly the 7,8-secoaldehyde (**2-7**), which might be expected to fragment as proposed in Scheme 2-4. On the other hand the mass spectrum of product 1 included strong *m/z* 220 and 233 ions, reminiscent of those which appeared in the starting material (**2-1**), possibly suggesting it to be an isomerised analogue (eg at C-21 or C-8) of the starting material (**2-1**).

Several attempts were made to isolate the believed secoaldehyde (**2-7**) from the product mixture, however on each occasion mainly un-reacted starting material (**2-1**) was recovered, possibly because of decomposition and/or rearrangement of the secoaldehyde (**2-7**) during attempted isolation.

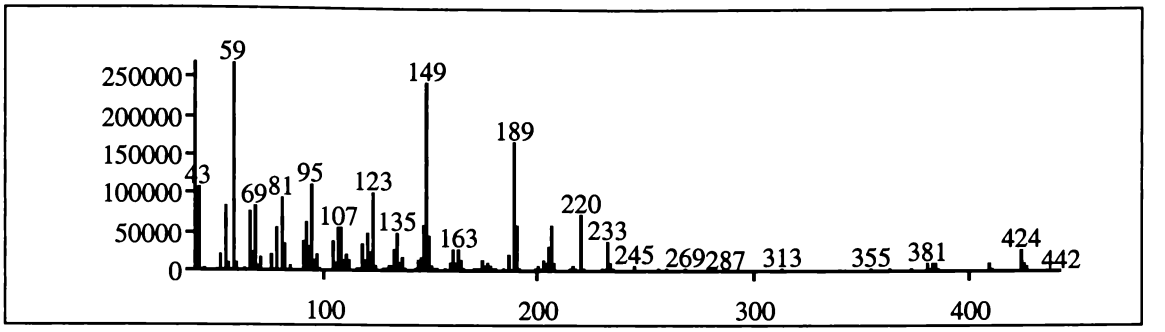

Figure 2-9. Mass spectrum of 22-hydroxyhopan-7-one (**2-1**) (starting material).

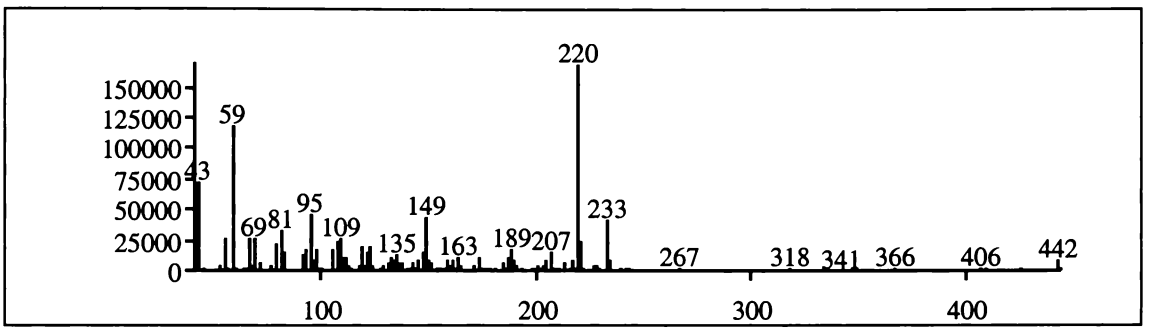

Figure 2-10. Mass spectrum of product 1.

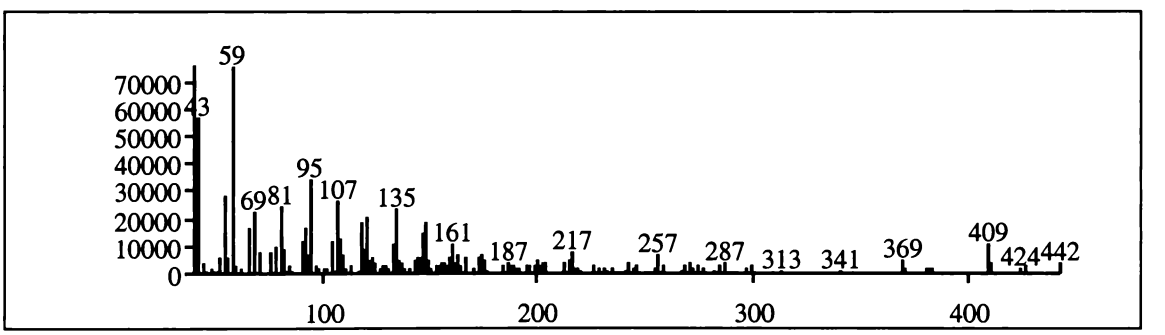

Figure 2-11. Mass spectrum of product 2 (possibly 7,8-secoaldehyde (**2-7**)).

Because of the low yield of photolysed products, and the difficulties experienced when attempting to separate the product mixture, efforts to isolate the secoaldehyde (**2-7**) were abandoned.

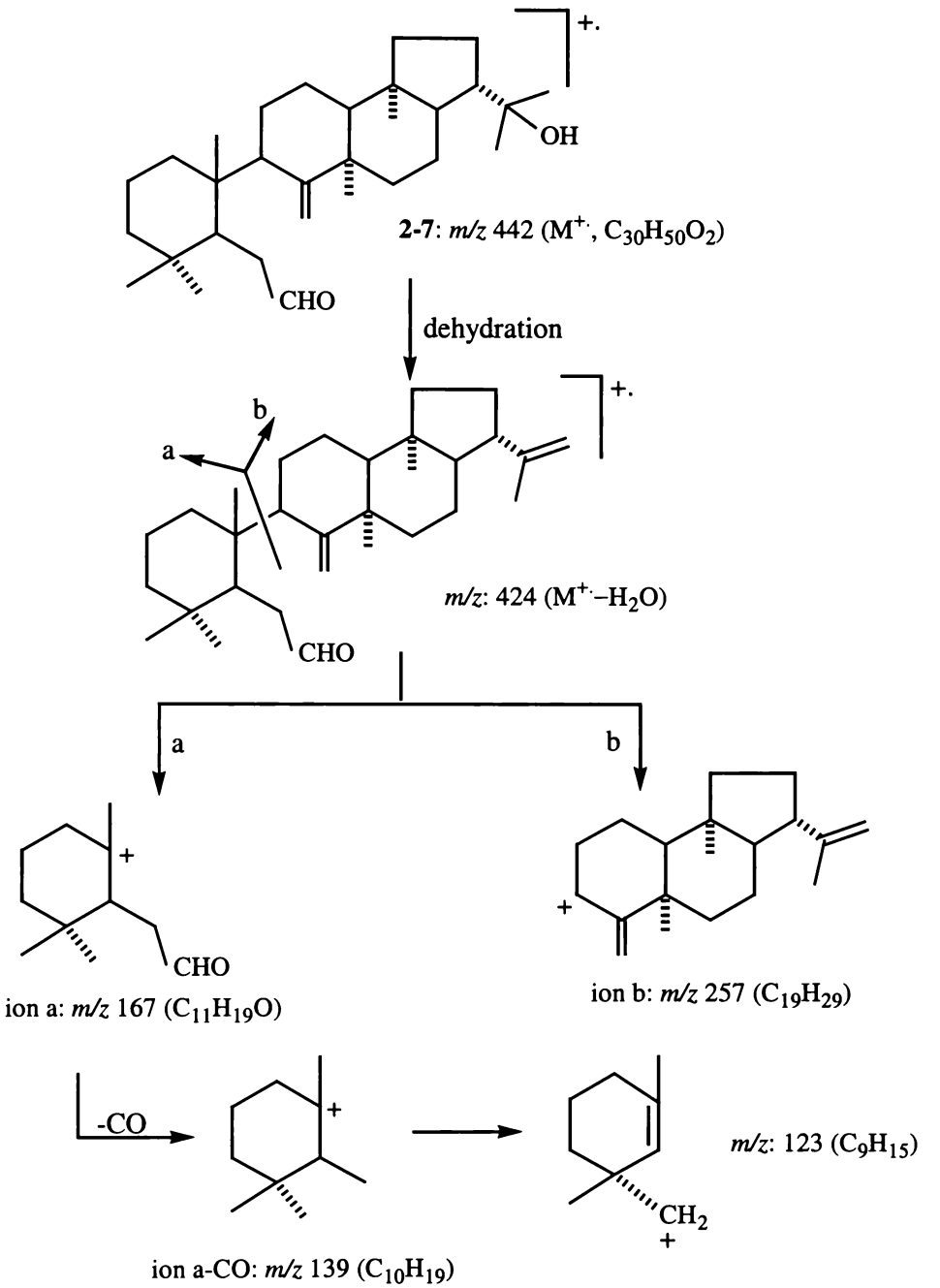

Scheme 2-4. Proposed mass spectral fragmentation pathways for 22-hydroxy-7,8-secohop-8(26)-en-7-al (**2-7**).

2.4 Photolysis of 22-Hydroxyhopan-7-one in Benzene-Isopropanol

2.4.1 Photolysis of 22-Hydroxyhopan-7-one (2-1)

Photolysis of 22-hydroxyhopan-7-one (**2-1**) in dry benzene-isopropanol for 8 h afforded product material which, when purified on radial PLC using light petroleum and diethyl ether as eluent, afforded isopropyl 22-hydroxy-7,8-secohopan-7-oate (**2-8**).

2.4.2 Structural Elucidation of Isopropyl 22-hydroxy-7,8-secohopan-7-oate (2-8)

2.4.2.1 Mass Spectral Analysis of Isopropyl 22-hydroxy-7,8-secohopan-7-oate (2-8)

The highest observed ion in the mass spectrum of isopropyl 22-hydroxy-7,8-secohopan-7-oate (**2-8**) occurred at *m/z* 484. This ion can be attributed to the loss of a water molecule from the expected molecular ion of *m/z* 502 ($C_{33}H_{58}O_3$).

The occurrence of a strong *m/z* 225 fragment in the mass spectrum of isopropyl 22-hydroxy-7,8-secohopan-7-oate (**2-8**), compared to a *m/z* 197 ion (ion "a") in the mass spectrum of methyl 22-hydroxy-7,8-secohopan-7-oate (**2-2**), is consistent with the replacement of the $COOCH_3$ group by a $COOCH(CH_3)_2$ group (see Scheme 2-5).

Loss of a propene molecule (C_3H_6, 42 mass units) from the *m/z* 225 fragment ion (ion "a") would afford a *m/z* 183 fragment ion, which may subsequently eliminate a molecule of methyl formate (60 mass units) to afford a *m/z* 123 fragment ion. Analogous *m/z* 123 fragment ions appeared in the mass spectra of methyl 22-hydroxy-7,8-sechopan-7-oate (**2-2**), and its LAH reduction product (**2-6**) (see Schemes 2-2 and 2-3). A strong *m/z* 259 ion corresponding to the "b" cleavage fragment (Scheme 2-5) was also observed in the mass spectra of **2-2** and **2-6**. Some other structurally significant ions, and their relative intensities are listed in Table 2-10.

Table 2-10. Selected mass spectral fragment ions observed for isopropyl 22-hydroxy-7,8-secohopan-7-oate (**2-8**).

ions	*m/z* (% relative intensities)
M^+	502 (not seen)
M^+- H_2O	484 (22)
M^+- H_2O-C_3H_7	441 (17)
M^+- C_5H_9 (ion c)	415 (4)
ion c - C_3H_6	373 (17)
$C_{19}H_{31}^+$ (ion b)	259 (22)
$C_{13}H_{21}O_2^+$ (ion a)	225 (26)
ion a-C_3H_6	183 (100)
ion a -C_3H_6-CH_3COOH	123 (65)
$C_5H_9^+$ (ion d)	69 (48)
$C_3H_7O^+$	59 (30)

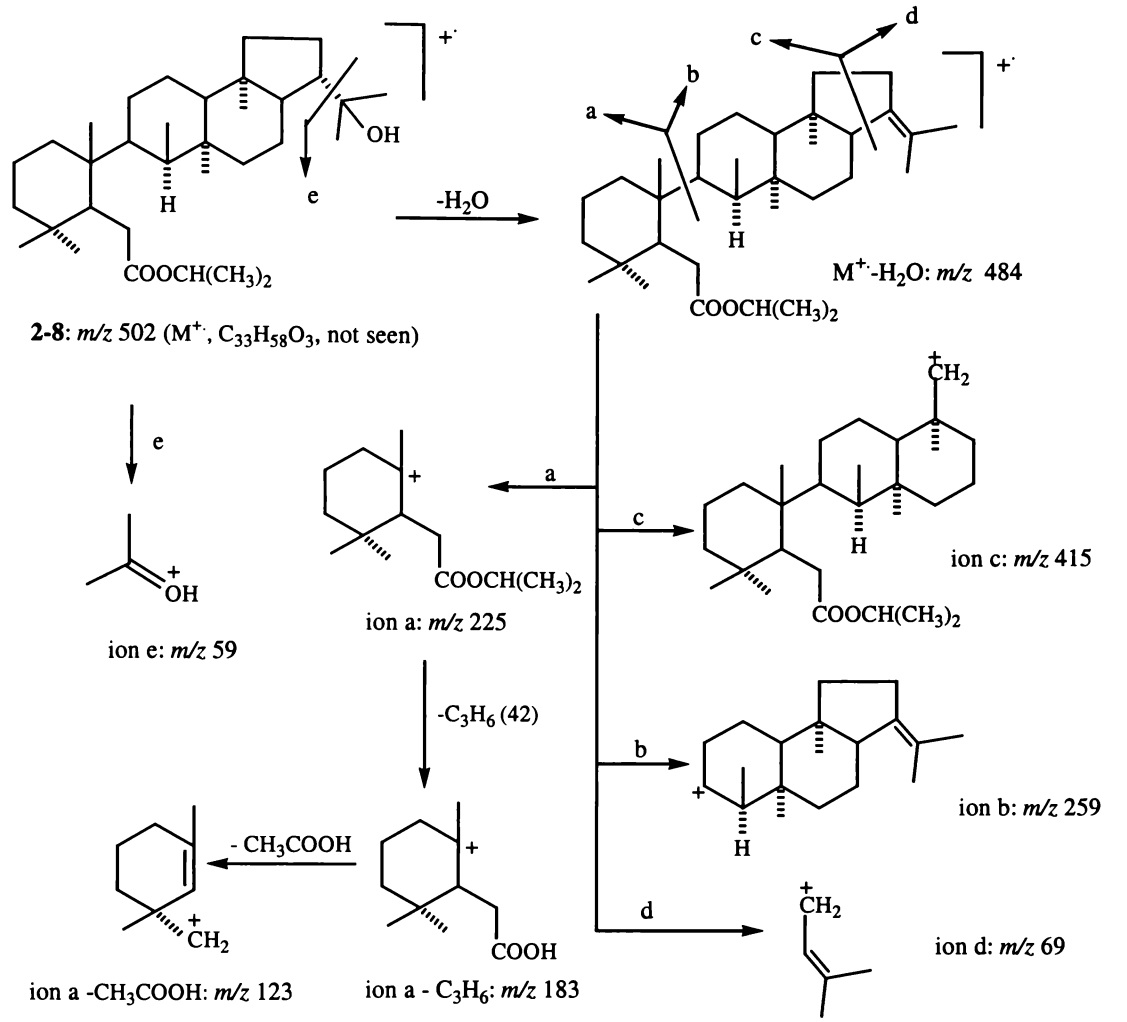

Scheme 2-5. Proposed mass spectral fragmentation pathways for isopropyl 22-hydroxy-7,8-secohopan-7-oate (**2-8**).

2.4.2.2 NMR Spectral Analyses of Isopropyl 22-hydroxy-7,8-secohopan-7-oate (2-8)

A complete assignment of the ^{13}C and ^{1}H NMR signals of **2-8**, presented in Table 2-11, was achieved in a manner similar to that described for **2-2**.

^{1}H NMR Spectrum of Isopropyl Secoester (2-8)

The ^{1}H NMR spectrum of **2-8** showed the presence of ten methyl groups, including seven tertiary methyl groups, three secondary methyl groups and a downfield resonance (5.00 ppm, m) attributable to the methine proton of the isopropyl ester group. The secondary methyl group resonance which occurred at 0.83 ppm (d, J = 6.9 Hz) could be readily identified as the 8β-methyl group signal by comparison with equivalent resonance of **2-2** (0.83 ppm, J = 6.9 Hz).

The secondary $OCH(CH_3)_2$ methyl signals appeared as the X_3 and X'_3 parts of an $AX_3X'_3$ system in which the inner lines of the two methyl signals centred at *ca.* 1.23 and 1.25 ppm respectively, were separated by 6.3 Hz. The A part of this spin system {that arising from the -$OCH(CH_3)_2$ proton} occurred at 5.00 ppm (~septet, J = 6.3 Hz).

Table 2-11. ^{13}C and ^1H NMR signals (δ ppm in $CDCl_3$ and C_5D_5N) observed for isopropyl 22-hydroxy-7,8-secohopan-7-oate (**2-8**).

atom	in $CDCl_3$			in C_5D_5N		
	^{13}C	$^1H_\alpha$	$^1H_\beta$	^{13}C	$^1H_\alpha$	$^1H_\beta$
1	34.2 t	1.33 t	1.51 d	34.5 t	1.38 t	1.54 d
2	18.6 t	1.35 d	1.52 q	18.9 t	1.35 d	1.53 t
3	41.7 t	1.15 t	1.38 d	42.0 t	1.18 t	1.39 d
4	35.1 s			35.2 s		
5	46.1 d	1.98 s (br)		46.4 d	2.20 s (br)	
6	33.4 t	2.21 q		33.6 t	2.37 t	
7	174.5 s			174.4 s		
8	44.1 d	1.38 d		44.5 d	1.45 q	
9	40.5 d	1.62 d		40.8 d	1.80 d	
10	39.8 s			39.7 s		
11	22.3 t	1.62 d	1.30 t	22.7 t	1.89 d	1.35 t
12	25.1 t	1.41 t	1.31 d	25.5 t	1.50 q	
13	49.8 d		1.08 d	50.2 d		1.19 d
14	39.3 s			40.1 s		
15	39.1 t	1.10 d	1.52 t	39.5 t	1.14 d	1.58 t
16	22.2 t	1.67 t	1.92 d	22.6 t	1.89 t	2.19 d
17	54.7 d		1.47 t	55.4 d		1.53 t
18	44.1 s			44.5 s		
19	40.7 t	1.52 t	0.95 q	41.3 t	1.59 q	1.01 q
20	26.6 t	1.50 t	1.76 q	27.0 t	1.78 t	1.82 q
21	51.1 d		2.21 q	51.5 d		2.38 q
22	74.0 s			72.5 s		
23	33.9 q	0.85 s		34.1 q	0.95 s	
24	22.7 q	0.93 s		22.8 q	1.00 s	
25	17.7 q	0.84 s		17.9 q	0.90 s	
26	10.7 d	0.84 d (J = 6.9 Hz)		11.0 d	0.90 d (J = 6.9 Hz)	
27	25.3 q	0.97 s		25.7 q	1.12 s	
28	16.2 q	0.72 s		16.5 q	0.96 s	
29	28.9 q	1.18 s		30.0 q	1.36 s	
30	30.9 q	1.21 s		31.5 q	1.43 s	
O<u>C</u>H$(CH_3)_2$	67.6 d	5.00 m (J = 6.3 Hz)		67.7 d	5.15 m (J = 6.3 Hz)	
OCH(<u>C</u>H$_3)_2$	21.9 q	1.23 d (J = 6.3 Hz)		22.0 q	1.25 d (J = 6.3 Hz)	
	21.9 q	1.25 d (J = 6.3 Hz)		22.0 q	1.27 d (J = 6.3 Hz)	

COSY Spectrum of Isopropyl Secoester (2-8)

Some structural significant COSY correlations observed for **2-8**, including those attributable to ^4J couplings between methyl groups and adjacent axially oriented methylene protons, are presented in Table 2-12.

Table 2-12. Selected ^{1}H-^{1}H COSY correlations (δ ppm in $CDCl_3$) observed for isopropyl 22-hydroxy-7,8-secohopan-7-oate (**2-8**).

^{1}H NMR signals	correlated ^{1}H signals
5.00 m {OC<u>H</u>$(CH_3)_2$}	1.23 d, 1.25 d (OCH (C<u>H</u>$_3)_2$)
2.21 q (H-6a/b)	1.98 br s (H-5α)
2.21 q (H-21β)	1.50 t/1.76 q (H-20α/β), 1.47 t (H-17β), 0.95 q (H-19β)
1.98 br s (H-5α)	2.21 q (H-6a/b)
1.92 d (H-16β)	1.67 t (H-16α), 1.47 t (H-17β), 1.10 d/1.52 t (H-15α/β)
1.76 q (H-20β)	2.21 q (H-21β), 1.50 q (H-20α), 1.52 t/ 0.95 q (H-19α/β)
1.62 d (H-11α)	1.62 d (H-9α), 1.41 t/1.31 d (H-12α/β), 1.29 t (H-11β)
1.47 t (H-17β)	2.21 q (H-21β), 1.92 d (H-16β)
1.38 d (H-8α)	0.83 d (8β-Me)
1.10 d (H-15α)	1.67 t/1.92 d (H-16α/β), 1.52 t (H-15β)
1.08 d (H-13β)	1.41 t/1.31 d (H-12α/β)
0.97 s (14α-Me)	1.52 t (H-15β)*
0.92 s (4β-Me)	1.15 t (H-3α)*, 0.85 s (4α-Me)*
0.85 s (10β-Me)	1.98 br s (H-5α), 1.33 t (H-1α)*
0.83 s (4α-Me)	0.92 s (4β-Me) *
0.72 s (18α-Me)	0.95 q (H-19β)*

* ^4J coupling

^{13}C and DEPT135 NMR Spectra of Isopropyl Secoester (2-8)

The ^{13}C NMR spectrum of **2-8** was comprised of thirty-three signals, which were characterised by a DEPT135 NMR spectrum to arise from ten quartet (CH_3), ten triplet (CH_2), seven doublet (CH) and six singlet (C) carbons.

The majority of the ^{13}C resonances of **2-8** corresponded closely to those determined for **2-2**, other than for minor differences in the resonances of atoms in close proximity to C-7, and for the presence of signals attributable to an oxygenated methine carbon at 67.6 ppm and two superimposed methyl group carbon signals at 21.9 ppm.

HMBC and HSQC Spectra of Isopropyl Secoester (2-8)

The seven tertiary methyl group resonances of **2-8** could be assigned by comparison with those of **2-2,** and by analyses of the HSQC and HMBC spectral data presented in Table 2-13.

The methyl group proton signals which occurred at 1.23 and 1.25 ppm correlated in the HMBC spectrum of **2-8** with the carbon signals which occurred at 67.6 and 21.9 ppm, while the proton signal at 5.00 ppm correlated with the carbonyl carbon which occurred at 174.5 ppm and the pair of methyl carbon signals which occurred at 21.9 ppm in **2-8**.

Table 2-13. ^{1}J, ^{2}J and ^{3}J heteronuclear ^{1}H-^{13}C correlations (δ ppm in $CDCl_3$) observed for isopropyl 22-hydroxy-7,8-secohopan-7-oate (**2-8**).

^{1}H signal	^{1}J correlated ^{13}Csignal	^{2}J and ^{3}J correlated ^{13}C signals
0.83 s (4α-Me)	33.9 (C-23)	46.1 (C-5), 41.7 (C-3), 35.1 (C-4), 22.7 (C-24)
0.92 s (4β-Me)	22.7 (C-24)	46.1 (C-5), 41.7 (C-3), 35.1 (C-4), 33.9 (C-23)
0.85 s (10β-Me)	17.7 (C-25)	46.1 (C-5), 40.5 (C-9), 39.8 (C-10), 34.2 (C-1)
0.83 d (8β-Me)	10.7 (C-26)	44.1 (C8), 40.5 (C9), 39.2 (C14)
0.97 s (14α-Me)	25.3 (C-27)	49.8 (C-13), 44.1 (C-8), 39.2 (C-14), 39.1 (C-15)
0.72 s (18α-Me)	16.2 (C-28)	54.7 (C-17), 49.8 (C-13), 44.1 (C-18), 40.7 (C-19)
1.17 s (22a-Me)	28.8 (C-29)	74.0 (C-22), 51.0 (C-21), 30.9 (C-30)
1.21 s (22b-Me)	30.9 (C-30)	74.0 (C-22), 51.0 (C-21), 28.8 (C-29)
5.00 m {OC<u>H</u>$(CH_3)_2$}	67.6 {O<u>C</u>H$(CH_3)_2$}	174.5 (C-7), 21.9 {OCH(<u>C</u>$H_3)_2$}
2.21 q (H-6a/b)	33.4 (C-6)	174.5 (C-7), 39.8 (C-10), 46.1 (C-5), 35.1 (C-4)
1.98 br s (H-5α)	46.1 (C-5)	174.5 (C-7), 39.8 (C-10), 35.1 (C-4), 33.9 (C-23), 33.4 (C-6), 22.7 (C-24)

ROESY Spectrum of Isopropyl Secoester (2-8)

The ROESY spectrum of **2-8** included correlations (see Table 2-14) which validated the methyl group assignments presented in Tables 2-11 and 2-13. The secondary 8β-methyl group signal (0.83, d, J = 6.9 Hz) exhibited correlations to H-8α (1.38 ppm), H-13β (1.08 ppm), and H-15β (1.52 ppm). These observations verified the secondary C-8 methyl group to be axially (β-) oriented.

The 10β-methyl group (0.84 ppm) of **2-8** exhibited ROESY correlations with the 4β-methyl group (0.93 ppm), H-2β (1.50 ppm), H-6a/b (2.21 ppm), H-8α (1.36 ppm) and H-9α (1.62 ppm). Correlations were also observed between the 4β- and 10β-methyl groups, and between the 14α- and 18α-methyl groups, but not between the 8β- and 10β-methyl groups. These observations were consistent with the conclusion (see Section **2.2.2.2**) for the product (**2-2**) obtained on photolysis of **2-1** that the cleavage of the C-7–C-8 bond resulted in rotation about the C-9–C-10 bond to relieve steric compression between the 8β- and 10β-methyl groups. The relative disposition of the 8β-and 10β-methyl groups could not however be ascertained in NOE or ROESY experiments since their signal resonances each occurred at 0.84 ppm.

Selected ROESY correlations observed for **2-8** are presented in Table 2-14.

Table 2-14. Selected ^{1}H-^{1}H ROESY correlations (δ ppm in $CDCl_3$) observed for isopropyl 22-hydroxy-7,8-secohopan-7-oate (**2-8**).

^{1}H NMR signals	correlated ^{1}H signals
1.98 br s (H-5α)	2.21 q (H-6a/b), 0.83 s (4α-Me)
1.76 q (H-20β)	2.21 q (H-21β), 1.50 t (H-20α), 0.95 q (H-19β)
1.67 t (H-16α)	1.10 d (H-15α)
1.21 s (22b-Me)	1.18 s (22a-Me)
1.18 s (22a-Me)	1.21 s (22b-Me)
0.97 s (14α-Me)	0.72 s (18α-Me), 1.38 d (H-8α), 1.23 d /1.25 d {CH(C<u>H</u>$_3$)$_2$}
0.93 s (4β-Me)	0.85 s (4α-Me)
0.85 s (4α-Me)	0.93 s (4β-Me), 1.98 br s (H-5α), 1.35 d (H-2α)
0.84 s (10β-Me)	0.93 s (4β-Me), 2.21 q (H-6a/b), 1.62 d (H-9α), 1.52 q (H-2β), 1.38 d (H-8α)
0.84 d (8β-Me)	1.52 d (H-15β), 1.38 d (H-8α), 1.08 d (H-13β)
0.72 s (18α-Me)	0.97 s (14α-Me)

Molecular modelling supported the conclusion that the preferred solution conformation of **2-8** was likely to be that in which ring A was rotated *ca.* 90° with respect to rings C/D/E, since the minimised energy of **2-8**, analogous to the Model B conformation of **2-2** (E = 90.6 Kcal), was 5.3 KCal lower than that determined for the corresponding Models A conformation (E = 95.9 KCal) (see Figure 2-12).

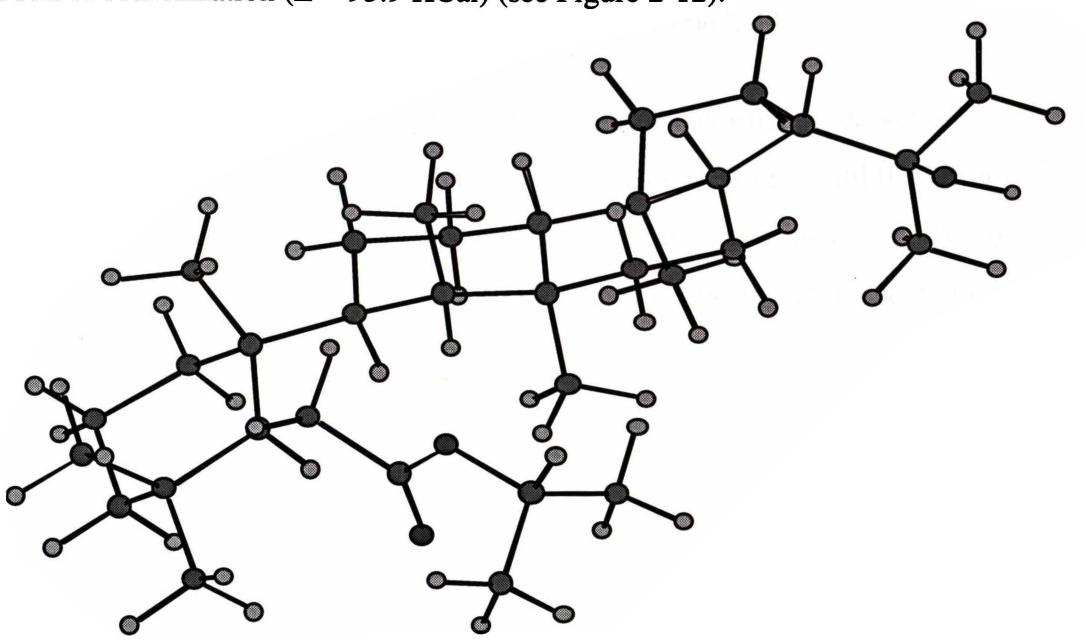

Model A: Refined without rotation about the C-9–C-10 bon (E = 95.9 KCal).

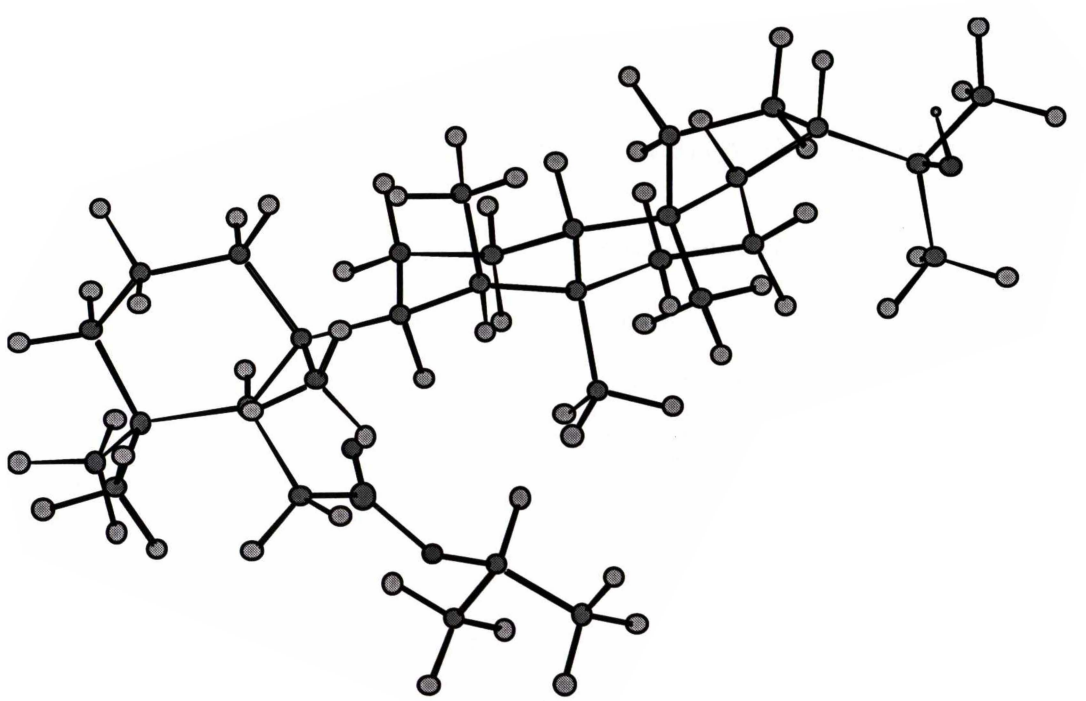

Model B: Refined after *ca.* 90° rotation about the C-9–C-10 bond (E = 90.6 KCal).

Figure 2-12. MM2 modelled confirmations determined for **2-8** without rotation (**model A**) and with rotation about the C-9-C-10 bond (**model B**).

NMR Data Analyses of Isopropyl Secoester (2-8) in Pyridine

It was anticipated that substitution of pyridine for $CDCl_3$ would lead to differing ^1H NMR chemical shifts being observed for the methyl groups. The complete assignment of the ^{13}C and ^1H NMR signals of **2-8** in pyridine, achieved from analyses of one- and two-dimensional NMR spectral data, is presented in Table 2-11.

The 14α-methyl and 18α-methyl groups exhibited significant downfield shifts to resonate at 1.12 ppm and 0.96 ppm respectively (from 0.97 ppm and 0.72 ppm), while the 8β-methyl (d) and 10β-methyl (s) groups also experienced a slightly downfield shift, however their signals were essentially coincident (the respective doublet and singlet signals were centered at 0.90 ppm),

Irradiation of H-1β (1.54 ppm) in an NOE-difference experiment enhanced the secondary C-8 methyl group (d, 0.90 ppm) and the tertiary 10β-methyl (s, 0.90 ppm), group signals, together with the H-1α (t, 1.38 ppm) and H-11β (t, 1.35 ppm) signals. These NOE's are consistent with the preferred solution conformation of **2-2** being that in which ring A is rotated *ca.* 90° relative to ring C.

2.5 Photolysis of Hop-22(29)-en-7-one in Benzene-Methanol

2.5.1 Preparation and Photolysis of Hop-22 (29)-en-7-one (2-3)

Dehydration of 22-hydroxyhopan-7-one (**2-1**) with phosphorus pentachloride, or phosphorus oxychloride in pyridine, afforded a mixture of hop-22(29)-en-7-one (**2-3**) and hop-21-en-7-one. Separation of this mixture on a silver nitrate impregnated alumina afforded a specimen of hop-22(29)-en-7-one (**2-3**) (Corbett & Young, 1966a) (see Scheme 2-1).

Photolysis of hop-22(29)-en-7-one (**2-3**) in dry benzene-methanol (1:1) as described for 22-hydroxyhopan-7-one (**2-1**) (see Section **2.2**) afforded product material which, when purified by radial chromatography on silica gel using mixtures of light petroleum and diethyl ether as eluents, gave methyl 7,8-secohop-22(29)-en-7-oate (**2-9**).

2.5.2 Structural Elucidation of Methyl 7,8-secohop-22(29)-en-7-oate (2-9)

2.5.2.1 Mass Spectral Analyses of Methyl 7,8-secohop-22(29)-en-7-oate (2-9) and Hop-22(29)-en-7-one (2-3)

The mass spectrum of **2-9** included a fragment ion at *m/z* 456, corresponding to the expected molecular formula $C_{31}H_{52}O_2$ (456 daltons). The base peak which occurred at *m/z* 197, and strong *m/z* 123 and 259 fragment ions (see Scheme 2-6), corresponded to fragment ions observed in the mass spectrum of methyl 22-hydroxy-7,8-secohopan-7-oate (**2-2**) (see Scheme 2-2).

On the other hand, the base peak at *m/z* 189 of **2-3** can be envisaged as arising from cleavage "b", while the *m/z* 205 fragment ion can be envisaged as arising from cleavage "a" (see Scheme 2-7).

Other significant fragment ions, and their intensities, observed in the mass spectrum of **2-9**, and the starting material (**2-3**), are compared in Table 2-15.

Table 2-15. Selected mass spectral fragment ions observed for methyl 7,8-secohop-22(29)-en-7-oate (**2-9**) and hop-22(29)-en-7-one (**2-3**).

methyl 7,8-secohop-22(29)-en-7-oate (**2-9**)		hop-22(29)-en-7-one (**2-3**)	
ions	***m/z*** **(% relative intensities)**	**ions**	***m/z*** **(% relative intensities)**
M^+	456 (11)	M^+	424 (26)
M^+-CH_3	441 (9)	M^+-CH_3	409 (15)
M^+– C_5H_9 (ion c)	387 (3)	M^+– C_5H_9 (ion c)	355 (8)
$C_{19}H_{31}^+$ (ion b)	259 (34)	ion c–C_3H_6	313 (26)
$C_{12}H_{21}O_2^+$ (ion a)	197 (100)	$C_{16}H_{25}O^+$ (ion f)	233 (21)
ion a-CH_3COOCH_3	123 (89)	$C_{15}H_{24}O^{+\cdot}$ (ion e)	220 (92)
$C_5H_9^+$ (ion d)	69 (58)	$C_{14}H_{21}O^+$ (ion a)	205 (32)
		$C_{14}H_{21}^+$ (ion b)	189 (100)

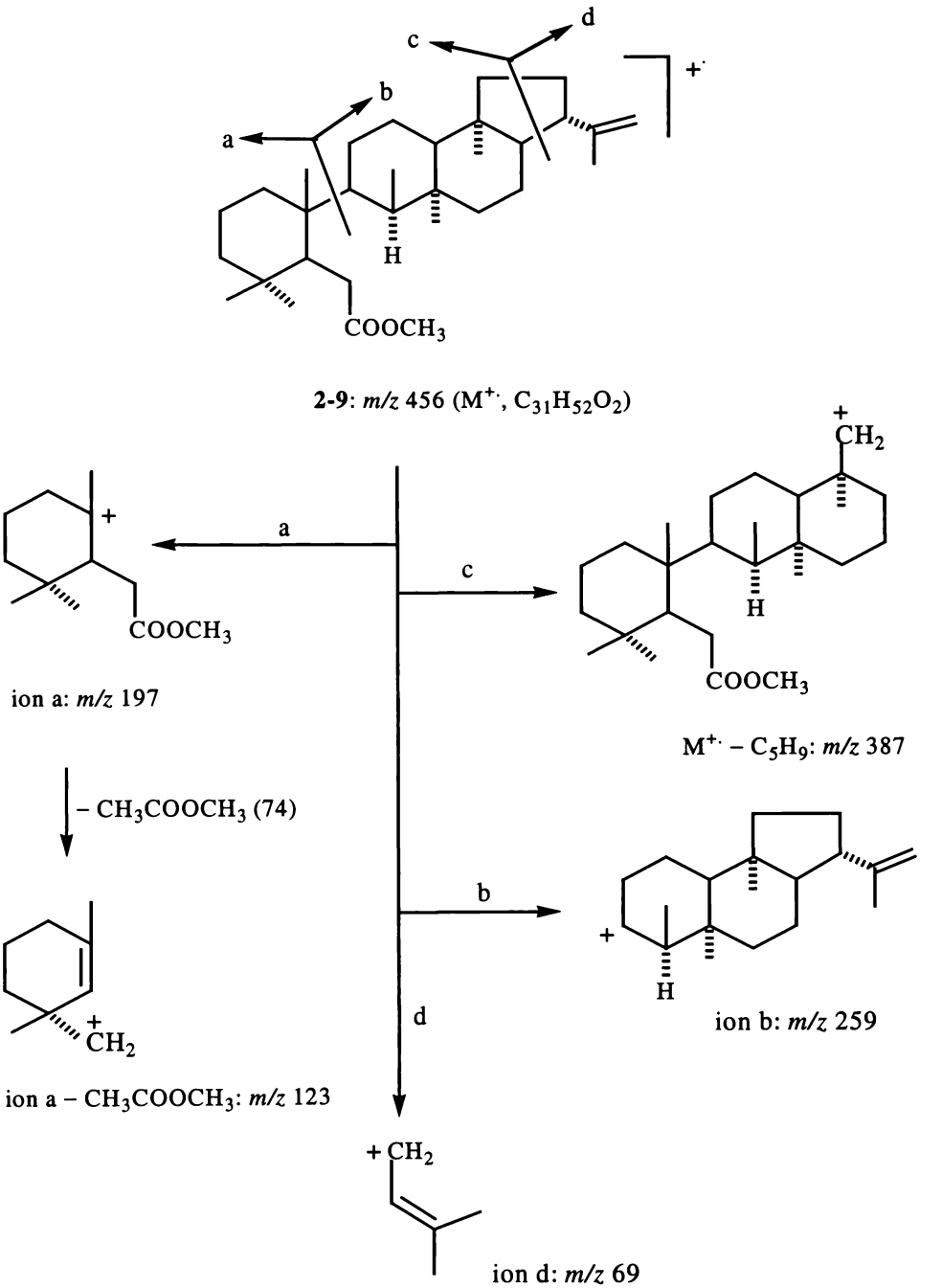

Scheme 2-6. Proposed mass spectral fragmentation pathways for methyl 7,8-secohop-22(29)-en-7-oate (**2-9**).

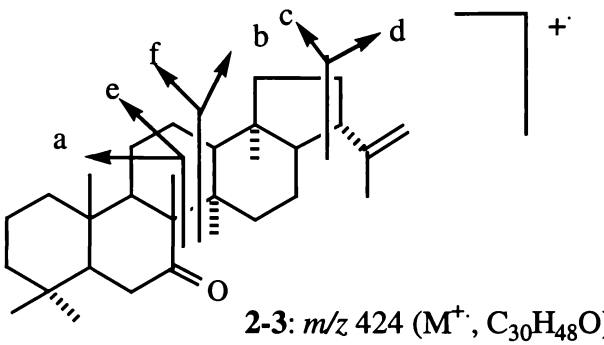

2-3: *m/z* 424 ($M^{+\cdot}$, $C_{30}H_{48}O$)

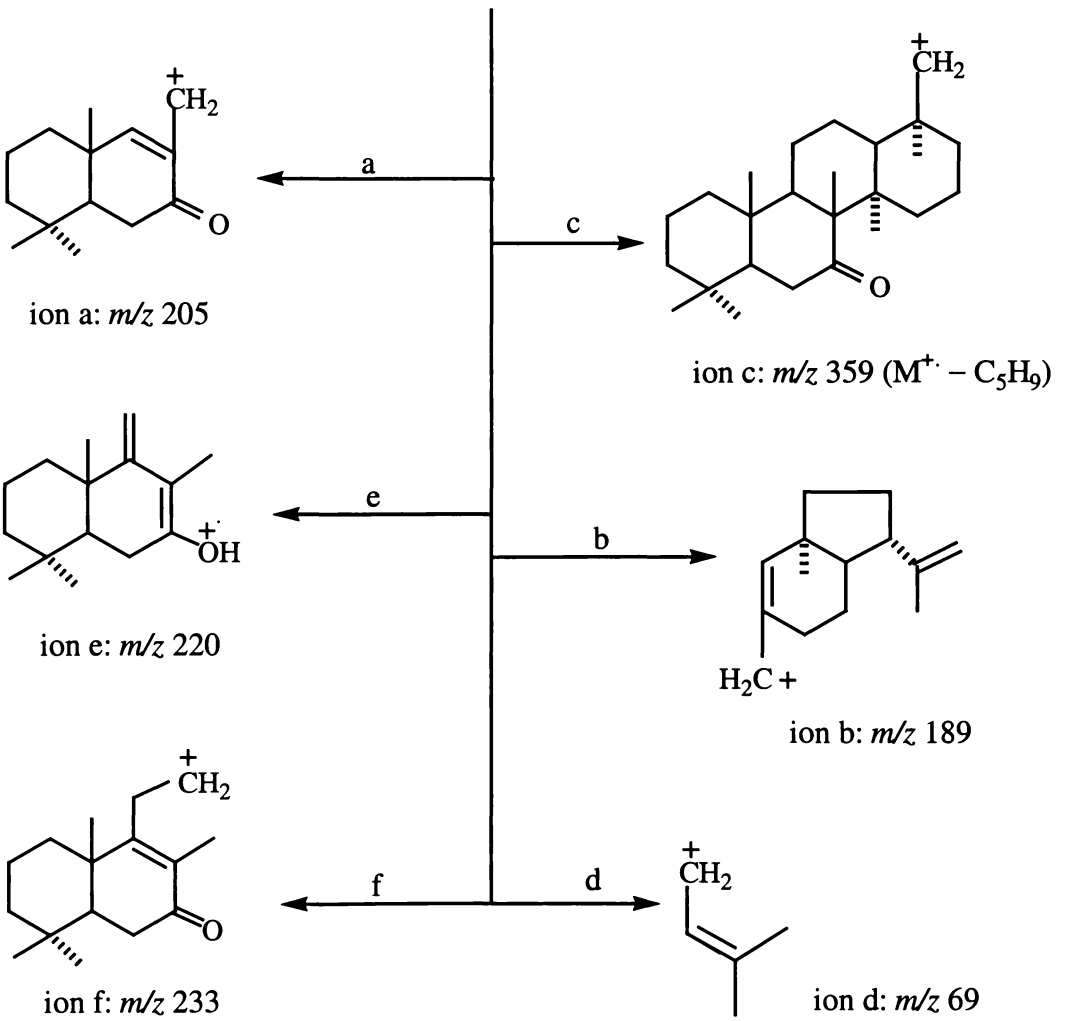

Scheme 2-7. Proposed mass spectral fragmentation pathways for hop-22(29)-en-7-one (**2-3**).

2.5.2.2 NMR Spectral Analyses of Methyl 7,8-secohop-22(29)-en-7-oate (2-9)

A complete assignment of the ^{13}C and ^{1}H NMR signals presented in Table 2-16 for methyl 7,8-secohop-22(29)-en-7-oate (**2-9**) can be compared with that elucidated for methyl 22-hydroxy-7,8-secohopan-7-oate (**2-2**) (see Section **2.2.2.2**), and the ^{13}C NMR assignments reported by Bird (1983) for hop-22(29)-en-7-one (**2-3**).

Table 2-16. ^{13}C and ^{1}H NMR signals (δ ppm in $CDCl_3$) observed for methyl 7,8-secohop-22(29)-en-7-oate (**2-9**), **2-2** and hop-22(29)-en-7-one (**2-3**).

atom	hop-22 (29)-en-7-on (**2-3**)[a]	methyl 22-hydroxy-7,8-seco-hop-22(29)-en-7-oate (**2-9**)			methyl 22-hydroxy-7,8 –seco-hopan-7-oate (**2-2**)		
	^{13}C	^{13}C	$^{1}H_{\alpha}$	$^{1}H_{\beta}$	^{13}C	$^{1}H_{\alpha}$	$^{1}H_{\beta}$
1	40.3 t	34.2 t	1.32 t	1.53 d	34.2 t	1.34 t	1.54 d
2	18.4 t	18.6 t	1.36 d	1.50 t	18.6 t	1.37 d	1.53 t
3	41.9 t	41.7 t	1.16 t	1.39 d	41.7 t	1.18 t	1.40 d
4	33.4 s	35.0 s			35.1 s		
5	52.9 d	46.5 d	1.99 s (br)		46.5 d	2.01 t	
6	37.9 t	32.6 t	2.23 t		32.6 t	2.24 t	
7	215.3 s	175.4 s			175.5 s		
8	58.3 s	44.1 d	1.39 d		44.1 d	1.40 d	
9	53.9 d	40.7 d	1.56 d		40.7 d	1.56 q	
10	37.6 s	40.0 s			40.0 s		
11	20.7 t	22.1 t	1.66 d	1.29 t	22.1 t	1.68 d	1.29 t
12	24.5 t	24.7 t	1.28 t	1.42 d	25.0 t	1.30 t	1.44 d
13	51.0 d	49.4 d		1.07 d	49.8 d		1.10 d
14	42.7 s	39.4 s			39.3 s		
15	34.9 t	38.4 t	1.08 d	1.55 t	39.2 t	1.12 d	1.54 t
16	22.0 t	21.9 t	1.55 t	1.64 d	22.2 t	1.66 t	1.94 d
17	55.0 d	55.6 d		1.40 t	54.7 d		1.49 t
18	45.3 s	44.8 s			44.1 s		
19	41.6 t	41.3 t	1.59 t	1.04 q	40.8 t	1.55 q	0.97 q
20	26.9 t	27.4 t	1.80 ~ 1.85		26.6 t	1.52 q	1.78 q
21	46.5 d	46.4 d		2.67 q	51.1 d		2.23 q
22	148.5 s	148.7 s			74.0 s		
23	32.6 q	34.0 q	0.86 s		34.0 q	0.85 s	
24	20.9 q	22.7 q	0.90 s		22.8 q	0.91 s	
25	15.7 q	17.7 q	0.85 s		17.8 q	0.87 s	
26	19.4 q	10.7 q	0.83 d (J = 7.0 Hz)		10.8 q	0.84 d (J = 6.9 Hz)	
27	15.8 q	24.8 q	0.91 s		25.2 q	0.94 s	
28	15.9 q	16.1 q	0.67 d (J = 0.53 Hz)		16.2 q	0.72 d (J = 0.77 Hz)	
29	110.0 t	110.1 t	4.77 d (J = 0.84 Hz)		28.9 q	1.18 s	
30	25.1 q	25.0 q	1.76 s		30.9 q	1.21 s	
31		51.5 q	3.70 s		51.6 q	3.70 s	

[a] assignments proposed by Bird (1984)

^{1}H NMR Spectrum of Methyl Secoester (2-9)

The ^{1}H NMR spectrum of **2-9** included signals attributable to five tertiary methyl group signals in the region 0.67~0.91 ppm, a secondary methyl group signal (0.83 ppm, J = 7.0 Hz), an olefinic methyl group signal (1.76 ppm), an ester methoxyl signal (3.70 ppm) and a two proton olefinic signal (4.77 ppm). One of the tertiary methyl group signals (18α-Me, 0.67 ppm, d, J = 0.53 Hz) exhibited a resolvable ^4J long range coupling to one of the adjacent methylene protons (H-19β, 1.04 ppm).

^{13}C and DEPT135 NMR Spectra of Methyl Secoester (2-9)

The ^{13}C NMR spectrum of **2-9** showed a total of thirty-one signal resonances, which were characterised by a DEPT135 NMR spectrum to arise from eight quartet (CH_3), eleven triplet (CH_2), six doublet (CH) and six singlet (C) carbons. The ^{13}C spectrum included signals attributable to the presence of a $\underline{C}OO\underline{C}H_3$ group (175.5 and 51.5 ppm) and a disubstituted olefinic system (CH_2=C–) (110.1 and 148.7 ppm). The chemical shifts of ring A, B and C carbons corresponded closely to those determined for methyl 22-hydroxy-7,8-secohopan-7-oate (**2-2**), while those of the ring D and E carbon resonances corresponded closely to those of hop-22(29)-en-7-one (**2-3**) and methyl 7,8-secohop-22(29)-en-7-oate (**2-9**) (see Table 2-16).

ROESY Spectrum of Methyl Secoester (2-9)

The ROESY spectrum of **2-9** included correlations between the 8β-methyl group and H-8α (1.39 ppm), H-15β (1.55 ppm) and H-13β (1.07 ppm), analogous to those observed for the equivalent protons of methyl 22-hydroxy-7,8-secohopan-7-oate (**2-2**) (see Section **2.2.2.2**) and isopropyl 22-hydroxy-7,8-secohopan-7-oate (**2-8**) (see Section **2.4.2.2**).

As was also the case for **2-2** and **2-8**, no ROESY correlation was observed between the 8β- and 10β-methyl groups of **2-9** due to the similar chemical shifts of the 8β-methyl (0.83 ppm, d) and 10β-methyl (0.85 ppm, s) groups.

The 10β-methyl group (0.85 ppm) exhibited ROESY correlations with H-8α (1.39 ppm), H-9α (1.56 ppm), H-2β (1.50 ppm), H-6a/b (2.23 ppm) and 4β-methyl group (0.90 ppm).

These ROESY correlations were analogous to those observed for **2-2** and **2-8**, and were consistent with the preferred solution conformation of **2-9** being that in which ring A is rotated *ca.* 90° with respect to rings C/D/E. Other ROESY correlations observed for **2-9** are listed in Table 2-17.

Table 2-17. Selected ^{1}H-^{1}H ROESY correlations (δ ppm in $CDCl_3$) observed for methyl 7,8-secohop-22(29)-ene-7-oate (**2-9**).

^{1}H NMR signals	correlated ^{1}H signals
4.77 d (H-29a/b)	1.80~1.85 (H-20α/β), 0.67 d (18α-Me)
2.67 q (H-21β)	1.84 q (H-20α), 1.55 t (H-16α), 1.40 t (H-17β)
2.23 t (H-6a/b)	1.99 br s (H-5α), 1.56 d (H-9α), 0.90 s (4β-Me), 0.84 s (10β-Me)
1.99 br s (H-5α)	2.23 t (H-6a/b), 1.66 d (H-11α), 1.56 d (H-9α), 0.86 s (4α-Me)
1.64 d (H-11α)	1.99 br s (H-5α), 1.29 t (H-11β), 1.28 t/1.42 d (H-12α/β)
1.16 t (H-3α)	1.39 d (H-3β)
1.08 d (H-15α)	1.55 t (H-15β)
1.76 s (22-Me)	4.77 d (H-29a/b), 2.67 q (H-21β), 1.64 d (H-16β), 0.67 d (18α-Me)
0.91 s (14α-Me)	3.70 s (COOC<u>H</u>$_3$), 1.55 t (H-16α), 1.39 d (H-8α), 1.28 t (H-12α) 1.08 d (H-15α), 0.67 s (18α-Me)
0.90 s (4β-Me)	2.23 t (H-6a/b), 0.87 s (4α-Me)
0.86 s (4α-Me)	0.90 s (4β-Me), 2.23 t (H-6a/b), 1.99 t (H-5α), 1.56 d (H-9α) 1.36 d (H-2α), 1.16 t (H-3α)
0.85 s (10β-Me)	0.90 s (4β-Me), 2.23 t (H-6a/b), 1.56 d (H-9α), 1.50 t (H-2β), 1.39 d (H-8α)
0.83 d (8β-Me)	1.54 d (H-15β), 1.39 d (H-8α), 1.07 d (H-13β)
0.67 d (18α-Me)	4.77 (H-29a/b), 1.76 s (22α-Me), 1.55 t (H-16α) 1.28 t/1.42 d (H-12α/β) 0.91s (14α-Me)

2.6 Mechanistic Aspects of the Formation of the Photochemical Reaction Products

The products obtained in the photochemical reactions of 22-hydroxyhopan-7-one (**2-1**) and hop-22(29)-en-7-one (**2-3**) (see Scheme 2-8), described in Sections **2.2**, **2.4** and **2.5**, can be envisaged as being derived mainly *via* an intermediate ketene which subsequently reacts with an alcohol (eg methanol or isopropanol) to afford a secoester (see Scheme 2-9 and 2-10).

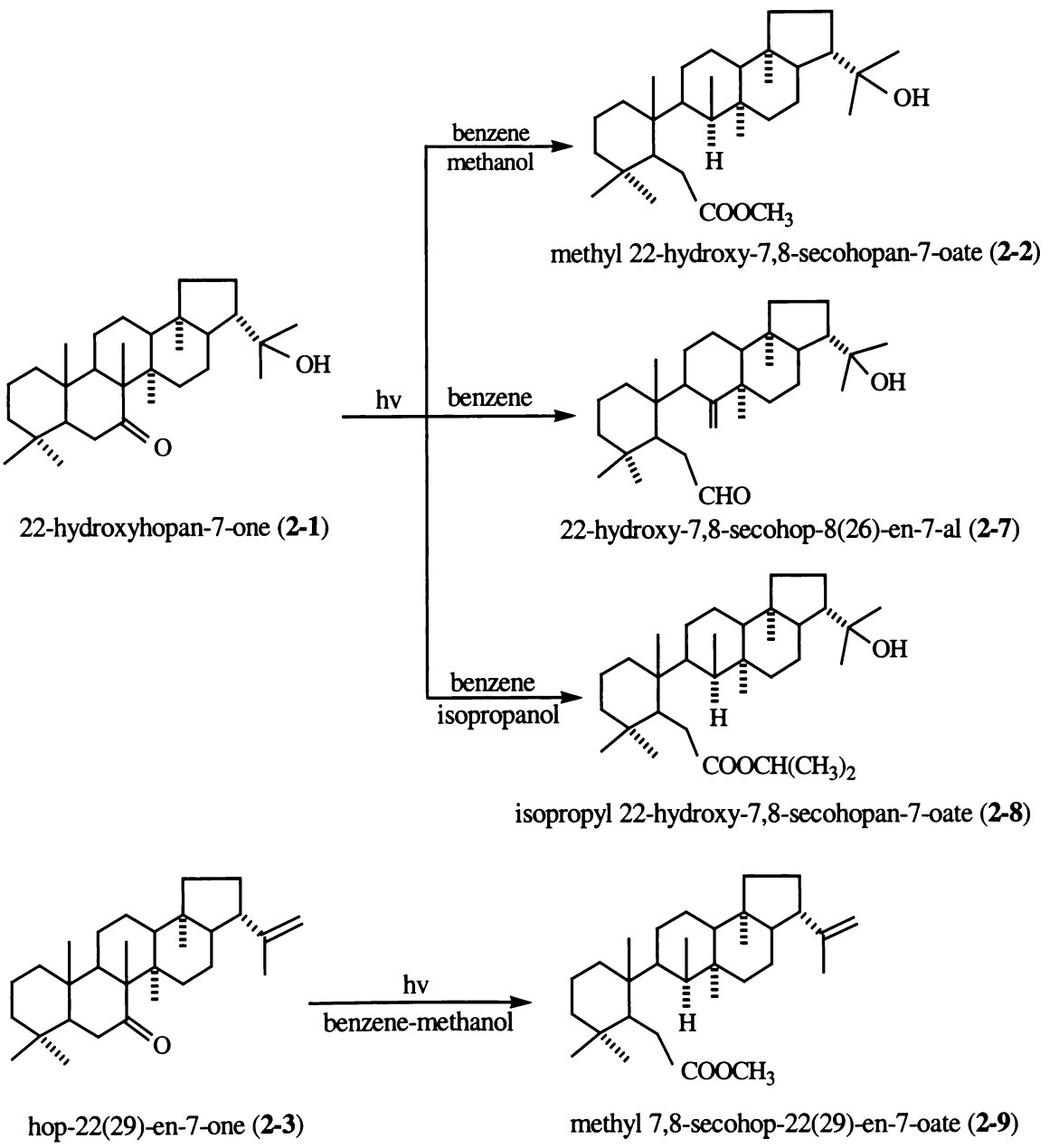

Scheme 2-8. Photoproducts of **2-2** and **2-3** in the presence of various solvents.

It can be proposed that photolysis of **2-1** affords biradical (**2-1a**) (Scheme 2-9), which undergoes hydrogen transfer from C-6 to C-8 (a 1,5 shift) *via* a six-membered transition state to give ketene (**2-1b**), which then reacts with methanol to afford a secoester (**2-2**). This conclusion is in agreement with the proposal of Hunter (1993).

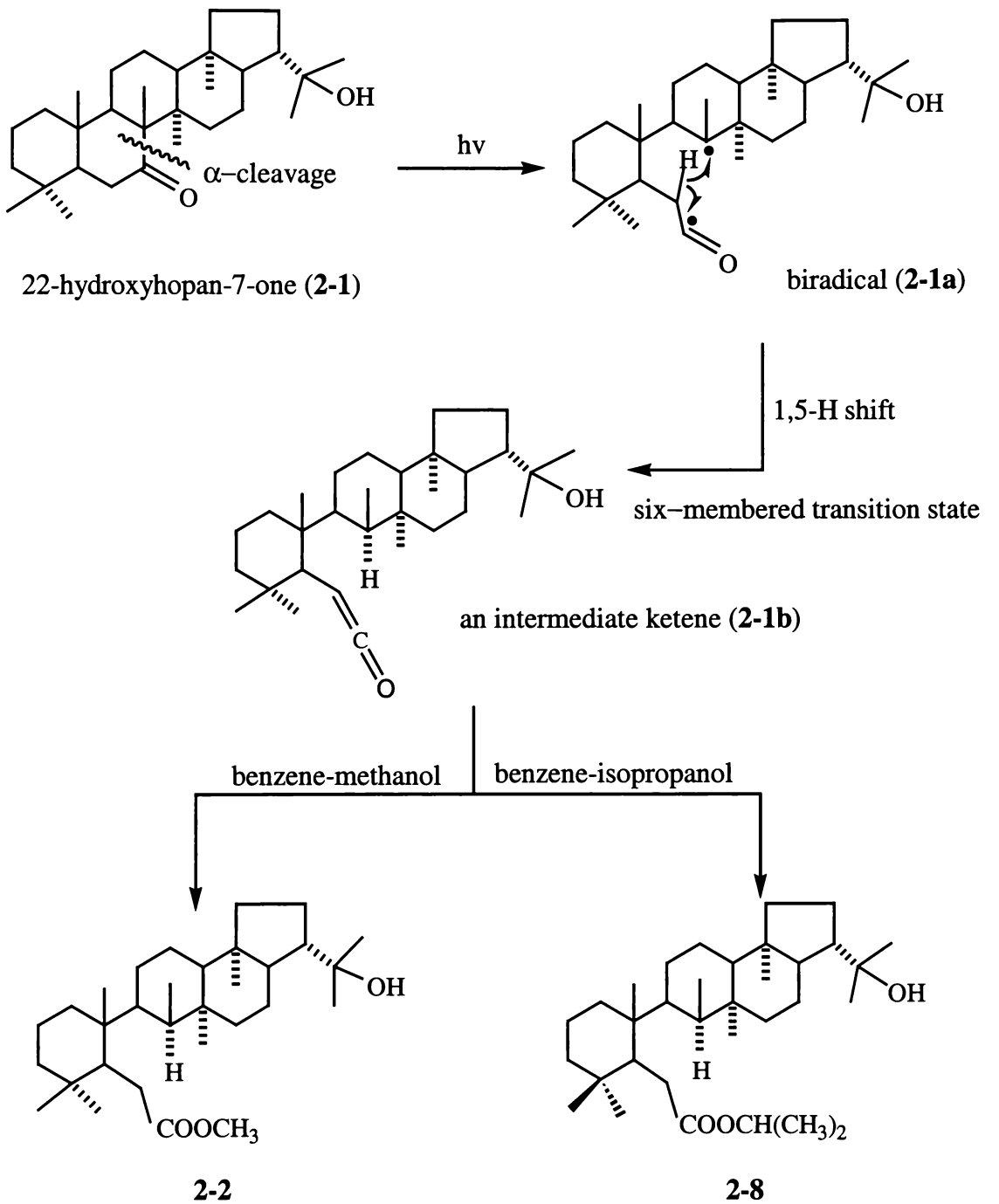

Scheme 2-9. Proposed mechanistic pathways for the formation of photolysis products (**2-2**) and (**2-8**) from 22-hydroxyhopan-7-one (**2-1**) in benzene-methanol or benzene-isopropanol.

The stereochemistry at C-8 was determined from analyses of ROESY data to be that in which the 8-methyl group was β-oriented (Scheme 2-9). This observation contrasts with that observed for the equivalent 15-oxo reaction (which afforded a mixture of C-14 isomers) (see Section **3.6**) and the results of Okogun *et al.* (1998) who observed that photolysis of 7-deacetoxy-7-oxokhivorin (**1-25**) proceeded with inversion at C-8 (see Scheme 2-11).

Secoester (**2-2**) can be envisaged as arising from biradical (**2-3a**) *via* a 1,5-hydrogen shift *via* a chair-like intermediate (see Scheme 2-12).

The formation of isopropyl 22-hydroxy-7,8-secohopan-7-oate (**2-8**) (Scheme 2-9), when 22-hydroxyhopan-7-one (**2-1**) was photolysed in benzene-isopropanol, shows that replacement of methanol by a more bulky alcohol does not influence the outcome of the photoreaction (other than by affording the corresponding secoester).

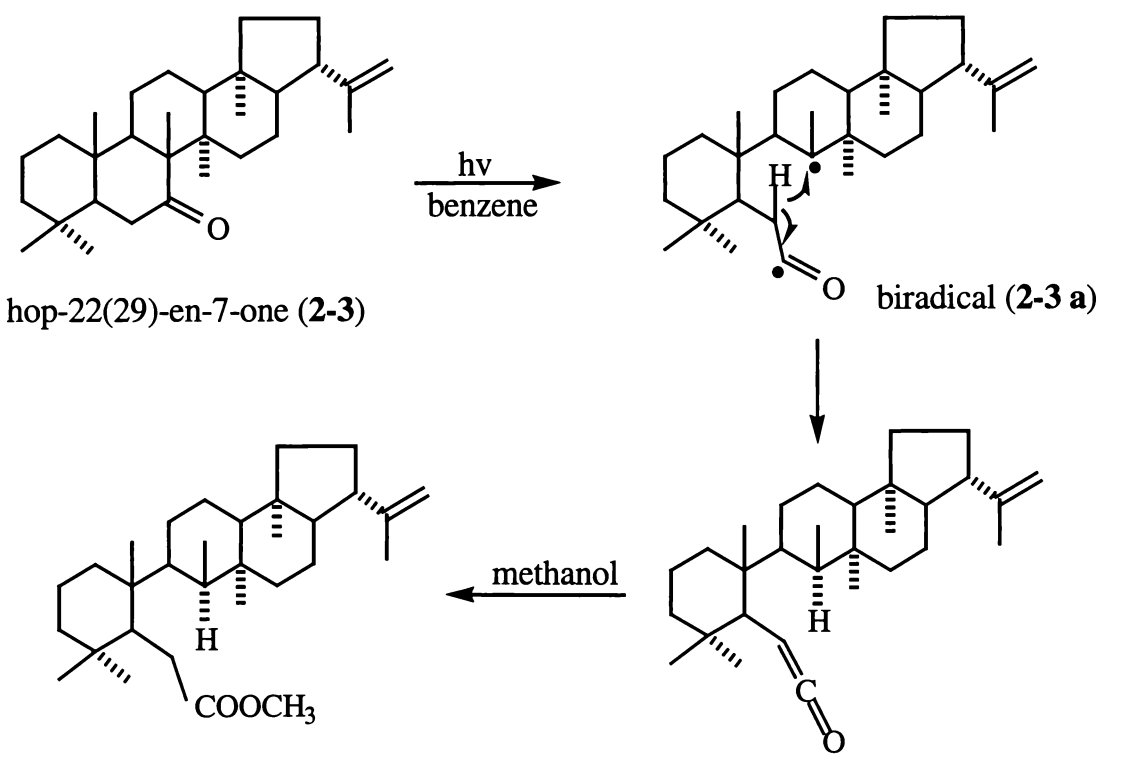

hop-22(29)-en-7-one (**2-3**) biradical (**2-3 a**)

methyl 7,8-secohop-22(29)-en-7-oate (**2-9**) ketene intermediate (**2-3 b**)

Scheme 2-10. Proposed pathway for the formation of the photolysis product from hop-22(29)-en-7-one (**2-3**) in benzene-methanol.

In the presence of methanol, photolysis of hop-22(29)-en-7-one (**2-3**) can also be envisaged as proceeding *via* α-cleavage (Scheme 2-10) to afford biradical (**2-3a**), followed by 1,5 hydrogen transfer to give ketene (**2-3b**), which subsequently reacts with methanol to give methyl 7,8-secohop-22(29)-en-7-oate (**2-9**). During the photolysis process, no dimeric Woodward Hoffmann $\pi 2_S + \pi 2_S$ addition product (see Scheme 2-13) was obtained.

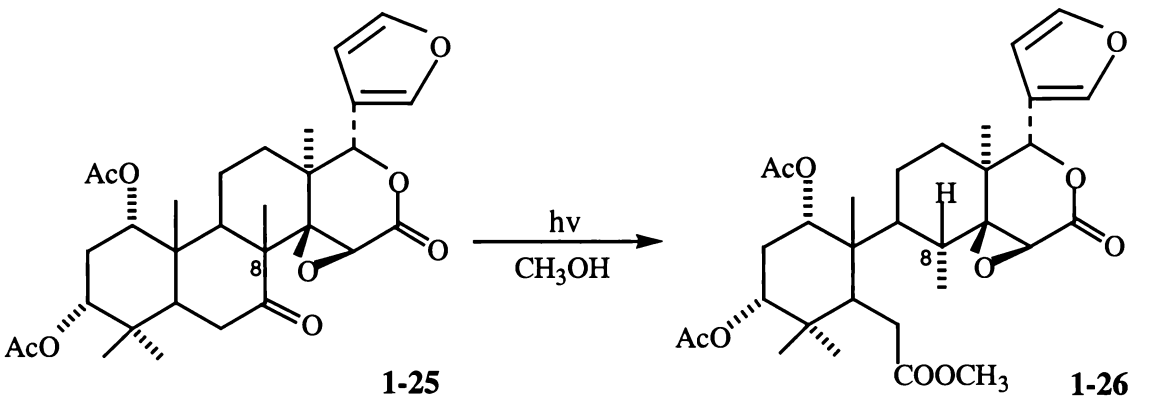

1-25 **1-26**

Scheme 2-11. Photolysis of 7-deacetoxy-7-oxokhivorin (**1-25**) to afford an inversion product at C-8 (**1-26**).

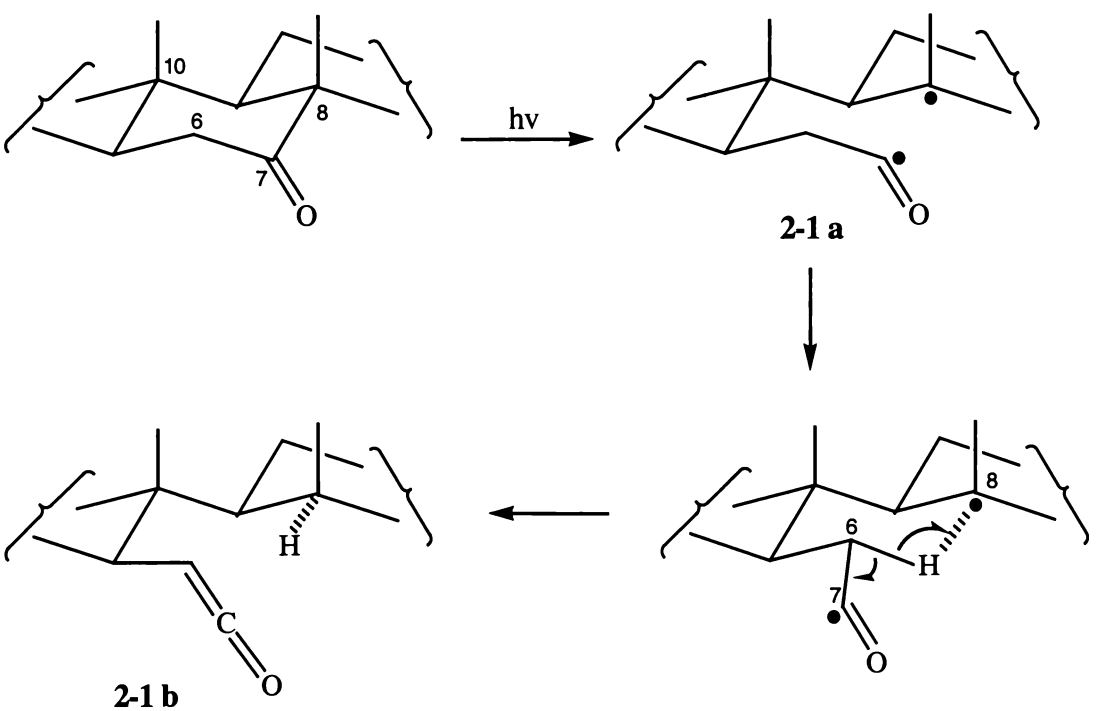

2-1 a **2-1 b**

Scheme 2-12. 1,5-Hydrogen transfer *via* a chair like conformation during the photochemical reaction of **2-1**.

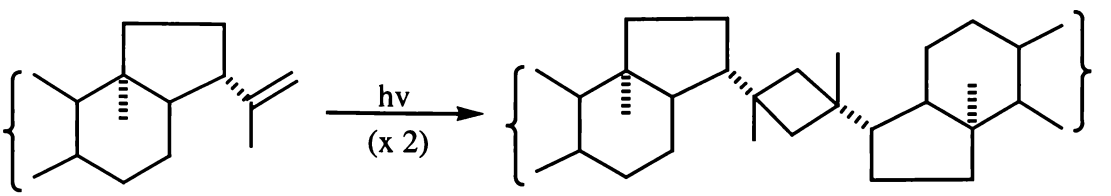

$\pi 2_S + \pi 2_S$ addition product

Scheme 2-13. Possible Woodward Hoffmann $\pi 2_S + \pi 2_S$ addition product arising from dimerisation of the 22(29)-double bond of hop-22(29)-en-7-one (**2-3**).

As noted in Section **2.3**, the possibility that in the absence of methanol, photolysis of 22-hydroxyhopan-7-one (**2-1**) might undergo a 1,7-hydrogen shift to afford a secoaldehyde (see scheme 2-14) was considered. The mass spectrum of one of the minor products (product 2) detected in the product mixture using GC/MS was consistent with the formation, in low yield, of secoaldehyde (**2-7**), however the presence of this compound was not confirmed by isolation.

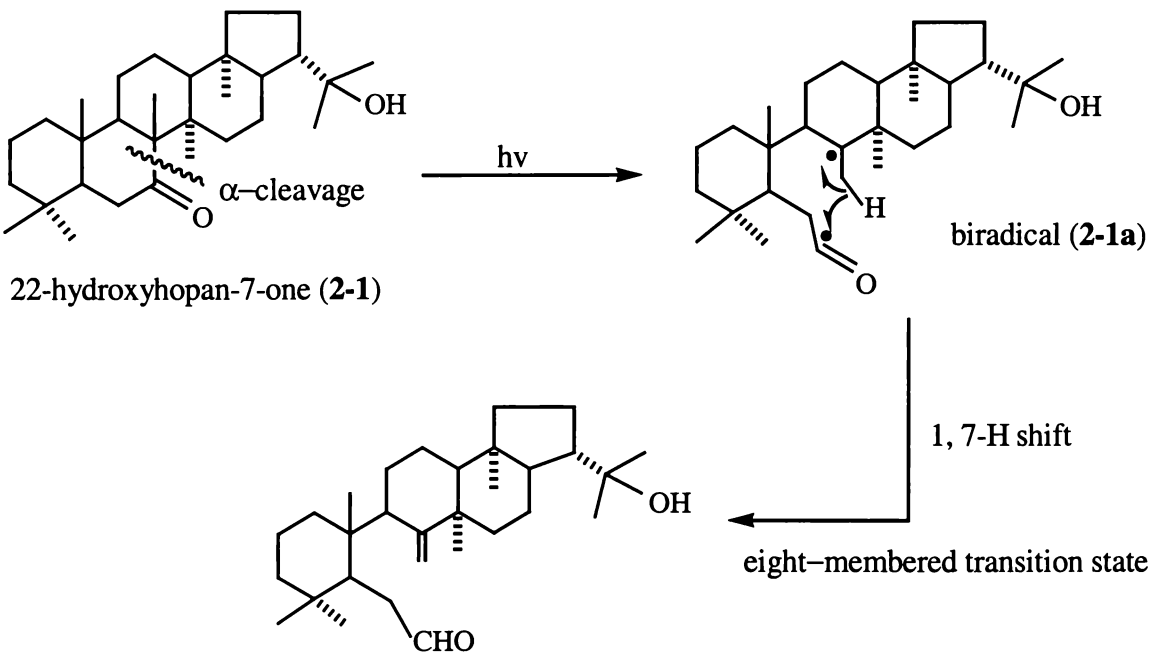

22-hydroxyhopan-7-one (**2-1**)

22-hydroxy-7,8-secohop-8(26)-en-7-al (**2-7**)

Scheme 2-14. Proposed pathways for the proposed photoproduct 2 (**2-7**) from 22-hydroxy-hopan-7-one (**2-1**) in the absence of an alcohol.

Chapter Three

Photochemical Reactions of Some 15-Oxohopanoids

3.1 Introduction

Photolysis of 22-hydroxyhopan-15-one (**3-1**) in benzene-methanol was first attempted by Hunter (1993), in a manner similar to that described in Chapter Two for 22-hydroxyhopan-7-one (**2-1**).

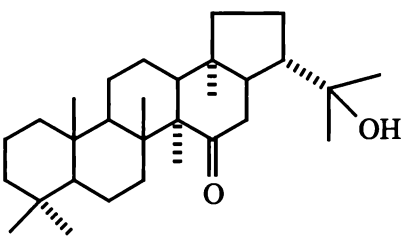

3-1

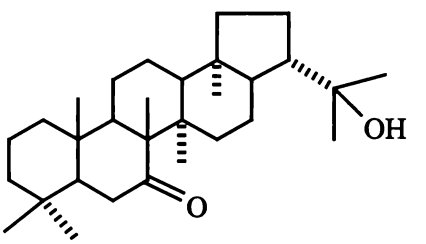

2-1

Hunter (1993) reported the formation of a complex mixture of products, which included the starting material and other several products. GC/MS analyses of the product mixture showed that one of the more dominant products exhibited a strong *m/z* 164 fragment ion, for which structure "a" was proposed (Figure 3-1). This ion can be envisaged as arising from a product generated *via* participation of the 22-hydroxyl group in the photolysis process, with the consequential formation of a 15,22-hemiacetal linkage (ie a new ring F system).

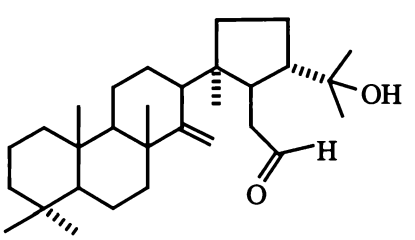

3-2

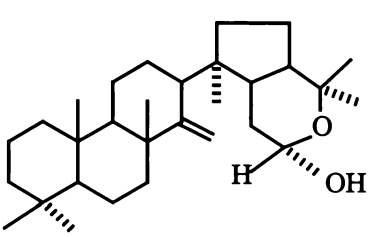

3-3

Hemiacetal (**3-3**) can be envisaged to have arisen from photoreaction of 22-hydroxy-hopan-15-one (**3-1**) to afford the unsaturated 14,15-secoaldehyde (**3-2**), which then cyclises with participation of the 22-hydroxyl group to give a hemiacetal (or a mixture of hemiacetals since C-15 is asymmetric) possessing structure (**3-3**).

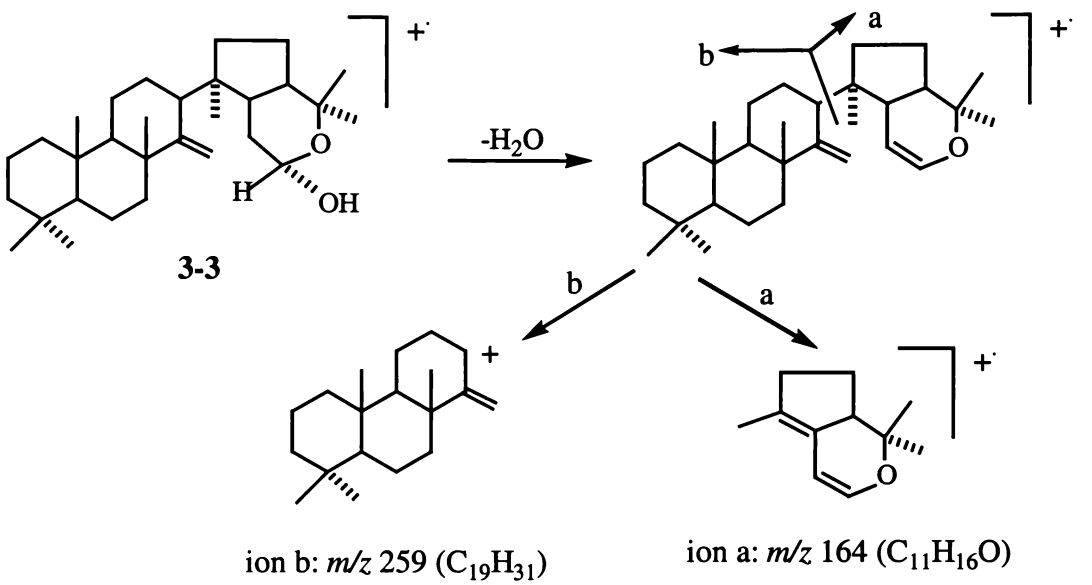

Figure 3-1. Proposed origin of the *m/z* 164 (ion a) and *m/z* 259 (ion b) fragment ions observed in the mass spectrum of hemiacetal (**3-3**).

In 1993, Hunter was not able to formally characterise the photoreaction product believed to be hemiacetal (**3-3**) and other companion products detected by GC/MS analyses, due to a combination of technical difficulties, including the failure of the UV lamp, unsuccessful attempts to separate the product mixture and time constraints.

The present investigation was undertaken in order that the supposed hemiacetal (**3-3**), and other companion products, might be isolated and formally characterised using modern one- and two-dimensional NMR techniques. The photoreactions of some other saturated and unsaturated 15-oxohopanoids, lacking a 22-hydroxyl group, were also investigated in the expectation that this would assist in defining the circumstances under which photolysis of 15-oxohopanoids proceeded with participation of the 22-hydroxyl group.

3.2 Photochemical Reactions of 22-Hydroxyhopan-15-one

3.2.1 Synthesis of 22-Hydroxyhopan-15-one (3-1)

22-Hydroxyhopan-15-one (**3-1**) was prepared from hopane-15α,22-diol (**3-4**), which was isolated from the lichen *Pseudocyphellaria homoeophylla*. Oxidation of hopane-15α,22-diol (**3-4**) with CrO_3 in pyridine, as described by Corbett & Young (1966b), afforded 22-hydroxyhopan-15-one (**3-1**).

3.2.2 Photolysis of 22-Hydroxyhopan-15-one (3-1) in

Solutions of 22-hydroxyhopan-15-one (**3-1**) in benzene-methanol (1:1), benzene-isopropanol (1:1), or neat benzene, were photolysed for 8 h at room temperature using a Hanovia 125 W medium pressure mercury lamp. In each case TLC analyses revealed the formation of complex mixtures of three or more products.

Unexpectedly (at least by analogy with outcomes observed for 22-hydroxyhopan-7-one (**2-1**)) (see Chapter Two), preliminary GC/MS analyses showed that reactions performed using benzene-methanol (1:1), benzene-isopropanol (1:1), or benzene, as solvents, afforded mixtures which contained (in the main) the same three product compounds. This indicated that alcohols such as methanol and isopropanol did not react with intermediate ketenes to afford the corresponding secoesters.

GC/MS analyses of the benzene-methanol product mixture revealed the apparent absence of a product exhibiting a molecular ion at *m/z* 456, attributable to the 14,15-secoester (Figure 3-2) analogous to the 7,8-secoester (**2-2**) generated on photolysis of 22-hydroxyhopan-7-one (**2-1**) (see Chapter two). Strong *m/z* 164 and *m/z* 181 fragment ions were observed in the mass spectra of some of the products.

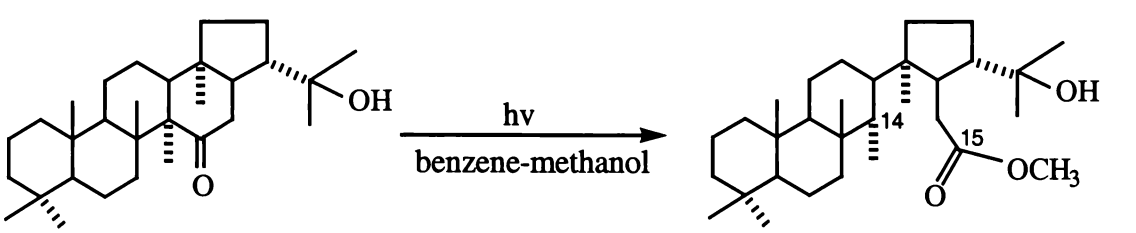

3–1 predicted product 14,15-secoester

Figure 3-2. Predicted photolysis product of 22-hydroxyhopan-15-one (**3-1**).

Separation of the product mixtures obtained on photolysis of 22-hydroxyhopan-15-one (**3-1**) in benzene-methanol, benzene-isopropanol, or benzene by radial PLC on silica gel afforded three products which were identified as 14,15-seco-15,22-*O*-*abeo*hop-14(27)-en-15α-ol (**3-3**) (m.p.168-170°C), 14,15-seco-15,22-*O*-*abeo*hop-14(27)-en-15-one (**3-5**) (m.p.174–178°C) and 14,15-seco-15,22-*O*-*abeo*hopa-14(27),15-diene (**3-6**) (m.p.144-147°C) (see Scheme 3-1), respectively.

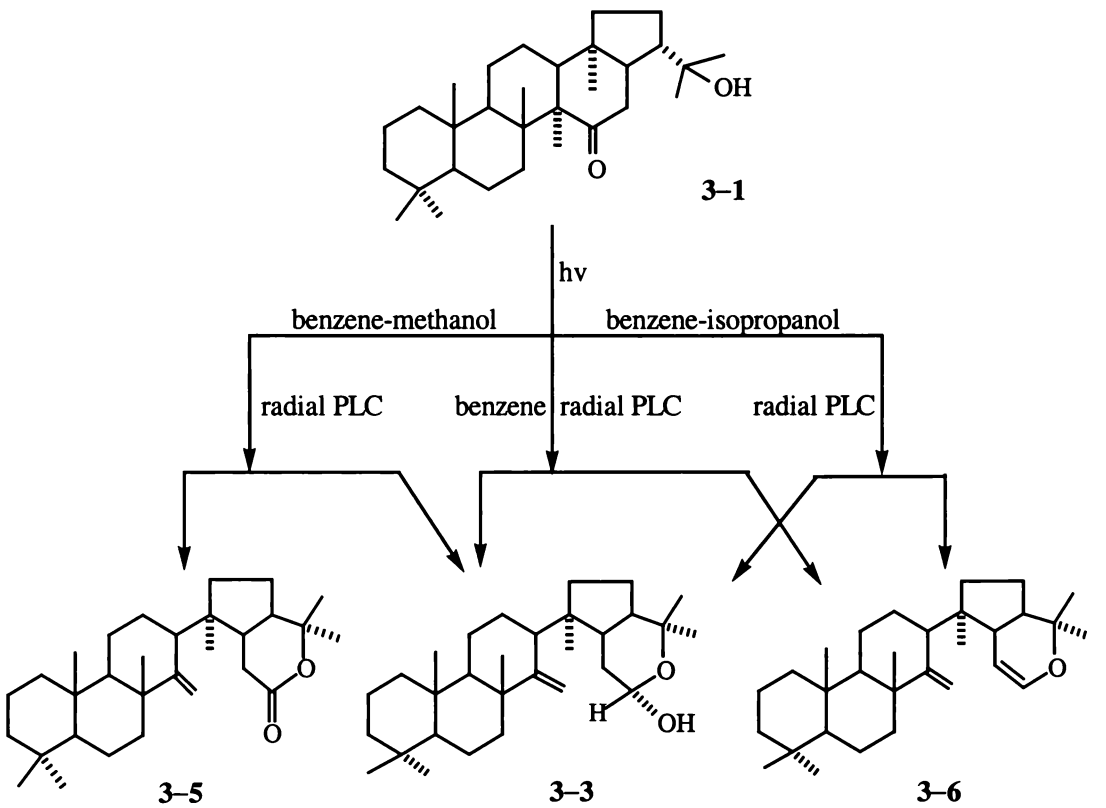

Scheme 3-1. Products obtained on photolysis of 22-hydroxyhopan-15-one (**3-1**).

3.3 Structural Elucidation of Photoreaction Products

The structures of the photoproducts (**3-3**), (**3-5**) and (**3-6**) were elucidated from analyses of mass spectral and one- and two-dimensional NMR spectral data determined for these compounds. The complete assignments of the ^{13}C and ^{1}H NMR signals of **3-3**, **3-5** and **3-6**, and the acetylation product (**3-7**), which was obtained on acetylation of **3-3** using pyridine-acetic anhydride, are presented in Tables 3-2 and 3-6.

These assignments can be compared with the ^{13}C and ^{1}H NMR assignments of **3-1** reported by Hunter (1993) (see Table 3-2).

3.3.1 14,15-Seco-15,22-*O*-*abeo*hop-14(27)-en-15α-ol (3-3)

3.3.1.1 Mass Spectral Analysis of Hemiacetal (3-3)

While the ^{13}C and ^{1}H NMR spectral data readily showed the presence of a 15-hydroxyl group in **3-3**, and were consistent with the molecular formula of **3-3** being $C_{30}H_{50}O_2$ (442 daltons) (see Section **3.3.1.2**), a fragment ion corresponding to the molecular ion of this compound was not observed in the mass spectrum of this compound.

Under GC/MS conditions the highest observed ion occurred at *m/z* 424. The mass spectrum of **3-3** also included a strong peak at *m/z* 164, considered to arise from ion a. The proposed origin of this fragment ion is shown in Scheme 3-2. This ion is considered to be indicative of a 14,15-secohopane possessing an additional ring F system, arising from a 15→22-*O*-linkage. Other structurally significant fragment ions are listed in Table 3-1.

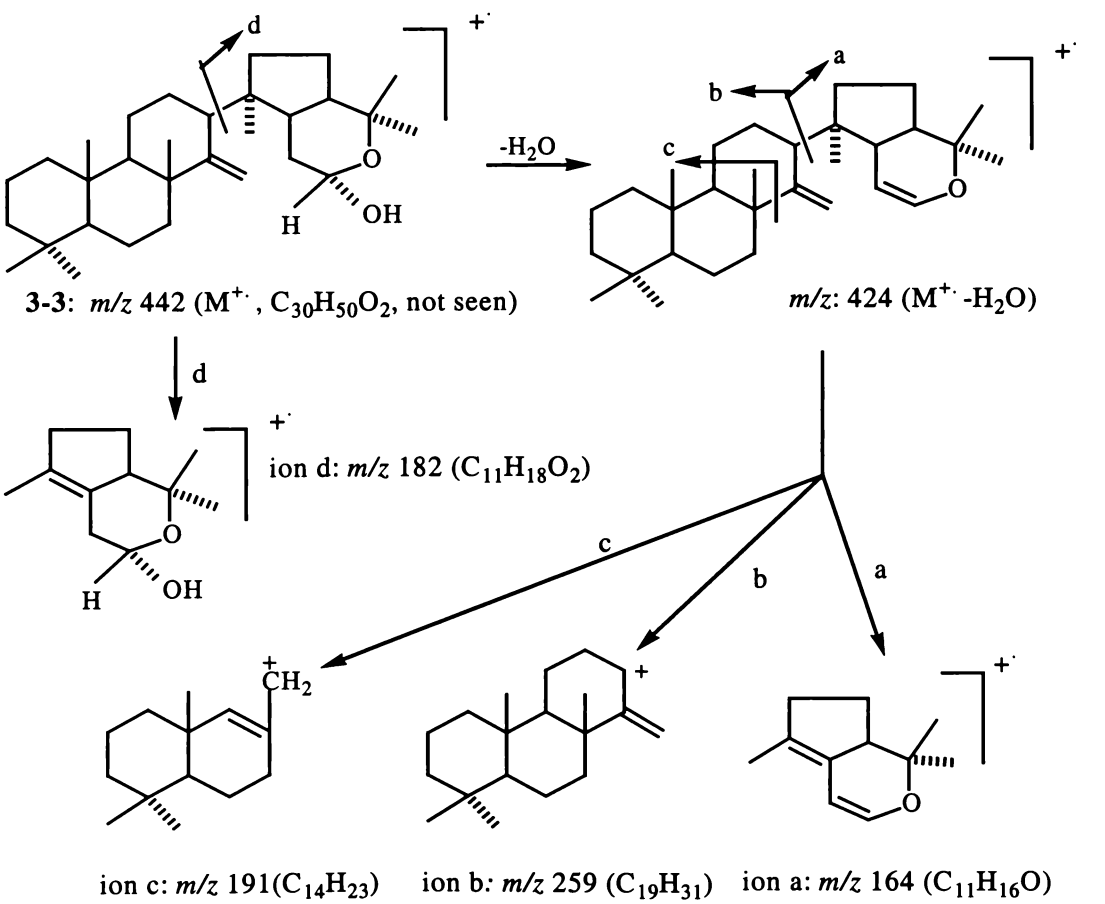

Scheme 3-2. Proposed mass spectral fragmentation pathways for 14,15-seco-15,22-*O*-*abeo*hop-14(27)-en-15α-ol (**3-3**).

Table 3-1. Selected mass spectral fragment ions observed for 14,15-seco-15,22-*O*-*abeo*hop-14(27)-en-15α-ol (**3-3**).

ions	*m/z* (% relative intensities)
M^+	442 (not seen)
M^+-H_2O	424 (0.2)
M^+-H_2O-CH_3	409 (1)
$C_{19}H_{31}^+$ (ion b)	259 (0.2)
$C_{14}H_{23}^+$ (ion c)	191 (0.4)
$C_{11}H_{18}O_2^{+\cdot}$ (ion d)	182 (2)
ion a	164 (100)
ion a-CH_3	149 (4)

3.3.1.2 NMR Spectral Analyses of Hemiacetal (3-3)

The complete assignment of the ^{13}C and ^1H NMR signals of **3-3**, presented in Table 3-2, was derived from the detailed analyses of one- and two-dimensional NMR spectral data determined for this compound. Signal assignments can be compared with those established in a like manner for **3-5** and **3-6** (Table 3-6), **3-7** (Table 3-2), and those reported by Hunter for **3-1** (Table 3-2).

^1H NMR Spectrum of Hemiacetal (3-3)

The 400 MHz ^1H NMR spectrum of hemiacetal (**3-3**) included signals attributable to seven tertiary methyl groups in the region of 0.80~1.35 ppm (one less than in the starting material), two olefinic protons at 4.83 ppm (br s) and 4.56 ppm (d, J = 1.4 Hz), a multiplet at 4.95 ppm (dd, J = 9.5, 2.6 Hz), and methylene or methine signals at 2.66 ppm (ddd, J = 13.1, 5.1, 5.1 Hz), 2.12 ppm (dd, J = 12.4, 2.3 Hz) and 1.94 ppm (dddd, J = 12.2, 3.2, 3.2, 3.2 Hz).

The chemical shift of the signal which occurred at 4.95 ppm was consistent with the presence of a hemiacetal {-O-CH(OH)-} group, rather than a secondary hydroxyl {-CH(OH)-} group, while the coupling constants exhibited by this signal (J = 9.5, 2.6 Hz) were consistent with the hydroxyl group being 15α-oriented and its companion methine proton therefore being 15β-oriented and coupled to a pair of methylene protons

which were axially and equatorially oriented with respect to the hemiacetal methine proton (see Figure 3-3).

Table 3-2. ^{13}C and ^{1}H NMR signals (δ ppm in $CDCl_3$) observed for 22-hydroxy-hopan-15-one (**3-1**), hemiacetal (**3-3**) and acetate (**3-7**).

atom	22-hydroxyhopan-15-one (3-1)			hemiacetal (3-3)			acetate (3-7)		
	^{13}C	$^{1}H_\alpha$	$^{1}H_\beta$	^{13}C	$^{1}H_\alpha$	$^{1}H_\beta$	^{13}C	$^{1}H_\alpha$	$^{1}H_\beta$
1	40.4 t	0.72 t	1.59 d	40.0 t	0.78 t	1.63 d	40.0 t	0.79 t	1.65 d
2	18.8 t	1.25-1.56*		18.7 t	1.38 d	1.58 t	18.8 t	1.41 d	1.59 t
3	42.0 t	1.07 t	1.30 d	42.2 t	1.11 t	1.36 d	42.2 t	1.14 t	1.38 d
4	33.2 s			33.4 s			33.4 s		
5	56.4 d	0.70 d		57.0 d	0.82 d		57.0 d	0.84 d	
6	18.8 t	1.25-1.58*		19.2 t	1.68 d	1.47 t	19.2 t	1.69 d	1.48 t
7	34.3 t	1.42 t	2.49 d	39.2 t	1.61 q	1.54 d	39.2 t	1.62 q	1.56 d
8	43.1 s			41.7 s			41.7 s		
9	51.8 d	1.10 d		60.2 d	0.92 d		60.2 d	0.94 d	
10	38.2 s			38.4 s			38.4 s		
11	21.4 t	1.58 d	1.20 q	22.4 t	1.75 d	1.35 t	22.4 t	1.75 d	1.38 q
12	24.0 t	1.68 q	1.46 d	30.8 t	1.12 q	1.94 dddd	30.7 t	1.13 q	1.95 dddd
13	50.6 d		1.68 d	47.4 d		2.12 dd	47.5 d		2.13 d
14	57.2 s			161.5 s			161.3 s		
15	214.8 s			91.7 d		4.95 dd	91.9 d		5.91 dd
16	41.3 t	2.78 t	2.59 d	32.1 t	1.13 q	1.71 d	29.0 t	1.34 q	1.68 d
17	51.0 d		1.79 t	39.6 d		2.66 ddd	39.6 d		2.74 ddd
18	44.1 s			46.5 s			47.4 s		
19	40.8 t	1.61 q	1.00 q	39.2 t	1.42 t	1.74 q	39.2 t	1.44 t	1.77 q
20	26.9 t	1.61 q	1.80 q	23.0 t	1.74 q	1.53 t	23.0 t	1.75 q	1.56 t
21	50.1 d		2.18 q	46.3 d		1.68 t	46.3 d		1.72 t
22	73.3 s			74.7 s			75.7 s		
23	33.4 q	0.80 s		33.5 q	0.87 s		33.5 q	0.87 s	
24	21.6 q	0.75 s		21.6 q	0.83 s		21.5 q	0.83 s	
25	15.9 q	0.77 s		16.2 q	0.86 d (0.8 Hz)		16.2 q	0.86 s	
26	19.4 q	1.00 s		22.3 q	1.00 s		22.3 q	1.00 s	
27	15.5 q	1.14 s		102.7 t	4.83 s	4.56 d (1.4 Hz)	102.9 t	4.83 s	4.54 s
28	16.0 q	0.91 s		17.9 q	0.98 s		18.0 q	0.98 s	
29	29.1 q	1.12 s		26.6 q	1.24 s (22β-Me)		26.3 q	1.30 s (22β-Me)	
30	31.1 q	1.16 s		28.5 q	1.18 s (22α-Me)		28.3 q	1.19 s (22α-Me)	
C=O							169.7 s		
OCH_3							21.6 q	2.10 s	

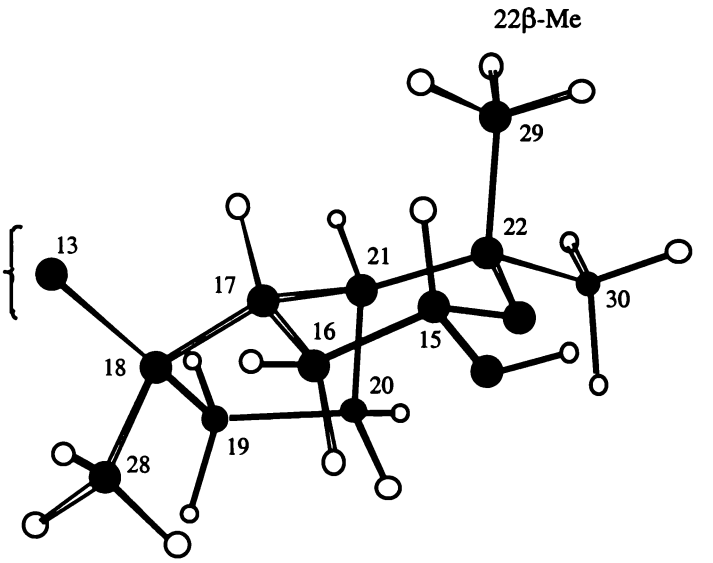

Figure 3-3. Proposed ring F conformation of hemiacetal (**3-3**).

COSY Spectrum of Hemiacetal (3-3)

The COSY spectrum of hemiacetal (**3-3**) included cross peaks arising from couplings between H-15β (4.95 ppm) and the adjacent H-16α (1.13 ppm) and H-16β (1.71 ppm) protons. H-13β (2.12 ppm) exhibited correlations to H-12α (1.12 ppm), H-12β (1.94 ppm) and H-17β (2.66 ppm), while the signal at 1.94 ppm (H-12β) also showed correlations to H-12α (1.12 ppm), H-11α (1.75 ppm), H-11β (1.35 ppm) and H-13β (2.12 ppm). This in turn allowed the corresponding carbon resonance to be identified *via* the correlation observed in the HSQC spectrum. Coupling constant information identified the signal at 1.94 ppm (dddd) as being attributable to H-12β since it experienced a large $^{2}J_{gem}$ (12.2 Hz) with H-12α, three smaller $^{3}J_{eq\text{-}ax}$ couplings (3.2 Hz) with H-13β and H-11α and H-11β.

Several of the methyl groups exhibited long range couplings to adjacent, 1,2-*trans* diaxially oriented methylene protons. Recognition of long range ^{4}J couplings greatly assisted the assignment of the methyl group resonances. In one case, the magnitude of the ^{4}J coupling (J = 0.8 Hz) was such that in the ^{1}H NMR of **3-3**, the10β-methyl group (0.86 ppm) appeared as a weakly coupled doublet. This coupling can be attributed to a ^{4}J coupling between H-25 and H-1α (Sanders & Hunter, 1987).

Table 3-3. Selected ^{1}H-^{1}H COSY correlations (δ ppm in $CDCl_3$) observed for 14,15-seco-15,22-*O*-*abeo*hop-14(27)-en-15α-ol (**3-3**).

^{1}H NMR signals	correlated ^{1}H signals
4.95 dd (H-15β)	2.66 ddd (H-17β)*, 1.71 d/1.13 q (H-16α/β)
4.83 br s (H-27a)	4.56 d (H-27b), 2.12 dd (H-13β)*, 1.61 q (H-7α)#
4.56 d (H-27b)	4.83 br s (H-27a), 2.12 dd (H-13β)*, 1.00 s (8β-Me)#
2.66 ddd (H-17β)	1.13 q/1.71 d (H-16α/β), 1.68 t (H-21β)
2.12 dd (H-13β)	4.83 br s/4.56 d (H-27a/b)*, 2.66 ddd (H-17β)*, 1.12 q/1.94 dddd (H-12α/β)
1.94 dddd (H-12β)	2.12 dd (H-13β), 1.75 d/1.35 t (H-11α/β), 1.12 q (H-12α)
1.71 d (H-16β)	4.95 dd (H-15β), 2.66 ddd (H-17β), 1.13 q (H-16α)
1.35 q (H-11β)	1.75 d (H-11α), 1.12 q/1.94 dddd (H-12α/β), 0.92 d (H-9α)
1.13 q (H-16α)	4.95 dd (H-15β), 2.66 ddd (H-17β), 1.71 d (H-16β)
1.00 s (8β-Me)	1.61 q (H-7α)*
0.92 d (H-9α)	1.75 d/1.35 t (H-11α/β)
0.82 d (H-5α)	1.68 d/1.47 t (H-6α/β)

* ^{4}J coupling , # ^{5}J coupling

^{13}C and DEPT135 NMR Spectra of Hemiacetal (3-3)

The ^{13}C NMR spectrum of **3-3** exhibited a total of thirty carbon signal resonances, which were characterised by a DEPT135 NMR spectrum to arise from 7 quartet (CH_3), 11 triplet (CH_2), 6 doublet (CH), and 6 singlet (C) carbons. The ^{13}C spectrum included signals attributable to an exocyclic methylene group (161.5 ppm, s, C-14; 102.7 ppm, t, C-27), a hemiacetal carbon (91.7 ppm, d, C-15), and an oxygenated quaternary carbon (74.7 ppm, s, C-22) (Table 3-2).

This data showed that a methyl carbon and a carbonyl carbon, present in the starting material (**3-1**), have been replaced in **3-3** by an exocyclic olefinic methylene carbon (102.7 ppm) and a hemiacetal methine carbon (91.7 ppm).

It was also consistent with the molecular formula of **3-3** being $C_{30}H_{50}O_2$ (442 daltons), rather than $C_{30}H_{48}O$ (424 daltons), as might be inferred from the highest observed mass spectral ion (see Section **3.2.4.1**).

The introduction into **3-3** of a 14(27)-double bond led to C-9 (60.2 ppm), C-12 (30.8 ppm) and C-7 (39.2 ppm) experiencing marked downfield shifts of 8.4, 6.8 and 4.9 ppm respectively relative to their positions in **3-1**, and to C-11 (22.4 ppm) exhibiting small downfield shifts of 1.0 ppm, while C-13 (47.4 ppm) and C-8 (41.7 ppm) exhibited only slight upfield shifts of 3.2 and 1.4 ppm respectively (Table 3-2).

The formation of a 15,22-*O*-*abeo* ring (ring F), and the removal of the 15-carbonyl group led to significant changes in the resonance positions for some of the ring E and F carbons, compared to their resonance positions in **3-1**.

For example, C-17 (39.6 ppm) and C-16 (32.1 ppm) exhibited significant upfield shifts of 10.4 and 9.2 ppm respectively, while C-20 (23.0 ppm), C-21 (46.3 ppm), C-29 (26.6 ppm) and C-30 (28.5 ppm) showed small upfield shifts (3.9, 3.8, 2.5 and 2.6 ppm respectively). Amongst the ring E/F carbons only C-18 (46.5 ppm) and C-28 (17.9 ppm) experienced small downfield shifts of 2.4 and 1.9 ppm, respectively compared to the equivalent resonances of **3-1** (Table 3-2).

HMBC and HSQC Spectra of Hemiacetal (3-3)

Correlations observed in the HMBC and HSQC spectra (see Figure 3-5 and Figure 3-6) greatly facilitated the complete assignment of the ^{13}C and ^{1}H NMR signals of **3-3**. Selected HMBC correlations observed for **3-3** are depicted in Figure 3-4.

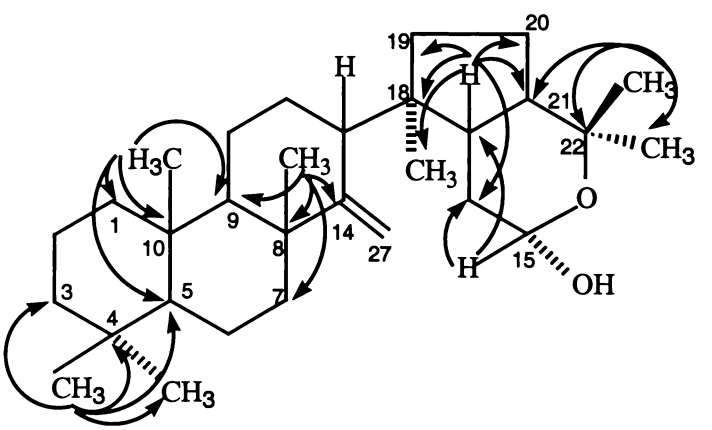

Figure 3-4. Selected HMBC correlations of the methyl groups and some methine protons observed for hemiacetal (**3-3**).

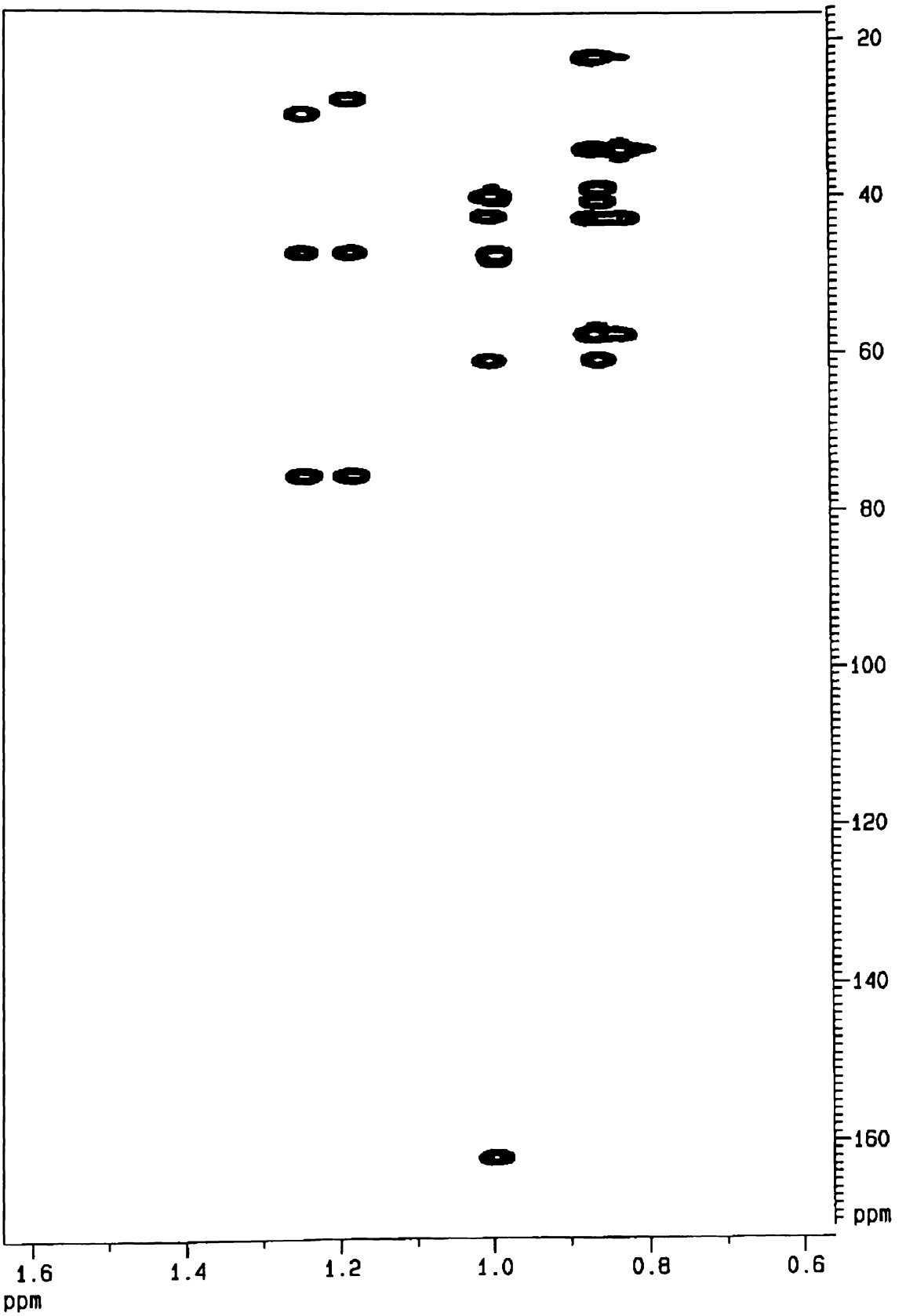

Figure 3-5. Selected HMBC correlations (the methyl group region) observed for hemiacetal (**3-3**).

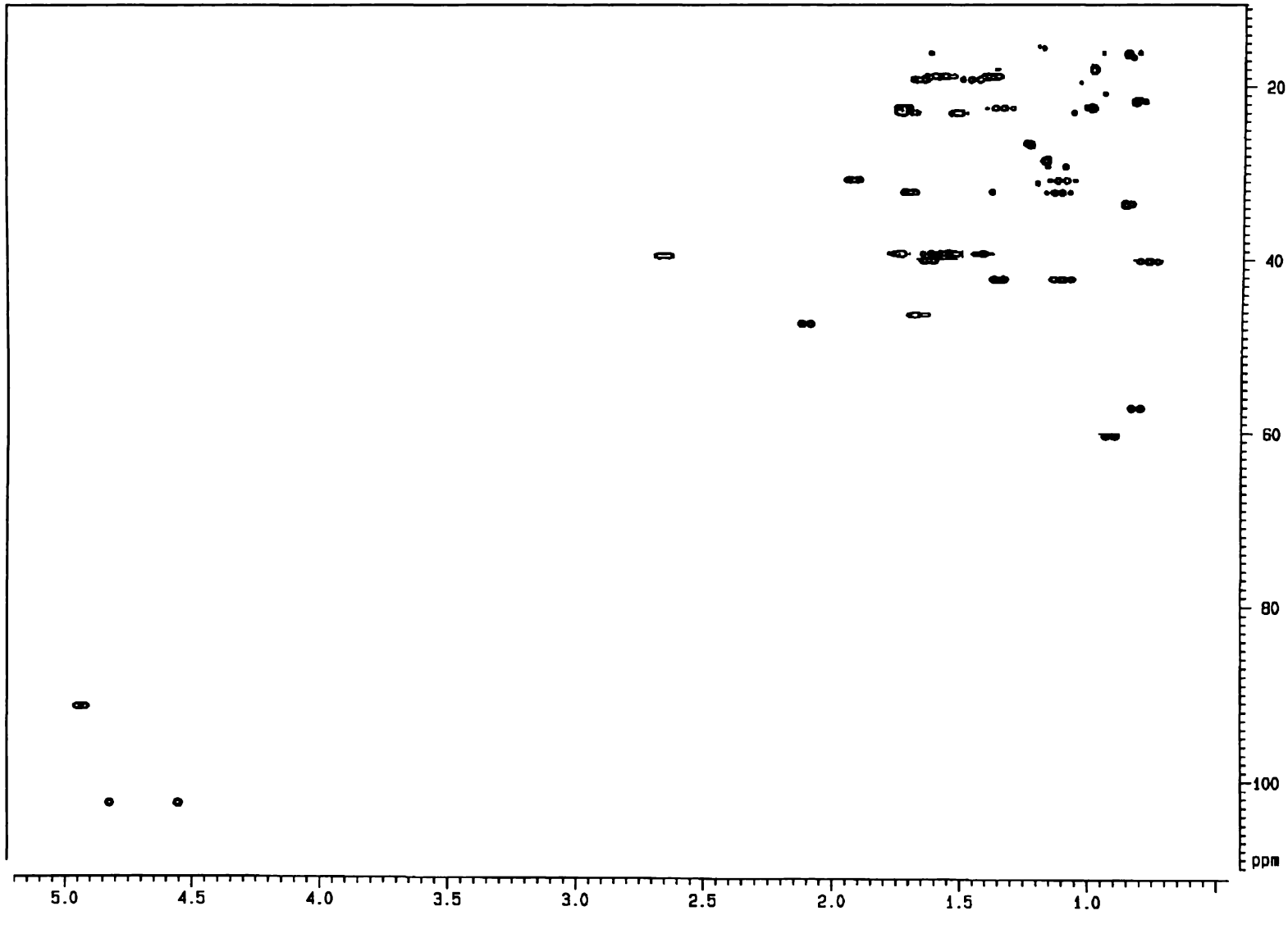

Figure 3-6. HSQC spectrum determined for hemiacetal (**3-3**).

Methyl group assignments

The ^{1}H and ^{13}C NMR signal assignments of the methyl groups were derived predominantly from analyses of HSQC and HMBC spectral data.

The protons of three methyl groups (H-25, H-26 and H-28) exhibited correlations to different quaternary carbons (C-10, C-8 and C-18 respectively), while two pairs of methyl groups (H-23/H-24, and H-29/H-30) exhibited correlations to the same quaternary carbons (C-4 and C-22 respectively). Further points of distinction were that (i) H-23, H-24 and H-25 each exhibited an HMBC correlation to C-5 (57.0 ppm); (ii) both H-25 and H-26 exhibited HMBC correlations to C-9 (60.2 ppm); (iii) both H-26 and H-27 showed HMBC correlations to C-8 (41.7 ppm) and C-14 (161.5 ppm) and (iv) H-15β and H-17β exhibited a correlation to C-16 (32.1 ppm).

Structurally significant correlations observed for the methyl groups, and some other protons of **3-3** are presented in Table 3-4. Identification of the methyl group resonances *via* their unique HMBC correlation patterns led in turn to the assignment of the corresponding ^{13}C resonances *via* correlations observed in the HSQC spectrum of **3-3** (see Table 3-2).

Methine proton assignments

The HSQC spectrum of **3-3** showed that H-15 (4.95 ppm) correlated with the ^{13}C signal which occurred at 91.7 ppm, while in the HMBC spectrum, this proton exhibited correlations to C-16 (32.1 ppm) and C-17 (39.6 ppm).

The five remaining methine protons of **3-3** were easily identified from a combination of HMBC correlations (see Table 3-4) and analyses of coupling patterns observed in the 400 MHz ^{1}H NMR spectrum of **3-3**. This information revealed the ^{13}C assignments of the methine carbons *via* correlations observed in the HSQC spectrum.

For example, the methine signal which resonated at 2.66 ppm (ddd, J = 13.1, 5.1, 5.1 Hz), exhibited HMBC correlations to C-13 (47.4 ppm), C-16 (32.1 ppm), C-18 (46.5 ppm), C-19 (39.2 ppm), C-20 (23.0 ppm) and C-21 (46.3 ppm), and was therefore assigned to H-17β. The corresponding H-17β resonance of **3-1** occurred at 1.79 ppm (0.87 ppm upfield of its position in **3-3**).

In a like manner, the methine proton signal at 2.12 ppm was assigned to H-13β since it exhibited a large coupling to H-12α ($^3J_{ax\text{-}ax}$ = 12.4 Hz) and a small coupling constant ($^3J_{ax\text{-}eq}$ = 2.3 Hz) to H-12β, while the carbon signal at 47.4 ppm to which this proton was correlated exhibited an HMBC correlation to H-28 (0.98 ppm).

Table 3-4. ^1J, ^2J and ^3J heteronuclear ^{1}H-^{13}C correlations (δ ppm in $CDCl_3$) observed for 14,15-seco-15,22-*O*-*abeo*hop-14(27)-en-15α-ol (**3-3**).

^{1}H signal	^1J correlated ^{13}C signal	^2J and ^3J correlated ^{13}C signals
0.87 s (4α-Me)	33.5 (C-23)	57.0 (C-5), 42.2 (C-3), 33.4 (C-4), 21.6 (C-24)
0.83 s (4β-Me)	21.6 (C-24)	57.0 (C-5), 42.2 (C-3), 33.4 (C-4), 33.5 (C-23)
0.86 d (10β-Me)	16.2 (C-25)	60.2 (C-9), 57.0 (C-5), 40.0 (C-1), 38.4 (C-10)
1.00 s (8β-Me)	22.3 (C-26)	161.5 (C-14), 60.2 (C-9), 41.7 (C-8), 39.2 (C-7)
0.98 s (18α-Me)	17.9 (C-28)	47.4 (C-13), 46.5 (C-18), 39.6 (C-17), 39.2 (C-19)
1.24 s (22β-Me)	26.6 (C-29)	74.7 (C-22), 46.3 (C-21), 28.5 (C-30)
1.18 s (22α-Me)	28.5 (C-30)	74.7 (C-22), 46.3 (C-21), 26.6 (C-29)
1.94 dddd (H-12β)	30.8 (C-12)	161.5 (C-14), 60.2 (C-9), 47.4 (C-13), 22.4 (C-11)
2.12 dd (H-13β)	47.4 (C-13)	161.5 (C-14), 102.7 (C-27), 46.5 (C-18), 41.7 (C-8) 39.6 (C-17), 30.8 (C-12), 22.4 (C-11), 17.9 (C-28)*
2.66 ddd (H-17β)	39.6 (C-17)	47.4 (C-13) 46.5 (C-18), 46.3 (C-21), 39.2 (C-19) 32.1 (C-16), 23.0 (C-20)
4.56 d (H-27b)	102.7 (C-27)	161.5 (C-14), 60.2 (C-9)*, 47.4 (C-13), 41.7 (C-8) 39.2 (C-7)*, 30.8 (C-12)*, 22.4 (C-11)#
4.83 br s (H-27a)	102.7 (C-27)	161.5 (C-14), 47.4 (C-13), 60.2 (C-9)*, 41.7 (C-8) 30.8 (C-12)*, 22.4 (C-11)#
4.95 dd (H-15β)	91.7 (C-15)	39.6 (C-17), 32.1 (C-16)

* ^4J coupling , # ^5J coupling

Methylene proton assignments

The HSQC spectrum of **3-3** showed that the signals at 4.83 ppm (br s) and 4.56 ppm (d, J = 1.4 Hz) were attached to the olefinic carbon (C-27) which resonated at 102.7 ppm.

As noted in Section **2.2.2.2**, the resolution HSQC spectrum was such that large axial-axial or geminal couplings of the order J = 10~16 Hz could be resolved, whereas smaller equatorial-equatorial or axial-equatorial couplings of the order J = 3~5 Hz were

not resolved. This information, in combination with COSY and HMBC correlations, was used to assign the resonances of the majority of axial and equatorial methylene protons. For example, H-25 (0.86 ppm) exhibited an HMBC correlation to C-1 (40.0 ppm) (see Figure 3-7) which in turn exhibited correlations in the HSQC spectrum to proton signals, which occurred at 0.78 ppm and 1.63 ppm.

The signal at 0.78 (~t) ppm was assignable to H-1α (in an axial position) since it would be expected to exhibit large $^{2}J_{\text{H-1α-H-1β}}$ and $^{3}J_{\text{H-1α-H-2β}}$ couplings with H-1β and H-2β respectively, whereas the signal at 1.63 (~d) was expected to only exhibit a large $^{2}J_{\text{H-1β-H-1α}}$ coupling.

Zhao (1983) has noted that, in a cyclohexane system with a chair conformation, axial protons normally experience larger shieldings than equatorial protons and therefore exhibit smaller chemical shifts (ca. 0.2~0.5 ppm) than those in equatorial positions.

The complete assignment of the methylene and methine protons of **3-3**, presented in Table 3-2, can be compared with those previously reported by Hunter (1993).

The marked difference in the resonance of the H-7β (1.54 ppm) signal of **3-3**, compared to that of this proton in **3-1** (2.49 ppm), can be attributed to it no longer being located within the anisotropic deshielding zone of the 15-carbonyl group of **3-1**.

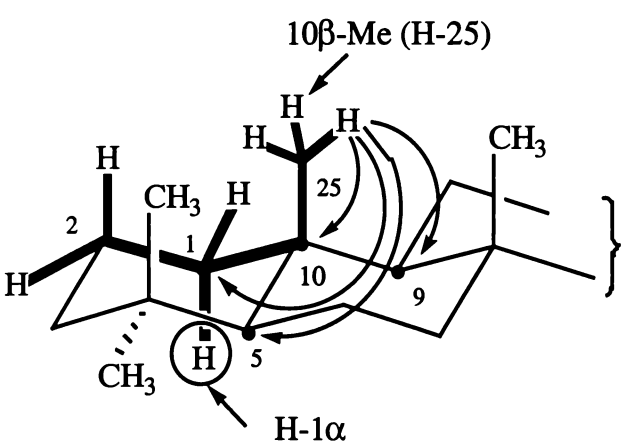

Figure 3-7. Ring A/B structure of **3-3** showing ^{2}J, ^{3}J and ^{4}J couplings exhibited by H-25 (10β-methyl group protons) and the ^{4}J COSY correlation between H-25 and H-1α (bold type).

NOESY Spectrum and Molecular Modelling Analyses of Hemiacetal (3-3)

Analyses of the phase sensitive NOESY spectral data determined for **3-3** were facilitated by the results of a molecular modelling investigation, performed using MacroModel and Chem3D Plus software (see Chapter Six).

Initial refinements afforded a twist boat conformation for ring F (steric energy E = 93.0 KCal), however this proved to be a local minimum. Further refinements (with manual re-positioning of ring F atoms in a chair like orientation prior to continued refinements) afforded a structure with an appreciably lower steric energy (E = 80.2 KCal) in which ring F adopted a ring chair conformation. The modelled conformation determined for **3-3** is depicted in Figure 3-8. The chair-like conformation of the 15,22-*O*-*abeo* ring is shown in Figure 3-9.

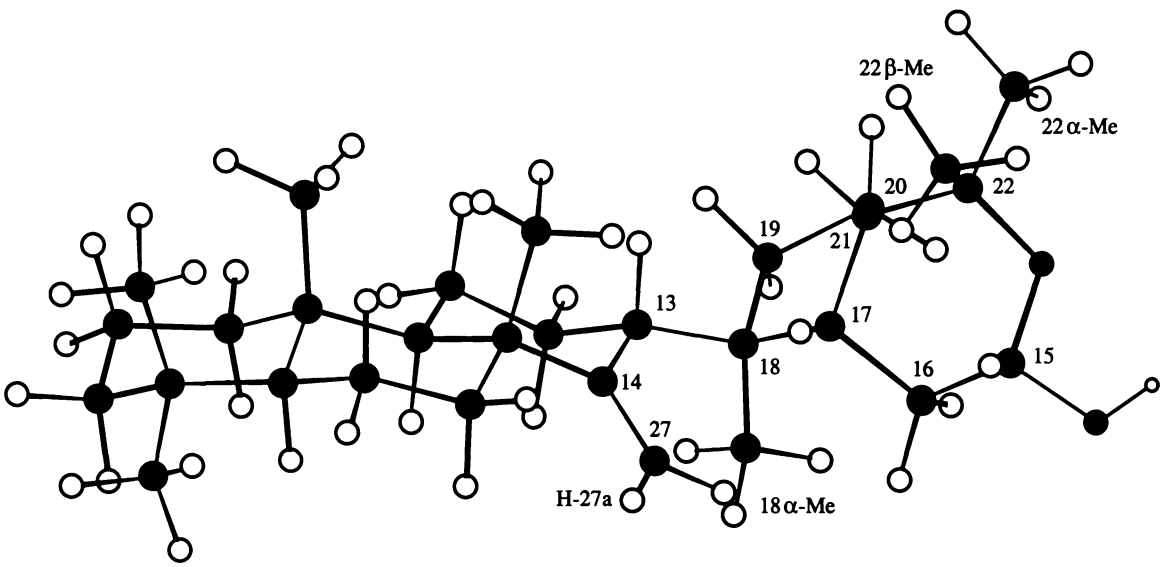

Figure 3-8. MM2 modelled conformation determined for hemiacetal (**3-3**).

H-15β exhibited NOESY correlations, which were consistent with the MM2 modelled conformation determined for **3-3**. Specifically, H-15β (4.95 ppm) exhibited correlations to H-16β (1.71 ppm), H-17β (2.66 ppm) and 22β-methyl group (1.24 ppm) (see Figure 3-9). The correlation between H-15β and the 22β-methyl group had particular significance in that it was consistent with the formation of a 15,22-*O*-*abeo* ring system.

The resonances of H-16α (1.13 ppm,) and H-16β (1.71 ppm,) were consequentially assigned from combination of coupling constants, COSY, HSQC and NOESY data. The coupling constants exhibited by H-15β ($^3J_{H\text{-}15\beta\text{–}H\text{-}16\alpha}$ = 9.5 Hz; $^3J_{H\text{-}15\beta H\text{-}16\beta}$ = 2.6 Hz) were consistent with those predicted by the generalised Karplus equations for dihedral angles of *ca.*174 and 59 degrees respectively.

The multiplicity of the H-17β signal (2.66 ppm, ddd, J = 13.1, 5.1, 5.1 Hz) was also consistent with the modelled conformation presented in Figure 3-8 since H-17β would be expected to exhibit a large ^3J coupling (J = 13.1 Hz) with H-16α, and lesser couplings (J = 5.1 Hz) with H-16β and H-21β. The dihedral angles from the MM2 model (Figure 3-9) were 175, 55 and 46° respectively.

The orientation of the H-27 protons was revealed by the analyses of NOESY spectral data. H-27b (4.56 ppm) exhibited correlations to H-27a (4.83 ppm), H-16β (1.71 ppm), H-17β (2.66 ppm) and 18α-methyl group (0.98 ppm) (see Figure 3-10). These correlations were consistent with modelled inter-nuclear distances of 1.83, 2.18, 2.32, and 2.11 Å, respectively.

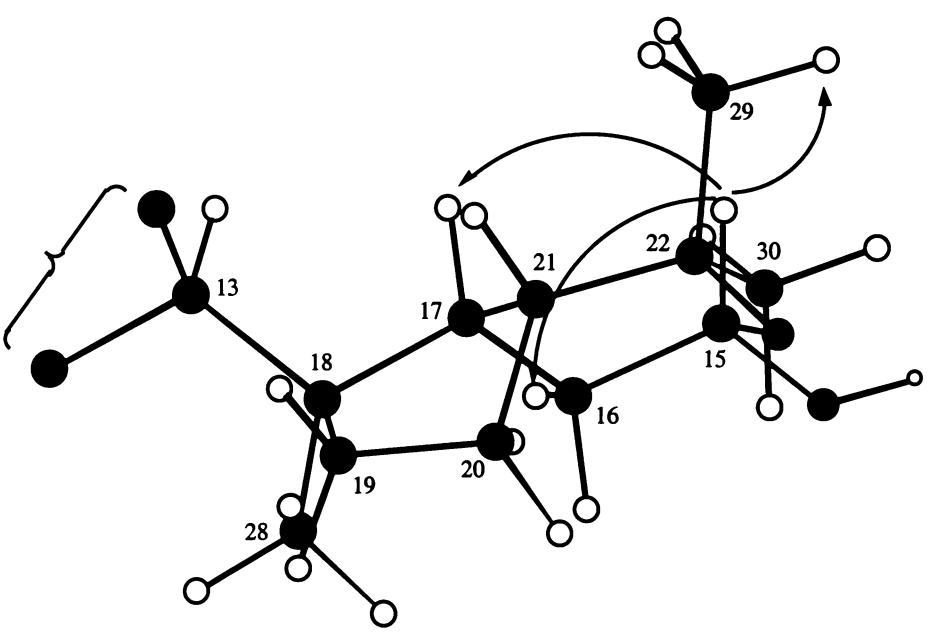

Figure 3-9. MM2 modelled conformation determined for rings E and F of **3-3**, showing NOESY correlations exhibited by H-15β.

On the other hand, H-27a (4.83 ppm) only exhibited correlations to H-27b (4.56 ppm) and H-7α/7β (1.56~162 ppm) (see Figure 3-10). The modelled inter-nuclear distance between these protons was 1.83, 2.23 and 2.27 Å, respectively.

Mutual NOESY correlations were observed between the 4β-methyl (0.83 ppm), 10β-methyl (0.86 ppm) and 8β-methyl (1.00 ppm) groups (see Figure 3-10). Other structurally significant NOESY correlations are presented in Table 3-5.

Table 3-5. Selected ^{1}H-^{1}H NOESY correlations (δ ppm in $CDCl_3$) observed for 14,15-seco-15,22-*O*-*abeo*hop-14(27)-en-15α-ol (**3-3**).

^{1}H NMR signal(s)	correlated ^{1}H signals
4.95 dd (H-15β)	2.66 ddd (H-17β), 1.71 d (H-16β), 1.24 s (22β-Me)
4.83 br s (H-27a)	4.56 d (H-27b), 1.61 q/1.54 d (H-7α/β)
4.56 d (H-27b)	4.83 br s (H-27a), 2.66 ddd (H-17β), 1.71 d (H-16β), 0.98 s (18α-Me)
2.66 ddd (H-17β)	4.95 dd (H-15β), 4.56 d (H-27b), 2.12 dd (H-13β), 1.68 t (H-21β) 1.24 s (22β-Me), 1.13 q/1.71 d (H-16α/β)
2.12 dd (H-13β)	2.66 ddd (H-17β), 1.74 q (H-19β), 1.35 t (H-11β) 1.12 q/1.94 dddd (H-12α/β), 1.00 s (8β-Me)
1.94 dddd (H-12β)	2.12 dd (H-13β), 1.75 d/1.35 t (H-11α/β), 1.12 q (H-12α), 0.98 s (18α-Me)
1.71 d (H-16β)	4.95 dd (H-15β), 4.56 d (H-27b), 2.66 ddd (H-17β), 1.13 q (H-16α) 0.98 s (18α-Me)
1.35 q (H-11β)	2.12 dd (H-13β), 1.75 d (H-11α), 1.12 q /1.94dddd (H-12α/β) 1.00 s (8β-Me), 0.86 s (10β-Me)
1.24 s (22β-Me)	1.18 s (22α-Me), 4.95 dd (H-15β), 2.66 ddd (H-17β), 1.68 t (H-21β)
1.00 s (8β-Me)	0.86 d (10β-Me), 2.12 dd (H-13β), 1.47 t (H-6β), 1.54 d (H-7β)
0.98 s (18α-Me)	4.56 d (H-27b), 1.42 t (H-19α), 1.71 d (H-16β), 1.12 q/1.94 dddd (H-12α/β)
0.87 s (4α-Me)	0.83 s (4β-Me), 1.68 d (H-6α), 1.11 t/1.36 d (H-3α/β), 0.82 d (H-5α)
0.86 d (10β-Me)	1.00 s (8β-Me), 0.83 s (4β-Me), 1.58 t (H-2β), 1.47 t (H-6β), 1.35 q (H-11β)

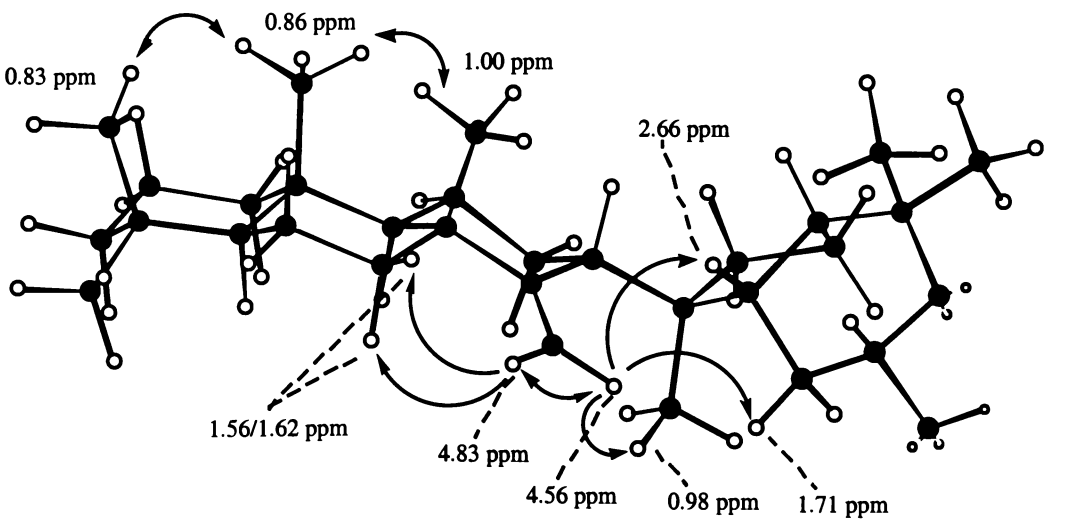

Figure 3-10. Selected NOESY correlations observed for hemiacetal (**3-3**).

3.3.2 Acetylation of 14,15-Seco-15,22-*O*-*abeo*hop-14(27)-en-15α-ol (3-3)

Acetylation of **3-3** with acetic anhydride and pyridine afforded the corresponding acetate product 15α-acetoxy-14,15-seco-15,22-*O*-*abeo*hop-14(27)-ene (**3-7**). This compound exhibited mass spectral and NMR spectral data which corresponded closely to that determined for hemiacetal (**3-3**).

3.3.2.1 Mass Spectral Analysis of Acetate (3-7)

The highest observed ion in the mass spectrum of the acetate (**3-7**), $C_{32}H_{52}O_3$ (molecular weight 484 daltons), appeared at *m/z* 424. This ion can be attributed to the loss of acetic acid (CH_3COOH). The mass spectrum of **3-7**, which was dominated by an *m/z* 164 ion (see Table 3-6), showed a similar series of fragment ions (see Scheme 3-3) to those observed for hemiacetal (**3-3**) (see Table 3-1 and Scheme 3-2).

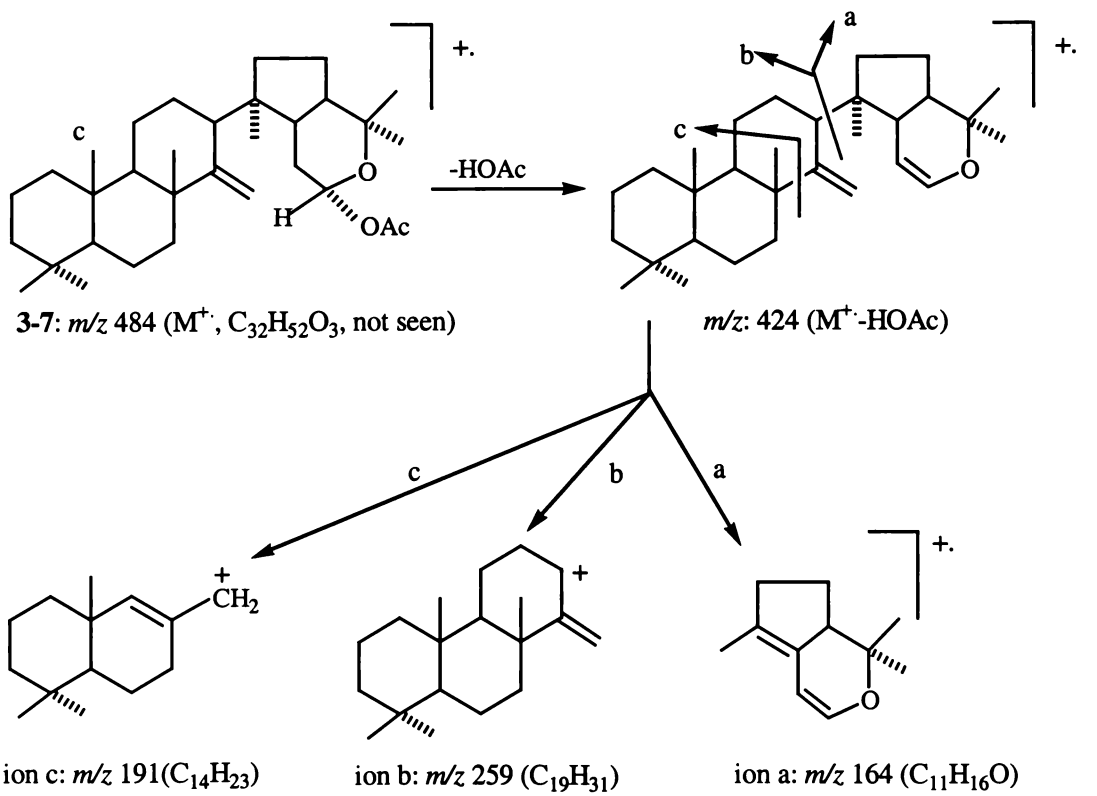

Scheme 3-3. Proposed mass spectral fragmentation pathways for 15α-acetoxy-14,15-seco-15,22-*O*-*abeo*hop-14(27)-ene (**3-7**).

Table 3-6. Selected mass spectral fragment ions observed for 15α-acetoxy-14,15-seco-15,22-*O*-*abeo*hop-14(27)-ene (**3-7**).

ions	*m/z* (% relative intensities)
M^+	484 (not seen)
M^+–HOAc	424 (0.2)
M^+– HOAc –CH_3	409 (1)
$C_{19}H_{31}^+$ (ion b)	259 (0.2)
$C_{14}H_{23}^+$ (ion c)	191 (0.6)
ion c–CH_3	177 (2)
ion a	164 (100)
ion a – CH_3	149 (5)

3.3.2.2 NMR Spectral Analyses of Acetate (3-7)

^{1}H NMR Spectrum of Acetate (3-7)

The ^{1}H NMR spectrum of **3-7** included signals attributable to 7 tertiary methyl groups in the region 0.70~1.30 ppm (see Table 3-2), two olefinic protons at 4.83 ppm (br s) and 4.54 ppm (br s), and an acetoxyl group (2.10 ppm). Downfield multiplets attributable to H-15β, H-17β and H-13β appeared at 5.91 ppm (dd, J = 10.3, 2.4 Hz), 2.74 ppm (ddd, J =13.5, 5.3, 5.3 Hz) and 2.13 ppm (d, J = 10.0 Hz) respectively.

Compared to the equivalent resonances of **3-3**, H-15β, H-16α and H-17β exhibited downfield shifts of 0.96, 0.21 and 0.08 ppm respectively, while H-16β experienced a modest upfield of 0.03 ppm. These differences can be attributed to the introduction of an acetoxyl group at C-15. With the exception only of the 22β-methyl group, which experienced a downfield shift (from 1.24 ppm in **3-3** compared to 1.30 ppm in **3-7**), the remaining proton resonances corresponded closely to those determined for **3-3** (see Table 3-2). These assignments were consistent with correlations observed in the COSY spectrum of **3-7** (see Table 3-7).

COSY Spectrum of Acetate (3-7)

The COSY correlations exhibited by **3-7** were similar to those observed for **3-3**, other than for chemical shift differences attributable to the presence of a 15α-acetoxyl group. In particular H-15β (5.91 ppm) correlated with H-17b (2.74 ppm), H-16α (1.34 ppm) and H-16β (1.68 ppm). Some other COSY correlations observed for **3-7** are presented in Table 3-7.

Table 3-7. Selected ^{1}H-^{1}H COSY correlations (δ ppm in $CDCl_3$) observed for 15α-acetoxy-14,15-seco-15,22-*O*-*abeo*hop-14(27)-ene (**3-7**).

^{1}H NMR signals	correlated ^{1}H signals
5.91 dd (H-15β)	2.74 ddd (H-17β)*, 1.34 q/1.68 d (H-16α/β)
4.83 br s (H-27a)	4.54 s (H-27b), 2.13 d (H-13β)*, 1.00 (8β-Me)#
4.54 br s (H-27b)	4.83 s (H-27a), 2.13 d (H-13β)*, 1.00 (8β-Me)#
2.74 ddd (H-17β)	1.72 t (H-21β), 1.34 q/1.68 d (H-16α/β)
2.13 d (H-13β)	4.83 br s/4.54 br s (H-27a/b)*, 1.13 q/1.95 dddd (H-12α/β)
1.95 dddd (H-12β)	2.13 d (H-13β), 1.75 d/1.38 q (H-11α/β), 1.13 q (H-12α)
1.75 d (H-11α)	1.38 q (H-11β), 1.13 q/1.95 dddd (H-12α/β), 0.94 d (H-9α)
1.68 d (H-16β)	5.91 dd (H-15β), 2.74 ddd (H-17β), 1.34 q (H-16α)
1.34 q (H-16α)	4 ddd (H-17β), 1.68 d (H-16β)

* ^{4}J coupling, # ^{5}J coupling

^{13}C and DEPT135 NMR Spectra of Acetate (3-7)

The ^{13}C NMR spectrum of **3-7** was comprised of 32 carbon resonances which were characterised by a DEPT135 NMR spectrum to arise from 7 quartet (CH_3), 11 triplet (CH_2), 6 doublet (CH), and 6 singlet (C) carbons. The ^{13}C NMR spectrum included signals assignable to the methyl and carbonyl carbons of an acetoxyl group (21.6 ppm, q; 169.7 ppm, s). The HMBC spectrum showed that the acetoxyl carbonyl carbon signal (169.7 ppm) correlated with the ^{1}H NMR signal which occurred at 2.13 ppm.

A complete assignment of the ^{13}C and ^{1}H NMR signals of **3-7** (see Table 3-2) was achieved in a manner analogous to that described for **3-3**. HMBC correlations observed for the methyl groups and some protons of **3-7** are presented in Table 3-8.

Amongst the carbon signals, only C-16 (29.0 ppm), C-18 (47.4 ppm) and C-22 (75.7 ppm) exhibited shifts, which differed similarly from those observed for the corresponding carbon signals of **3-3**, which resonated at 32.1, 46.5 and 74.7 ppm respectively.

Table 3-8. ^{1}J, ^{2}J and ^{3}J heteronuclear ^{1}H–^{13}C correlations (δ ppm in $CDCl_3$) observed for 15α-acetoxy-14,15-seco-15,22-*O*-*abeo*hop-14(27)-ene (**3-7**).

^{1}H signal	^{1}J correlated ^{13}C signal	^{2}J and ^{3}J correlated ^{13}C signals
0.87 s (4α-Me)	33.5 (C-23)	57.0 (C-5), 42.2 (C-3), 33.4 (C-4), 21.5 (C-24)
0.83 s (4β-Me)	21.5 (C-24)	57.0 (C-5), 42.2 (C-3), 33.4 (C-4), 33.5 (C-23)
0.86 s (10β-Me)	16.2 (C-25)	60.2 (C-9), 57.0 (C-5), 40.0 (C-1), 38.4 (C-10)
1.00 s (8β-Me)	22.3 (C-26)	161.3 (C-14), 60.2 (C-9), 41.7 (C-8), 39.2 (C-7)
0.98 s (18α-Me)	18.0 (C-28)	47.5 (C-13), 47.4 (C-18), 39.6 (C-17), 39.2 (C-19)
1.30 s (22β-Me)	26.3 (C-29)	75.7 (C-22), 46.3 (C-21), 28.3 (C-30)
1.19 s (22α-Me)	28.3 (C-30)	75.7 (C-22), 46.3 (C-21), 26.3 (C-29)
2.10 s ($OOCCH_3$)	21.6 (15-$OOCCH_3$)	169.7 (15-$OOCCH_3$)
4.83 br s/4.54 br s (H-27a/b)	102.9 (C-27)	161.3 (C-14), 47.5 (C-13), 41.7 (C-8)

* ^{4}J coupling

NOESY Spectrum of Acetate (3-7)

The NOESY spectrum of acetate (**3-7**) included correlations between (i) H-15β (5.91 ppm) and H-17β (2.74 ppm), H-16α (1.34 ppm) and H-16β (1.68 ppm); (ii) H-27a (4.83 ppm) and H-27b (4.54 ppm), H-7α (1.62 ppm) and H-7β (1.56 ppm); and (iii) H-27b (4.54 ppm) and H-17β (2.72 ppm), H-16β (1.68 ppm) and the 18β-methyl group (0.98 ppm). These correlations showed that the preferred three-dimensional conformation of **3-7** was similar to that of **3-3**.

Other structurally significant NOESY correlations observed for **3-7** are presented in Table 3-9.

Table 3-9. Selected ^{1}H-^{1}H NOESY correlations (δ ppm in $CDCl_3$) observed for 15α-acetoxy-14,15-seco-15,22-*O*-*abeo*hop-14(27)-ene (**3-7**).

^{1}H NMR signal(s)	correlated ^{1}H signals
5.91 dd (H-15β)	2.74 ddd (H-17β), 1.68 d (H-16β), 1.30 s (22β-Me)
4.83 br s (H-27a)	4.54 br s (H-27b), 1.62 q/1.56 d (H-7α/β)
4.54 br s (H-27b)	4.83 br s (H-27a), 2.74 ddd (H-17β), 1.68 d (H-16β), 0.98 s (18α-Me)
2.74 ddd (H-17β)	5.91 dd (H-15β), 4.54 br s (H-27b), 2.13 d (H-13β), 1.72 t (H-21β) 1.68 d (H-16β), 1.30 s (22β-Me)
2.13 d (H-13β)	2.74 ddd (H-17β), 1.95 dddd (H-12β), 1.77 q (H-19β), 1.38 q (H-11β) 1.00 s (8β-Me)
1.95 dddd (H-12β)	2.13 d (H-13β), 1.75 d/1.38 q (H-11α/β), 1.13 q (H-12α), 0.98 s (18α-Me)
1.30 s (22β-Me)	1.19 s (22α-Me), 5.91 dd (H-15β), 2.74 ddd (H-17β), 1.72 t (H-21β)
1.19 s (22α-Me)	1.30 s (22β-Me), 1.72 t (H-21β), 1.56 t (H-20β)
1.00 s (8β-Me)	0.86 s (10β-Me), 2.13 d (H-13β), 1.56 d (H-7β), 1.48 t (H-6β)
0.98 s (18α-Me)	4.54 br s (H-27b), 1.68 d (H-16β), 1.44 t (H-19α), 1.13 q/1.95 dddd (H-12α/β)
0.87 s (4α-Me)	0.83 s (4β-Me), 1.69 d (H-6α), 1.14 t/1.38 d (H-3α/β), 0.84 d (H-5α)
0.86 s (10β-Me)	1.00 s (8β-Me), 0.83 s (4β-Me), 1.59 t (H-2β), 1.48 t (H-6β), 1.38 q (H-11β)

3.3.3 14,15-Seco-15,22-*O*-*abeo*hop-14(27)-en-15-one (3-5)

3.3.3.1 Mass Spectral Analysis of Lactone (3-5)

The highest observed ion in the mass spectrum of lactone (**3-5**) occurred at *m/z* 425. This ion can be attributed to the loss of a methyl group from a substance of molecular formula $C_{30}H_{48}O_2$ (440 daltons).

The mass spectrum of **3-5** was dominated by an intense *m/z* 181 fragment ion, rather than by a *m/z* 164 fragment ion as was the case for hemiacetal (**3-3**) (see Section **3.3.1**). The *m/z* 181 ion can be attributed to cleavage across the C-13–C-18 bond (see Scheme 3-4). Other structurally significant fragment ions are listed in Table 3-10.

Table 3-10. Selected mass spectral fragment ions observed for 14,15-seco-15,22-*O*-*abeo*hop-14(27)-en-15-one (**3-5**).

ions	*m/z* (% relative intensities)
M^+	440 (not seen)
M^+-CH_3	425 (0.5)
$C_{19}H_{31}^+$ (ion b)	259 (11)
$C_{16}H_{25}^+$	217 (10)
$C_{14}H_{23}^+$ (ion c)	191 (7)
$C_{11}H_{17}O_2^+$ (ion a)	181 (100)
$C_{11}H_{15}O^+$	163 (11)
$C_{10}H_{13}O^+$	149 (6)

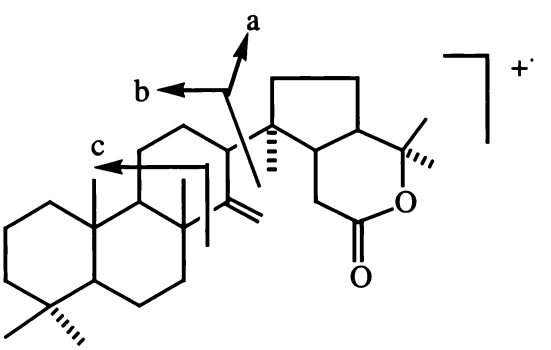

3-5: *m/z* 440 ($M^{+\cdot}$, $C_{30}H_{48}O_2$, not seen)

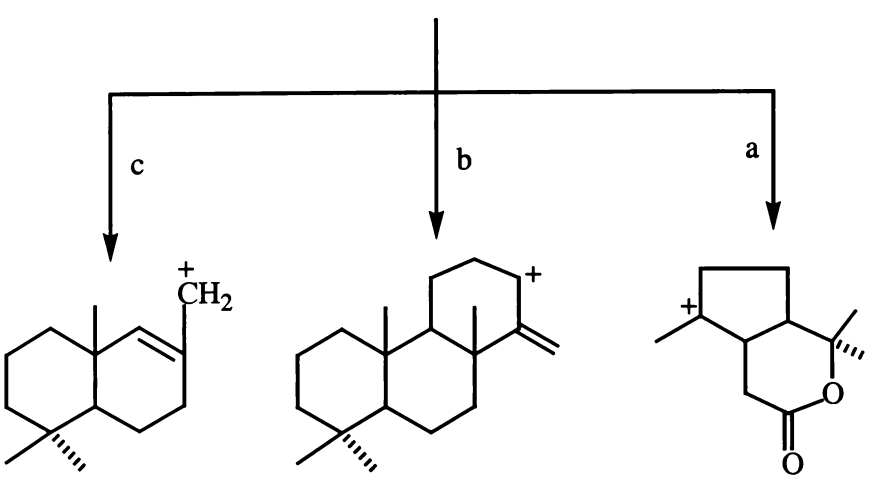

ion c: *m/z* 191($C_{14}H_{23}$) ion b: *m/z* 259 ($C_{19}H_{31}$) ion a : *m/z* 181 ($C_{11}H_{17}O_2$)

Scheme 3-4. Proposed mass spectral fragmentation pathways for 14,15-seco-15,22-*O*-*abeo*hop-14(27)-en-15-one (**3-5**).

3.3.3.2 NMR Spectral Analyses of Lactone (3-5)

The complete assignments of the ^{13}C and ^{1}H NMR signals of lactone (**3-5**) and diene (**3-6**) (see Section **3.3.4**), presented in Table 3-11, were derived from detailed analyses of one- and two-dimensional NMR data determined for these compounds. Signal assignments can be compared with those established in a like manner for **3-3** (see Table 3-2).

Table 3-11. ^{13}C and ^{1}H NMR signals (δ ppm in $CDCl_3$) observed for 22-hydroxy-hopan-15-one (**3-1**), 14,15-seco-15,22-*O*-*abeo*hop-14(27)-en-15-one (**3-5**) and 14,15-seco-15,22-*O*-*abeo*hopa-14(27),15-diene (**3-6**).

atom	22-hydroxyhopan-15-one (**3-1**)			lactone (**3-5**)			diene (**3-6**)		
	^{13}C	$^{1}H_{\alpha}$	$^{1}H_{\beta}$	^{13}C	$^{1}H_{\alpha}$	$^{1}H_{\beta}$	^{13}C	$^{1}H_{\alpha}$	$^{1}H_{\beta}$
1	40.4 t	0.72 t	1.59 d	40.0 t	0.78 t	1.65 d	40.1 t	0.80 t	1.66 d
2	18.8 t	1.25~1.56*		18.7 t	1.41 d	1.58 t	18.8 t	1.39 d	1.58 t
3	42.0 t	1.07 t	1.30 d	42.1 t	1.13 t	1.38 d	42.2 t	1.13 t	1.38 d
4	33.2 s			33.3 s			33.4 s		
5	56.4 d	0.70 d		56.9 d	0.84 d		56.9 d	0.85 d	
6	18.8 t	1.25~1.58		19.1 t	1.69 d	1.48 t	19.2 t	1.68 d	1.48 t
7	34.3 t	1.42 t	2.49 d	39.2 t	1.61 q	1.55 d	39.4 t	1.61 q	1.58 d
8	43.1 s			41.7 s			41.6 s		
9	51.8 d	1.10 d		59.8 d	0.94 d		59.8 d	0.94 d	
10	38.2 s			38.3 s			38.3 s		
11	21.4 t	1.58 d	1.20 q	22.2 t	1.76 d	1.38 q	22.2 t	1.73 d	1.38 q
12	24.0 t	1.68 q	1.46 d	30.9 t	1.15 q	1.95 dddd	30.7 t	1.15 q	1.94 dddd
13	50.6 d		1.68 d	48.6 d		2.13 d	48.9 d		2.12 dd
14	57.2 s			161.0 s			161.3 s		
15	214.8 s			172.9 s			140.8 d		6.19 dd
16	41.3 t	2.78 t	2.59 d	29.4 t	2.41 dd	2.50 dd	101.6 d		4.59 m
17	51.0 d		1.79 t	39.0 d		2.81 dd	39.6 d		2.76 d
18	44.1 s			47.5 s			46.5 s		
19	40.8 t	1.61 q	1.00 q	40.0 t	1.52 d	1.75 t	41.6 t	1.53 q	1.62 q
20	26.9 t	1.61 q	1.80 q	24.3 t	1.74 d	1.54 q	24.2 t	1.58 t	1.56 q
21	50.1 d		2.18 q	46.7 d		2.14 q	48.0 d		1.84 m
22	73.3 s			81.9 s			74.9 s		
23	33.4 q	0.80 s		33.4 q	0.86 s		33.5 q	0.87 s	
24	21.6 q	0.75 s		21.6 q	0.82 s		21.6 q	0.83 s	
25	15.9 q	0.77 s		16.2 q	0.85 s		16.2 q	0.86 s	
26	19.4 q	1.00 s		22.3 q	1.01 s		22.3 q	1.02 s	
27	15.5 q	1.14 s		102.8 t	4.82 s 4.45 d (1.0 Hz)		102.8 t	4.82 s	4.59 s
28	16.0 q	0.91 s		18.6 q	1.03 s		19.8 q	1.06 s	
29	29.1 q	1.12 s		27.6 q	1.39 s (22β-Me)		25.4 q	1.21 s (22β-Me)	
30	31.1 q	1.16 s		29.1 q	1.35 s (22α-Me)		27.5 q	1.20 s (22α-Me)	

^{1}H NMR Spectrum of Lactone (3-5)

The 400 MHz ^{1}H NMR spectrum of lactone (**3-5**) included signals attributable to seven tertiary methyl groups, and two olefinic protons, assignable to H-27a (4.82 ppm, br s,) and H-27b (4.45 ppm, d, J = 1.0 Hz). The resonances of the four methyl groups which occurred in the region 0.82~1.03 ppm corresponded closely to those determined for the 4α-, 4β-, 8β- and 10β-methyl groups (ie the H-23, H-24, H-26 and H-25 respectively) of **3-3**. This spectral data was consistent with the presence of a ring A/B/C system identical to that identified in **3-3** (see Figure 3-11).

The three remaining tertiary methyl groups of lactone (**3-5**) occurred at 1.03 ppm (18α-Me), 1.39 ppm (22β-Me) and 1.35 ppm (22α-Me) (Table 3-11), slightly downfield of their resonance positions in **3-3**.

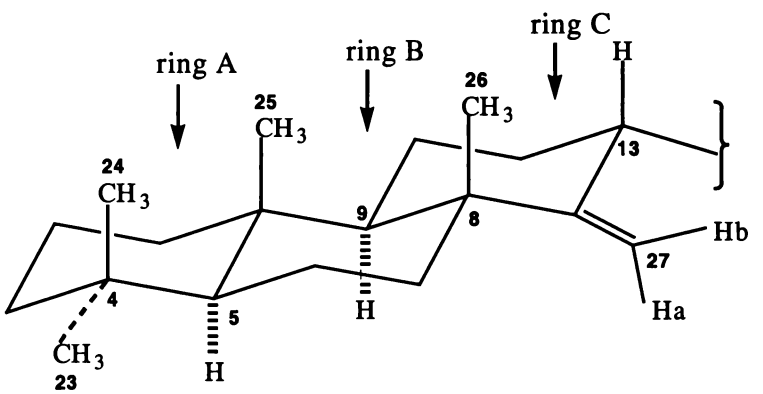

Figure 3-11. The common ring A/B/C partial structure identified for **3-3** and **3-5**.

Other features of the ^{1}H NMR spectrum of lactone (**3-5**) included the absence of a signal at 4.95 ppm attributable to H-15β in hemiacetal (**3-3**), and the appearance of a pair of methylene protons at 2.41 ppm (dd, J = 17.7, 7.5 Hz) and 2.50 ppm (dd, J = 17.7, 9.1 Hz). HSQC and HMBC data (see Tables 3-11 and 3-14) and the large ^2Jvicinal coupling exhibited by these protons demonstrated that they arose from H-16α and H-16β respectively, and were located adjacent to a carbonyl carbon (C-15) which resonated at 172.9 ppm.

The differing $^3J_{H\text{-}16\beta\text{-}H\text{-}17\beta(cis)}$ and $^3J_{H\text{-}16\alpha\text{-}H\text{-}17\beta(trans)}$ couplings (J = 9.1 and 7.5 Hz respectively) are consistent with the dihedral angles (75.5 and 50° respectively) experienced by these protons, as revealed by a Chem3D modelling investigation (see Figure 3-11). Hitherto (Zhao, 1983) has reported that $^3J_{cis}$ is normally larger than $^3J_{trans}$. The $^3J_{H\text{-}16\beta\text{-}H\text{-}17\beta(cis)}$ and $^3J_{H\text{-}16\alpha\text{-}H\text{-}17\beta(trans)}$ coupling constants can be compared to those exhibited by H-6α/β and H-16α/β in 22-hydroxyhopan-7-one (**2-1**) and 22-hydroxyhopan-15-one (**3-1**) respectively (see Tables 2-2 and 3-2).

The presence in lactone (**3-5**) of a carbonyl group led to H-21β (2.14 ppm) and H-17β (2.81 ppm) experiencing downfield shifts of 0.46 ppm and 0.15 ppm relative to the resonance positions of these protons in **3-3** (see Table 3-2).

COSY Spectrum of Lactone (3-5)

The proton NMR signal assignments presented in Table 3-11 for lactone (**3-5**) were elucidated from analyses of COSY (Table 3-12), NOESY (Table 3-14) and HSQC spectral data, as described for **3-3**. The majority of the proton assignments corresponded closely to those determined for **3-3**.

Table 3-12. Selected ^{1}H-^{1}H COSY correlations (δ ppm in $CDCl_3$) observed for 14,15-seco-15,22-*O*-*abeo*hop-14(27)-en-15-one (**3-5**).

^{1}H NMR signals	correlated ^{1}H signals
4.82 br s (H-27a)	4.45 d (H-27b), 2.13 ddd (H-13β)*
4.45 d (H-27b)	4.83 br s (H-27a), 2.13 ddd (H-13β)*
2.81 dd (H-17β)	2.41dd/2.50 dd (H-16α/β), 2.14 ddd (H-21β)
2.41dd /2.50 dd (H-16α/β)	2.81 dd (H-17β)
2.14 q (H-21β)	2.81 dd (H-17β), 1.74 d/1.54 q (H-20α/β)
2.13 d (H-13β)	4.82 br s (H-27a), 4.56 d (H-27b), 1.52 q (H-19β)* 1.15 q/1.95 dddd (H-12α/β)
1.95 dddd (H-12β)	2.13 ddd (H-13β), 1.76 d/1.38 q (H-11α/β), 1.15 q (H-12α)
1.76 d (H-11α)	2.13 ddd (H-13β)*, 1.38 q (H-11β), 1.15 q/1.95 dddd (H-12α/β)
1.74 d (H-20α)	2.14 ddd (H-21β), 1.54 q (H-20β)
1.54 q (H-20β)	2.14 dd (H-20β)
1.38 q (H-11β)	1.76 d (H-11α), 1.15 q/1.95 dddd (H-12α/β), 0.94 d (H-9α)
1.01 s (8β-Me)	1.61 q (H-7α)*
0.94 d (H-9α)	1.76 d/1.38 q (H-11α/β)
0.84 d (H-5α)	1.69 d/1.48 t (H-6α/β)

* ^4J coupling

^{13}C and DEPT135 NMR Spectra of Lactone (3-5)

The ^{13}C NMR spectrum of **3-5** was comprised of thirty carbon resonances, which were characterised by a DEPT135 NMR spectrum to arise from 7 quartet (CH_3), 11 triplet (CH_2), 5 doublet (CH), and 7 singlet (C) carbons. The ^{13}C NMR spectrum included signals attributable to an exocyclic methylene group (161.0 ppm, s, C-14; 102.8 ppm, t, C-27), a carbonyl carbon (172.9, s, C-15), and an oxygenated quaternary carbon (81.9 ppm, s, C-22) (see Table 3-11).

This data was consistent with the identification of this compound as the lactone (**3-5**). Other than for the resonances of carbons in close proximity to C-15, the ^{13}C signal resonances of **3-5** corresponded closely to those reported for **3-3**.

Table 3-13. ^1J, ^2J and ^3J heteronuclear ^1H-^{13}C correlations (δ ppm in $CDCl_3$) observed for 14,15-seco-15,22-*O*-*abeo*hop-14(27)-en-15-one (**3-5**).

^1H signal	^1J correlated ^{13}C signal	^2J and ^3J correlated ^{13}C signals
0.86 s (4α-Me)	33.4 (C-23)	56.9 (C-5), 42.1 (C-3), 33.3 (C-4), 21.6 (C-24)
0.82 s (4β-Me)	21.6 (C-24)	56.9 (C-5), 42.1 (C-3), 33.3 (C-4), 33.4 (C-23)
0.85 s (10β-Me)	16.2 (C-25)	59.8 (C-9), 56.9 (C-5), 40.0 (C-1), 38.3 (C-10)
1.01 s (8β-Me)	22.3 (C-26)	161.0 (C-14), 59.8 (C-9), 41.7 (C-8), 39.2 (C-7)
1.03 s (18α-Me)	18.6 (C-28)	48.6 (C-13), 47.5 (C-18), 40.0 (C-19), 39.0 (C-17)
1.39 s (22β-Me)	27.6 (C-29)	81.9 (C-22), 46.7 (C-21), 29.1 (C-30)
1.35 s (22α-Me)	29.1 (C-30)	81.9 (C-22), 46.7 (C-21), 27.6 (C-29)
1.95 dddd (H-12β)	30.9 (C-12)	59.8(C-9), 48.6 (C-13), 22.2 (C-11)
2.13 d (H-13β)	48.6 (C-13)	161.0 (C-14), 102.8 (C-27), 47.5 (C-18), 30.9 (C-12)
2.41dd/2.50 dd (H-16α/β)	29.4 (C-16)	172.9 (C-15), 39.0 (C-17), 47.5 (C-18), 46.7 (C-21)
2.81 dd (H-17β)	39.0 (C-17)	172.9 (C-15), 48.6 (C-13), 47.5 (C-18), 29.4 (C-16), 24.3 (C-20)
4.45 d (H-27b)	102.8 (C-27)	161.0 (C-14), 48.6 (C-13), 41.7 (C-8), 39.2 (C-7)*, 30.9 (C-12)*
4.84 br s (H-27a)	102.8 (C-27)	161.0 (C-14), 48.6 (C-13), 59.8 (C-9)*, 41.7 (C-8), 30.9 (C-12)*

* ^4J couplings

C-16 was shifted slightly upfield to resonate at 29.4 ppm, compared to 32.1 ppm in **3-3**. In addition, carbons at C-18, C-19, and C-22 all experienced downfield shifts to resonate at 47.5, 40.0 and 81.9 ppm. The C-28, C-29 and C-30 methyl group carbons also experienced small downfield shifts, compared to the resonances observed for the corresponding carbons of **3-3**.

HMBC correlations for selected protons of **3-5** are presented in Table 3-14. Of particular note are the correlations which H-16α/β exhibited to C-15 (172.9 ppm), C-17 (39.0 ppm), C-18 (47.5 ppm) and C-21 (46.7 ppm). These correlations demonstrated the close proximity of the carbonyl group to the ring D/E junction.

The HMBC correlations exhibited by the methyl group protons of **3-5** (see Table 3-13) were fully consistent with those exhibited by hemiacetal (**3-3**).

NOESY Spectrum of Lactone (3-5)

The NOESY correlations exhibited by **3-5** were consistent with the MM2 minimised conformation determined for this compound. In particular H-27a (4.82 ppm) exhibited NOESY correlations to H-27b (4.45 ppm), H-7α (1.61 ppm) and H-7β (1.55 ppm), while H-27b (4.45 ppm) exhibited NOESY correlations to H-27a (4.82 ppm), H-16α (2.41 ppm), H-16β (2.50 ppm), H-17β (2.81 ppm) and the18α-methyl group (1.03 ppm) (see Figure 3-12). The modelled inter-nuclear distances determined for these protons were 1.83, 2.17, 2.84, 2.53 and 2.14 Å respectively.

H-17β (2.81 ppm, dd, J = 16.5, 7.9 Hz) exhibited the NOESY correlations to H-27b (4.45 ppm), H-16α (2.41 ppm), H-16β (2.50 ppm), H-21β (2.14 ppm) and 22β-methyl group (1.39 ppm). Other structurally significant NOESY correlations observed for **3-5**, presented in Table 3-14, were similar to those observed for **3-3**.

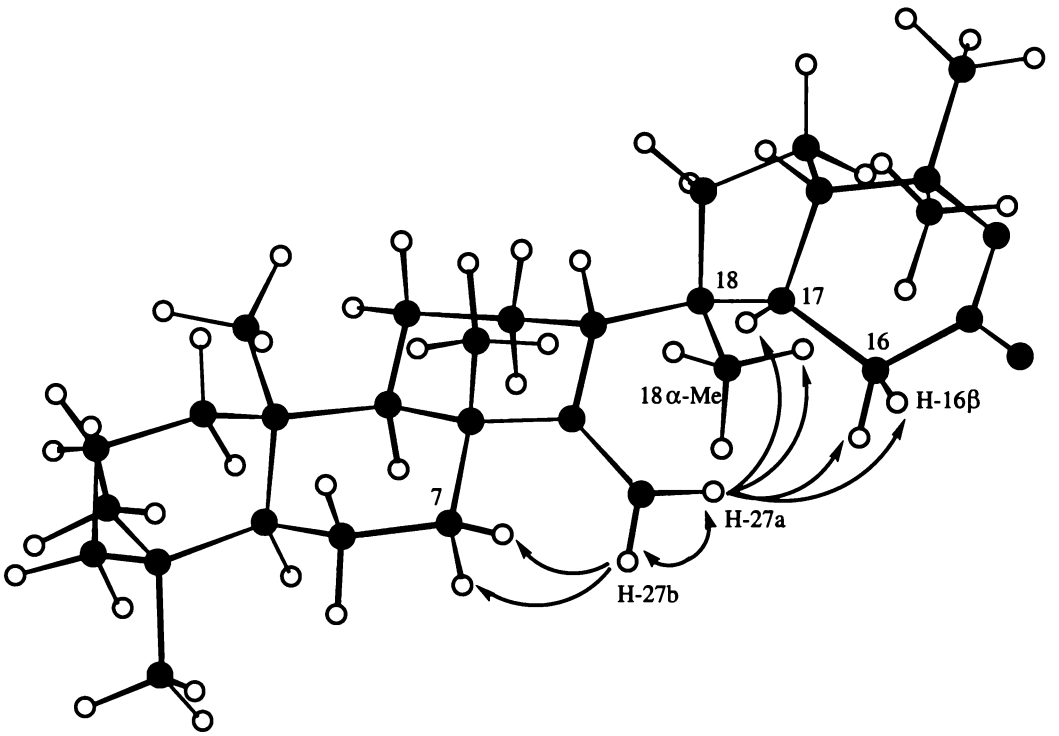

Figure 3-12. MM2 refined conformation of **3-5** showing NOESY correlations exhibited by H-27a (4.82 ppm) and H-27b (4.45 ppm).

Table 3-14. Selected ^1H-^1H NOESY correlations (δ ppm in $CDCl_3$) observed for 14,15-seco-15,22-*O*-*abeo*hop-14(27)-en-15-one (**3-5**).

^1H NMR signals	correlated ^1H signals
4.82 br s (H-27a)	4.45 d (H-27b), 1.61 q/1.55 d (H-7α/β)
4.45 d (H-27b)	4.82 s (H-27a), 2.81 dd (H-17β), 2.41dd/2.50 dd (H-16α/β), 1.03 s (18α-Me)
2.81 dd (H-17β)	4.45 d (H-27b), 2.41 dd/2.50 dd (H-16α/β), ~2.13 {H-13β, H-21β), 1.39 s (22β-Me)
2.50 dd (H-16β)	4.45 d (H-27b), 2.81 dd (H-17β), 2.41 dd (H-16α), 1.39 s (22β-Me)
2.41 dd (H-16α)	4.45 d (H-27a), 2.81 dd (H-17β), 2.50 dd (H-16β), 1.39 s (22β-Me), 1.03 s (18α-Me)
2.13 d (H-13β)	2.81 dd (H-17β), 1.75 t (H-19β), 1.38 q (H-11β), 1.15 q/1.95 dddd (H-12α/β) 1.01 s (8β-Me)
1.95 dddd (H-12β)	2.13 d (H-13β), 1.76 d/1.38 q (H-11α/β), 1.52 d/1.75 t (H-19α/β), 1.15 q (H-12α) 1.03 s (18β-Me)
1.76 d (H-11α)	1.38 q (H-11β), 1.15 q/1.95 dddd (H-12α/β), 0.94 d (H-9α)
1.61 q/1.55 d (H-7α/β)	4.82 br s (H-27a)
1.03 s (18α-Me)	4.45 d (H-27b), 2.41 dd (H-16α)
1.01 s (8β-Me)	0.85 s (10β-Me), 2.13 ddd (H-13β), 1.55 d (H-7β), 1.48 t (H-6β), 1.38 q (H-11β)
0.85 s (10β-Me)	1.01s (8β-Me), 0.82 s (4β-Me), 1.58 t (H-2β), 1.48 t (H-6β), 1.38 q (H-11β)

3.3.4 14,15-Seco-15,22-*O*-*abeo*hopa-14(27),15-diene (3-6)

3.3.4.1 Mass Spectral Analysis of Diene (3-6)

The highest observed ion in the mass spectrum of diene (**3-6**) occurred at *m/z* 424, in agreement with its molecular formula of $C_{30}H_{48}O$ (424 dalton).

The base peak, which occurred at *m/z* 164, can be attributed to cleavage across the C-13 –C-18 bond (see Scheme 3-5). Other significant fragment ions are listed in Table 3-15. In general, there was a close similarity between the mass spectrum of the hemiacetal (**3-3**) and that of the diene (**3-6**).

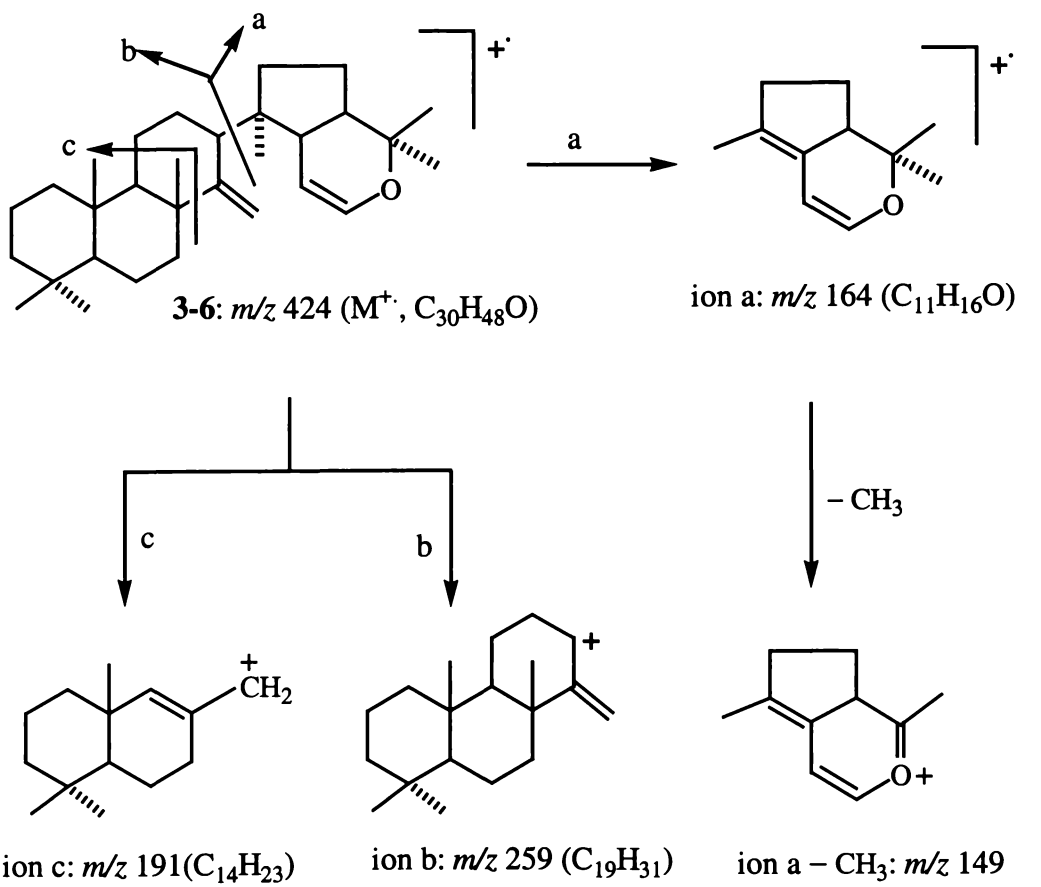

Scheme 3-5. Proposed mass spectral fragmentation pathways for 14,15-seco-15,22-*O*-*abeo*hopa-14(27),15-diene (**3-6**).

Table 3-15. Selected mass spectral fragment ions observed for 14,15-seco-15,22-*O*-*abeo*hopa-14(27),15-diene (**3-6**).

ions	*m/z* (% relative intensities)
M^+	424 (0.2)
M^+–CH_3	409 (0.8)
$C_{19}H_{31}^+$ (ion b)	259 (0.2)
$C_{14}H_{23}^+$ (ion c)	191(0.5)
$C_{11}H_{16}O^{+\cdot}$ (ion a)	164 (100)
Ion a – CH_3	149 (6)

3.3.4.2 NMR Spectral Analyses of Diene (3-6)

^{1}H NMR Spectrum of Diene (3-6)

The ^{1}H NMR spectrum of **3-6** included seven tertiary methyl group signals in the region at 0.80~1.25 ppm, a pair of olefinic protons at δ 4.82 ppm (br, s) and at δ 4.59 ppm (br s), as well as signals at 2.76 ppm (br d, J = 7.3 Hz), 2.12 ppm (dd, J = 12.5, 2.8 Hz) and 1.94 ppm (dddd, J = 12.2, 3.3, 3.3, 3.3 Hz). These ^{1}H NMR spectral features were similar to those observed for hemiacetal (**3-3**).

Downfield proton resonances at 6.19 ppm (dd, J = 6.5, 2.0 Hz) and 4.59 ppm (m), respectively, were assigned to the olefinic H-15 and H-16 signals. The coupling constants of the H-16 signal could not be determined due to overlap with one of the olefinic H-27 (4.59 ppm) signals. The $^3J_{\text{H-15—H-16}}$ coupling constant (J = 6.5 Hz) exhibited by H-15 was consistent with the presence in ring F of a *cis*-double bond, since olefinic $^3J_{cis}$ couplings are typically in the range 6~8 Hz, compared to 10~16 Hz for the corresponding $^3J_{trans}$ couplings (Zhao, 1983).

COSY Spectrum of Diene (3-6)

The proton NMR assignments presented in Table 3-11 for diene (**3-6**) were elucidated from analyses of COSY (Table 3-16), NOESY (Table 3-18) and HSQC spectral data, as described for **3-3**. The majority of the proton assignments corresponded closely to those determined for **3-3**. The COSY spectrum of **3-6** verified that the olefinic H-15 and H-16 signals were mutually coupled, and that each of them was also coupled to H-17β (2.76 ppm).

Table 3-16. Selected ^{1}H-^{1}H COSY correlations (δ ppm in $CDCl_3$) observed for 14,15-seco-15,22-*O*-*abeo*hopa-14(27),15-diene (**3-6**).

^{1}H NMR signals	correlated ^{1}H signals
6.19 dd (H-15)	4.59 dd (H-16), 2.76 br d (H-17β)*
4.59 m (H-16)	6.19 dd (H-15), 2.76 br d (H-17β), 1.84 dd (H-21β)*
4.82 br s (H-27a)	4.59 br s (H-27b), 2.12 dd (H-13β)*
4.59 br s (H-27b)	4.83 br s (H-27a), 2.12 dd (H-13β)*
2.76 br d (H-17β)	6.19 dd (H-15)*, 4.59 m (H-16), 1.84 dd (H-21β)
2.12 dd (H-13β)	4.82 br s/4.59 br (H-27a/b), 1.15 q /1.94 dddd (H-12α/β), 1.60 t (H-19β)*
1.94 dddd (H-12β)	2.12 d (H-13β), 1.73 d /1.38 q (H-11α/β), 1.15 q (H-12α)
1.84 m (H-21β)	2.76 br d (H-17β), 1.58 t/1.56 q (H-20α/β)
1.73 d (H-11α)	1.38 q (H-11β), 1.15 q/1.94 dddd (H-12α/β), 0.94 d (H-9α)
1.38 q (H-11β)	1.73 d (H-11α), 1.15 q/1.94 dddd (H-12α/β), 0.94 d (H-9α)
1.02 s (8β-Me)	1.61 q (H-7α)*
0.94 d (H-9α)	1.73 d/1.38 q (H-11α/β)
0.85 d (H-5α)	1.68 d/1.48 t (H-6α/β)

* ^{4}J coupling

^{13}C and DEPT135 NMR Spectra of Diene (3-6)

The ^{13}C NMR spectrum of **3-6** was comprised of thirty carbon resonances, which were characterised by a DEPT135 NMR spectrum to arise from 7 quartet (CH_3), 10 triplet (CH_2), 7 doublet (CH), and 6 singlet (C) carbons. The ^{13}C NMR spectrum included signals attributable to an exocyclic methylene group (161.3 ppm, s, C-14; 102.8 ppm, t, C-27), two olefinic methine carbons (140.8 ppm, d, C-15; 101.6 ppm, d, C-16), and an oxygenated quaternary carbon (74.9 ppm, s, C-22) (see Table 3-11).

This data was consistent with the identification of **3-6** as the dehydrated analogue of **3-3**. HMBC correlations observed for the methyl group protons of this compound, and also some of the methylene and methine protons are presented in Table 3-17. The ^{3}J HMBC coupling which H-15 (4.59 ppm) exhibited with C-22 (74.9 ppm) verified the presence of a 15,22-*O*-*abeo* ring system (ring F) in **3-6**.

Table 3-17. ^1J, ^2J and ^3J heteronuclear ^1H-^{13}C correlations (δ ppm in $CDCl_3$) observed for 14,15-seco-15,22-*O*-*abeo*hopa-14(27),15-diene (**3-6**).

^1H signal	^1J correlated ^{13}C signal	^2J and ^3J correlated ^{13}C signals
0.87 s (4α-Me)	33.5 (C-23)	56.9 (C-5), 42.2 (C-3), 33.4 (C-4), 21.6 (C-24)
0.83 s (4β-Me)	21.6 (C-24)	56.9 (C-5), 42.2 (C-3), 33.4 (C-4), 33.5 (C-23)
0.86 s (10β-Me)	16.2 (C-25)	59.8 (C-9), 56.9 (C-5), 40.1 (C-1), 38.3 (C-10)
1.02 s (8β-Me)	22.3 (C-26)	161.3 (C-14), 59.8 (C-9), 41.6 (C-8), 39.4 (C-7)
1.06 s (18α-Me)	19.8 (C-28)	48.9 (C-13), 46.5 (C-18), 41.6 (C-19), 39.6 (C-17)
1.21 s (22β-Me)	25.4 (C-29)	74.9 (C-22), 48.0 (C-21), 27.5 (C-30)
1.20 s (22α-Me)	27.5 (C-30)	74.9 (C-22), 48.0 (C-21), 25.4 (C-29)
6.19 dd (H-15)	140.8 (C-15)	101.6 (C-16), 74.9 (C-22), 39.6 (C-17)
4.59 m (H-16)	101.6 (C-16)	140.8 (C-15), 48.0 (C-21), 46.5 (C-18), 39.6 (C-17)
4.82 br s/4.59 br s (H-27a/b)	102.8 (C-27)	161.3 (C-14), 59.8 (C-9)*, 48.9 (C-13), 41.6 (C-8) 30.7 (C-12)*, 22.2 (C-11)*
2.76 br d (H -17β)	39.6 (C-17)	140.8 (C-15), 101.6 (C-16), 48.9 (C-13), 46.5 (C-18) 41.6 (C-19), 24.2 (C-20), 48.0 (C-21)
2.12 dd (H-13β)	48.9 (C-13)	161.3 (C-14), 102.8 (C-27), 46.5 (C-18), 30.7 (C-12)
1.94 dddd (H-12β)	30.7 (C-12)	48.9 (C-13), 22.2 (C-11)
1.84 m (H-21β)	48.0 (C-21)	101.6 (C-16), 39.6 (C-17), 24.2 (C-20)

* ^4J coupling

NOESY Spectrum and Molecular Modelling Analyses of Diene (3-6)

The NOESY spectrum of **3-6** included correlations between H-27b (4.59 ppm) and H-27a (4.82 ppm), H-17β (2.76 ppm), H-16 (4.59 ppm) and the 18α-methyl group (1.06 ppm), and between H27a (4.82 ppm) and H-27b (4.59 ppm) and H-7α/β (1.61/1.58 ppm). These NOESY correlations (see Table 3-18) were analogous to correlations observed for the equivalent protons of **3-3** and **3-5**. They were also consistent with the MM2 modelled structure depicted in Figure 3-13. Other NOESY correlations are presented in Table 3-18.

Table 3-18. Selected ^{1}H-^{1}H NOESY correlations (δ ppm in $CDCl_3$) observed for 14,15-seco-15,22-*O*-*abeo*hopa-14(27),15-diene (**3-6**).

^{1}H NMR signals	correlated ^{1}H signals
6.19 dd (H-15)	4.59 m (H-16)
4.59 m (H-16)	6.19 dd (H-15)
4.82 br s (H-27a)	4.59 br s (H-27b), 1.61q/1.58 d (H-7α/β)
4.59 br s (H-27b)	4.83 br s (H-27a), 2.76 br d (H-17β), 1.06 s (18α-Me)
2.76 br d (H-17β)	4.59 {H-27b, H-16}, 2.12 dd (H-13β), 1.84 m (H-21β), 1.21 s (22β-Me)
2.12 dd (H-13β)	2.76 br d (H-17β), 2.12 dd (H-13β), 1.60 t (H-19β), 1.15 q/1.94 dddd (H-12α/β) 1.38 q (H-11β), 1.02 s (8β-Me)
1.94 dddd (H-12β)	2.12 dd (H-13β), 1.73 d/1.38 q (H-11α/β), 1.53 d (H-19α), 1.15 q (H-12α)
1.84 m (H-21β)	2.76 br d (H-17β), 2.12 dd (H-13β), 1.56 t/1.59 d (H-20α/β), 1.20 s/1.21 s (22α/β-Me)
1.21 s (22β-Me)	2.76 br d (H-17β), 1.84 m (H-21β)
1.02 s (8β-Me)	0.86 s (10β-Me), 2.12 dd (H-13β), 1.58 d (H-7β), 1.48 t (H-6β), 1.38 q (H-11β)
0.86 s (10β-Me)	1.02 s (8β-Me), 1.66 d (H-1β), 1.58 t (H-2β), 1.48 t (H-6β), 1.38 q (H-11β)
0.83 s (4β-Me)	0.87 s (4α-Me), 0.86 s (10β-Me), 1.58 t (H-2β), 1.48 t (H-6β), 1.38 d (H-3β)

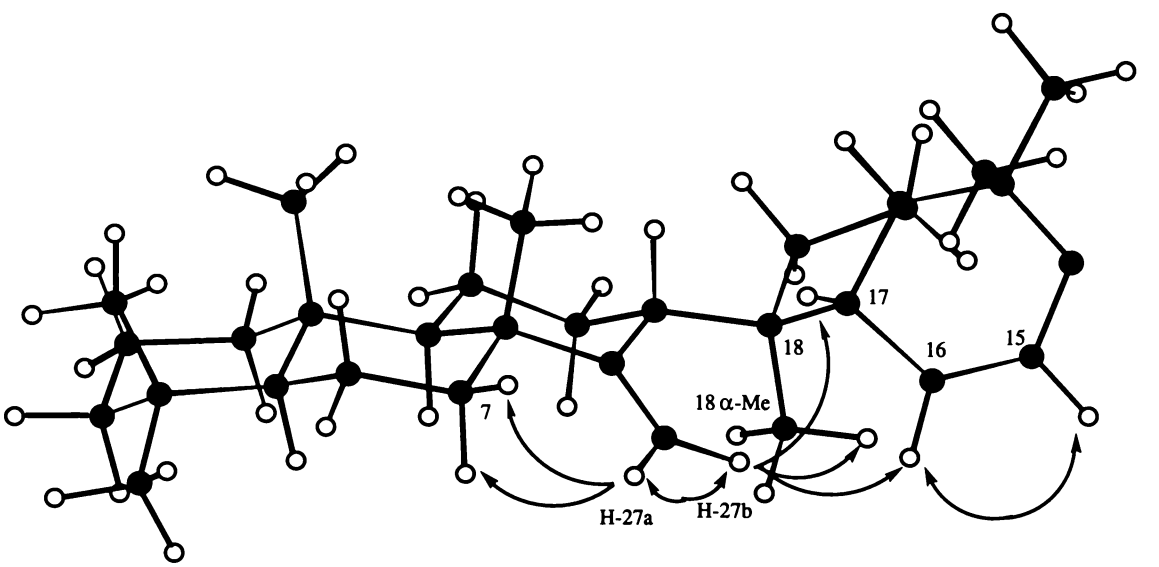

Figure 3-13. MM2 modelled conformation determined for diene (**3-6**).

3.4 Photochemical Reactions of Hop-21-en-15-one and Hop-22(29)-en-15-one

The demonstration in Section **3.3** that photolysis of 22-hydroxyhopan-15-one (**3-1**) proceeded *via* an eight-membered transition state, and with participation of the 22-OH group prompted the synthesis of some 15-oxohopenoids, in order that the outcomes of photochemical reactions performed in the absence of a 22-hydroxyl group might be ascertained.

Four 15-oxohopenoids were synthesised from 22-hydroxyhopan-15-one (**3-1**) using standard methods (Corbett & Young, 1966b) (see Scheme 3-6). Synthetic details are reported in Chapter Six (Experimental).

Dehydration of 22-hydroxyhopan-15-one (**3-1**) with $POCl_3$ in pyridine afforded a mixture of hop-21-en-15-one (**3-8**) and hop-22(29)-en-15-one (**3-9**) which were separated using a silver nitrate impregnated alumina column and mixtures of light petroleum and diethyl ether as eluents. Hydrogenation of **3-8** and **3-9** over Adam's catalyst yielded 21α-H-hopan-15-one (**3-11**) and hopan-15-one (**3-10**) respectively (see Scheme 3-6).

The complete assignments of ^{13}C and ^{1}H NMR signals of ketones (**3-8**), (**3-9**), (**3-10**) and (**3-11**) were established by detailed analyses of one- and two-dimensional NMR spectral data, analogous to those described in Section **3.3** for photoproducts (**3-3**), (**3-5**) and (**3-6**). Signal assignments established for **3-8**, **3-9**, **3-10** and **3-11** are presented in Table 3-20, 3-24 and 3-31, respectively.

The photolysis of hop-21-ene-15-one (**3-8**), hopan-15-one (**3-10**) and 21α-H-hopan-15-one (**3-11**), are reported in Sections **3.4, 3.5** and **3.6** respectively. Photolysis of hop-22(29)-ene-15-one (**3-9**) in benzene-methanol afforded a complex mixture of products which was not considered worth of further investigation.

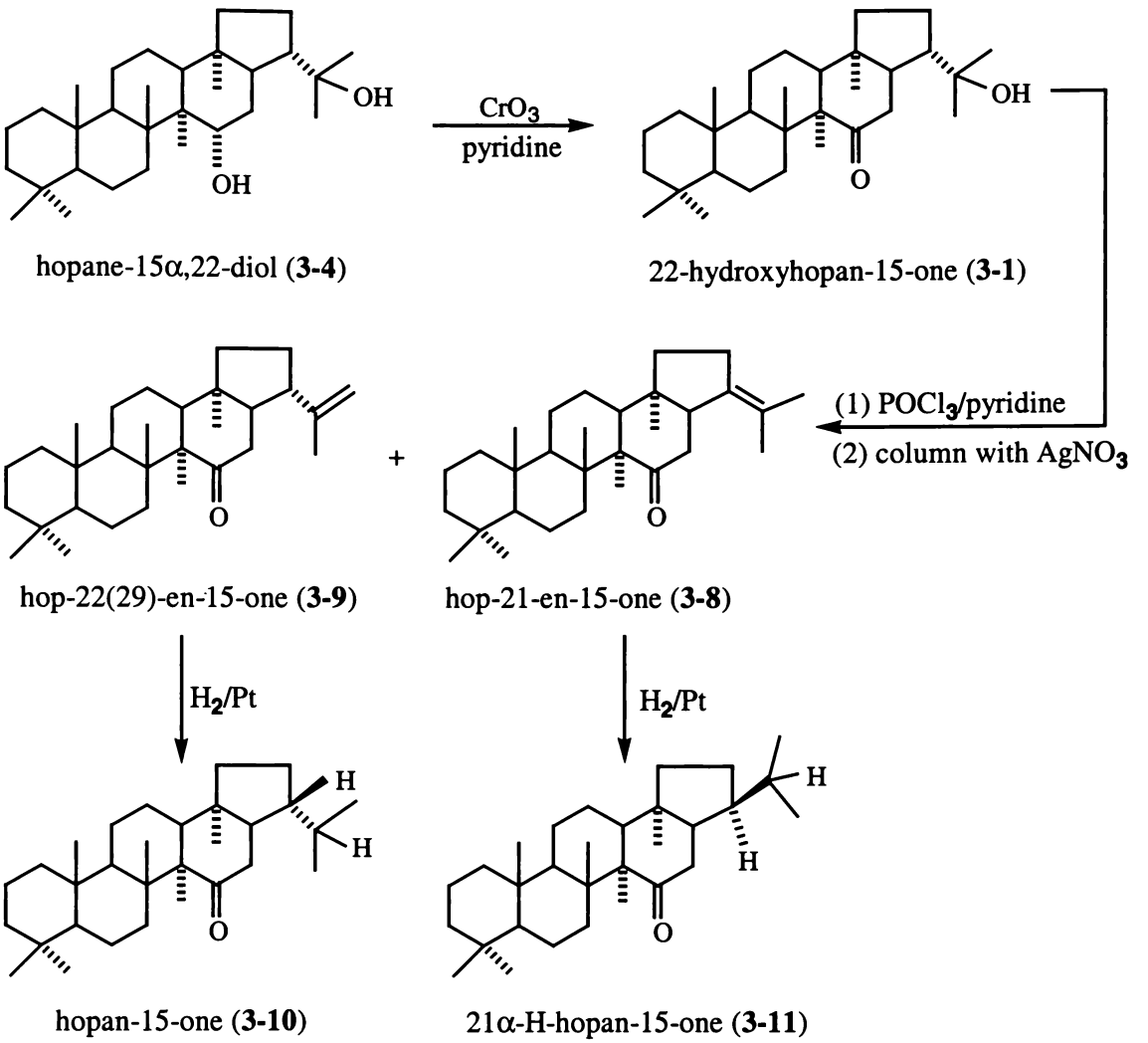

Scheme 3-6. Reaction sequences used to prepare photolysis substrates from 22-hydroxyhopan-15-one (**3-1**).

3.4.1 Photolysis of Hop-21-en-15-one (3-8) in Benzene-Methanol

Photolysis of hop-21-ene-15-one (**3-8**) in mixture of dry benzene-methanol afforded a mixture of products which were separated by radial chromatography using mixtures of light petroleum and benzene as eluents. This afforded a fraction which consisted mainly of starting material hop-21-en-15-one (**3-8**) and an unsaturated secoaldehyde (**3-12**).

Efforts to separate **3-8** and **3-12** using several solvent systems were not successful, however the major component of the mixture was readily identified as 14,15-secohopa-14(27),21-dien-15-al (**3-12**) by detailed analyses of the NMR spectral data obtained on subtraction of the spectrum of the starting material (**3-8**). A complete assignment of the ^{13}C and ^{1}H NMR signals of **3-12** is presented in Table 3-20.

3.4.2 Structural Elucidation of 14,15-Secohopa-14(27),21-dien-15-al (3-12)

3.4.2.1 Mass Spectral Analysis of Secoaldehyde (3-12)

The highest observed fragment ion observed in the mass spectrum of secoaldehyde (**3-12**) occurred at *m/z* 424. This was consistent with the molecular formula of **3-12** being $C_{30}H_{48}O$ (424 daltons). Pronounced *m/z* 164, 136 and 121 fragment ions appeared in the mass spectrum of **3-12**, possibly arising from the loss of a ring E fragment ion (ion a) (see Scheme 3-7), followed by the loss of a CO group, and a methyl group. Significant *m/z* 191 and 245 ions also appeared in the mass spectrum of **3-12**. Other structurally significant fragment ions are listed in Table 3-19.

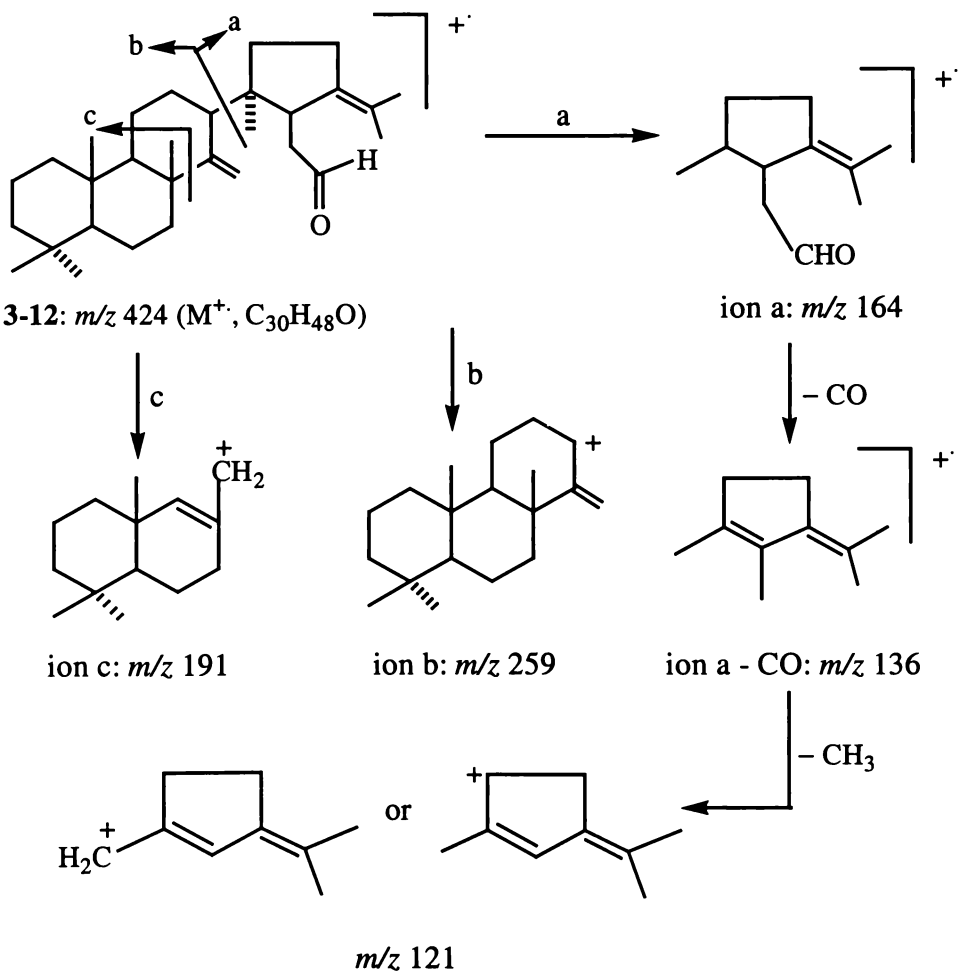

Scheme 3-7. Proposed mass spectral fragmentation pathways for 14,15-secohopa-14(27),21-dien-15-al (**3-12**).

Table 3-19. Selected mass spectral fragment ions observed for 14,15-secohopa-14(27),21-dien-15-al (**3-12**).

ions	*m/z* (% relative intensities)
M^+	424 (11)
M^+-CH_3	409 (30)
M^+-C_3H_7	381 (3)
M^+- ion d	355 (2)
$C_{19}H_{31}^+$ (ion b)	259 (0.2)
$C_{14}H_{23}^+$ (ion c)	191 (14)
$C_{11}H_{16}O^{+\cdot}$ (ion a)	164 (100)
related ion	147 (22)
ion a-CO	136 (36)
ion a-CO-CH_3	121 (97)
$C_7H_{11}^+$	95 (38)
$C_6H_9^+$	81 (30)
$C_5H_9^+$ (ion d)	69 (28)

3.4.2.2 NMR Spectral Analyses of Secoaldehyde (3-12)

A complete assignment of the ^{13}C and ^1H NMR signals determined for **3-12** is presented in Table 3-20. These assignments can be compared with those established for hop-21-en-15-one (**3-8**) and hop-22(29)-en-15-one (**3-9**).

^1H NMR Spectrum of Secoaldehyde (3-12)

The ^1H NMR spectrum of **3-12** included signals attributable to seven methyl groups (one less than the starting material (**3-8**) (see Table 3-20), two olefinic methylene protons (4.87 ppm, br s, H-27a and 4.75 ppm, br s, H-27b) and an aldehyde proton (9.76 ppm, ~t, J = 2.6 Hz, H-15).

Other distinctive features of the ^1H NMR spectrum of **3-12** were the appearance of a downfield methine proton at 3.75 ppm (t, J = 7.5 Hz) and two methylene signals at 2.21 and 2.57 ppm, each of which appeared as finely resolved eight-line patterns (J = 12.8, 7.3 and 2.7 Hz).

Table 3-20. ^{13}C and ^{1}H NMR signals (δ ppm in $CDCl_3$) observed for **3-8**, **3-9** and 14,15-secohopa-14(27),21-dien-15-al (**3-12**).

atom	hop-21-en-15-one (**3-8**)			aldehyde (**3-12**)			hop-22(29)-en-15-one (**3-9**)		
	^{13}C	$^{1}H_{\alpha}$	$^{1}H_{\beta}$	^{13}C	$^{1}H_{\alpha}$	$^{1}H_{\beta}$	^{13}C	$^{1}H_{\alpha}$	$^{1}H_{\beta}$
1	40.5 t	0.77 t	1.64 d	40.0 t	0.77 t	1.64 d	40.4 t	0.77 t	1.64 d
2	18.8 t	1.37~1.59		18.7 t	1.40 d	1.59 t	18.8 t	1.36~1.57	
3	42.0 t	1.13 t	1.38 d	42.1 t	1.13 t	1.38 d	42.0 t	1.10 t	1.34 d
4	33.3 s			33.3 s			33.2 s		
5	56.5 d	0.76 d		57.0 d	0.82 d		56.4 d	0.74 d	
6	18.8 t	1.37~1.59		19.1 t	1.68 t	1.06 d	18.8 t	1.36~1.57	
7	34.3 t	1.49 t	2.51 m	39.2 t	1.54 t	1.61 d	34.2 t	1.44 t	2.53 m
8	43.1 s			41.9 s			43.0 s		
9	51.8 d	1.16 d		60.2 d	0.92 d		51.8 d	1.14 d	
10	38.2 s			38.3 s			38.2 s		
11	21.4 t	1.64 t	1.28 t	22.4 d	1.75 d	1.36 q	21.4 t	1.61 d	1.25 q
12	23.4 t	1.11 t	1.57 d	30.6 t	1.10 t	1.97 d	23.9 t	~1.48 overlapped	
13	48.8 d		1.80 d	43.0 d		2.00 d	50.3 d		1.71 d
14	56.7 s			161.0 s			56.5 s		
15	215.4 s			203.6 d	9.76 t (2.6 Hz)		215.1 s		
16	42.8 t	~2.83 overlapped		46.1 t	2.57 m	2.21 m	41.4 t	2.62 dd	2.29 dd
17	53.5 d		2.27 t	41.9 d		3.75 t	52.0 d		1.85 d
18	44.3 s			46.7 s			44.7 s		
19	38.6 t	1.66 t	1.14 d	35.7 t	1.42 q	1.93 t	40.8 t	1.65 t	1.08 q
20	28.8 t	2.21 d	2.34 t	25.8 t	~2.19 overlapped		27.8 t	1.65 t	1.95 t
21	133.3 s			138.2 s			45.5 d		1.98 q
22	122.4 s			123.5 s			146.8 s		
23	33.4 q	0.85 s		33.5 q	0.86 s		33.4 q	0.84 s	
24	21.6 q	0.80 s		21.6 q	0.82 s		21.6 q	0.79 s	
25	15.9 q	0.82 s		16.1 q	0.84 s		15.9 q	0.81 s	
26	19.5 q	1.06 s		21.4 q	0.85 s		19.3 q	1.04 s	
27	15.7 q	1.22 s		102.9 t	4.87 s	4.75 s	15.4 q	1.17 s	
28	14.5 q	0.87 s		17.8 q	0.98 s		15.9 q	0.92 d (0.8 Hz)	
29	19.4 q	1.66 s		20.7 q	1.54 s		111.5 t	4.86 s	4.80 s
30	22.9 q	1.58 s		21.3 q	1.56 s		25.0 q	1.71 s	

COSY Spectrum of Secoaldehyde (3-12)

The COSY spectrum of **3-12** revealed that the foregoing pair of methylene protons (2.57 and 2.21 ppm) was coupled to the H-15 aldehydic proton (9.76 ppm) and the downfield methine proton (3.75 ppm) (see Table 3-21). These correlations demonstrated that these signals arose from H-15 (9.76 ppm), H-16α/β (2.57 and 2.21

ppm) and H-17β (3.75 ppm). H-13β (2.00 ppm, d) was identified by ^4J correlations which this proton exhibited with H-27a (4.87 ppm, br s) and H-27b (4.75 ppm, br s).

Table 3-21. Selected ^{1}H-^{1}H COSY correlations (δ ppm in $CDCl_3$) observed for 14,15-secohopa-14(27),21-dien-15-al (**3-12**).

^{1}H NMR signals	correlated ^{1}H signals
9.76 t (H-15)	2.57 m/2.21 m (H-16α/β)
4.87 br s (H-27a)	4.75 br s (H-27b), 2.00 d (H-13β)
4.75 br s (H-27b)	4.87 br s (H-27a), 2.00 d (H-13β)
3.75 t (H-17β)	2.57 m/2.21 m (H-16α/β)
2.57 m (H-16α)	9.76 t (H-15), 3.75 t (H-17β), 2.21 m (H-16β)
2.21 m (H-16β)	9.76 t (H-15), 3.75 t (H-17β), 2.57 m (H-16α)

^{13}C and DEPT135 NMR Spectra of Secoaldehyde (3-12)

The ^{13}C NMR spectrum of secoaldehyde (**3-12**) was comprised of 30 carbon resonances, which were characterised by a DEPT135 NMR spectrum to arise from 7 quartet (CH_3), 11 triplet (CH_2), 5 doublet (CH), and 7 singlet (C) carbons. The ^{13}C NMR spectrum included signals attributable to two non-protonated olefinic carbons (123.5 ppm, s and 138.2 ppm, s) and an aldehyde carbon (203.6 ppm) (see Table 3-20).

Most carbon signals could be assigned by analyses of the ^1J and ^2J, ^3J and sometimes ^4J correlations observed in the HSQC and HMBC spectra of **3-12** (see Table 3-22).

Comparisons with signal assignments determined for ring A/B/C carbons of **3-3**, and for ring A/B and olefinic ring E carbons of **3-8**, also facilitated the derivation of signal assignments. For example, HMBC data did not differentiate the C-2 and C-6 assignments of **3-12**. This problem was resolved by comparison with assignments established for these carbons in **3-3** and **3-8**.

Table 3-22. ^{1}J, ^{2}J and ^{3}J heteronuclear ^{1}H-^{13}C correlations (δ ppm in $CDCl_3$) observed for 14,15-secohopa-14(27),21-dien-15-al (**3-12**).

^{1}H signal	^{1}J correlated ^{13}C signal	^{2}J and ^{3}J correlated ^{13}C signals
0.86 s (4α-Me)	33.5 (C-23)	57.0 (C-5), 42.1 (C-3), 33.3 (C-4), 21.6 (C-24)
0.85 s (4β-Me)	21.6 (C-24)	57.0 (C-5), 42.1 (C-3), 33.3 (C-4), 33.5 (C-23)
0.84 s (10β-Me)	16.1 (C-25)	60.2 (C-9), 57.0 (C-5), 40.0 (C-1), 38.3 (C-10)
0.85 s (8β-Me)	21.4 (C-26)	161.0 (C-14), 60.2 (C-9), 41.9 (C-8), 39.2 (C-7)
0.98 s (18α-Me)	17.8 (C-28)	46.7 (C-18), 43.0 (C-13), 41.9 (C-17), 35.7 (C-19)
1.54 s (22a-Me)	20.7 (C-29)	138.2 (C-21), 123.5 (C-22), 21.3 (C-30)
1.56 s (22b-Me)	21.3 (C-30)	138.2 (C-21), 123.5 (C-22), 20.7 (C-29)
9.76 t (H-15)	203.6 (C-15)	46.1 (C-16), 41.9 (C-17)
4.87 br s (H-27a)	102.9 (C-27)	161.0 (C-14), 60.2 (C-9)*, 43.0 (C-13), 41.9 (C-8) 30.6 (C-12)*, 21.4 (C-26)*
4.75 br s (H-27b)	102.9 (C-27)	161.0 (C-14), 43.0 (C-13), 41.9 (C-8), 39.2 (C-7)*, 30.6 (C-12)*
3.75 t (H-17β)	41.9 (C-17)	203.6 (C-15), 138.2 (C-21), 123.5 (C-22), 46.7 (C-18) 46.1 (C-16), 43.0 (C-13), 35.7 (C-19), 25.8 (C-20)
2.57 m/2.21 m (H-16α/β)	46.1 (C-16)	203.6 (C-15), 138.2 (C-21), 46.7 (C-18), 41.9 (C-17)

* ^{4}J coupling

The methyl group proton and carbon resonances were identified from the analyses of HSQC and HMBC spectral data similar to that described in Section **3.3.1** for **3-3**. For example each of the 4α-, 4β- and 10β-methyl group protons (0.86, 0.82 and 0.84 ppm respectively) exhibited correlations with C-5 (57.0 ppm), while the protons of the 8β- and 10β-methyl groups showed correlations with C-9 (60.2 ppm). The 4α- and 4β-methyl group protons also exhibited correlations to C-3 (42.1 ppm) and C-4 (33.3 ppm), while the 10β-methyl group protons exhibited correlations to C-1 (40.0 ppm), C-9 (60.2 ppm) and C-10 (38.3 ppm).

Notwithstanding the very small differences in resonance frequencies of the foregoing methyl groups, the resolution of the 400 MHz difference HMBC spectrum of **3-12** (obtained after subtraction of signals arising from **3-8**), was such that individual sets of methyl group HMBC correlations could be adequately resolved. The HSQC data demonstrated that the C-23, C-24 and C-25 signals occurred at 33.5, 21.6 and 16.1 ppm respectively.

The location of the aldehyde group was revealed by correlations which H-15 (9.76 ppm) exhibited to C-16 (46.1 ppm) and C-17 (41.9 ppm), and by the correlations which H-17β (3.75 ppm) exhibited to C-15 (203.6 ppm), C-21 (138.2 ppm), C-22 (123.5 ppm), C-13 (43.0 ppm), C-18 (46.7 ppm), C-16 (46.1 ppm), C-19 (35.7 ppm) and C-20 (25.8 ppm).

3.5 Photochemical Reaction of Hopan-15-one

3.5.1 Photolysis of Hopan-15-one (3-10) in Benzene-Methanol

Irradiation of a solution of hopan-15-one (**3-10**) in a mixture of dry benzene and methanol for 24 h gave a complex mixture of products, which when separated by radial chromatography on silica gel using mixtures of light petroleum and diethyl ether as eluents, afforded moderate quantities of two products. These compounds exhibited significant *m/z* 426 fragment ions, and were identified as the epimeric alcohols 14,15-seco-15,22-*abeo*hop-14(27)-en-15α-ol (**3-13**) and 14,15-seco-15,22-*abeo*hop-14(27)-en-15β-ol (**3-14**) respectively (see Figure 3-14).

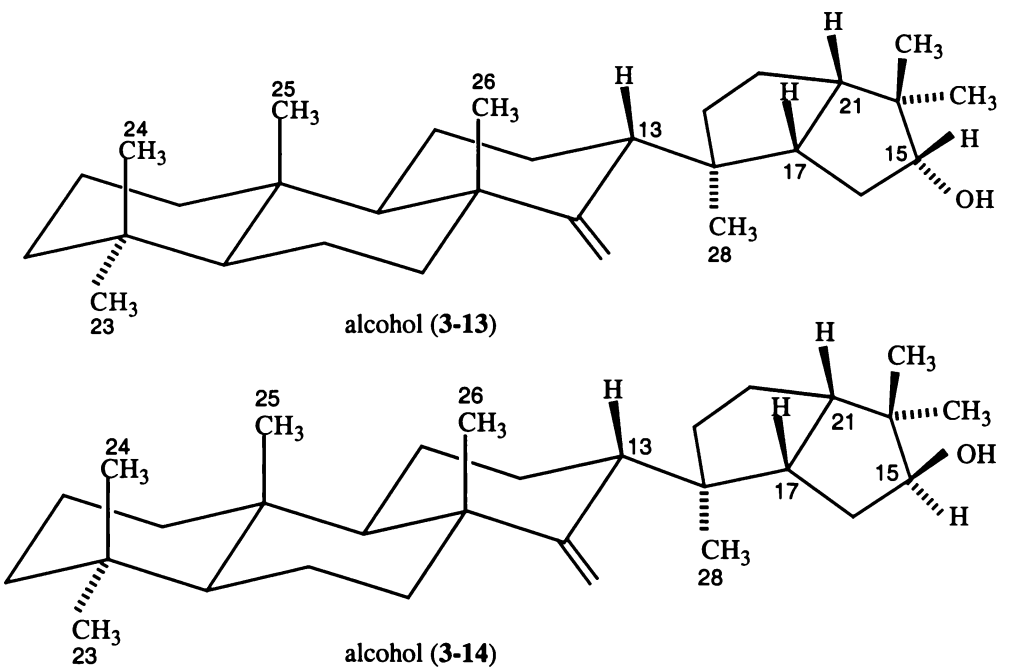

Figure 3-14. Proposed structures of 15,22-*abeo*-15-ols (**3-13**) and (**3-14**) obtained on photolysis of hopan-15-one (**3-10**).

3.5.2 Structural Elucidation of Alcohols (3-13) and (3-14)

3.5.2.1 Mass Spectral Analysis of Alcohols (3-13) and (3-14)

The mass spectra of alcohols (**3-13**) and (**3-14**) included molecular ions at *m/z* 426, corresponding to molecular formulae of $C_{30}H_{50}O$ (426 daltons). Pronounced *m/z* 166, 165, 149 and 148 fragment ions, and less intense *m/z* 260 and 245 fragment ions were observed in the mass spectra of the respective compounds. The postulated fragmentation pathways leading to these ions are shown in Scheme 3-8.

The *m/z* 260 and 166 fragment ions can be envisaged as radical ions formed by cleavage of the C-13-C-18 bond. Loss of a methyl group from the *m/z* 260 fragment ion would lead to a *m/z* 245 ion, while loss of water from the *m/z* 166 fragment ion would lead to a *m/z* 148 ion.

The ratio of the *m/z* 166 to *m/z* 148 ion intensities was ~ 0.9 for alcohol (**3-13**), compared to ~1.4 for alcohol (**3-14**), possibly indicating that alcohol (**3-13**) is more prone to dehydration under mass spectral conditions than is the case for alcohol (**3-14**). Other significant fragment ions, and their relative intensities are listed in Table 3-23.

Table 3-23. Selected mass spectral fragment ions observed for 14,15-seco-15,22-*abeo*hop-14(27)-en-15α-ol (**3-13**) and 14,15-seco-15,22-*abeo*hop-14(27)-en-15β-ol (**3-14**).

ions	*m/z* (% relative intensities)	
	alcohol (3-13)	alcohol (3-14)
M^+	426 (2)	426 (2)
M^+-CH_3	411 (2)	411 (2)
$C_{19}H_{32}^{+\cdot}$ (ion b)	260 (5)	260 (5)
ion b-CH_3	245 (5)	245 (6)
$C_{11}H_{19}O^+$(ion a)	167 (11)	167 (20)
$C_{11}H_{18}O^{+\cdot}$ (ion a')	166 (23)	166 (33)
$C_{11}H_{17}O^+$	165 (13)	165 (14)
ion a -H_2O	149 (86)	149 (17)
ion a'-H_2O	148 (25)	148 (23)
ion a'-H_2O-CH_3	133 (36)	133 (38)
$C_9H_{15}^+$ (ion c)	123 (47)	123 (70)
$C_9H_{13}^+$	121 (33)	121 (23)

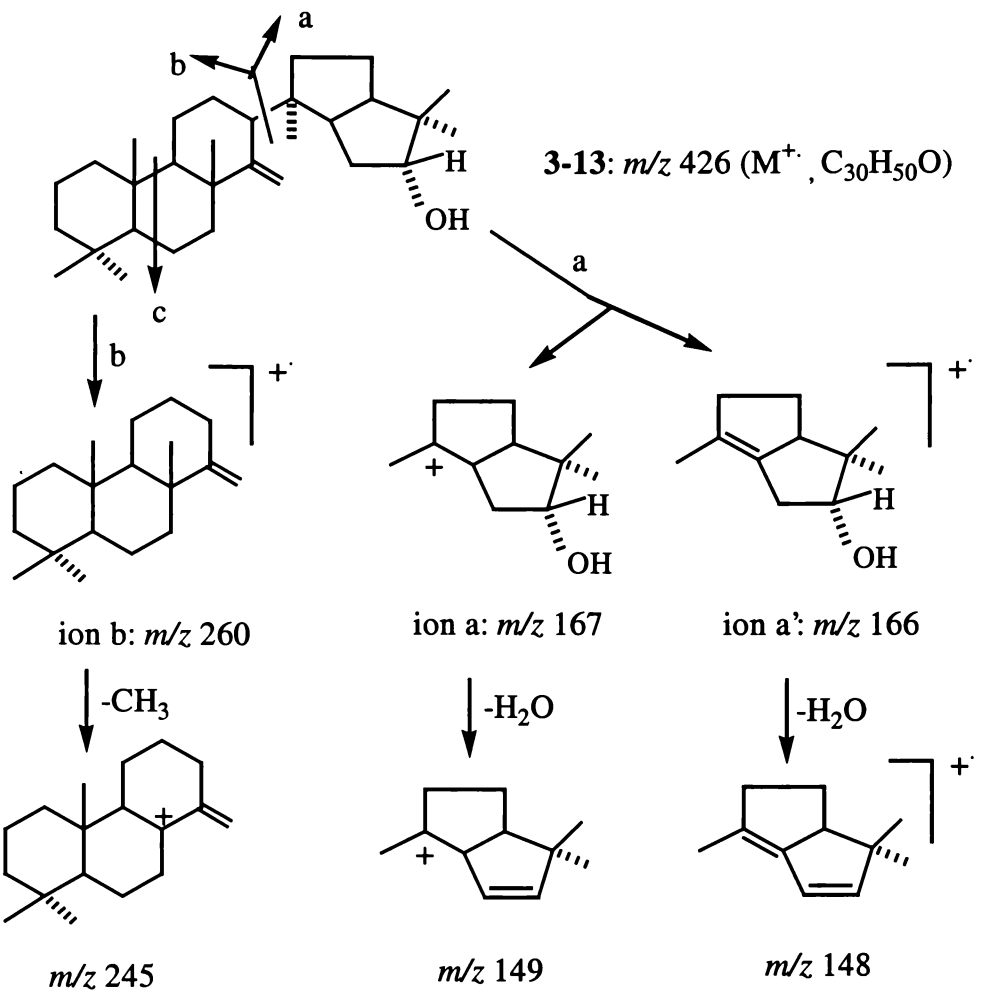

Scheme 3-8. Proposed mass spectral fragmentation pathways for 14,15-seco-15,22-*abeo*hop-14(27)-en-15α-ol (**3-13**).

3.4.2.2 NMR Spectral Analyses of Alcohols (3-13) and (3-14)

Complete assignments of the ^{13}C and ^{1}H NMR signals of alcohols (**3-13**) and (**3-14**), derived from a combination of one- and two-dimensional NMR spectral data, are presented in Table 3-24.

^{1}H NMR Spectrum of Alcohol (3-13)

The ^{1}H NMR spectrum of alcohol (**3-13**) included signals arising from seven tertiary methyl groups, two olefinic protons (4.76 ppm, br s and 4.51 ppm, br s), a downfield methine proton (3.70 ppm, t, J = 6.1 Hz), and methylene or methine signals at 2.37 ppm (dd, J = 18.1, 9.4 Hz) and 1.90 ppm (dddd, J = 12.3, 3.4, 3.4, 3.4 Hz).

The resonances of the two olefinic protons (4.76 and 4.51 ppm) corresponded closely to the H-27a and H-27b resonances of **3-3**, **3-5**, **3-6** and **3-12** (Sections **3.3** and **3.4**), thereby indicating the presence of a similar ring A/B/C structural unit in **3-13**.

Table 3-24. ^{13}C and ^{1}H NMR signals (δ ppm in $CDCl_3$) observed for hopan-15-one (**3-10**), 14,15-seco-15,22-*abeo*hop-14(27)-en-15α-ol (**3-13**) and 14,15-seco-15,22-*abeo*hop-14(27)-en-15β-ol (**3-14**).

atom	Hopan-15-one (**3-10**)			alcohol (**3-13**)			alcohol (**3-14**)		
	^{13}C	$^{1}H_\alpha$	$^{1}H_\beta$	^{13}C	$^{1}H_\alpha$	$^{1}H_\beta$	^{13}C	$^{1}H_\alpha$	$^{1}H_\beta$
1	40.5 t	0.77 t	1.64 d	40.1 t	0.77 t	1.64 d	40.1 t	0.76 t	1.64 d
2	18.8 t	1.36~1.57		18.8 t	1.39 d	1.59 q	18.8 t	1.38 d	1.57 q
3	42.1 t	1.10 t	1.34 d	42.2 t	1.11 t	1.36 d	42.2 t	1.11 t	1.36 d
4	33.3 s			33.4 s			33.4 s		
5	56.5 d	0.74 d		56.9 d	0.82 d		56.8 d	0.81 d	
6	18.8 t	1.36~1.57		19.2 t	1.64 d	1.46 q	19.1 t	1.66 d	1.44 q
7	34.2 t	1.44 t	2.53 m	39.5 t	~1.59		39.6 t	~1.59	
8	42.9 s			41.4 s			41.3 s		
9	51.9 d	1.14 d		59.4 d	0.89 d		59.2 d	0.87 d	
10	38.2 s			38.3 s			38.2 s		
11	21.4 t	1.61 d	1.25 q	22.0 t	1.68 d	1.38 q	21.9 t	1.68 d	1.37 q
12	23.9 t	~1.48 overlapped		31.0 t	1.14 q	1.90 dddd	31.0 t	1.14 q	1.87 dddd
13	50.1 d		1.69 d	51.1 d		2.02 d	52.4 d		2.00 d
14	56.9 s			161.6 s			161.5 s		
15	215.4 s			82.8 d	(6.1 Hz) 3.70 t		79.5 d	3.81 dd (9.6, 7.6 Hz)	
16	41.8 t	2.74 dd	2.39 dd	36.6 t	1.64 q	2.01 q	35.4 t	1.60 q	2.05 t
17	52.0 d		1.70 d	47.5 d		2.37 dd	46.5 d		2.37 ddd
18	44.3 s			46.0 s			45.3 s		
19	41.1 t	1.63 t	0.99 q	45.0 t	1.56 t	1.50 d	45.4 t	1.58 d	1.37 q
20	28.0 t	1.62 t	1.87 q	26.0 t	1.63 t	1.49 q	27.0 t	1.51 t	1.19 q
21	47.0 d		1.67 q	55.6 d		2.04 q	56.3 d		2.06 q
22	31.3 d	1.60 d		43.1 s			42.3 s		
23	33.4 q	0.85 s		33.5 q	0.86 s		33.5 q	0.86 s	
24	21.6 q	0.79 s		21.6 q	0.83 s		21.6 q	0.83 s	
25	16.0 q	0.82 d (0.5 Hz)		16.2 q	0.86 s		16.2 q	0.86 s	
26	19.1 q	1.04 s		22.3 q	1.02 s		22.4 q	1.02 s	
27	15.5 q	1.20 s		102.6 t	4.76 s	4.51 s	102.7 t	4.74 s	4.48 d (1 Hz)
28	15.6 q	0.92 d (0.9 Hz)		18.9 q	1.01 s		18.5 q	0.96 s	
29	22.5 q	0.84 d (6.4 Hz)		29.3 q	0.94 s (22β-Me)		22.7 q	0.97 s (22β-Me)	
30	23.7 q	0.88 d (6.4 Hz)		18.6 q	0.92 s (22α-Me)		21.9 q	0.87 s (22α-Me)	

HSQC spectral data established that the H-15 signal which occurred at 3.70 ppm was ^1J coupled to an oxygenated carbon (82.8 ppm) (see Table 3-24), which HMBC spectral data showed was located within a five membered ring F (see below). The chemical shift of H-15 (3.70 ppm) was consistent with the presence of a secondary alcohol group in alcohol (**3-13**).

^{1}H NMR Spectrum of Alcohol (3-14)

The ^{1}H NMR spectrum of alcohol (**3-14**) corresponded closely to that observed for alcohol (**3-13**). In particular it included methyl group signals attributable to a common ring A/B/C partial structural unit (see Table 3-24), two olefinic proton signals (4.74 ppm, br s; 4.48 ppm, d, J = 1.0 Hz) assignable to H-27a and H-27b, and a downfield methine signal at 3.81 ppm (dd, J = 9.6, 7.6 Hz), and methylene or methine multiplet signals at 2.37 ppm (ddd, J = 10.9, 10.9 and 3.5 Hz), and 1.87 ppm (dddd, J = 12.1, 3.4, 3.4, 3.4 Hz).

Similarly, the ^{1}H NMR signal at 3.81 ppm correlated in the HSQC spectrum with an oxygenated carbon signal which occurred at 79.5 ppm (see Table 3-24). The above observations were consistent with the formulation of **3-14** as the C-15 epimer of **3-13**.

COSY Spectrum of Alcohol (3-14)

The COSY spectrum of alcohol (**3-14**) showed that H-15 (3.81 ppm) coupled to a pair of methylene protons which resonated at 1.60 and 2.05 ppm (H-16α and H-16β respectively), and that each of these protons coupled to H-17β (2.37 ppm).

H-13β (2.00 ppm, d) was identified by ^4J correlations with two olefinic protons (4.74 ppm, s, H-27a and 4.48 ppm, d, J = 1.0 Hz, H-27b) and a pair of methylene protons at 1.14 and 1.87 ppm (H-12α and H-12β). Similarly, H-21β (2.06 ppm) was identified by correlations with H-17β (2.37 ppm) and H-20α/β (1.51 and 1.19 ppm).

Several of the methyl group protons exhibited ^4J couplings to adjacent 1,2-*trans* diaxially oriented methylene protons (Sanders and Hunter, 1987). For example, ^4J couplings where observed between H-25 and H-1α and between H-26 and H-7α. The H-29 and H-30 protons were also mutually ^4J coupled (see Table 3-25).

Table 3-25. Selected ^{1}H-^{1}H COSY correlations (δ ppm in $CDCl_3$) observed for 14,15-seco-15,22-*abeo*hop-14(27)-en-15β-ol (**3-14**).

^{1}H NMR signals	correlated ^{1}H signals
4.74 br s (H-27a)	4.48 d (H-27b), 2.00 d (H-13β), ~1.59 (H-7α/β)*
4.48 d (H-27b)	4.74 br s (H-27a), 2.00 d (H-13β)
3.81 dd (H-15α)	1.60 q/2.05 t (H-16α/β), 0.97 s (22β-Me)
2.37 ddd (H-17β)	2.06 q (H-21β), 1.60 q/2.05 t (H-16α/β)
2.06 q (H-21β)	2.37 ddd (H-17β), 1.51 t/1.19 q (H-20α/β)
2.00 d (H-13β)	4.74 s/4.48 d (H-27a/b)*, 1.14 q/1.87 dddd (H-12α/β)
1.87 dddd (H-12β)	2.00 d (H-13β), 1.68 d/1.37 q (H-11α/β), 1.14 q (H-12α)
1.68 d (H-11α)	1.37 q (H-11β), 1.14 q/1.87 dddd (H-12α/β), 0.87 d (H-9α)
1.60 q (H-16α)	3.81 dd (H-15α), 2.37 ddd (H-17β), 2.05 t (H-16β)
1.51 t (H-20α)	2.06 q (H-21β), 1.19 q (H-20β)
1.38 d (H-2α)	0.76 t /1.64 d (H-1α/β), 1.56 q (H-2β), 1.11 t (H-3α)
1.19 q (H-20β)	2.06 q (H-21β), 1.58 d (H-19α), 1.51 t (H-20α)
1.11 t (H-3α)	1.38 d (H-2α), 1.36 d (H-3β), 0.83 s (4β-Me)*, 0.81 d (H-5α)
0.87 d (H-9α)	1.68 d/1.37 q (H-11α/β)
0.81 d (H-5α)	1.68 d/1.44 q (H-6α/β)
0.86 s (10β-Me)*	0.76 t (H-1α)
1.02 s (8β-Me)*	1.59 (H-7α)
0.97 s (22β-Me)*	0.87 s (22α-Me)

* ^{4}J coupling

^{13}C and DEPT135 NMR Spectra of Alcohols (3-13) and (3-14)

The ^{13}C NMR spectra of alcohols (**3-13**) and (**3-14**) were each comprised of 30 carbon resonances, which were characterised by DEPT135 NMR spectra to arise from 7 quartet (CH_3), 11 triplet (CH_2), 6 doublet (CH), and 6 singlet (C) carbons. Signals attributable to two olefinic carbons and an oxygenated methine carbon appeared in the ^{13}C NMR spectra of alcohol (**3-13**) (102.6, 161.6 and 82.8 ppm respectively) and of alcohol (**3-14**) (102.7, 161.6 and 79.5 ppm respectively).

The resonances of the ring A/B/C carbons of alcohol (**3-13**) and (**3-14**) were essentially identical (see Table 3-24), other than for a 3.3 ppm difference in their C-15 resonances, and minor differences in the resonances of C-16, C-17, C-18, C-21, C-22, C-29 and C-30. These differences were consistent with the formulation of **3-13** and **3-14** as a pair of epimeric C-15 alcohols.

HSQC spectral data showed that most of ring A, B and C methylene, and methine proton resonances of alcohols (**3-13**) and (**3-14**) corresponded closely to those determined for hemiacetal (**3-3**), and related compounds (**3-5**) and (**3-6**). Complete assignments of the ^{13}C and ^{1}H NMR signals of alcohols (**3-13**) and (**3-14**) are given in Table 3-24.

The existence of a five-membered 15,22-*abeo* ring system (ring F) in alcohols (**3-13**) and (**3-14**) was established by detailed analyses of HMBC correlations exhibited by ring F protons of the respective compounds (see Table 3-26 and 3-27). HMBC correlations observed for the ring F protons of alcohol (**3-13**) are depicted Figure 3-15.

Table 3-26. ^{1}J, ^{2}J and ^{3}J heteronuclear ^{1}H-^{13}C correlations (δ ppm in $CDCl_3$) observed for 14,15-seco-15,22-*abeo*hop-14(27)-en-15α-ol (**3-13**).

^{1}H signal	^{1}J correlated ^{13}C signal	^{2}J and ^{3}J correlated ^{13}C signals
0.86 s (4α-Me)	33.5 (C-23)	56.9 (C-5), 42.2 (C-3), 33.4 (C-4), 21.6 (C-24)
0.83 s (4β-Me)	21.6 (C-24)	56.9 (C-5), 42.2 (C-3), 33.4 (C-4), 33.5 (C-23)
0.86 s (10β-Me)	16.2 (C-25)	59.4 (C-9), 56.9 (C-5), 40.1 (C-1), 38.3 (C-10)
1.02 s (8β-Me)	22.3 (C-26)	161.6 (C-14), 59.4 (C-9), 41.4 (C-8), 39.5 (C-7)
1.01 s (18α-Me)	18.9 (C-28)	51.1 (C-13), 47.5 (C-17), 46.0 (C-18), 45.0 (C-19)
0.94 s (22β-Me)	29.3 (C-29)	82.8 (C-15), 55.6 (C-21), 43.1 (C-22), 18.6 (C-30)
0.92 s (22α-Me)	18.6 (C-30)	82.8 (C-15), 55.6 (C-21), 43.1 (C-22), 29.3 (C-29)
1.90 dddd (H-12β)	31.0 (C-12)	161.6 (C-14), 59.4 (C-9), 51.1 (C-13), 22.0 (C-11)
2.01 q (H-16β)	36.6 (C-16)	82.8 (C-15), 55.6 (C-21), 47.5 (C-17), 46.0 (C-18), 43.1 (C-22)
2.02 d (H-13β)	51.1 (C-13)	161.6 (C-14) 102.6 (C-27), 36.6 (C-16)*, 31.0 (C-12) 26.0 (C-20)* 22.0 (C-11), 18.9 (C-28)
2.37 dd (H-17β)	47.5 (C-17)	82.8 (C-15), 55.6 (C-21), 51.1 (C-13),46.0 (C-18), 45.0 (C-19) 36.6 (C-16), 26.0 (C-20), 18.9 (C-28)
3.70 t (H-15β)	82.8 (C-15)	55.6 (C-21), 47.5 (C-17), 36.6 (C-16), 29.3 (C-30), 18.6 (C-29)
4.51 br s (H-27b)	102.6 (C-27)	161.6 (C-14), 51.1 (C-13), 41.4 (C-8), 39.5 (C-7)*, 31.0 (C-12)*
4.76 br s (H-27a)	102.6 (C-27)	161.6 (C-14), 59.4 (C-9)*, 51.1 (C-13), 41.4 (C-8) 31.0 (C-12)*, 22.0 (C-11)*

*^{4}J coupling

In particular, H-15β (3.70 ppm) of alcohol (**3-13**) exhibited HMBC correlations with C-16 (36.6 ppm), C-17 (47.5 ppm), C-21 (43.1 ppm), C-29 (29.3 ppm), and C-30 (18.6 ppm). Correlations were also observed between H-15α (3.81 ppm) and C-29 (22.7 ppm), and C-30 (21.9 ppm) in the HMBC spectrum of alcohol (**3-14**).

These correlations, which demonstrated that H-15 was situated within 3 bonds of C-29 and C-30, were consistent with the presence of 15,22-*abeo* ring F system in alcohols (**3-13**) and (**3-14**).

Other structurally significant HMBC correlations observed for alcohols (**3-13**) and (**3-14**) are presented in Tables 3-26 and 3-27 respectively.

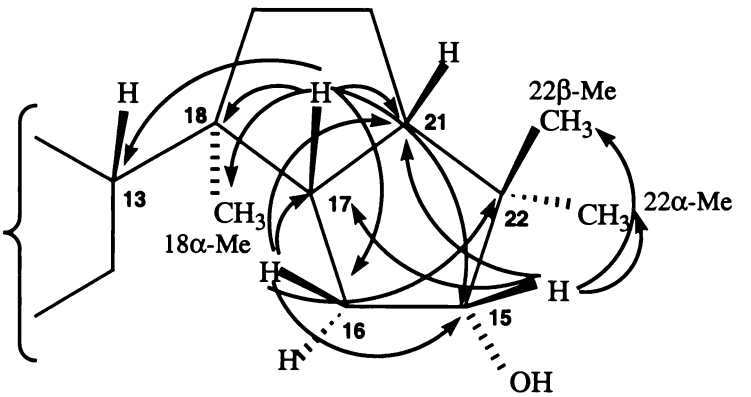

Figure 3-15. Selected HMBC correlations observed for the ring F protons of alcohol (**3-13**).

Table 3-27. ^{1}J, ^{2}J and ^{3}J heteronuclear ^{1}H-^{13}C correlations (δ ppm in $CDCl_3$) observed for 14,15-seco-15,22-*abeo*hop-14(27)-en-15β-ol (**3-14**).

^{1}H signal	^{1}J correlated ^{13}C signal	^{2}J and ^{3}J correlated ^{13}C signals
0.86 s (4α-Me)	33.5 (C-23)	56.8 (C-5), 42.2 (C-3), 33.4 (C-4), 21.6 (C-24)
0.83 s (4β-Me)	21.6 (C-24)	56.9 (C-5), 42.2 (C-3), 33.4 (C-4), 33.5 (C-23)
0.86 s (10β-Me)	16.2 (C-25)	59.2 (C-9), 56.8 (C-5),40.1 (C-1), 38.2 (C-10)
1.02 s (8β-Me)	22.4 (C-26)	161.5 (C-14), 59.2 (C-9), 41.3 (C-8), 39.6 (C-7)
0.96 s (18α-Me)	18.5 (C-28)	52.4 (C-13), 46.5 (C-17), 45.4 (C-19), 45.3 (C-18)
0.97 s (22β-Me)	22.7 (C-29)	79.5 (C-15), 56.3 (C-21), 42.3 (C-22), 22.7 (C-30)
0.87 s (22α-Me)	21.9 (C-30)	79.5 (C-15), 56.3 (C-21), 42.3 (C-22), 21.9 (C-29)
2.00 d (H-13β)	52.4 (C-13)	46.5 (C-17), 45.4 (C-19), 45.3 (C-18), 31.0 (C-12)
2.05 t (H-16β)	35.4 (C-16)	79.5 (C-15), 56.3 (C-21), 46.5 (C-17), 45.3 (C-18)
2.37 ddd (H-17β)	46.5 (C-17)	79.5 (C-15), 56.3 (C-21), 52.4 (C-13), 45.3 (C-18) 35.4 (C-16), 27.0 (C-20)
3.81 dd (H-15α)	79.5 (C-15)	22.7 (C-30), 21.9 (C-29)
4.48 d (H-27b)	102.7 (C-27)	161.5 (C-14), 52.4 (C-13), 41.3 (C-8), 39.6 (C-7)*
4.74 s (H-27a)	102.7 (C-27)	161.5 (C-14), 52.4 (C-13), 41.3 (C-8), 22.4 (C-26)*

* ^{4}J coupling

NOE Data and Molecular Modelling Analyses of Alcohols (3-13) and (3-14)

The C-15 configuration of alcohols (**3-13**) and (**3-14**) were defined by NOE-difference data (see Table 3-28 and 3-29). Enhancements observed for the protons of the ring A/B/C methyl groups of **3-13** are depicted in Figure 3-16.

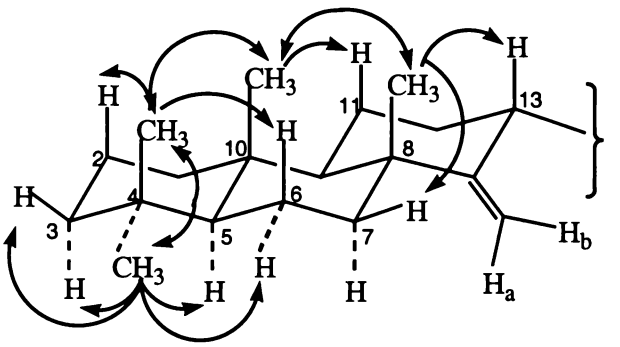

Figure 3-16. Selected NOE's observed for ring A/B/C protons of alcohol (**3-13**).

The observation that irradiation of H-15 (3.70 ppm) of alcohol (**3-13**) enhanced H-16β (2.01 ppm), H-17β (2.37 ppm) and the 22β-methyl group (0.94 ppm) showed H-15 to be β-orientated and revealed the hydroxyl group at C-15 to be α-oriented (Figure 3-17). Other structurally significant NOE's are presented in Table 3-28.

Table 3-28. NOE effects (δ ppm in $CDCl_3$) observed for alcohol (**3-13**).

irradiated ^{1}H NMR signal	enhanced ^{1}H signals
4.76 br s (H-27a)	4.51 br s (H-27b), ~1.59 (H-7α/β)
4.51 br s (H-27b)	4.76 br s (H-27a), 2.37 dd (H-17β), 2.01 q (H-16β), 1.01 s (18α-Me)
3.70 t (H-15β)	2.37 dd (H-17β), 2.01 q (H-16β), 0.94 s (22β-Me)
2.37 dd (H-17β)	4.51 br s (H-27b), 3.70 t (H-15β), ~2.02 {H-13β, H-16β, H-21β}, 0.94 s (22β-Me)
0.94 s (22β-Me)	0.92 s (22α-Me), 3.70 t (H-15β), 2.37 dd (H-17β), 2.04 q (H-21β)
0.92 s (22α-Me)	0.94 s (22β-Me), 1.64 q (H-16α), 1.63 t (H-20α)
1.02 s (8β-Me)	0.86 s (10β-Me), 2.02 d (H-13β), ~1.59 (H-7β), 1.46 q (H-6β)
1.01s (18α-Me)	4.51 br s (H-27b), 1.64 q/2.01 q (H-16α/β), 1.14 q/1.90 dddd (H-12α/β)
0.86 s (4α-Me)	0.83 s (4β-Me), 1.64 d (H-6α), 1.11 t/1.36 d (H-3α/β), 0.82 d (H-5α)
0.86 s (10β-Me)	1.02 s (8β-Me), 0.83 s (4β-Me), 1.59 q (H-2β), 1.46 q (H-6β), 1.38 q (H-11β),
0.83 s (4β-Me)	0.86 s (4α-Me), 0.86 s (10β-Me), 1.59 q (H-2β), 1.46 q (H-6β)

Irradiation of H-17β (2.37 ppm) enhanced H-27b (4.51 ppm), H-15β (3.70 ppm), H-21β (2.04 ppm), H-13β (2.02 ppm), H-16β (2.01 ppm) and the 22β-methyl group (0.94 ppm). Irradiation of the 18α-methyl group (1.01 ppm) did not enhance H-15 (3.70 ppm). These observations were consistent with the conclusion that in alcohol (**3-13**), H-15 is β-oriented (see Figure 3-17).

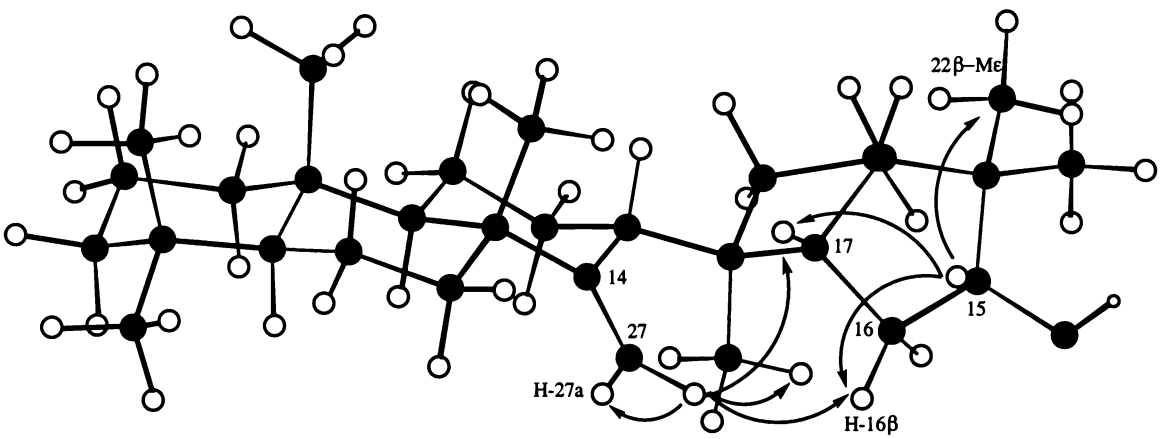

Figure 3-17. MM2 modelled conformation determined for alcohol (**3-13**).

The disposition of the H-27a and H-27b protons of alcohol (**3-13**) was revealed by the analyses of NOE-difference spectral data (see Figure 3-16). Irradiation of H-27a (4.76 ppm) enhanced H-27b (4.51 ppm), and H-7α/β (~1.59 ppm), while irradiation of H-27b (4.51 ppm) enhanced H-27a (4.76 ppm), H-17β (2.37 ppm), H-16β (2.01 ppm), and the 18α-methyl group (1.01 ppm). These correlations are consistent with modelled inter-nuclear distances of 1.83, 2.48, 2.25 and 2.08 Å respectively.

The ring A/B/C protons and the methyl groups of alcohol (**3-14**) exhibited similar NOE-difference enhancements to those observed for the equivalent protons of alcohol (**3-13**) (see Table 3-29). Other structurally significant NOE's observed for alcohol (**3-14**) are presented in Table 3-29.

Irradiation of the 18α-methyl group (0.96 ppm) of alcohol (**3-14**) enhanced H-15 (3.81 ppm), while irradiation of H-17β (2.37 ppm) did not enhance H-15 (3.81 ppm). These observations indicated H-15 to be α-oriented, and showed that in alcohol (**3-14**), the C-15 hydroxyl group was β-oriented (see Figure 3-18).

Table 3-29. NOE effects (δ ppm in $CDCl_3$) observed for alcohol (**3-14**).

irradiated ^{1}H NMR signals	enhanced ^{1}H signals
4.74 br s (H-27a)	4.48 d (H-27b), ~1.59 (H-7α/β)
4.48 d (H-27b)	4.74 br s (H-27a), 2.37 ddd (H-17β), 1.60 q/2.05 t (H-16α/β), 0.96 s (18α-Me)
3.81 dd (H-15α)	1.60 q (H-16α), 1.51 q (H-20α), 0.96 s (18α-Me), 0.87 s (22α-Me)
2.37 ddd (H-17β)	4.48 d (H-27b), 2.00-2.06 {H-13β, H-16β, H-21β}, 1.60 q (H-16α), 0.97 s (22β-Me)
0.97s (22β-Me)	0.87 s (22α-Me), 2.37 ddd (H-17β), 2.06 q (H-21β)
0.87 s (22α-Me)	0.97 s (22β-Me), 3.81 dd (H-15α), 2.06 q (H-21β), 1.51 t /1.19 q (H-20α/β)
1.02 s (8β-Me)	0.86 s (10β-Me), 2.00 d (H-13β), 1.59 (H-7β), 1.44 q (H-6β)
0.96 s (18α-Me)	4.48 d (H-27b), 3.81 dd (H-15α), 1.58 -1.60 {H-19α, H-16α}, 1.14 q (H-12α)
0.86 s (4α-Me)	0.83 s (4β-Me), 1.66 d (H-6α), 1.11 t/1.36 d (H-3α/β), 0.81 d (H-5α)
0.86 s (10β-Me)	1.02 s (8β-Me), 0.83 s (4β-Me), 1.57 q (H-2β), 1.44 q (H-6β), 1.37 q (H-11β)
0.83 s (4β-Me)	0.86 s (4α-Me), 0.86 s (10β-Me), 1.57 q (H-2β), 1.44 q (H-6β)

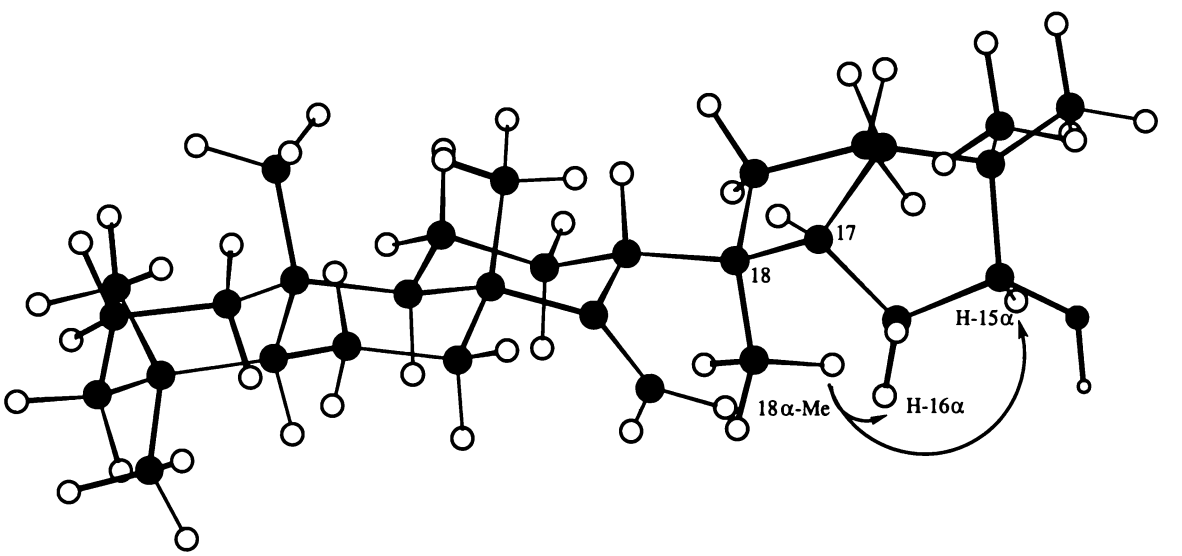

Figure 3-18. MM2 modelled conformation determined for (**3-14**).

3.6 Photochemical Reaction of 21α-H-Hopan-15-one

3.6.1 Photolysis of 21α-H-Hopan-15-one (3-11) in Benzene-Methanol

Photolysis of 21α-H-hopan-15-one (**3-11**) in a mixture of dry benzene and methanol afforded a complex mixture. Separation of the mixture by radial PLC on silica gel using mixtures of light petroleum and benzene as eluents afforded fractions which were shown by GC/MS analyses to be comprised of two compounds. These compounds each exhibited similar mass spectra with highest observed ions at *m/z* 458 and were believed to be isomers at C-14.

These compounds were subsequently identified as methyl 14α,21α-H-14,15-secohopan-15-oate (**3-15**) (secoester 1) and methyl 21α-H-14,15-secohopan-15-oate (**3-16**) (secoester 2). These secoesters can be viewed as ketene addition products, analogous to those obtained on photolysis of 22-hydroxyhopan-7-one (**2-1**) in benzene-methanol (see Section **2.2**).

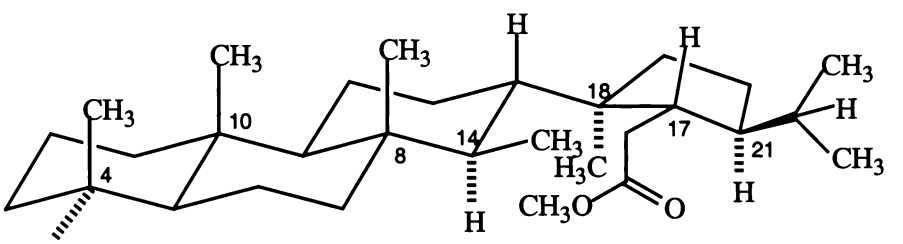

secoester 1 (**3-15**)

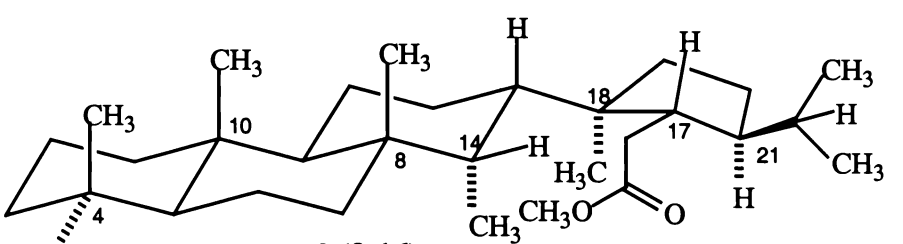

secoester 2 (**3-16**)

Figure 3-19. Structures of methyl 14α,21α-H-14,15-secohopan-15-oate (**3-15**) (secoester 1) and methyl 21α-H-14,15-secohopan-15-oate (**3-16**) (secoester 2).

Repeated efforts to separate the pair of secoesters by radial chromatography on silica gel, including recovery of the early and later portions of the chromatographic band,

repetitively afforded mixtures of the two secoesters. Earlier eluting fractions (eg fraction 8) contained a greater level of **3-16** while later eluting fractions (eg fraction 10) contained a greater level of **3-15**.

3.6.2 Structural Elucidation of Secoesters (3-15) and (3-16)

3.6.2.1 Mass Spectral Analyses of Secoesters (3-15) and (3-16)

The mass spectra of secoesters (**3-15**) and (**3-16**) included weak M^+ ions at *m/z* 458, corresponding to the molecular formulae of $C_{31}H_{54}O_2$ (458 daltons). Significant *m/z* 261, 197, 191, 153, 137 and 123 ions appeared in the mass spectra of each of the secoesters. The proposed origin of these fragment ions is depicted in Scheme 3-9. Other significant fragment ions observed in the mass spectra of the two secoesters (**3-15**) and (**3-16**) are listed in Table 3-30.

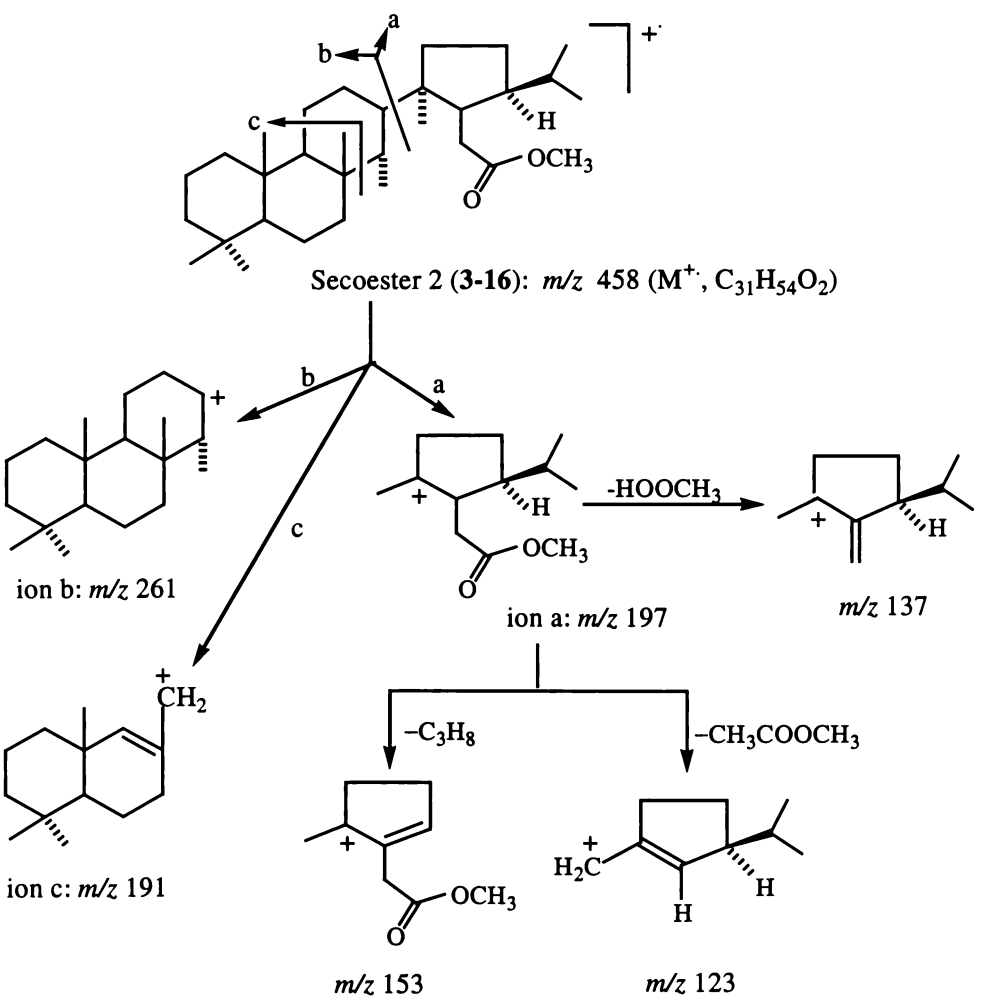

Scheme 3-9. Proposed mass spectral fragmentation pathways for methyl 21α-H-14,15-secohopan-15-oate (**3-16**) (secoester 2).

Table 3-30. Selected mass spectral fragment ions observed for methyl 14α,21α-H-14,15-secohopan-15-oate (**3-15**) (secoester 1).and methyl 21α-H-14,15-secohopan-15-oate (**3-16**) (secoester 2).

ions	*m/z* (% relative intensities)	
	secoester 1 (3-15)	secoester 2 (3-16)
M^+	458 (3)	458 (2)
M^+ -CH_3	443 (5)	443 (5)
M^+-OCH_3	427 (2)	427 (2)
M^+-OCH_3-H_2O	409 (2)	409 (2)
$C_{19}H_{33}^+$ (ion b)	261 (33)	261 (34)
$C_{12}H_{21}O_2^+$ (ion a)	197 (100)	197 (86)
$C_{14}H_{23}^+$ (ion c)	191 (38)	191 (34)
$C_{13}H_{21}^+$	177 (9)	177 (8)
ion a - CH_3OH	165 (20)	165 (30)
ion a - C_3H_8	153 (13)	153 (28)
ion a - $HCOOCH_3$	137 (48)	137 (52)
ion a - CH_3COOCH_3	123 (88)	123 (100)

3.6.2.2 NMR Spectra Analyses of Secoesters (3-15) and (3-16)

Acquisition (under identical conditions) and Fourier transformation of one- and two-dimensional NMR spectral data determined for the secoester fractions recovered from radial chromatography afforded one- and two-dimensional NMR data sets which were manipulated using spectral addition/subtraction software to afford ^1H, ^{13}C, DEPT135, HSQC and HMBC spectra attributable to each of secoester 1 (**3-15**) and secoester 2 (**3-16**) respectively. ^{13}C and ^1H NMR signal assignments established for secoesters (**3-15**) and (**3-16**) are presented in Table 3-31.

^1H NMR Spectrum of Secoester 1 (3-15)

The ^1H NMR spectrum of secoester 1 (**3-15**) included singlet and doublet signals in the region 0.78~0.90 ppm, attributable to five tertiary and three secondary methyl groups, together with a sharp three proton singlet (3.63 ppm) attributable to an ester methoxyl group, and three downfield multiplets at 2.39 ppm (dd, J = 13.7, 3.5 Hz), 2.20 ppm (appeared as finely resolved seven-line patterns, J = 6.9, 6.9, 3.2 Hz) and 2.00 ppm (dd, J = 13.8, 3.6 Hz).

Two of the secondary methyl group signals (0.81 and 0.85 ppm, J = 6.8 Hz) were readily assignable to the 22a- and 22b-methyl groups by comparison with the corresponding signals observed for 21α-H-hopan-15-one (**3-11**). HMBC data also validated this assignment (see Table 3-33). Assignments of the methyl groups were facilitated by ^4J COSY correlations to appropriately 1,2-*trans* diaxially oriented methylene protons (see Table 3-32), and by an extensive series of HMBC correlations (see Table 3-33).

Table 3-31. ^{13}C and ^1H NMR signals (δ ppm in $CDCl_3$) observed for 21α-H-hopan-15-one (**3-11**), secoesters (**3-15**) and (**3-16**).

atom	21α-H-hopan-15-one (**3-11**)			secoester 1 (**3-15**)			secoester 2 (**3-16**)		
	^{13}C	$^1H_\alpha$	$^1H_\beta$	^{13}C	$^1H_\alpha$	$^1H_\beta$	^{13}C	$^1H_\alpha$	$^1H_\beta$
1	40.5 t	0.77 t	1.64 d	40.0 t	0.76 t	1.64 d	40.1 t	0.79 t	1.64 d
2	18.8 t	1.37~1.59		18.8 t	1.38 d	1.60 t	18.8 t	1.39 d	1.56 t
3	42.0 t	1.11 t	1.34 d	42.2 t	1.12 t	1.35 d	42.3 t	1.12 t	1.35 d
4	33.3 s			33.3 s			33.4 s		
5	56.5 d	0.74 d		56.4 d	0.77 d		57.0 d	0.74 d	
6	18.8 t	1.37~1.59		19.1 t	1.53 d	1.34 t	18.9 t	1.52 d	1.38 t
7	34.3 t	1.45 t	2.53 m	41.6 t	0.93 t	1.80 d	38.0 t	1.55 t	1.07 d
8	43.1 s			38.5 s			38.6 s		
9	51.9 d	1.14 d		59.9 d	0.74 d		50.4 d	1.03 d	
10	38.2 s			37.6 s			37.3 s		
11	21.4 t	1.61 d	1.26 q	21.2 t	1.60 d	1.24 d	*21.8 t	1.58 t	1.20 q
12	23.7 t	1.54 d	1.49 q	28.5 t	0.93 d	1.86 d	23.5 t	1.55 t	1.28 d
13	49.7 d		1.81 q	42.9 d		1.20 d	40.1 d		1.65 d
14	57.2 s			49.8 d	1.05 d (ax)		44.4 d		1.29 q (eq)
15	215.2 s			174.7 s			175.0 s		
16	41.2 t	2.46 t	2.20 dd	36.9 t	2.00 m	2.39 dd	35.0 t	2.25 t	2.12 t
17	51.2 d		1.28 t	45.1 d		2.20 d	45.1 d		2.12 t
18	44.3 s			47.2 s			46.4 s		
19	39.3 t	1.57 t	1.00 q	34.8 t	1.55 q,	1.23 d	33.7 t	1.55 t,	1.21 d
20	23.4 t	1.41 q	1.73 q	23.7 t	1.54 t	1.24 d	* 21.8 t	1.58 t	1.20 q
21	45.9 d	1.63 q		51.3 d	1.60 t		48.1 d	1.53 d	
22	29.0 d	1.63 q		30.6 d	1.52 q		28.7 d	1.62 t	
23	33.4 q	0.84 s		33.4 q	0.84 s		33.5 q	0.85 s	
24	21.6 q	0.79 s		21.5 q	0.79 s		21.7 q	0.80 s	
25	16.0 q	0.82 d (0.8 Hz)		16.3 q	0.80 s		16.1 q	0.78 s	
26	19.4 q	1.06 s		14.6 q	0.78 d (0.64 Hz)		24.5 q	0.97 s	
27	15.5 q	1.19 s		14.0 q	0.89 d (eq) (6.8 Hz)		9.9 q	0.79 d (ax) (6.8 Hz)	
28	15.1 q	0.86 d (1.1 Hz)		21.1 q	0.85 s		20.5 q	0.76 s	
29	17.8 q	0.79 d (6.6 Hz)		17.7 q	0.81 d (6.8 Hz)		16.1 q	0.80 d (6.8 Hz)	
30	22.0 q	0.88 d (6.6 Hz)		22.5 q	0.85 d (6.8 Hz)		22.6 q	0.88 d (6.8 Hz)	
COOMe				51.3 q	3.63 s		51.5 q	3.66 s	

*assignments are interchangeable.

The third secondary methyl group signal at 0.89 ppm (d, J = 6.8 Hz) was assigned to the C-14 methyl group since it exhibited HMBC correlations to C-8 (38.5 ppm), C-13 (42.9 ppm) and C-14 (49.8 ppm) (see Table 3-31). The ^{13}C NMR data subsequently showed that the methyl group at C-14 was equatorially oriented (see Section ^{13}C).

The signal at 2.20 ppm was identified to be H-17β by the combination of HSQC and HMBC correlations (Table 3-33). This was confirmed by the observation of the cross peaks between H-17β and a pair of methylene protons (2.39 and 2.00 ppm) in the COSY spectrum of secoester 1 (**3-15**) (see Table 3-32).

COSY Spectrum of Secoester 1 (3-15)

The COSY spectrum of secoester 1 (**3-15**) showed that the 14β-methyl group protons coupled to the methine signal which occurred at 1.05 ppm (H-14α). The COSY spectrum also included correlations between H-16α (2.00 ppm), H-16β (2.39 ppm) and H-17β (2.20 ppm). The chemical shifts of the H-16 methylene protons were consistent with the presence of an adjacent $COOCH_3$ group.

Table 3-32. Selected ^1H-^1H COSY correlations (δ ppm in $CDCl_3$) observed for methyl 14α,21α-H-14,15-secohopan-15-oate (**3-15**) (secoester 1).

^1H NMR signals	correlated ^1H signals
2.39 dd (H-16β)	2.20 dd (H-17β), 2.00 m (H-16α)
2.20 dd (H-17β)	2.39 dd (H-16β), 2.00 m (H-16α)
2.00 m (H-16α)	2.38 dd (H-16β), 2.20 dd (H-17β)
1.86 d (H-12β)	1.60 d /1.23 q (H-11α/β), 1.20 d (H-13β), 0.93 d (H-12α)
1.80 d (H-7β)	1.53 d/1.34 t (H-6α/β), 0.93 t (H-7α)
1.60 d (H-11α)	1.23 q (H-11β), 0.93 d (H-12α), 0.74 d (H-9α)
1.52 q (H-22)*	0.81 d /0.85 d (22a/b-Me)
1.34 t (H-6β)	0.77 d (H-5α)
1.20 d (H-13β)	1.86 d (H-12β), 1.05 d (H-14α)
1.05 d (H-14α)	0.89 d (14β-Me) (eq)
0.80 s (4β-Me)	1.12 t (H-3α)*
0.79 s (8β-Me)	0.93 t (H-7α)*
0.80 s (10β-Me)	0.76 t (H-1α)*
0.81 d/0.85 d (22a/b-Me)	1.52 d (H-22)*
0.89 d (14β-Me) (eq)	1.05 d (H-14α)*

* ^4J coupling.

^{1}H NMR Spectrum of Secoester 2 (3-16)

The ^{1}H NMR spectrum of secoester 2 (**3-16**) included signals attributable to five tertiary methyl groups and three secondary methyl groups in the region 0.78~0.98 ppm, together with a sharp three proton singlet (3.66 ppm) attributable to an ester methoxyl group. Assignments of the methyl group were facilitated by an extensive series of HMBC correlations (see Table 3-34).

Two of the secondary methyl group signals (0.80 and 0.88 ppm) were readily assignable to the 22a- and 22b-methyl groups by comparisons with the corresponding signals observed for 21α-H-hopan-15-one (**3-11**) and secoester 1 (**3-15**). HMBC correlations exhibited by these methyl groups (see Table 3-34) also validated this assignment.

The third secondary methyl group signal at 0.79 ppm (d, J = 6.8 Hz) was assigned to the C-14 methyl group since it exhibited HMBC correlations to C-8 (38.6 ppm), C-13 (40.1 ppm) and C-14 (44.4 ppm) (see Table 3-31). The ^{13}C NMR chemical shift subsequently showed this methyl group was axially oriented (see below).

^{13}C and DEPT135 NMR Spectra of Secoesters (3-15) and (3-16)

The ^{13}C NMR spectra of secoesters (**3-15**) and (**3-16**) were each comprised of a total of thirty-one carbon signal resonances, which were characterized by DEPT135 NMR spectra to arise from 9 quartet (CH_3), 10 triplet (CH_2), 7 doublet (CH) and 5 singlet (C) carbon. This data was consistent with the conclusion that photolysis of 21α-H-hopan-15-one (**3-11**) had proceeded with incorporation of a mole of methanol.

Methyl group carbon assignments were facilitated by HSQC correlations with the corresponding protons (see Table 3-31). The ^{13}C NMR signals of **3-15** and **3-16** that occurred at 51.3 and 51.5 ppm respectively, correlated with proton signals which occurred at 3.63 and 3.66 ppm respectively, hence these ^{13}C NMR signals were assigned to the COO$\underline{C}H_3$ group carbons of **3-15** and **3-16**.

Except for the C-7 and C-9 resonances, the ring A and B ^{13}C NMR signal assignments elucidated for secoesters (**3-15**) and (**3-16**) were similar to those determined for 21α-H-hopan-15-one (**3-11**) (see Table 3-31). Among the ring C atoms, there were marked

differences in the C-12, C-13, C-14 and C-26 chemical shifts. These variations can be attributed to the epimeric H-14 configurations of the two secoesters.

Structurally significant HMBC and HSQC correlations observed for the methyl groups of **3-15** and **3-16** are presented in Table 3-33 and Table 3-34. Identification of the methyl group resonances *via* their unique HMBC correlation patterns led to the assignment of the corresponding ^{13}C resonances *via* their HSQC correlations observed for secoesters (**3-15**) and (**3-16**). It was of note in particular that 14-methyl groups in **3-15** and **3-16**, correlated only to three carbon signals (C-8, C-13 and C-14), rather than four carbon signals (C-8, C-13, C-14 and C-15) in starting material (**3-11**).

Table 3-33. ^{1}J, ^{2}J and ^{3}J heteronuclear ^{1}H-^{13}C correlations (δ ppm in $CDCl_3$) observed for methyl 14α,21α-H-14,15-secohopan-15-oate (**3-15**) (secoester 1).

^{1}H signal	^{1}J correlated ^{13}C signal	^{2}J and ^{3}J correlated ^{13}C signals
0.84 s (4α-Me)	33.4 (C-23)	56.4 (C-5), 42.2 (C-3), 33.3 (C-4), 21.5 (C-24)
0.79 s (4β-Me)	21.5 (C-24)	56.4 (C-5), 42.2 (C-3), 33.3 (C-4), 33.4 (C-23)
0.80 s (10β-Me)	16.3 (C-25)	59.9 (C-9), 56.4 (C-5), 40.0 (C-1), 37.6 (C-10)
0.78 s (8β-Me)	14.6 (C-26)	59.9 (C-9), 49.8 (C-14), 41.6 (C-7), 38.5 (C-8)
0.89 d (14β-Me) (eq)	14.0 (C-27)	49.8 (C-14), 42.9 (C-13), 38.5 (C-8)
0.85 s (18α-Me)	21.1 (C-28)	47.2 (C-18), 45.1 (C-17), 42.9 (C-13), 34.8 (C-19)
0.81 d (22a-Me)	17.7 (C-29)	51.3 (C-21), 30.6 (C-22), 22.5 (C-30)
0.85 d (22b-Me)	22.5 (C-30)	51.3 (C-21), 30.6 (C-22), 17.7 (C-29)

Table 3-34. ^{1}J, ^{2}J and ^{3}J heteronuclear ^{1}H-^{13}C correlations (δ ppm in $CDCl_3$) observed for methyl 21α-H-14,15-secohopan-15-oate (**3-16**) (secoester 2).

^{1}H signal	^{1}J correlated ^{13}C signal	^{2}J and ^{3}J correlated ^{13}C signals
0.85 s (4α-Me)	33.5 (C-23)	57.0 (C-5), 42.3 (C-3), 33.4 (C-4), 21.7 (C-24)
0.80 s (4β-Me)	21.7 (C-24)	57.0 (C-5), 42.3 (C-3), 33.4 (C-4), 33.5 (C-23)
0.78 s (10β-Me)	16.1 (C-25)	57.0 (C-5), 50.4 (C-9), 40.1 (C-1), 37.3 (C-10)
0.97 s (8β-Me)	24.5 (C-26)	50.4 (C-9), 44.4 (C-14), 38.6 (C-8), 38.0 (C-7)
0.79 d (14α-Me) (ax)	9.9 (C-27)	44.4 (C-14), 40.1 (C-13), 38.6 (C-8)
0.76 s (18α-Me)	20.5 (C-28)	46.4 (C-18), 45.1 (C-17), 40.1 (C-13), 33.7 (C-19)
0.80 d (22a-Me)	16.1 (C-29)	48.1 (C-21), 28.7 (C-22), 22.6 (C-30)
0.88 d (22b-Me)	22.6 (C-30)	51.3 (C-22), 30.7 (C-21), 16.1 (C-29)

3.6.3 C-14 Stereochemistry of Secoester 1 (3-15) and Secoseter 2 (3-16)

Because of the occurrence of the C-14 methyl group and the nearby proton signals (eg H-13β, H-7α and H-9α signals) at similar chemical shifts in crowded part of the ^{1}H NMR spectra of respective secoesters it was not possible to elucidate the C-14 stereochemistry of secoesters 1 (**3-15**) and 2 (**3-16**) *via* correlations observed in NOESY spectra, or in NOE–difference experiments.

Detailed comparisons of the ^{13}C and ^{1}H NMR chemical shifts, summarised in Figure 3-20, identified the C-14 configuration of the pair of secoesters. It is well established that in six-membered cyclohexane ring systems, an axial methyl group appears at higher field (smaller chemical shift) than the corresponding equatorial methyl group (Breitmaier & Voelter, 1987).

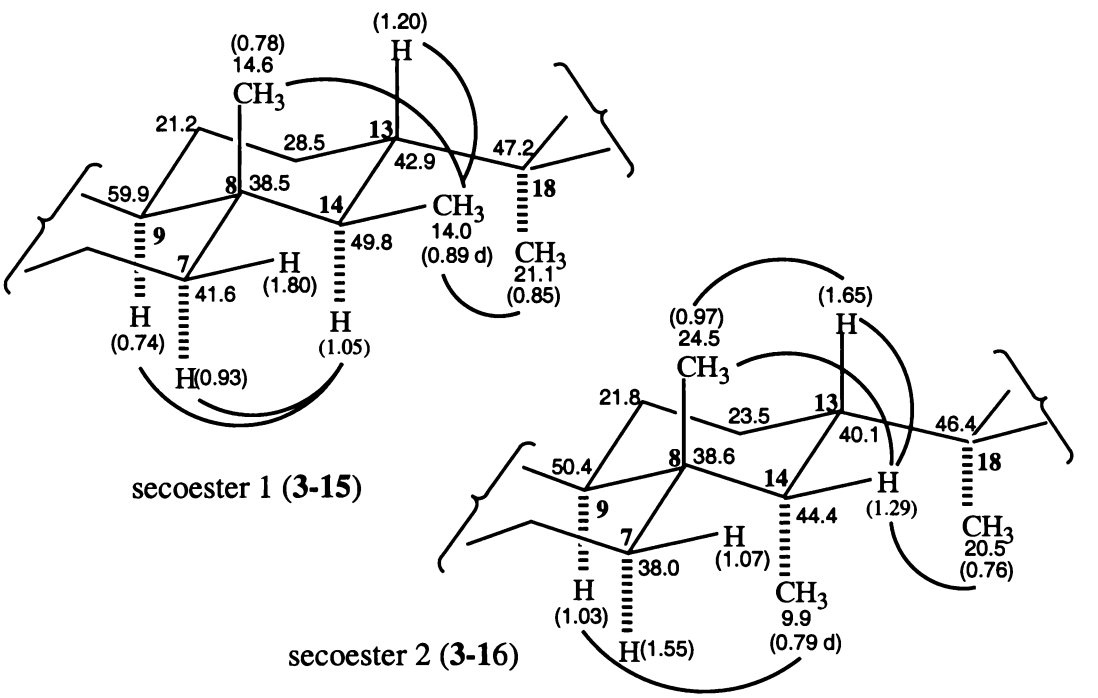

Figure 3-20. Comparison of selected ^{1}H and ^{13}C NMR signals observed for secoesters (**3-15**) and (**3-16**). ^{13}C resonances are given in plain text, ^{1}H resonances are bracketed and atom numbers are given in bold type. Curved lines designate resonances discussed in the text.

This data indicated the C-14 methyl group to be axially oriented in secoester 2 (**3-16**) and equatorially oriented in secoester 1 (**3-15**), since the C-27 resonances of these compounds occurred at 9.9 ppm and at 14.0 ppm, respectively. Consistent with this conclusion, the presence of an axial C-14 methyl group in **3-16** led to C-9 and C-7 experiencing upfield shifts to resonate at 50.4 and 38.0 ppm respectively, compared to 59.9 and 41.6 ppm respectively in **3-15**.

The presence of an axial C-14 methyl group (α-face) in secoester 2 (**3-16**) also led to the axially oriented 9α- and 7α-protons experiencing marked downfield shifts to resonate at 1.03 and 1.55 ppm respectively, compared to 0.74 and 0.93 ppm, respectively, in secoester 1 (**3-15**). The H-9α (1.14 ppm) and H-7α (1.45 ppm) resonances of 21α-H-hopan-15-one (**3-11**), in which the C-14 methyl group is axially orientated, are comparable with those of secoester 2 (**3-16**), but not secoester 1 (**3-15**). The ^{1}H and ^{13}C chemical shifts of the H-13β and the 8β- and 18α-methyl groups were also sensitive to the orientation of the C-14 methyl group (see Figure 3-20).

In accordance with established substituent group effects for cyclohexane ring compounds (Breitmaier & Voelter, 1987), the presence of an axial C-14 (α-face) methyl group in secoester 2 (**3-16**) led to C-14 experiencing a lesser chemical shift (44.4 ppm) than was the case for secoester 1 (**3-15**) (49.8 ppm) in which the C-14 methyl group was equatorially (β-face) oriented.

3.6.4 Kinetic vs. Thermodynamic Control

The formation of a pair of epimeric 14,15-secoesters (**3-15**) and (**3-16**) can be rationalised as being a consequence of kinetic vs. thermodynamic control.

Cleavage of the C-14-C-15 bond would initially afford a biradical species (**3-11a**) which would then be expected to undergo hydrogen radical transfer *via* a six-membered chair-like conformation to afford intermediate ketene II (see Scheme 3-10). This would then react with methanol to afford secoester 2 (**3-16**) in which the C-14 methyl group retains its original axial orientation. This product can be viewed as the rapidly formed, kinetic, product of the photolysis reaction.

Another possibility is that partial rotation about the C-13–C-18 bond (presumably to relieve steric strain), may occur prior to hydrogen radial transfer, which would then take place with inversion of the original C-14 configuration (see Scheme 3-10). This would afford intermediate ketene I, which would then react with methanol to give secoester 1 (**3-15**) in which the C-14 methyl group is equatorially oriented (β-face). This product can be viewed as the thermodynamically favoured product of the photolysis reaction, since it affords the product molecule with the sterically more favourable orientation of the C-14 methyl group (ie that with the C-14-methyl group equatorially oriented).

The MM2 modelled conformations of secoester 1 (**3-15**) and 2 (**3-16**) are shown in Figures 3-21 and 3-22 respectively. The presence in the mixture of photolysis products of approximately equal amounts of **3-15** (equatorial C-14 methyl group, modelled E = 79.6 KCal) and **3-16** (axial C-14 methyl group, modelled E = 80.8 KCal) is consistent with the conclusion that the thermodynamic product is not greatly favoured over the kinetic product.

Other mechanistic considerations, relating to outcomes of the photochemical reactions reported in Sections **3.3**, **3.4** and **3.5** are discussed in Section **3.7**.

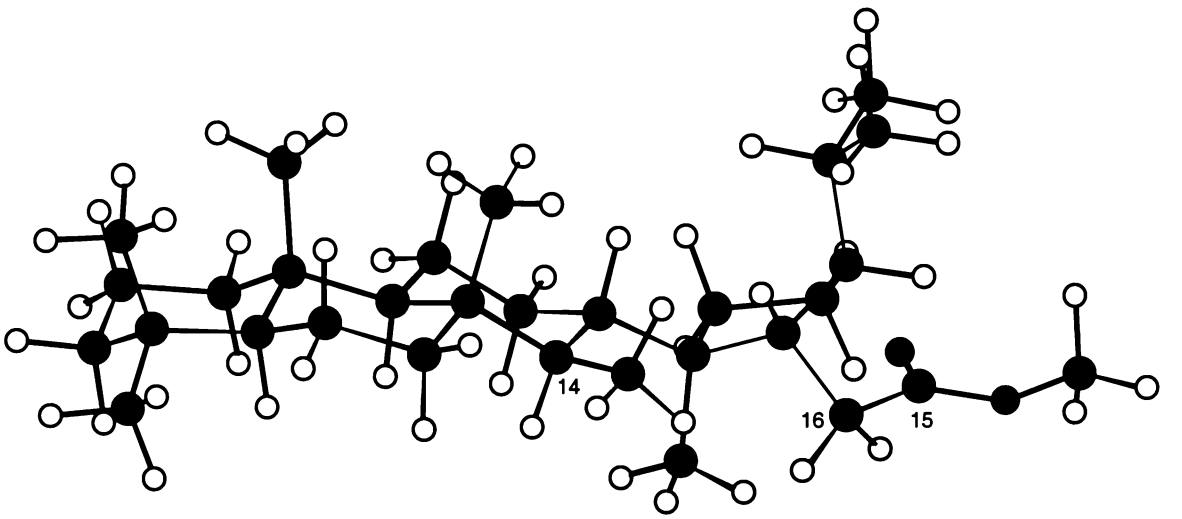

Figure 3-21. MM2 modelled conformation of methyl 14α,21α-H-14,15-secohopan-15-oate (**3-15**) (secoester 1).

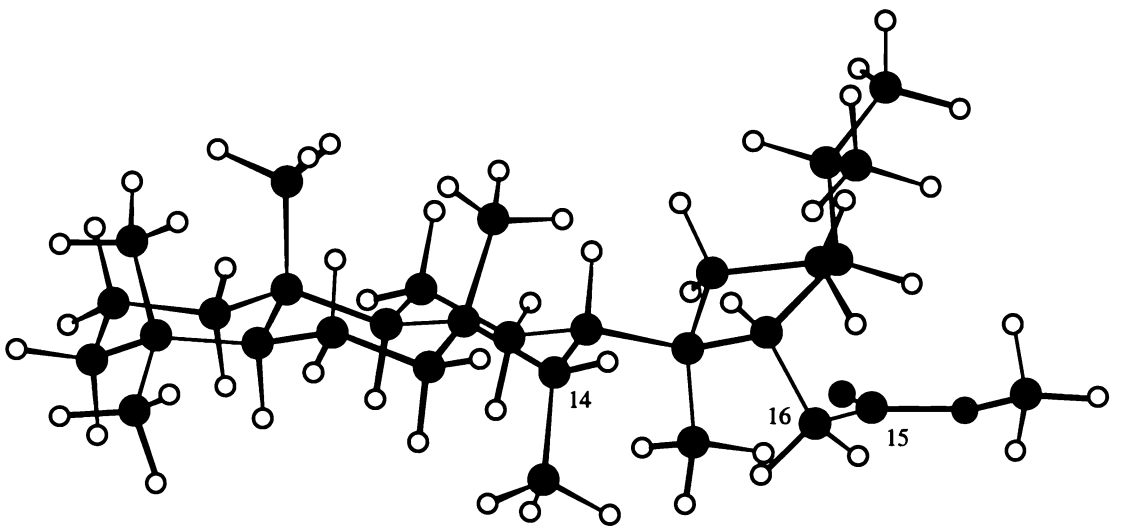

Figure 3-22. MM2 modelled conformation of methyl 21α-H-14,15-secohopan-15-oate (**3-16**) (secoester 2).

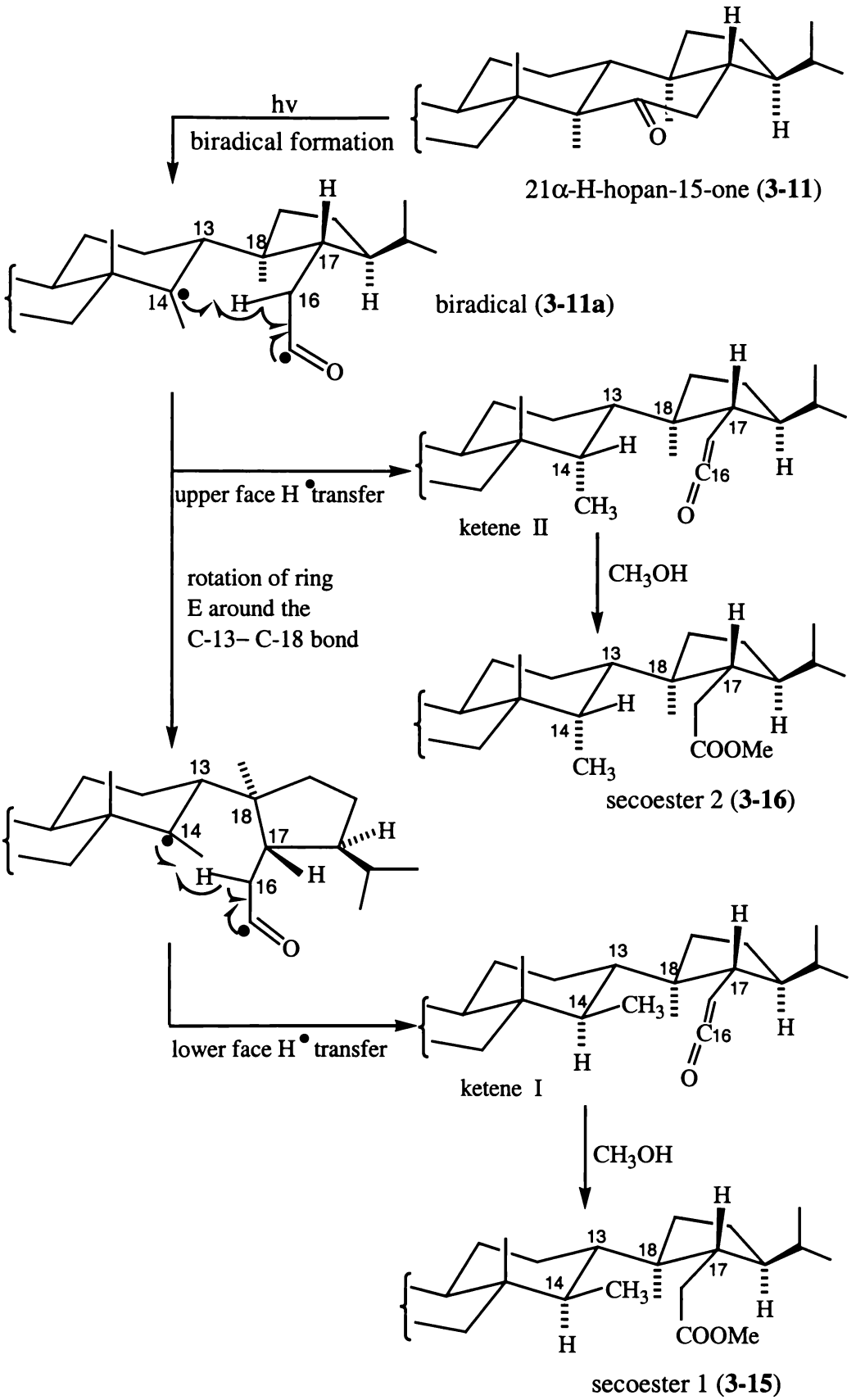

Scheme 3-10. Proposed mechanistic pathways for the formation of secoesters 1 (**3-15**) and 2 (**3-16**) obtained on photolysis of 21α-H-hopan-15-one (**3-11**).

3.7 Attempted X-Ray Crystallographic Analyses

Efforts to define the structures of some unexpected photolysis products (eg. **3-3**, **3-5**, and **3-13**) by X-ray crystallographic analyses were not successful. In each case repeated attempts to obtain crystals for X-ray analyses afforded crystals that were twinned, of inadequate size, or of irregular shape.

The ROESY, NOESY or NOE-difference spectral data, presented in Section **3.3** and **3.5**, together with MM2 modelling results, were therefore used to define the stereochemistry of the new photolysis products.

3.8 Mechanistic Aspects of the Formation of the Photochemical Reaction Products

It is apparent from the structures of the photoreaction products obtained in the investigations described in Sections **3.2**, **3.4**, **3.5** and **3-6**, that photolysis of 15-oxohopanoids can proceed:

(a) *via* an intermediate secoaldehyde, and followed by participation of the 22-OH group or 22-H of hopanoids possessing a 21α-isopropyl group, or

(b) *via* an intermediate ketene which subsequently reacted with an alcohol to afford a secoester.

Type (b) products were only obtained for 21α-H-hopanes, in which the 22-proton was more distant from C-15, and orientated towards the upper face of the hopane skeleton.

The formation of type (a) participation products can be rationalised as follows: Upon irradiation of 22-hydroxyhopan-15-one (**3-1**) α-cleavage (Norrish Type I process) occurred between C-14 and C-15, as depicted in Scheme 3-11. This is consistent with the well-established preference of C-C bonds adjacent to a carbonyl group to be cleaved to afford the most substituted biradical species. The acyl-alkyl biradical (**3-1a**) generated by this process then undergoes hydrogen transfer from C-27 methyl group *via* an eight-membered transition state to give the secoaldehyde (**3-2**).

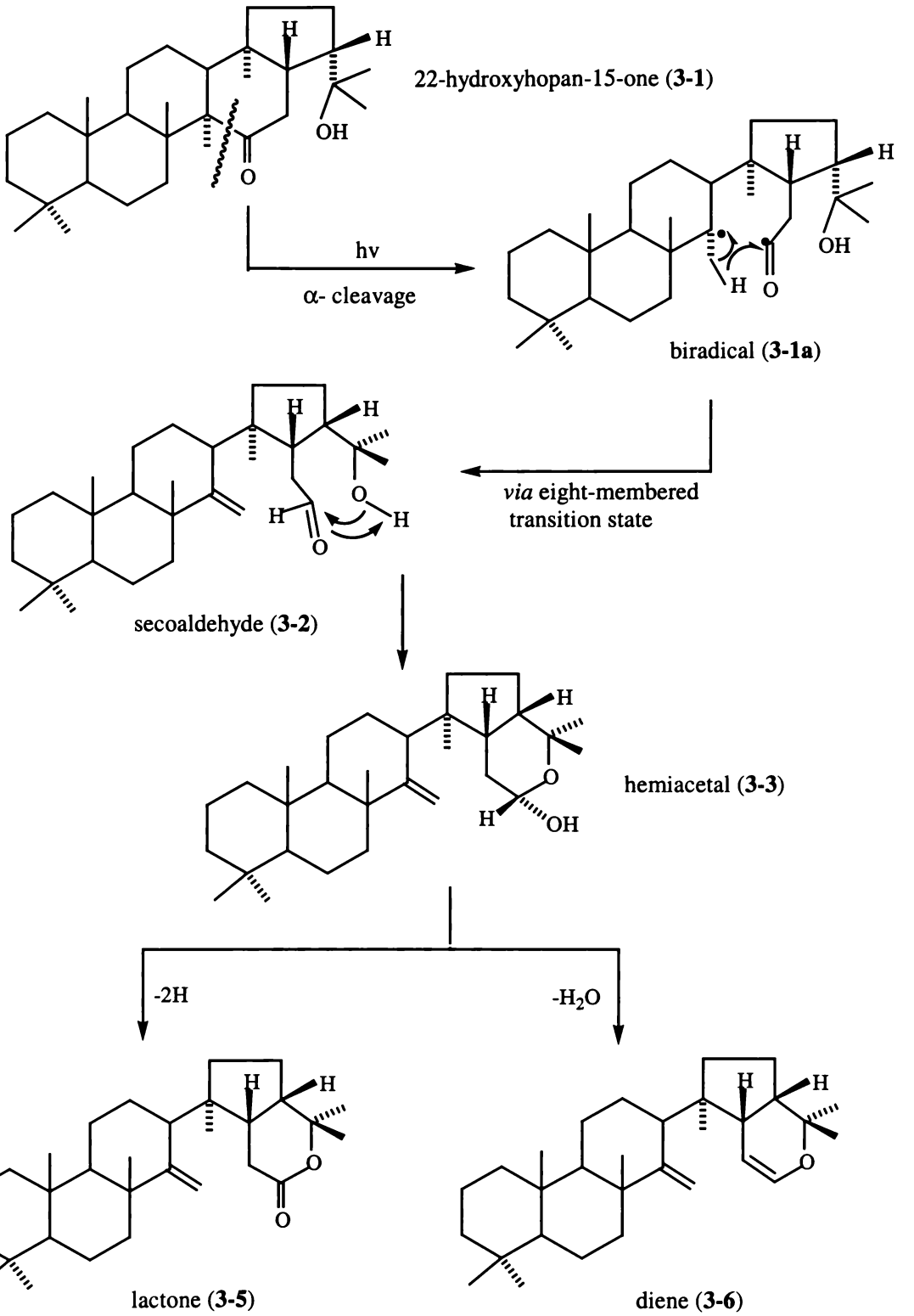

Scheme 3-11. Proposed mechanistic pathways for the formation of photolysis products from 22-hydroxyhopan-15-one (**3-1**).

The disposition of the 22-hydroxyl group of secoaldehyde (**3-2**) is such that it can intramolecularly cyclize with the carbonyl group of the initially formed secoaldehyde

(**3-2**), to afford hemiacetal (**3-3**) as the major photoreaction product. The tendency for an aldehyde to intermolecularly cyclize with a suitably oriented hydroxyl group is well known and can be compared to the predominant existence of D-(+)-glucopyranose (a polyhydroxyaldehyde) in α- and β-hemiacetal forms (McMurry, 1992)

The two minor products, lactone (**3-5**) and diene (**3-6**) isolated on photolysis of **3-1** in benzene-methanol, benzene-isopropanol, or benzene, can be viewed as dehydrogenation (photo-oxidation) and dehydration products, respectively, of hemiacetal (**3-3**).

Photolysis of hop-21-en-15-one (**3-8**) can be envisaged as proceeding in a manner analogous to that described above for 22-hydroxyhopan-15-one (**3-1**). Rearrangement of the initially formed acyl-alkyl biradical (**3-8a**) *via* an eight-membered transition state with hydrogen transfer from C-27 to C-15 will afford the secoaldehyde (**3-12**) (see Scheme 3-12), which does not react further due to the absence of a 22-hydroxyl group, or a suitably oriented 'activated' hydrogen (see below).

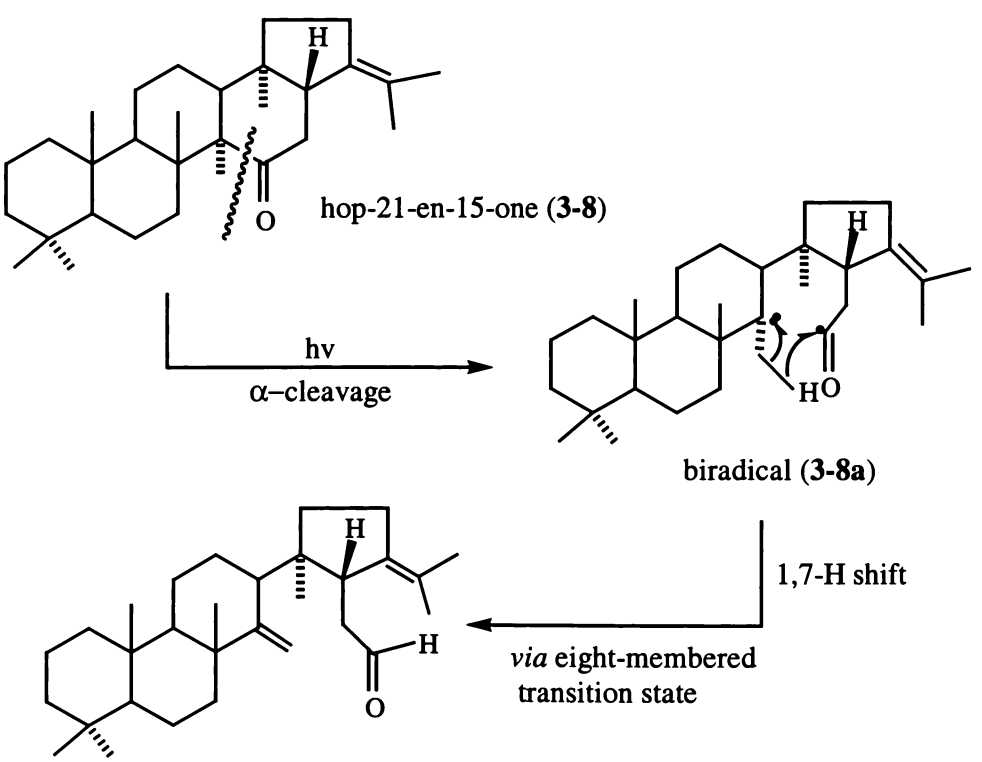

Scheme 3-12. Proposed mechanistic pathway for the formation of secoaldehyde (**3-12**) obtained on photolysis of hop-21-en-15-one (**3-8**).

The photolysis of hopan-15-one (**3-10**) can be envisaged as proceeding in a manner analogous to that described above for hop-21-en-15-one (**3-8**). Rearrangement of the initially formed acyl-alkyl biradical (**3-10a**), *via* an eight-membered transition state with hydrogen transfer from C-27 to C-15 will afford secoaldehyde (**3-17**) (Scheme 3-13). The secoaldehyde (**3-17**) then appears to undergo photo-induced cyclization to C-22, with transfer of H-22 to the aldehyde oxygen to afford the 15α- or 15β-alcohols (**3-13**) and (**3-14**) respectively.

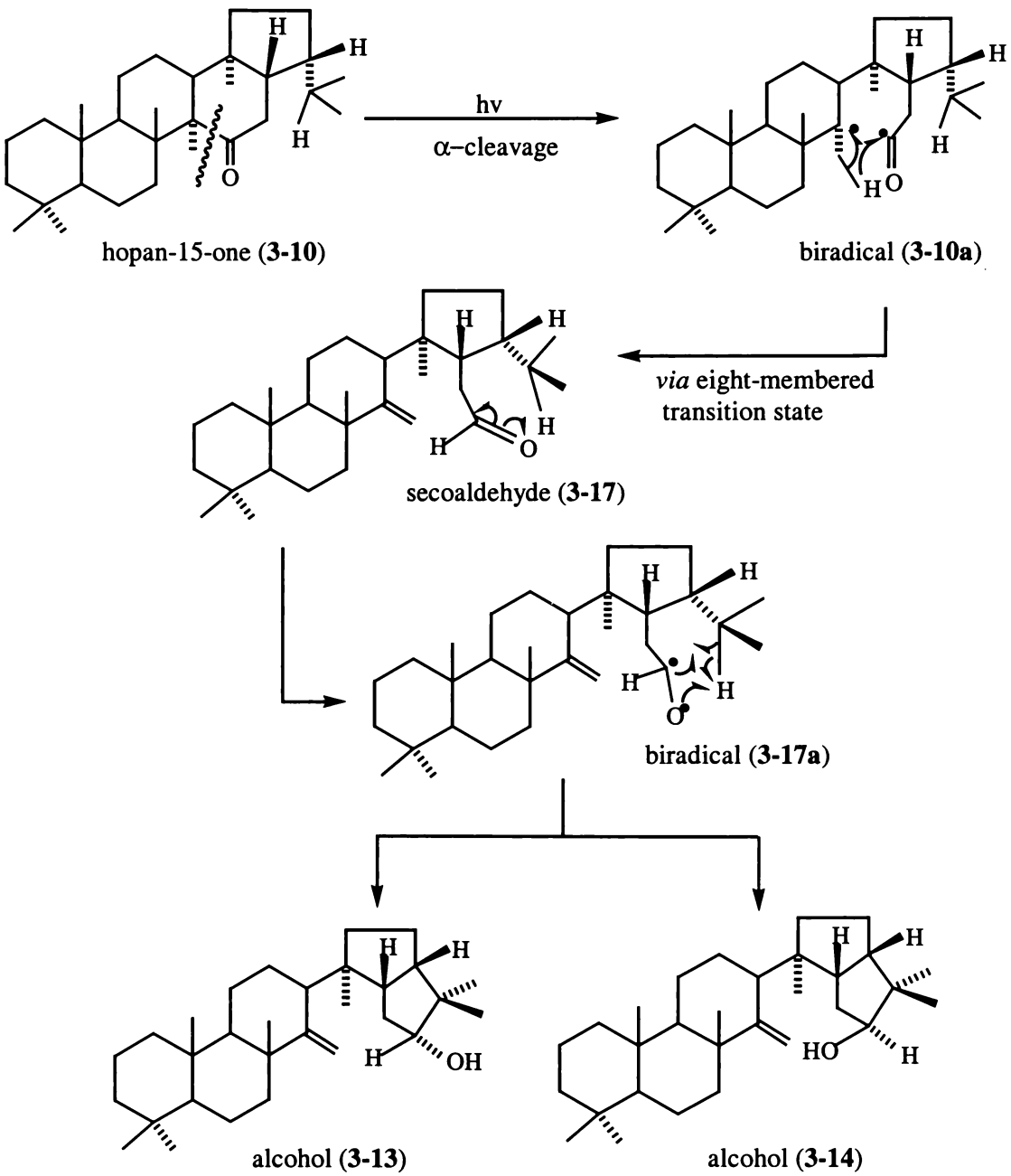

Scheme 3-13. Proposed mechanistic pathways for the formation of photolysis products from hop-21-en-15-one (**3-10**).

The photo-cyclization process leading to the formation of the 15,22-*abeo* rings of alcohols (**3-13**) and (**3-14**) can be envisaged as proceeding *via* a biradical intermediate (**3-17a**) generated from the aldehyde carbonyl (see Scheme 3-13). In the absence of a "reactive" proton (or other group), it can be anticipated that this secoaldehyde could be isolated, as was the case for secoaldehyde (**3-12**) (see Scheme 3-12). Alternatively, radical induced transfer of H-22 to the carbonyl oxygen, as depicted in Scheme 3-13, can be envisaged as being facilitated by the +I effects of the two methyl groups attached to C-22.

In the absence of a 21α-isopropyl side chain, as is the case for 21α-H-hopan-15-one (**3-11**), photolysis in benzene-methanol afforded the epimeric 21α-H-secoesters (**3-15**) and (**3-16**). These secoesters can be envisaged as arising from α-cleavage of the C-14--C-15 bond (α-cleavage), followed by hydrogen transfer from C-16 to C-14 *via* a six-membered transition state to give the intermediate ketenes I and II (see Scheme 3-10) which then react with methanol to afford the 14,15-secoesters (**3-15**) and (**3-16**) respectively (see Scheme 3-10).

As noted in Section **3.6**, the secoesters 1 (**3-15**) and 2 (**3-16**) can be rationalized as the kinetically and thermodynamically controlled reaction products generated from the initial tertiary C-14 radical. Rapid (kinetically controlled) hydrogen abstraction can be envisaged as affording secoester 2 (**3-16**), in which the C-14 methyl group retains its original axial orientation, whereas thermodynamically controlled hydrogen abstraction can be envisaged as affording secoester 1 (**3-15**) in which the C-14 methyl group is equatorially oriented.

The formation of secoesters (**3-15**) and (**3-16**) can be compared with that observed on photolysis of 22-hydroxyhopan-7-one (**2-1**). In this case only a single secoester (**2-2**), possessing an axial C-8 methyl group (β-oriented), corresponding to the kinetic product, was isolated (see Scheme 3-10).

The presence of a more distant upper face (β-oriented) C-21 substituent leads to photoreactions proceeding *via* a chair-like six-membered transition state. The formation of the epimeric secoesters (**3-15**) and (**3-16**), attributable to kinetic and thermodynamic

control of the hydrogen abstraction process, suggests the presence of a 21β-substituted five-membered ring E system in 21α-H-hopan-15-one (**3-11**), as opposed to an adjacent six-membered ring C system in 22-hydroxyhopan-7-one (**2-1**), leads to intermolecular hydrogen transfer occurring at a slower rate for **3-11**, than is the case for **2-1**, thereby accounting for the detection of the thermodynamically favoured secoester on photolysis of **3-11**, but not on photolysis of **2-1**.

3.9 Summary of Photoreaction Outcomes

It is apparent from the array of products isolated in this work, that the nature and orientation of ring E substituent groups strongly influences the outcomes of photolysis reactions of 15-oxohopanoids. In particular the presence of a 21α-side chain (eg an oxygenated 22-hydroxyisopropyl group, or a saturated isopropyl group) leads to rearrangement of an initially formed 14,15-seco biradical species proceeding *via* an eight-membered transition states (see Schemes 3-11, 3-12 and 3-13), whereas six-membered transition state products (secoesters (**3-15**) and (**3-16**)) are only found when the C-21 side chain was β-oriented (see Scheme 3-10).

The foregoing observations can be interpreted as indicating that the steric influence(s) of bulky lower face (α-oriented) substituents attached to C-21 is such that the corresponding 14,15-seco biradical species are not able to undergo 'conventional' intramolecular hydrogen abstraction *via* a chair-like six-membered transition state. Instead they undergo intramolecular hydrogen transfer *via* a less sterically demanding eight-membered transition state.

Presumably this is a consequence of the differing steric interaction between the 21α-isopropyl group and the 17α-CH_2-C=O side chain in **3-10a**, which is adjacent to a 21α-isopropyl group, compared to an H-21α in **3-11a** (see Scheme 3-10). The lower face 21α-isopropyl group appears to prevent rearrangement proceeding *via* a six-membered transition state, possibly because the radical side chain is prevented from adopting the required conformation.

Chapter Four

A New 6α-Substituted Stictane Triterpene

4.1 Introduction

Stictane triterpenes, a unique group of triterpene substances with a boat ring B (see Figure 4-1), were first isolated from some New Zealand *Pseudocyphellaria* lichens by Chin *et al.* (1973). Apart from yellow medulla *Pseudocyphellaria* species (Galloway, 1985), they have also been isolated from Himalayan collections of *Lobaria retigera* (Corbett & Wilkins, 1976c) and a Norwegian collection of *Cetraria nivalis* (Wilkins 1977a) (see Section **1.2.1** in Chapter One).

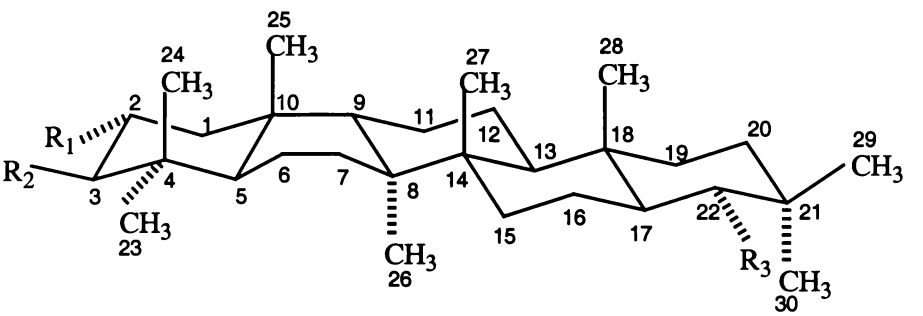

Figure 4-1. Structural representation of stictane triterpenes, showing the boat ring B system.

To date, ten stictane triterpenes have been isolated from the extracts of *P. colensoi*, *P. coronata*, and *P. pickeringii* (syn. *P. flavicans*) (Chin *et al.*, 1972; Corbett & Wilkins, 1976c), and three 3,4-secostictane triterpenes have been isolated from *P. degelii* (Goh *et al.*, 1978) (see Section **1.2.1**).

Careful TLC analyses of the chloroform extracts of *P. colensoi* suggested the presence of some other minor unidentified triterpenes, possibly stictane triterpenes, in the extracts. Accordingly, the isolation and structural elucidation of these triterpenes were

undertaken and, a new ring B substituted stictane triterpene (**4-1**) and a new flavicane triterpene (**5-3**) (see Chapter Five) were isolated from the extracts.

The novel stictane lactone, 22α-hydroxystictano-25,3β-lactone (**4-2**) (Figure 4-2), first isolated by Wilkins *et al.* (1989), was also isolated from the extracts, and a complete assignment of its proton resonances, and some revision to its ^{13}C NMR assignments, were elucidated. A search for possible biosynthetic precursors of this lactone (eg 3β,22α-dihydroxy-stictan-25-oic acid) did not result in the isolation of other new triterpenes.

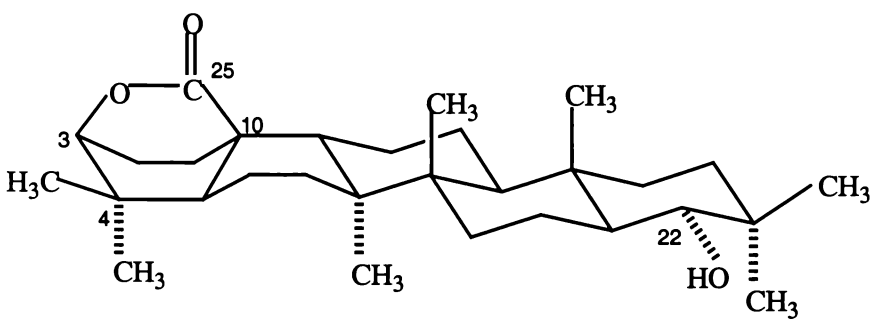

Figure 4-2. The structure of 22α-hydroxystictano-25,3β-lactone (**4-2**).

4.2 Structural Elucidation of the New Stictane Triterpene

Detailed analyses of mass spectral and one- and two-dimensional NMR spectral data determined for the new stictane triterpene showed it to be 3β,6α,22α-triacetoxystictane (**4-1**) (Figure 4-3).

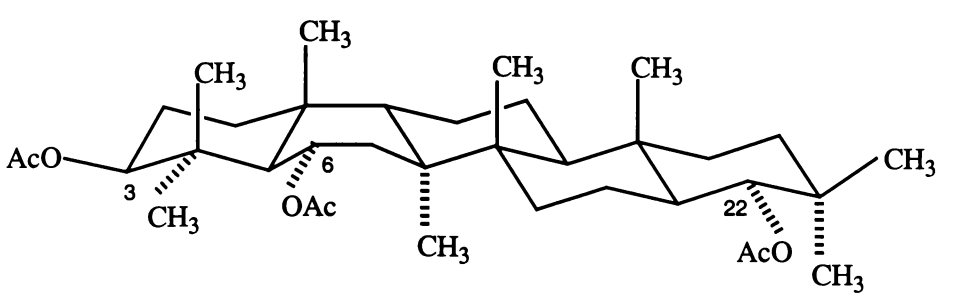

Figure 4-3. The structure of 3β,6α,22α-triacetoxystictane (**4-1**).

4.2.1 Isolation of the New Triterpene

Extraction of finely ground lichen material with light petroleum afforded an extract, which was shown by TLC analyses to be comprised mainly of 2α,3β,22α-triacetoxystictane (**4-3**), 2α,3β-diacetoxystictan-22α-ol (**4-4**), 2α-acetoxystictane-3β,22α-diol (**4-5**), 3β-acetoxystictane-2α,22α-diol (**4-6**), stictane-3β,22α-diol (**4-7**) and 22α-hydroxystictan-3-one (**4-8**) (see Figure 4-4). TLC analyses also revealed the presence of some additional, minor compounds.

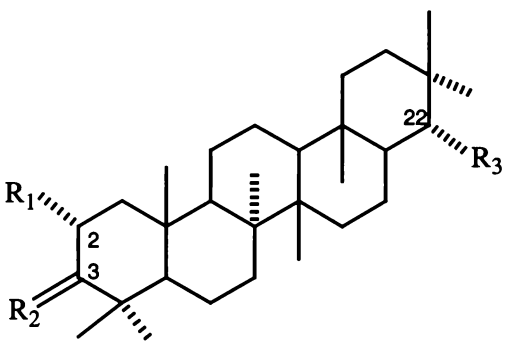

(**4-3**) R_1=OAc, R_2=H, β-OAc, R_3=OAc	2α,3β,22α-triacetoxystictane
(**4-4**) R_1=OAc, R_2=H, β-OAc, R_3=OH	2α,3β-diacetoxystictan-22α-ol
(**4-5**) R_1=OAc, R_2=H, β-OH, R_3=OH	2α-acetoxystictane-3β,22α-diol
(**4-6**) R_1=OH, R_2=H, β-OAc, R_3=OH	3β-acetoxystictane-2α,22α-diol
(**4-7**) R_1=H, R_2=H, β-OH, R_3=OH	stictane -3β,22α-diol
(**4-8**) R_1=H, R_2=O, R_3=OH	22α-hydroxystictan-3-one

Figure 4-2. Structures of the major triterpenes isolated from the extracts of *P. colensoi.*

Separation of the extractives by column chromatography on alumina, afforded 14 fractions, two of which (fractions 7 and 8), appeared to be mixtures of a new triterpene triacetate and 2α,3β,22α-triacetoxystictane (**4-3**). A total of six acetoxy methyl group signals were identified in the ^{1}H NMR spectra of the mixtures of the two compounds. GC/MS analyses of fractions 7 and 8 also suggested the new compound to be a triacetate, however the intensity of its *m/z* 187, 189 and 43 fragment ions differed significantly from those determined for 2α,3β,22α-triacetoxystictane (**4-3**).

Repeated attempts to separate the new triterpene from 2α,3β,22α-triacetoxystictane (**4-3**) by radial chromatography on silica gel were not successful, due to the almost identical polarity (TLC R_f's) of the two compounds. Close inspection of the ^{1}H NMR spectrum of the mixture suggested that unlike 2α,3β,22α-triacetoxystictane (**4-3**),

the new triacetate did not have adjacent substitutent groups (ie it was not 2α,3β-disubstituted), hence it was reasoned that room temperature hydrolysis of the mixture, in the presence of KOH, would convert 2α,3β,22α-triacetoxystictane (**4-3**) to 22α-acetoxystictane-2α,3β-diol (**4-9**) (see Figure 4-5) while the new triacetate would not be hydrolysed. It was then anticipated that the more polar dihydroxyacetate (**4-9**) could be readily separated from the new triacetate.

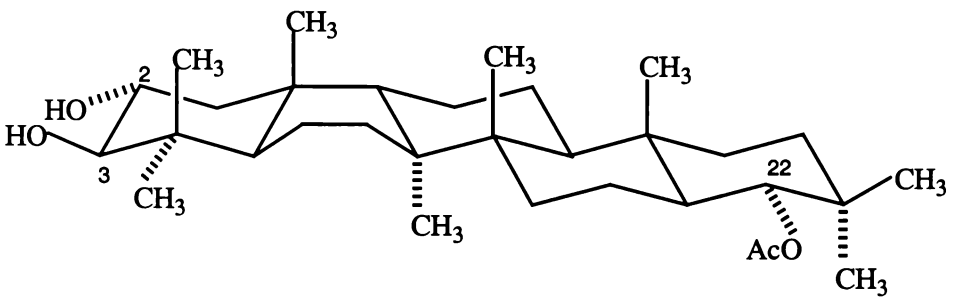

Figure 4-3. The structure of 22α-acetoxystictane-2α,3β-diol (**4-9**).

A pilot scale hydrolysis reaction, monitored by TLC, verified this conclusion. Separation of a larger scale reaction mixture by radial chromatography on silica gel afforded a specimen of 3β,6α,22α-triacetoxystictane (**4-1**).

4.3 Structural Elucidation of 3β,6α,22α-Triacetoxystictane (4-1)

4.3.1 Mass Spectral Analysis of 3β,6α,22α-Triacetoxystictane (4-1)

The highest observed fragment ion in the mass spectrum of **4-1** occurred at *m/z* 586. This is consistent with the molecular formula of **4-1** being $C_{36}H_{58}O_6$ (586 daltons). Significant *m/z* 526, 466, and 406 fragment ions, consistent with the loss of one, two or three acetoxyl groups respectively from the molecular ion, were also observed.

The ring C cleavages are dominant in the mass spectra of stictane triterpene compounds. These cleavages typically give rise to the fragment ions "a", "b" and "c" shown in Scheme 4-1 (Holland & Wilkins, 1979). Strong peaks at *m/z* 187, 189, and 203 observed in the mass spectrum of **4-1** corresponded to the loss of acetoxyl groups from "a", "b" and "c" fragment ions. Other structurally significant fragment ions observed for **4-1** are listed in Table 4-1.

Table 4-1. Selected mass spectral fragment ions observed for 3β,6α,22α-triacetoxystictane (**4-1**).

ions	*m/z* (% relative intensities)
M^+	586 (1)
M^+-AcOH	526 (4)
M^+-AcOH-CH_3	511 (46)
M^+-AcOH-C_3H_7	483 (4)
M^+-2×AcOH	466 (27)
M^+–2×AcOH-CH_3	451 (13)
M^+-2×AcOH-CH_2=C=O	424 (6)
M^+-3×AcOH	406 (10)
ion b-AcOH	203 (19)
ion c-AcOH	189 (71)
ion a-2×AcOH	187 (80)
CH_3CO	43 (100)

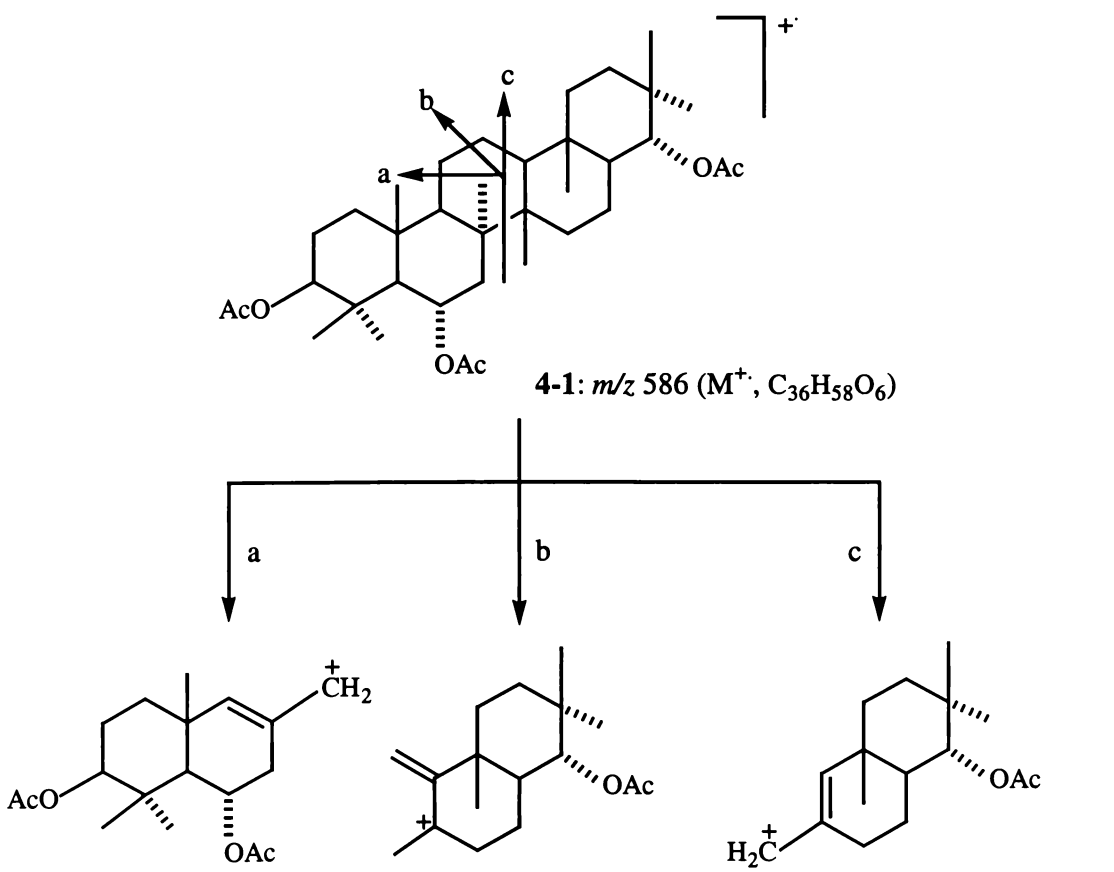

ion a: *m/z* 307 ($C_{18}H_{27}O_4$) ion b: *m/z* 263 ($C_{17}H_{27}O_2$) ion c: *m/z* 249 ($C_{16}H_{25}O_2$)

Scheme 4-1. Proposed mass spectral fragment pathways for 3β,6α,22α-triacetoxystictane (**4-1**).

4.3.2 NMR Spectral Analyses of 3β,6α,22α-Triacetoxystictane (4-1)

The complete assignment of the ^{13}C and ^{1}H NMR signals of 3β,6α,22α-triacetoxystictane (**4-1**), presented in Table 4-2, was facilitated by analyses of one- and two-dimensional NMR spectral data, and by comparison with those reported for 2α,3β,22α-triacetoxystictane (**4-3**) (Wilkins *et al.*, 1989) and the ^{13}C and ^{1}H signal resonances established in a like manner for a specimen of 3β,22α-diacetoxystictane (**4-10**) (see Table 4-2), prepared by acetylation of stictane-3β,22α-diol (**4-7**). Hitherto only the ^{13}C assignments of (**4-10**) have been reported (Wilkins *et al.*, 1989).

4.3.2.1 ^{1}H NMR Spectrum of 3β,6α,22α-Triacetoxystictane (4-1)

The 400 MHz ^{1}H NMR spectrum of **4-1** included signals attributable to eight tertiary methyl groups in the region of 0.80~1.25 ppm, three acetoxy methyl groups (δ 2.05, 2.05 and 2.03 ppm), three lowfield multiplet signals at 4.48 ppm (dd, J = 11.7, 5.1 Hz), 4.68 ppm (d, J = 10.9 Hz), and 5.11 ppm (ddd, J = 10.8, 8.2 and 6.4 Hz), and methylene or methine signals at 2.18 ppm (dd, J = 13.9, 6.4 Hz), and 1.92 ppm (d, J = 10.8 Hz).

The chemical shift of the signal which occurred at 4.68 ppm corresponded with that of the H-22 methine protons of 2α,3β,22α-triacetoxystictane (**4-3**) and 3β,22α-diacetoxystictane (**4-10**), while the signal at 4.48 ppm corresponded with that of the methine proton at C-3 in 3β,22α-diacetoxystictane (**4-10**) (see Table 4-2).

The coupling constants exhibited by the signal which occurred at 4.48 ppm (dd, J = 11.7, 5.1 Hz) were consistent with the presence of an acetoxyl group at C-3 being β-oriented while the signal at 4.68 ppm exhibited a doublet (d, J = 10.9 Hz), which was consistent with the presence of a 22α-oriented acetoxyl group (Chin *et al.*, 1976).

A distinctive feature of the ^{1}H NMR spectrum of **4-1** was the appearance of a downfield methine proton, finely resolved eight-line pattern, at 5.11 ppm (ddd, J = 10.8, 8.2, 6.4 Hz). The coupling pattern exhibited by this proton indicated it to be adjacent to three protons and pointed to the third acetoxyl group (assuming the presence of a stictane skeleton) being attached to one of C-6, C-11, C-12, C-16, C-19 or C-20.

Table 4-2. ^{13}C and ^{1}H NMR signals (δ ppm in $CDCl_3$) observed for three stictane triterpenes (**4-3**), (**4-1**) and (**4-10**).

atom	2α,3β,22α-triacetoxystictane (4-3)			3β,6α,22α-triacetoxystictane (4-1)			3β, 22α-diacetoxystictane (4-10)		
	^{13}C	$^{1}H_\alpha$	$^{1}H_\beta$	^{13}C	$^{1}H_\alpha$	$^{1}H_\beta$	^{13}C	$^{1}H_\alpha$	$^{1}H_\beta$
1	39.2 t	1.44 t	1.81 d	33.0 t	1.48 t	1.44 d	32.9 t	1.43 q	1.45 t
2	72.0 d		5.15 ddd	24.9 t	1.73 d	1.62 t	25.4 t	1.73 d	1.63 q
3	81.2 d	4.72 d		80.7 d	4.48 dd		81.2 d	4.49 dd	
4	38.8 s			38.3 s			38.3 s		
5	47.7 d	1.60 d		50.9 d	1.92 d		48.1 d	1.45 d	
6	18.8 t	1.16 d	1.54 t	71.4 d		5.11 ddd	18.9 t	1.16 d	1.54 q
7	34.1 t	1.15 d	1.94 d	41.3 t	1.12 t	2.18 q	34.4 t	1.13 t	1.91 d
8	41.8 s			42.5 s			41.8 s		
9	46.2 d		1.38 d	46.7 d		1.49 d	45.9 d		1.39 d
10	37.5 s			38.4 s			36.8 s		
11	22.7 t	1.27 t	1.51 d	22.9 t	1.26 t	1.51 d	22.6 t	1.27 q	1.48 d
12	21.4 t	1.58 d	1.23 t	21.6 t	1.58 d	1.22 t	21.6 t	1.58 d	1.24 q
13	48.7 d	1.33 d		48.5 d	1.32 d		48.8 d	1.32 d	
14	42.6 s			42.5 s			42.6 s		
15	31.6 t	~1.28		31.7 t	1.28 q	1.24 d	31.7 t	1.28 t	1.23 d
16	19.7 t	~1.22		19.7 t	1.21 d	1.22 t	19.7 t	1.25 d	1.21 t
17	46.6 d	1.22 d		46.7 d	1.22 s (br)		46.6 d	1.22 s (br)	
18	39.1 s			38.8 s			38.8 s		
19	34.9 t	1.06 t	1.46 d	35.0 t	1.06 t	1.46 d	34.9 t	1.06 t	1.45 d
20	34.9 t	1.28 d	1.55 t	34.9 t	1.28 d	1.55 t	34.9 t	1.28 d	1.55 t
21	35.3 s			35.3 s			35.3 s		
22	78.5 d		4.68 d	78.4 d		4.68 d	78.6 d		4.69 d
23	29.5 q	0.90 s		31.0 q	1.03 s		29.0 q	0.86 s	
24	18.0 q	0.90 s		17.7 q	0.94 s		17.2 q	0.85 s	
25	23.7 q	1.03 s		24.5 q	1.04 s		22.8 q	0.93 s	
26	22.5 q	1.15 s		21.7 q	1.21 s		22.6 q	1.14 s	
27	17.1 q	0.90 s		17.1 q	0.94 s		17.2 q	0.89 s	
28	13.5 q	0.81 s		13.5 q	0.81 s		13.5 q	0.81 s	
29	29.5 q	0.85 s		29.5 q	0.85 s		29.5 q	0.85 s	
30	19.7 q	0.93 s		19.6 q	0.93 s		19.7 q	0.93 s	
	21.2 q	1.99 s ($\underline{C}H_3COOC$-2)		21.3 q	2.05 s ($\underline{C}H_3COOC$-3)		21.3 q	2.04 s ($\underline{C}H_3COOC$-3)	
	21.0 q	2.06 s ($\underline{C}H_3COOC$-3)		21.9 q	2.03 s ($\underline{C}H_3COOC$-6)				
	21.0 q	2.06 s ($\underline{C}H_3COOC$-22)		21.0 q	2.05 s ($\underline{C}H_3COOC$-22)		21.0 q	2.06 s ($\underline{C}H_3COOC$-22)	
	170.6 s	($CH_3\underline{C}OOC$-2)		171.1 s	($CH_3\underline{C}OOC$-3)		171.1 s	($CH_3\underline{C}OOC$-3)	
	171.0 s	($CH_3\underline{C}OOC$-3)		170.4 s	($CH_3\underline{C}OOC$-6)				
	171.2 s	($CH_3\underline{C}OOC$-22)		171.1 s	($CH_3\underline{C}OOC$-22)		171.2 s	($CH_3\underline{C}OOC$-22)	

The ^{13}C NMR spectrum of **4-1** (see Table 4-2) included upfield methylene carbon signals attributable to C-11 (22.9 ppm), C-12 (21.6 ppm), and C-16 (19.7 ppm) thereby excluding substitution in ring C and D, while the downfield shifts displayed by C-5 (50.9 ppm), and C-7 (41.3 ppm), in comparison to the corresponding signals of **4-3**, were consistent with the attachment of acetoxyl group at C-6.

Since the acetoxyl methine proton experienced two large $^{3}J_{ax\text{-}ax}$ couplings of 10.8, 8.2, and 6.4 Hz, it can be concluded that this proton was oriented 1,2-*trans* with respect to H-5α and one of the H-7 protons, and it was therefore axially oriented (β-face). This conclusion was subsequently supported by NOE-difference (see Section **4.3.2.5**).

4.3.2.2 COSY Spectrum of 3β,6α,22α-Triacetoxystictane (4-1)

The COSY spectrum of **4-1** included cross peaks arising from the couplings between H-6β (5.11 ppm) and the adjacent pair of methylene protons H-7α (1.12 ppm) and H-7β (2.18 ppm), and H-5α (1.92 ppm). H-3α (4.48 ppm) exhibited correlations to H-2α (1.73 ppm) and H-2β (1.62 ppm), while H-22β (4.68 ppm) only showed a correlation to H-17α (1.22 ppm).

The signal at 2.18 ppm (H-7β) exhibited a long range ^{4}J coupling to 8α-methyl group together with correlations to H-6β (5.11 ppm) and H-7α (1.12 ppm). H-5α (1.92 ppm) exhibited a correlation to H-6β (5.11 ppm).

Most of the methyl groups exhibited long range couplings to adjacent 1,2-*trans* diaxially oriented methylene protons. Recognition of long range ^{4}J couplings greatly assisted the assignment of the methyl group resonances (see Table 4-3 and Figure 4-6).

Table 4-3. Selected ^{1}H-^{1}H COSY correlations (δ ppm in $CDCl_3$) observed for 3β,6α,22α-triacetoxystictane (**4-1**).

^{1}H NMR signals	correlated ^{1}H NMR signals
5.11 ddd (H-6β)	1.92 d (H-5α), 1.12 t / 2.18 q (H-7α/β)
4.68 d (H-22β)	1.22 s (br) (H-17α)
4.48 dd (H-3α)	1.73 d / 1.62 t (H-2α/β)
2.18 q (H-7β)	5.11 ddd (H-6β), 1.21 s (8α-Me)*, 1.12 t (H-7α)
1.92 d (H-5α)	5.11 ddd (H-6β)
1.73 d (H-2α)	4.48 dd (H-3α), 1.62 t (H-2β), 1.48 t (H-1α)
1.62 t (H-2β)	4.48 dd (H-3α), 1.73 d (H-2α), 1.48 t/1.44 d (H-1α/β)
1.28 (H-20α)	1.55 t H-20β), 1.06 t / 1.46 d (H-19α/β)
1.22 s (br) (H-17α)	4.68 d (H-22β)
1.12 t (H-7α)	5.11 ddd (H-6β), 2.18 q (H-7β)
1.06 t (H-19α)	1.46 d (H-19β), 1.28 d (H-20α), 0.81 s (18β-Me)*
1.12 t (H-7α)	5.11 ddd (H-6β), 2.18 q (H-7β)
0.94 s (4β-Me)*	1.03 s (4α-Me)*
1.04 s (10β-Me)*	1.46 t (H-1α)*
1.21 s (8α-Me)*	2.18 q (H-7β)*, 0.94 s (14β-Me)#
0.94 s (14β-Me)*	1.28 t (H-15α)*, 1.21 s (8α-Me)#
0.81 s (18β-Me)*	1.06 t (H-19α)*
0.93 s (21α-Me)*	1.55 t (H-20β)*, 0.85 s (21β-Me)*
0.85 s (21β-Me)*	0.93 s (21α-Me)*

* ^4J couplings, # ^5J coupling (weak)

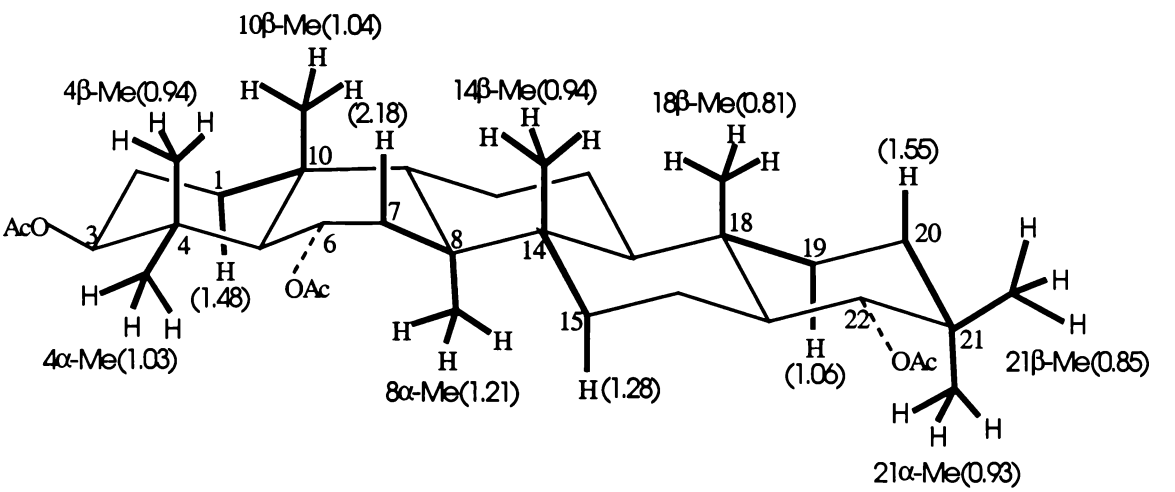

Figure 4-4. Selected ^4J ^{1}H-^{1}H COSY correlations observed for 3β,6α,22α-triacetoxystictane (**4-1**).

4.3.2.3 ^{13}C and DEPT135 NMR Spectra of 3β,6α,22α-Triacetoxystictane (4-1)

Thirty-six signals, including 9 less intense quaternary carbon resonances, appeared in the ^{13}C NMR spectrum of **4-1** while 11 quartet (CH_3), 9 triplet (CH_2), and 7 doublet (CH) signals appeared in the DEPT135 NMR spectrum. These spectra included signals attributable to three carbonyl carbons (171.1, 170.4 and 171.1 ppm) and three acetoxy methyl groups carbons (21.3, 21.9 and 21.0 ppm) respectively (Table 4-2).

In ring B, C-6 experienced a significant downfield shift to resonate at 71.4 ppm, compared to 18.8 ppm in **4-3**. C-7 also experienced a downfield shift and resonated at 41.3 ppm, compared to 34.1 and 34.4 ppm respectively in **4-3** and **4-10**.

Most of the ^{13}C chemical shifts of rings C/D/E carbons closely resembled those determined for **4-3** and **4-10**, except for C-8 which experienced a modest downfield shift of 0.7 ppm to resonate at 42.5 ppm, compared to 41.8 ppm in 3β,22α-diacetoxy stictane (**4-10**).

4.3.2.4 HMBC and HSQC Spectra of 3β,6α,22α-Triacetoxystictane (4-1)

Correlations observed in the HSQC and HMBC spectra (see Figure 4-7 and 4-8) facilitated the complete assignment of the ^{13}C and ^{1}H NMR signals of **4-1**. Selected HMBC correlations observed for **4-1** are depicted in Figure 4-9.

Methyl group assignments

The HMBC spectrum of **4-1** readily identified the resonances of the two pair of methyl groups attached to C-4 and C-22 since the protons of the 4α- and 4β-methyl groups (ie, H-23, H-24) and the 21α- and 21β-methyl groups (ie, H-29, H-30) exhibited ^{2}J heteronuclear correlations to the same quaternary carbons (C-4 or C-21 respectively). Additionally, (i) H-23, H-24 and H-25 each exhibited an HMBC correlation to C-5 (50.9 ppm); (ii) H-25 and H-26 exhibited correlations to C-9 (46.7 ppm), and (iii) both H-26 and H-27 showed HMBC correlations to C-8 (42.5 ppm) and C-14 (42.5 ppm) (see Table 4-4).

Structurally significant correlations observed for the methyl groups, and some other protons of **4-1** are presented in Table 4-4.

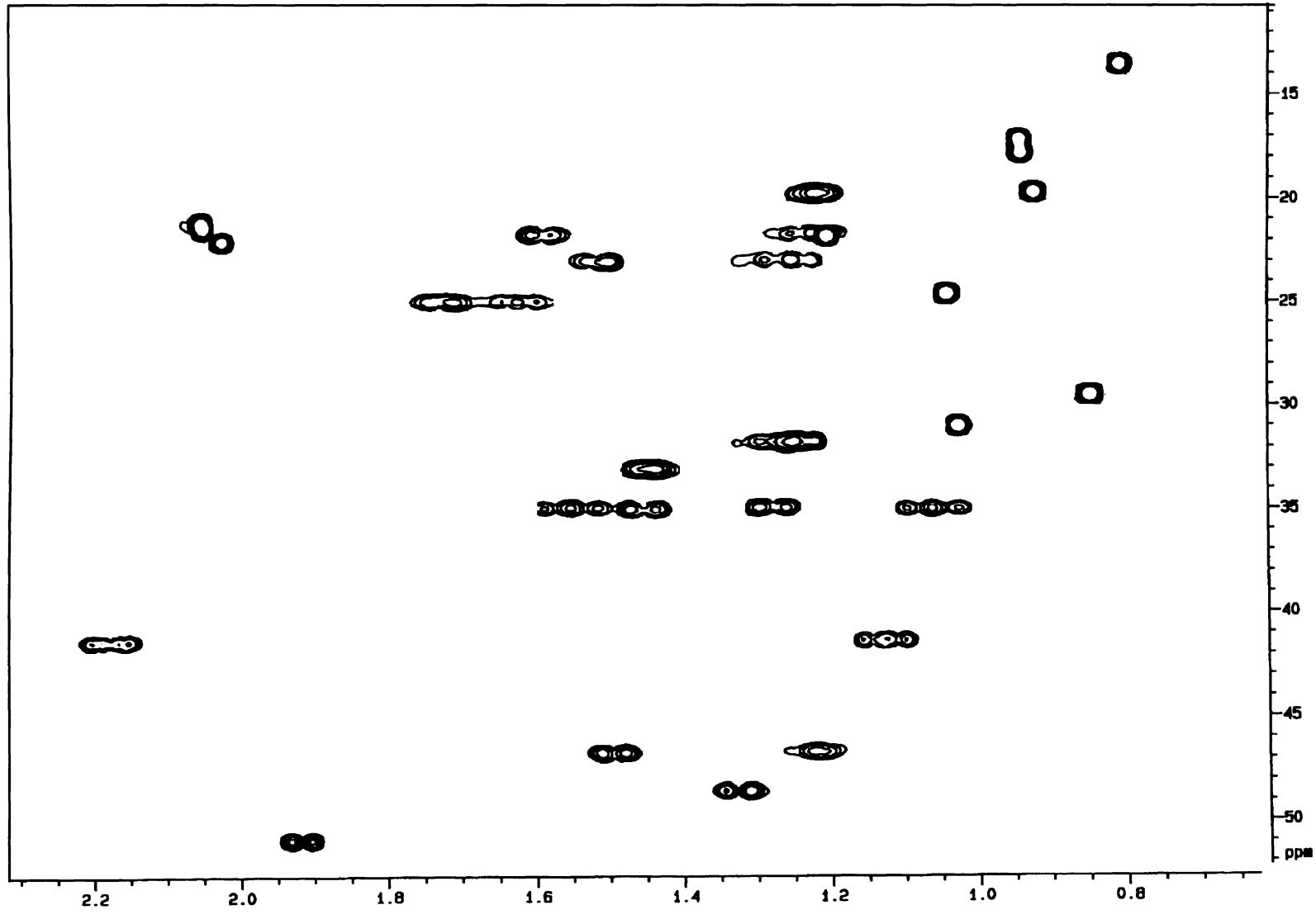

Figure 4-5. The HSQC spectrum (^{1}H, δ 0.6-2.4 ppm region) of 3β,6α,22α-triacetoxystictane (**4-1**).

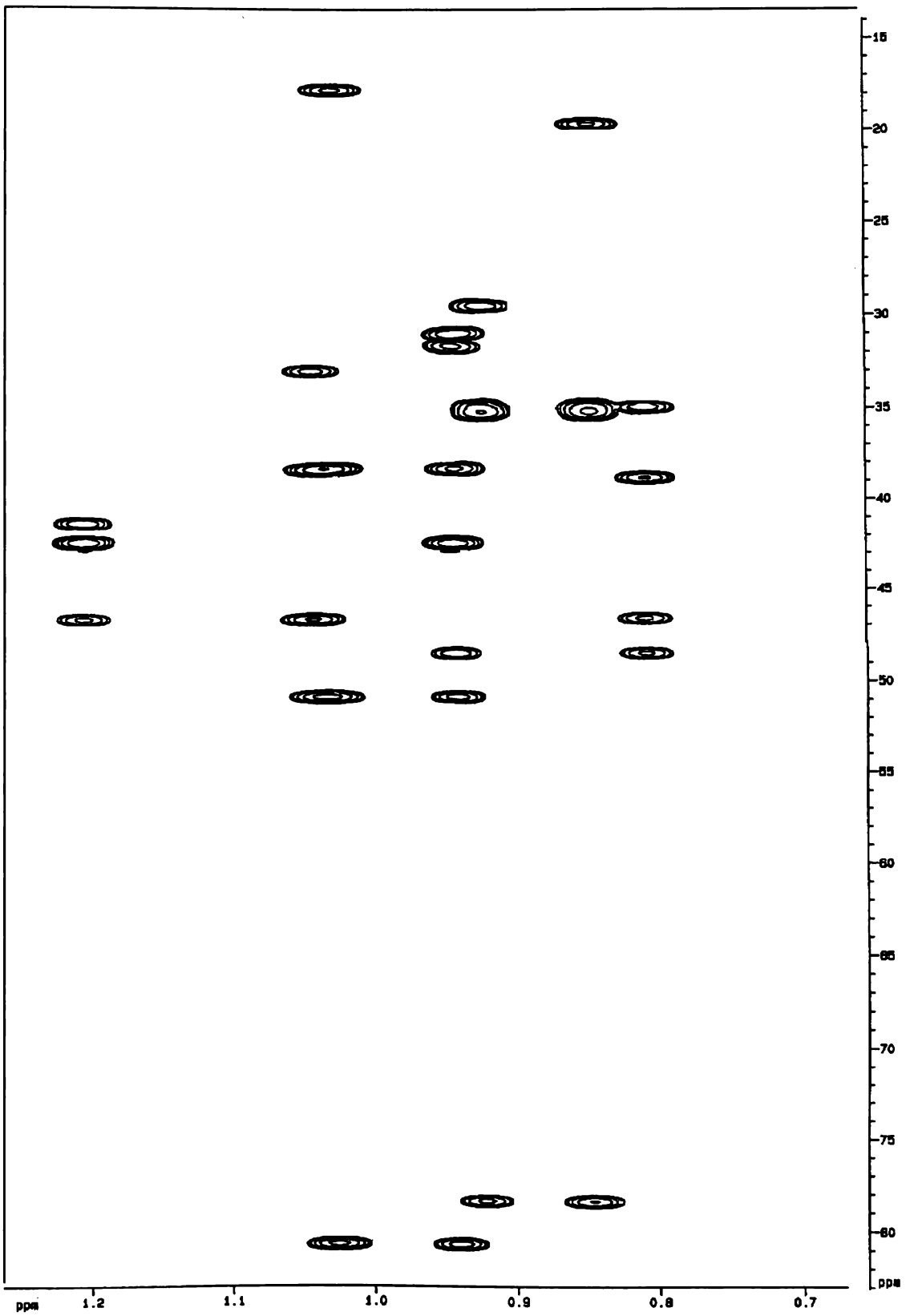

Figure 4-6. Selected HMBC correlations (the methyl group region) observed for 3β,6α,22α-triacetoxystictane (**4-1**).

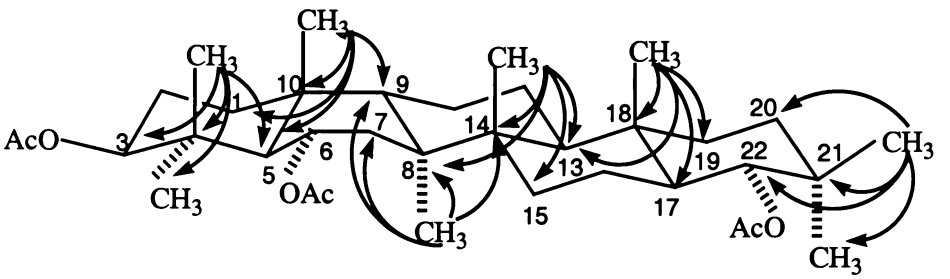

Figure 4-7. Selected HMBC correlations observed for the methyl groups of 3β,6α,22α-triacetoxystictane (**4-1**).

Table 4-4. ^{1}J, ^{2}J and ^{3}J heteronuclear ^{1}H-^{13}C correlations (δ ppm in $CDCl_3$) observed for 3β,6α,22α-triacetoxystictane (**4-1**).

^{1}H signal	^{1}J correlated ^{13}C signal	^{2}J and ^{3}J correlated ^{13}C signals
1.03 s (4α-Me)	31.0 (C-23)	80.7 (C-3), 50.9 (C-5), 38.3 (C-4), 17.7 (C-24)
0.94 s (4β-Me)	17.7 (C-24)	80.7 (C-3), 50.9 (C-5), 38.3 (C-4), 31.0 (C-23)
1.04 s (10β-Me)	24.5 (C-25)	50.9 (C-5), 46.7 (C-9), 38.4 (C-10), 33.0 (C-1)
1.21 s (8α-Me)	21.7 (C-26)	46.7 (C-9), 42.5 (C-8), 41.3 (C-7), 42.5 (C-14)
0.94 s (14β-Me)	17.1 (C-27)	48.5 (C-13), 42.5 (C-8), 42.5 (C-14), 31.7 (C-15)
0.81 s (18β-Me)	13.5 (C-28)	48.5 (C-13), 46.6 (C-17), 38.8 (C-18), 35.0 (C-19)
0.85 s (21β-Me)	29.5 (C-29)	78.4 (C-22), 35.3 (C-21), 34.9 (C-20), 19.6 (C-30)
0.93 s (21α-Me)	19.6 (C-30)	78.4 (C-22), 35.3 (C-21), 34.9 (C-20), 29.5 (C-29)
1.12 t (H-7β) (ax)	41.3 (C-7)	71.4 (C-6), 50.9 (C-5), 46.7 (C-9), 42.5 (C-8) 42.5 (C-14), 21.7 (C-26)
1.92 d (H-5α) (ax)	50.9 (C-5)	80.7 (C-3), 71.4 (C-6), 41.3 (C-7), 38.3 (C-4) 33.0 (C-1), 31.0 (C-23), 24.5 (C-25), 17.7 (C-24)
2.18 q (H-7α) (eq)	41.3 (C-7)	71.4 (C-6), 50.9 (C-5), 42.5 (C-8), 42.5 (C-14), 21.7 (C-26)
4.48 d (H-3α) (ax)	80.7 (C-3)	171.1 ($CH_3\underline{C}OO$-C-3), 38.3 (C-4), 31.0 (C-23), 17.7 (C-24)
4.68 d (H-22β) (ax)	78.4 (C-22)	171.1 ($CH_3\underline{C}OO$-C-22), 46.6 (C-17), 19.6 (C-30)
5.11 ddd (H-6β) (ax)	71.4 (C-6)	170.4 ($CH_3\underline{C}OO$-C-6), 50.9 (C-5), 41.3 (C-7)

* ^{4}J coupling

Identification of the methyl group resonances *via* their unique HMBC correlation patterns led in turn to the assignment of the corresponding ^{13}C resonances *via* correlations observed in the HSQC spectrum of **4-1**. These assignments are presented in Table 4-2.

Methine proton assignments

The HSQC spectrum of **4-1** showed that H-3α (4.48 ppm), H-6β (5.11 ppm) and H-22β (4.68 ppm) correlated with the ^{13}C signals which occurred at 80.3, 71.4 and 78.4 ppm respectively. In the HMBC spectrum H-3α (4.48 ppm) exhibited correlations with C-4 (38.3 ppm), C-23 (31.0 ppm), C-24 (17.7) and the acetoxy carbonyl carbon at C-3 (171.1 ppm); H-6β (5.11 ppm) exhibited correlations with C-5 (50.9 ppm), C-7 (41.3 ppm) and the acetoxy carbonyl carbon at C-6 (170.4 ppm), and H-22β (4.68 ppm) exhibited correlations with C-17 (46.6 ppm), C-30 (19.6 ppm) and the acetoxy carbonyl carbon at C-22 (171.1 ppm).

The four remaining methine protons of **4-1** were easily identified from a combination of HMBC correlations (see Table 4-4), HSQC correlations and analyses of coupling patterns observed in the 400 MHz ^{1}H NMR spectrum. This information revealed the ^{13}C assignments of the methine carbons *via* correlations observed in the HSQC spectrum.

For example, the methine signal which resonated at 1.92 ppm (d, J = 10.8 Hz), exhibited HMBC correlations to C-1 (33.0 ppm), C-3 (80.7), C-4 (38.3 ppm), C-6 (71.4 ppm), C-7 (41.3 ppm), C-23 (31.0 ppm), C-24 (17.7 ppm) and C-25 (24.5 ppm), and was therefore assigned to H-5α. The corresponding H-5α resonances of **4-3** and **4-10** occurred at 1.60 and 1.45 ppm. This difference can be attributed to an introduction of the substituted acetoxyl group at C-6.

Methylene proton assignments

Assignments of individual methylene protons of **4-1**, including their orientation (α- or β-), were achieved by the combination of COSY, HSQC and HMBC data, along with the information that the resolution HSQC spectrum was such that large axial-axial or geminal couplings of the order J = 10~16 Hz could be resolved, whereas smaller equatorial-equatorial or axial-equatorial couplings of the order J = 3~5 Hz were not resolved (as described in Section **2.2.2.2** for most methylene protons in **2-2**).

For instance, a pair of signals at 1.28 (~d) ppm and 1.55 (~t) ppm were readily assigned as the H-20α and H-20β methylene proton resonances since (i) these signals correlated with C-20 (34.9 ppm) in the HSQC spectrum (Table 4-2), and (ii) H-20α (in an equatorial position) would be expected to exhibit a doublet coupling arising from a ^2J coupling with H-20β and unresolved couplings to H-19α and H-19β, while H-20β (in an axial position) would like to exhibit a triplet-like pattern due to one large ^2J coupling with H-20α and another large ^3J coupling with H-19α. Additionally, a ^4J coupling between H-20β and the 21α-methyl group (0.93 ppm), detected in a COSY spectrum (see Table 4-3), validated the above assignments.

In a like manner, signals at 1.06 (~t) ppm and 1.46 (~d) ppm can be assigned to H-19α (in an axial position) and H-19β (in an equatorial position), respectively.

The complete assignments of the methylene and methine protons of **4-1** are presented in Table 4-2, and the resonances for most of methylene protons in rings C, D and E can be compared with those previously reported for **4-3** by Wilkins *et al.* (1989) and the assignments for **4-10** made in this investigation (see Table 4-2).

4.3.2.5 NOE Data and Molecular Modelling Analyses of 3β,6α,22α-Triacetoxystictane (4-1)

Irradiation of H-6β (5.11 ppm) of **4-1** enhanced H-7β (2.18 ppm), H-9β (1.49 ppm), and the 10β-methyl (1.04 ppm) and 4β-methyl (0.94 ppm) groups. This showed H-6 to be β-orientated.

Irradiation of H-22β (4.68 ppm) enhanced H-19β (1.46 ppm), H-20β (1.55 ppm), H-16β (1.22 ppm), and the 18β-methyl (0.81 ppm) and 21β-methyl (0.85 ppm) groups, while irradiation of H-3α (4.48 ppm) enhanced H-5α (1.92 ppm), H-1α (1.48 ppm) and the 4α-methyl group (1.03 ppm). These observations are consistent with the conclusion that the acetoxyl groups at C-3 and C-22 of **4-1** have the same orientation as **4-3** and **4-10**.

Other structurally significant enhancements observed for **4-1** are presented in Table 4-5. Selected NOE's observed for **4-1** are depicted in Figure 4-10.

Table 4-5. NOE effects (δ ppm in $CDCl_3$) observed for 3β,6α,22α-triacetoxystictane (**4-1**).

irradiated ^{1}H NMR signals	enhanced ^{1}H signals
1.03 s (4α-Me)	0.94 s (4β-Me), 4.48 dd (H-3α), 1.92 d (H-5α),
0.94 s (4β-Me)	1.04 s (10β-Me), 1.03 s (4α-Me)
1.04 s (10β-Me)	0.94 s (4β-Me), 5.11 ddd (H-6β), 1.62 t (H-2β), 1.49 d (H-9β)
1.21 s (8α-Me)	1.92 d (H-5α), 1.33 q (H-13α)
0.94 s (14β-Me)	0.81s (18β-Me), 2.18 q (H-7β), 1.49 d (H-9β), 1.22 t (H-12β), 1.22 t (H-16β)
0.81 s (18β-Me)	0.94 s (14β-Me), 4.68 d (H-22β)
0.93 s (21α-Me)	0.85 s (21β-Me), 1.33 d (H-13α), 1.22 br s (H-17α)
0.85 s (21β-Me)	0.93 s (21α-Me), 4.68 d (H-22β)
4.48 dd (H-3α)	1.03 s (4α-Me), 1.92 d (H-5α), 1.45 q (H-1α)
4.68 d (H-22β)	0.85 s (21β-Me), 0.81 s (18β-Me), 1.55 t (H-20β), 1.46 d (H-19β), 1.22 t (H-16β)
5.11 ddd (H-6β)	1.04 s (10β-Me), 0.94 s (4β-Me), 2.18 q (H-7β), 1.49 d (H-9β),

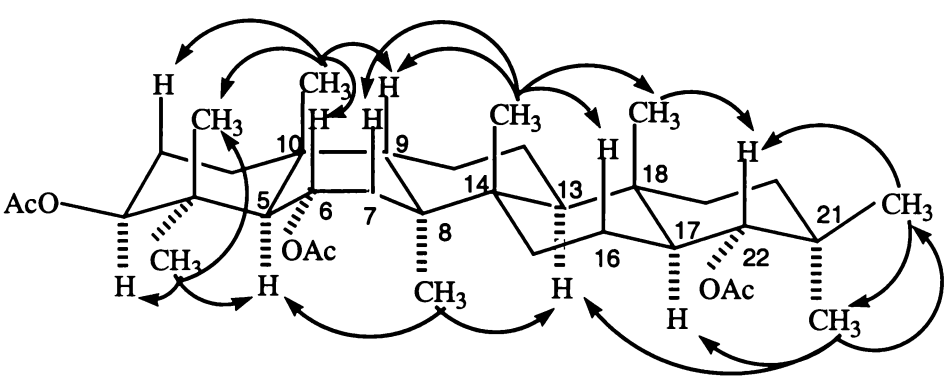

Figure 4-8. Selected NOE's observed for 3β,6α,22α-triacetoxystictane (**4-1**).

The MM2 modelled structure of **4-1** is presented in Figure 4-11. The coupling constants of the H-6β proton (J = 10.4, 8.6, 6.2 Hz) are consistent with the twist boat conformation of the ring B shown in Figure 4-11.

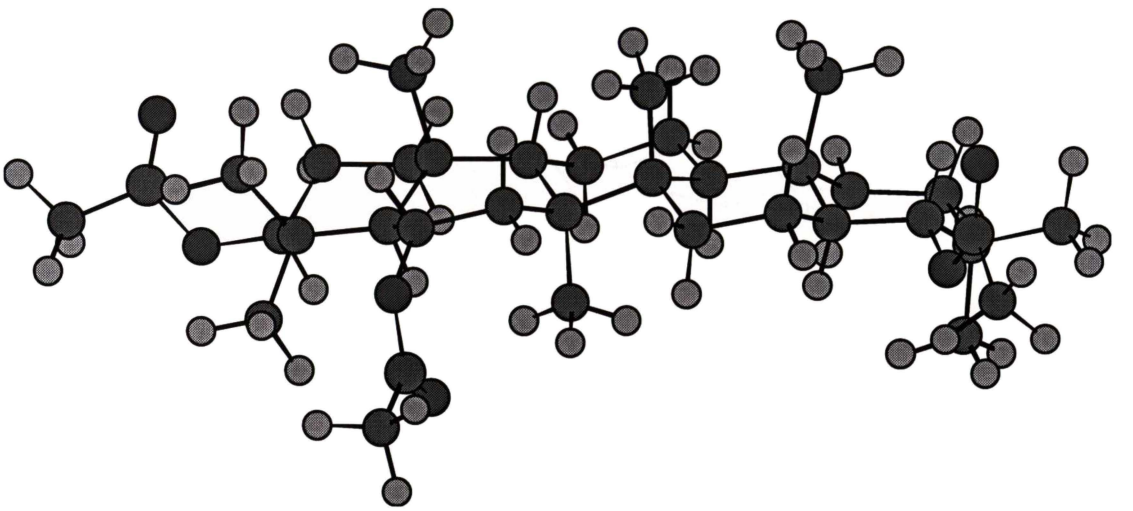

Figure 4-9. MM2 modelled structure of 3β,6α,22α-triacetoxystictane (**4-1**).

4.4 NMR Spectral Analyses of 22α-Hydroxystictano-25,3β-lactone

One of the fractions isolated from the *P. colensoi* extracts was identified as 22α-hydroxystictano-25,3β-lactone (**4-2**) (Wilkins *et al.*, 1989). Hitherto only the ^{13}C NMR assignments of **4-2** have been reported by Wilkins *et al.* (1989). During the course of the present investigation the complete assignments of the ^{13}C and ^{1}H NMR assignments of the lactone (**4-2**) were achieved by analyses of a combination of one- and two-dimensional NMR data. This lead to revision in some of the reported ^{13}C NMR assignments.

The revised ^{13}C NMR assignments reported here have significance in respect of the structure of a new flavicano-25,3β-lactone (**5-3**) reported in Chapter 5. The biosynthetic precursor of this lactone (**4-2**) is believed to be 3β,22α-dihydroxystictan-25-oic acid (**4-10**) (See Figure 4-12).

The complete assignment of the ^{13}C and ^{1}H NMR signals of **4-2** is presented in Table 4-6. The ^{13}C NMR assignments of stictane-3β,22α-diol (**4-7**) reported by Wilkins *et al.* (1989), are also listed in Table 4-6.

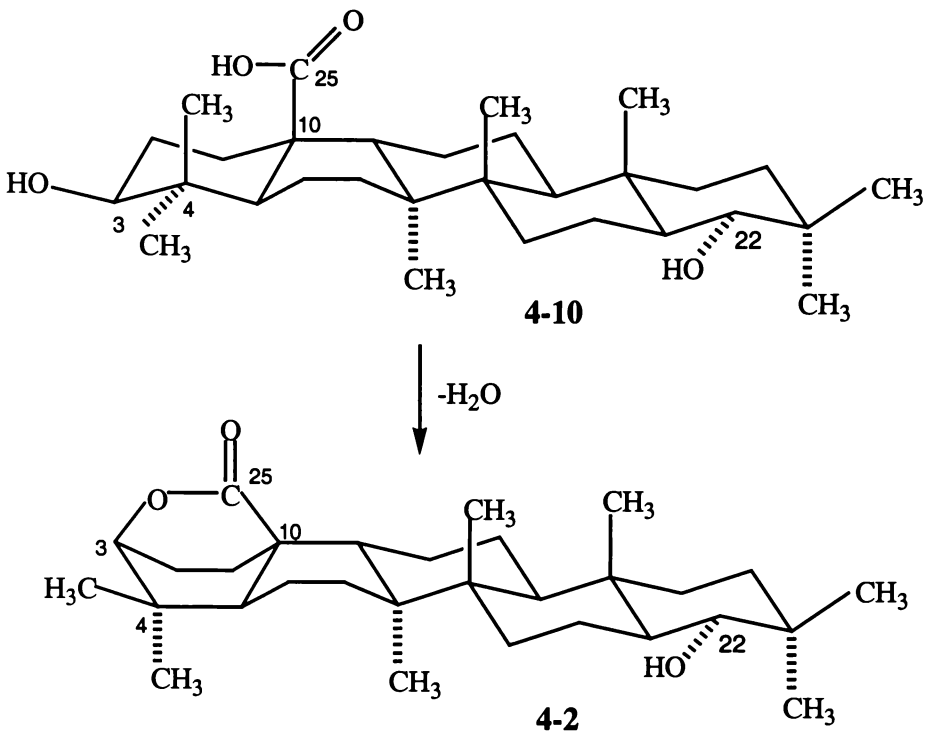

Figure 4-10. Structure of 3β,22α-dihydroxystictan-25-oic acid (**4-10**), the proposed biosynthetic precursor of lactone (**4-2**).

4.4.1 ^{1}H and ^{13}C NMR Spectra of 22α-Hydroxystictano-25,3β-lactone (4-2)

The 400 MHz ^{1}H NMR spectrum of **4-2** included signals attributable to seven tertiary methyl groups in the region of 0.85~1.15 ppm, downfield multiplet signals observed at 4.03 ppm (d, J = 4.6 Hz), 3.17 ppm (d, J = 11.0 Hz) and 2.58 ppm (dd, J = 12.5, 3.3 Hz), and methylene signals at 1.86 ppm (ddd, J = 9.5, 9.5, 3.5 Hz), 1.75 ppm (dd, J =10.9, 3.1 Hz).

The signal at 4.03 ppm, assigned to H-3α, was consistent with the presence of a 3β,25-lactone group {-CHO-CO-C-}, while the chemical shift and coupling constant of the methine signal at 3.17 ppm was consistent with the presence of a 22α-hydroxyl group.

The ^{13}C NMR signals of the specimen of **4-2** isolated in the present investigation corresponded with those previously reported for this lactone (Wilkins *et al.*, 1989), however two-dimensional HSQC and HMBC spectral data showed that some of the reported ring A/B signal assignments should be revised (see below). There was however a close correspondence between the ring C/D/E assignments and those

determined for **4-2** (see Table 4-6), other than for the reversal of the C-13 and C-17 assignments.

Table 4-6. ^{13}C and ^{1}H NMR signals (δ ppm in $CDCl_3$) determined for 22α-hydroxystictano-25,3β-lactone (**4-2**) and stictane-3β,22α-diol (**4-7**).

atom	stictane-3β,22α-diol (**4-7**)	(**4-2**)*	22α-hydroxystictano-25,3β-lactone (**4-2**)		
	^{13}C	^{13}C	^{13}C	$^{1}H_{\alpha}$	$^{1}H_{\beta}$
1	33.2 t	23.9 t	24.0 t	1.53 d	1.29 d
2	29.2 t	25.7 t	20.3 t[a]	~1.98 (overlapped)	
3	79.3 d	82.5 d	82.5 d	4.03 d	
4	39.2 s	38.3 s	38.3 s		
5	48.0 d	33.4 d	46.8 d[b]	1.63 d	
6	19.1 t	20.2 t	25.8 t[a]	1.86 ddd	1.63 q
7	34.5 t	32.7 t	32.7 t	0.97 d	1.98 q
8	41.9 d	40.3 s	40.4 s		
9	45.8 d	46.7 d	33.5 d[b]	2.58 dd	
10	36.9 s	44.9 s	45.0 s		
11	22.6 t	20.8 t	20.9 t	1.55 t	1.46 d
12	21.5 t	21.7 t	21.8 t	1.47 d	1.03 t
13	48.6 d	48.5 d	49.1 d[c]	1.28 d	
14	42.8 s	42.8 s	42.3 s?		
15	31.8 t	31.6 t	31.7 t	~1.37 (overlapped)	
16	19.4 t	19.2 t	19.3 t	1.75 dd	1.23 q
17	49.0 d	49.0 d	48.6 d[c]	1.05 d	
18	38.5 s	38.5 s	38.6 s		
19	34.9 t[d]	34.9 t[d]	35.0 t[d]	1.03 t	1.45 d
20	35.0 t[d]	35.0 t[d]	34.9 t[d]	1.26 d	1.49 t
21	35.8 s	35.8 s	35.8 s		
22	76.5 d	76.5 d	76.5 d	3.17 d	
23	29.1 q	26.4 q	26.5 q	1.03 s	
24	16.1 q	20.2 q	20.3 q	0.87 s	
25	22.7 q	178.2 s	178.3 s		
26	22.7 q	22.1 q	22.2 q	1.11 s	
27	17.3 q	17.1 q	17.2 q	1.01 s	
28	13.5 q	13.5 q	13.6 q	0.76 s	
29	29.9 q	29.8 q	29.9 q	0.87 s	
30	18.6 q	18.5 q	18.6 q	0.99 s	

[a] reassignment for C-2 and C-6 [b] reassignment for C-5 and C-9
[c] reassignment for C-13 and C-17 [d] interchangeable
*^{13}C assignments reported by Wilkins *et al.* (1989)

4.4.2 COSY Spectrum of 22α-Hydroxystictano-25,3β-lactone (4-2)

The COSY spectrum of **4-2** included cross peaks arising from the couplings between H-3α (4.03 ppm) and the adjacent pair of methylene protons H-2α/β (~1.98 ppm), H-22β (3.17 ppm) and H-17α (1.05 ppm), and H-9β (2.58 ppm) and H-11α (1.55 ppm) (see Table 4-7).

The 4α- and 4β-methyl groups, and the 21α- and 21β-methyl groups, respectively, exhibited mutual long range ^4J couplings, while the 18α-methyl (0.76 ppm) and 21α-methyl (0.99 ppm) groups exhibited ^4J couplings to H-19α (1.03 ppm) and H-20β (1.49 ppm), respectively (see Table 4-7). Other selected ^{1}H-^{1}H COSY correlations observed for **4-2** are presented in Table 4-7.

Table 4-7. Selected ^{1}H-^{1}H COSY correlations (δ ppm in $CDCl_3$) observed for 22α-hydroxystictano-25,3β-lactone (**4-2**).

^{1}H NMR signals	correlated ^{1}H signals
4.03 d (H-3α)	~1.98 (H-2α/β)
3.17 d (H-22β)	1.05 t (H-17α)
2.58 dd (H-9β)	1.55 t (H-11α)
~1.98 (H-2α/β)	4.03 d (H-3α)
1.98 q (H-7β)	1.86 ddd/1.63 q (H-6α/β), 0.97 d (H-7α)
1.86 ddd (H-6α)	1.98 q (H-7β), 1.63 q (H-6β), 1.63 d (H-5α)
1.75 d (H-16α)	1.37 (H-15α/β), 1.23 q (H-16β), 1.05 t (H-17α)
1.63 q (H-6β)	1.98 q (H-7β), 1.86 ddd (H-6α)
1.55 t (H-11α)	2.58 dd (H-9β)
1.46 d (H-11β)	1.55 t (H-11α), 1.47 d (H-12α)
~1.37 (H-15α/β)	1.75 dd /1.23 q (H-16α/β)
1.28 d (H-13α)	1.47 d / 1.03 t (H-12α/β)
1.23 q (H-16β)	1.75 dd (H-16α), ~1.37 (H-15α/β), 1.05 t (H-17α)
1.05 t (H-17α)	3.17 d (H-22β), 1.75 dd/1.23 q (H-16α/β), 0.76 s (18β-Me)*
0.99 s (21α-Me)	1.49 t (H-20β)*, 0.87 s (21β-Me)*
0.97 d (H-7α)	1.98 q (H-7β)
0.87 s (4β-Me)	1.03 s (4α-Me)*
0.76 s (18β-Me)	1.03 t (H-19α)*

* ^4J coupling

4.4.3 HMBC and HSQC Spectra of 22α-Hydroxystictano-25,3β-lactone (4-2)

Correlations observed in the HMBC and HSQC spectra greatly facilitated the complete assignment of the ^{13}C and ^{1}H NMR signals of **4-2**. The HMBC correlations observed for the methyl groups and selected methylene or methine protons of **4-2** are presented in Table 4-8.

HMBC and HSQC spectral data, in combination with COSY data, established that the C-2 and C-6, C-13 and C-17, and C-5 and C-9 signal assignments of **4-2** reported by Wilkins *et al.* (1989) should be revised.

Table 4-8. ^{1}J, ^{2}J and ^{3}J heteronuclear ^{1}H-^{13}C correlations (δ ppm in $CDCl_3$) observed for 22α-hydroxystictano-25,3β-lactone (**4-2**).

^{1}H signal	^{1}J correlated ^{13}C signal	^{2}J and ^{3}J correlated ^{13}C signals
1.03 s (4α-Me)	26.5 (C-23)	82.5 (C-3), 46.8 (C-5), 38.3 (C-4), 20.3 (C-24)
0.87 s (4β-Me)	20.3 (C-24)	82.5 (C-3), 46.8 (C-5), 38.3 (C-4), 26.5 (C-23)
1.11 s (8α-Me)	22.2 (C-26)	32.7 (C-7), 42.3 (C-14), 40.4 (C-8), 33.5 (C-9)
1.01 s (14β-Me)	17.2 (C-27)	49.1 (C-13), 42.3 (C-14), 40.4 (C-8), 31.7 (C-15)
0.76 s (18β-Me)	13.6 (C-28)	49.1 (C-13), 48.6 (C-17), 38.6 (C-18), 35.0 (C-19)
0.87 s (21β-Me)	29.9 (C-29)	76.5 (C-22), 35.8 (C-21), 34.9 (C-20), 18.6 (C-30)
0.99 s (21α-Me)	18.6 (C-30)	76.5 (C-22), 35.8 (C-21), 34.9 (C-20), 29.9 (C-29)
4.03 d (H-3α)	82.5 (C-3)	178.3 (C-25), 46.8 (C-5), 38.3 (C-4), 26.5 (C-23), 20.3 (C-24)
3.17 d (H-22β)	76.5 (C-22)	48.6 (C-17), 38.6 (C-18), 35.8 (C-21), 29.9 (C-29), 18.6 (C-30)
2.58 dd (H-9α)	33.5 (C-9)	178.3 (C-25), 45.0 (C-10), 42.3 (C-14), 40.4 (C-8) 24.0 (C-1), 20.9 (C-11)
1.98 q (H-7β)	32.7 (C-7)	46.8 (C-5), 42.3 (C-14), 40.4 (C-8), 22.2 (C-26)
1.86 ddd (H-6α)	25.8 (C-6)	178.3 (C-25), 82.5 (C-3), 45.0 (C-10), 20.3 (C-24)
1.63 d (H-5α)	46.8 (C-5)	178.3 (C-25), 45.0 (C-10), 38.3 (C-4), 32.7 (C-7), 20.3 (C-24)
1.36 d (H-15α)	31.7 (C-15)	49.1 (C-13), 42.3 (C-14), 19.3 (C-16), 17.2 (C-27)

Revision of C-5 and C-9 assignments

The HMBC spectrum of **4-2** showed correlations between H-3α (4.03 ppm) and C-4 (38.3 ppm), C-5 (46.8 ppm), C-23 (26.5 ppm), C-24 (20.3 ppm), C-25 (178.3 ppm), while the signal at 2.58 ppm (dd, J = 12.5 and 3.3 Hz) was assigned to H-9β since it

exhibited HMBC correlations to C-1 (24.0 ppm), C-8 (40.4 ppm), C-10 (45.0 ppm), C-11 (20.9 ppm), C-14 (42.3 ppm) and C-25 (178.3 ppm) (see Table 4-8). In the HSQC spectrum of **4-2** H-9β (2.58 ppm) correlated with the ^{13}C NMR signal which occurred at 33.5 ppm.

These observations demonstrated that the reported assignments of C-5 and C-9 should be reversed (see Table 4-6).

Revision of C-13 and C-17 assignments

The ^{13}C signal which occurred at 48.6 ppm was reassigned to C-17 since in the HMBC spectrum of **4-2** the 18β-methyl group (0.76 ppm) correlated to both C-13 (49.1 ppm) and C-17 (48.6 ppm), while H-22β (3.17 ppm) showed correlations to C-17 (48.6 ppm), C-18 (38.6 ppm), C-21 (35.8), C-29 (29.9 ppm) and C-30 (18.6 ppm), rather than C-13 (49.1 ppm).

Revision of C-2 and C-6 assignments

The resonances of the ring B protons of **4-2** were defined by COSY correlations between H-6α (1.86 ppm) and H-6β, H-5α (1.63 ppm) and H-7β (1.98 ppm) (see Table 4-7). Correlations observed in the HSQC spectrum showed that the C-5, C-6 and C-7 signals occurred at 46.8 ppm, 25.8 ppm and 32.7 ppm, respectively.

The COSY spectrum of **4-2** also exhibited correlations between H-3α (4.03 ppm) and the overlapping H-2α/β signals (1.98 ppm). The HSQC spectrum showed that these protons correlated with the ^{13}C resonance which occurred at 20.3 ppm.

The foregoing correlations showed that the reported C-2 and C-6 assignments should be reversed

Methylene and methine proton assignments

The orientation (α or β-) of most of the ring C/D/E methylene protons were readily assigned by the analyses of coupling patterns observed in the HSQC spectrum (see Table 4-6) and some case, also by ^{4}J COSY couplings (see Table 4-7).

4.4.4 NOE Data Analyses of 22α-Hydroxystictano-25,3β-lactone (4-2)

Irradiation of H-22β (3.17 ppm) enhanced H-20β (1.49 ppm), and the 18β-methyl (0.76 ppm) and 21β-methyl (0.87 ppm) groups, while irradiation of H-3α (4.03 ppm) enhanced H-2α/β (~1.98 ppm), and the 4α-methyl (1.03 ppm) and 4β-methyl (0.87 ppm) groups. Irradiation of H-9β (2.58 ppm) enhanced H-7β (1.98 ppm), H-6β (1.63 ppm), H-12β (1.03 ppm) and the 14β-methyl (1.01 ppm) group.

Other structurally significant enhancements observed for the methyl groups and some methine protons are presented in Table 4-9.

Table 4-9. NOE effects (δ ppm in $CDCl_3$) observed for 22α-hydroxystictano-25,3β-lactone (**4-2**).

irradiated ^{1}H NMR signals	enhanced ^{1}H signals
1.03 s (4α-Me)	0.87 s (4β-Me), 1.63 d (H-5α), 4.03 d (H-3α)
0.87 s (4β-Me)	1.03 s (4α-Me), 4.03 d (H-3α)
1.11 s (8α-Me)	1.86 ddd (H-6α), 1.63 d (H-5α), ~1.37 (H-15α/β), 0.97 d (H-7α)
1.01 s (14β-Me)	0.76 s (18β-Me), 2.58 dd (H-9β), 1.98 q (H-7β)
0.76 s (18β-Me)	1.01 s (14β-Me), 3.17 d (H-22β), 1.49 t (H-20β), 1.23 q (H-16β)
0.99 s (21α-Me)	0.86 s (21β-Me), 1.05 t (H-17α)
0.87 s (21β-Me)	0.99 s (21α-Me), 3.17 d (H-22β), 1.26 d/1.49 t (H-20α/β)
2.58 dd (H-9β) (ax)	1.01 s (14β-Me), 1.98 q (H-7β), 1.63 d (H-6β), 1.03 t (H-12β)
3.17 d (H-22β)	0.87 s (21β-Me), 0.76 s (18β-Me), 1.49 t (H-20β)
4.03 d (H-3α)	1.03 s (4α-Me), 0.87 s (4β-Me), ~1.98 (H-2α/β)

Chapter Five

A New Flavicane Triterpene

5.1 Introduction

Chin *et al.* (1973) and Corbett & Wilkins (1976) have reported that dehydration of 22-hydroxystictane triterpenes with phosphoryl chloride in pyridine affords ring E contracted flavicane (**5-1**) triterpenes, rings C, D and E of which were antipodally related to those of the corresponding rings of 21α-H-hopane (**5-2**) (see Figure 5-1).

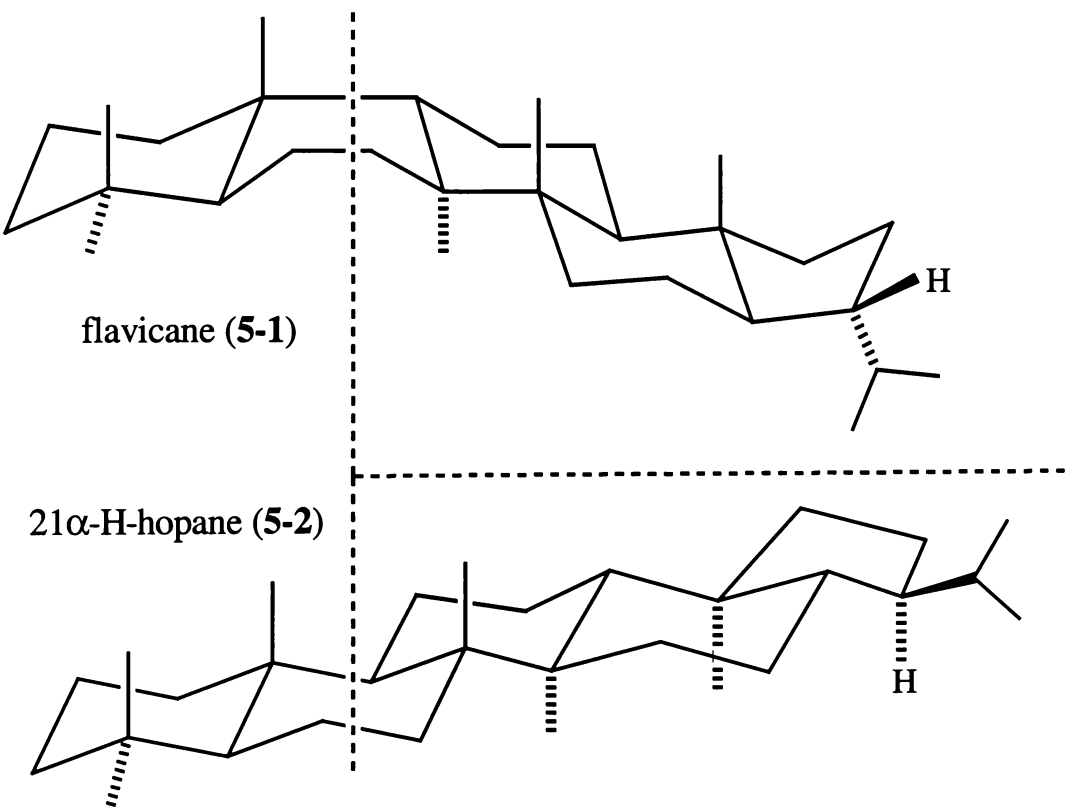

Figure 5-1. The antipodal relationship of rings C, D and E of flavicane (**5-1**) and 21α-H-hopane (**5-2**) triterepenes.

To date flavicane triterpenes have only been prepared by ring contraction of naturally occurring 22-hydroxystictane triterpenes. In this chapter the isolation of a flavicane triterpene from natural sources is reported.

Detailed analyses of mass spectral and one- and two-dimensional NMR spectral data identified the new flavicane triterpene as 22-hydroxyflavicano-25,3β-lactone (**5-3**). Due to the striking similarities in the ^{13}C and ^{1}H NMR spectra of flavicane (**5-1**) and 21α-H-hopane (**5-2**) (Corbett & Wilkins, 1976), 21α-H-hopan-22-ol (**5-4**) and 22α-hydroxystictano-25,3β-lactone (**4-2**) were used as model compounds to establish the complete assignment of the ^{13}C and ^{1}H NMR signals of the new triterpene (**5-3**).

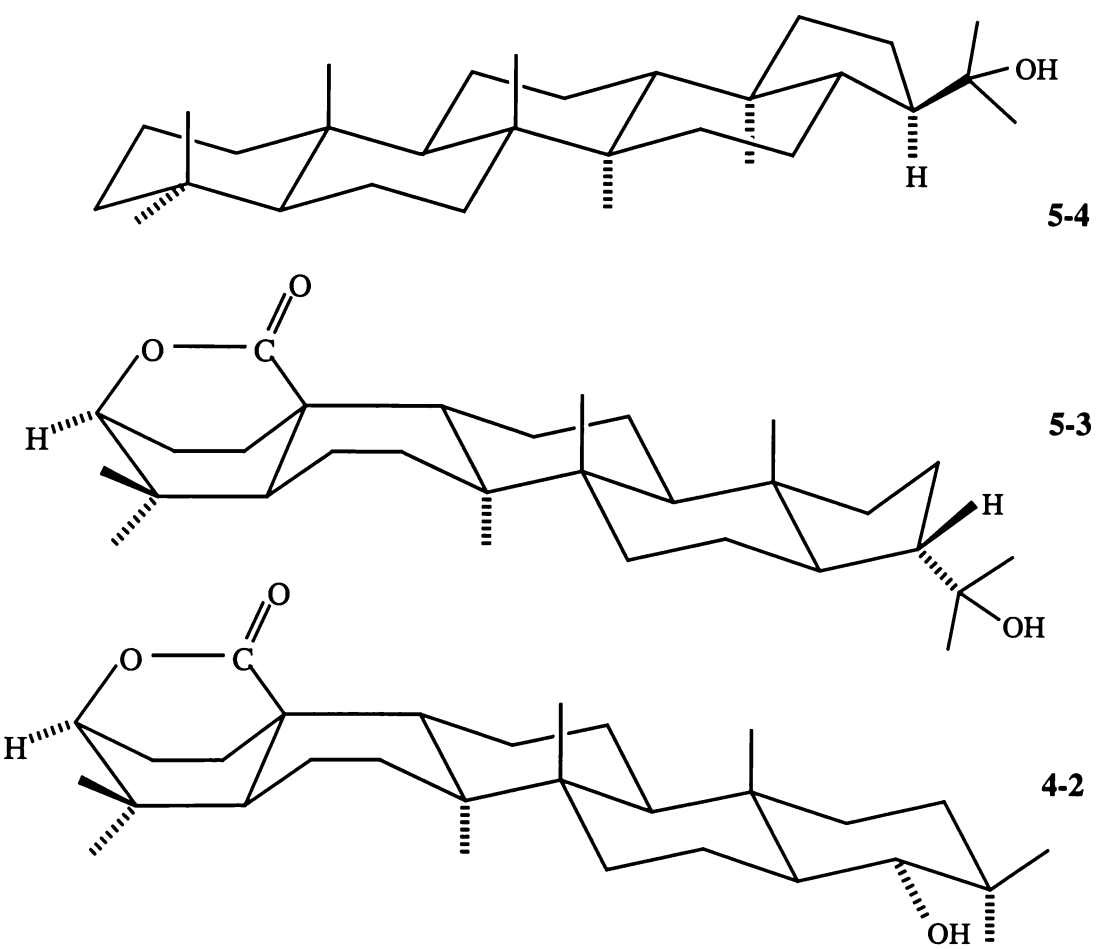

Figure 5-2. The structures of 21α-H-hopan-22-ol (**5-4**), 22-hydroxyflavicano-25,3β-lactone (**5-3**) and 22α-hydroxystictano-25,3β-lactone (**4-2**).

5.2 Isolation of the New Flavicane Triterpene

As noted in Chapter Four, 14 fractions were obtained from the column chromatography on the extracts of the lichen *P. colensoi*. The possible presence of a new triterpene (possibly one possessing a hydroxyisopropyl group analogous to that present in 22-hydroxyhopanoids) was suggested by an intense *m/z* 59 fragment ion observed during GC/MS analyses for the dominant constituent of fraction 10. Separation of this fraction by radial PLC on silica gel with the mixtures of light petroleum and diethyl ether as eluents led to the isolation of the new triterpene (**5-3**).

5.3 Structural Elucidation of 22-Hydroxyflavicano-25,3β-lactone (5-3)

5.3.1 Mass Spectrum Analysis of 22-Hydroxyflavicano-25,3β-lactone (5-3)

The mass spectral fragmentation pattern of **5-3** was similar to that of **4-2**, other than for the strong fragment ion which occurred at *m/z* 59. This ion suggested the presence of a $-C(CH_3)_2OH$ group. The highest fragment ion observed in the mass spectrum of **5-3** occurred at *m/z* 438 can be attributed to the loss of a water molecule (under mass spectral conditions) from the expected molecule, $C_{30}H_{48}O_3$ (456 daltons). Other significant fragment ions observed for **5-3** are presented in Table 5-1 and Scheme 5-1.

Table 5-1. Selected mass spectral fragment ions observed for 22-hydroxyflavicano-25,3β-lactone (**5-3**).

ions	*m/z* (% relative intensities)
M^+	456 (not seen)
M^+-H_2O	438 (14)
M^+-H_2O-CH_3	423 (3)
M^+- H_2O-C_3H_7	395 (3)
M^+-H_2O-C_5H_9	369 (6)
M^+-H_2O-$C_{13}H_{19}O^+$	247 (5)
Ion b	203 (8)
ion a-CO	191 (30)
related fragment	190 (27)
ion c	189 (100)
related fragment	187 (11)
ion c- C_3H_6O	149 (23)
$C_3H_7O^+$ (ion d)	59 (84)

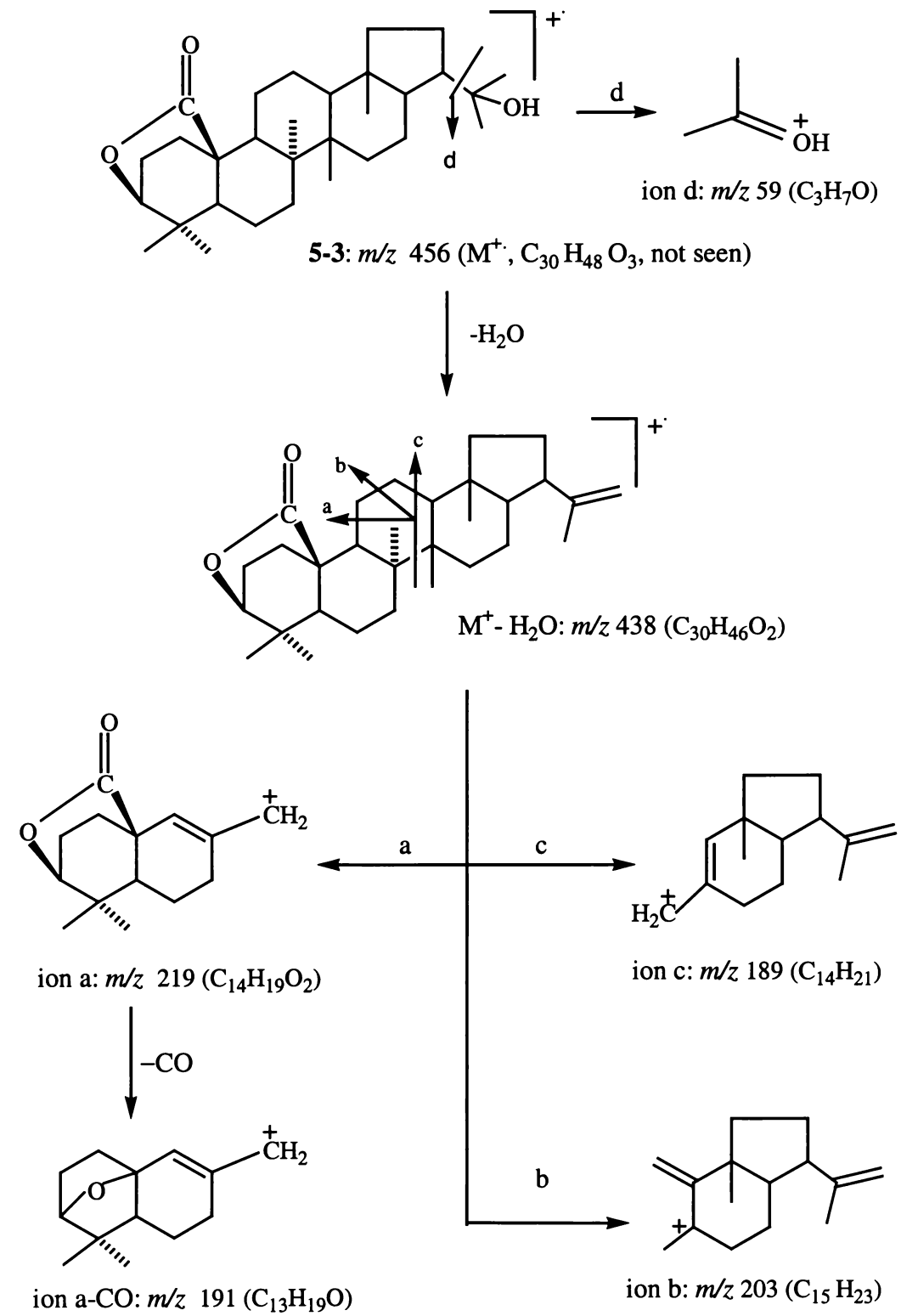

Scheme 5-1. Proposed mass spectral fragmentation pathways for 22-hydroxyflavicano-25,3β-lactone (**5-3**).

5.3.2 NMR Spectral Analyses of 22-Hydroxyflavicano-25,3β-lactone (5-3)

The complete assignment of the ^{13}C and ^{1}H NMR signals of **5-3**, presented in Table 5-2, was derived from detailed analyses of one- and two-dimensional NMR spectral data determined for this compound. Signal assignments can be compared with those established in a like manner for 22α-hydroxystictano-25,3β-lactone (**4-2**) (see Section **4.4** in Chapter Four) and for 21α-H-hopan-22-ol (**5-4**), as reported by Ageta *et al.* (1993, 1994) (see Table 4-2).

5.3.2.1 ^{1}H NMR Spectrum of 22-Hydroxyflavicano-25,3β-lactone (5-3)

The 400 MHz ^{1}H NMR spectrum of **5-3** included signals attributable to seven tertiary methyl groups in the region of 0.85~1.20 ppm (rather than the usual eight methyl groups encountered in sticane triterpenoids) and lowfield signals at 4.03 ppm (d, J = 4.6 Hz) and 2.58 ppm (dd, J = 12.4, 3.5 Hz). The methyl group signal which occurred at 0.71 ppm appeared as a finely split doublet (J = 0.9 Hz).

The signal that appeared at 2.58 ppm (dd, J = 12.4 and 3.5 Hz) was identified as the H-9β of **5-3** by comparison with the corresponding signal observed for **4-2**. The coupling constants exhibited by this proton were consistent with it experiencing a large $^{3}J_{ax\text{-}ax}$ (12.4 Hz) coupling with H-11α and a small $^{3}J_{ax\text{-}eq}$ (3.5 Hz) coupling with H-11β. The HMBC correlations exhibited by this signal validated the assignment to H-9β since it showed HMBC correlations to C-6 (25.8 ppm) C-8 (40.2 ppm), C-10 (45.1 ppm), C-11 (23.5ppm), C-14 (42.7 ppm) and C-25 (178.3 ppm) (see Table 5-3).

The signal at 4.03 ppm (d, J = 4.6 Hz) was readily assigned to the methine proton at C-3 since its chemical shift and couplings constants corresponded closely to those observed for the equivalent proton of **4-2**.

However, the 22a- and 22b-methyl groups (ie H-29 and H-30) (1.18 and 1.19 ppm) only showed HMBC correlations to two ring E carbons {ie C-21 (51.0 ppm) and C-22 (73.6 ppm)} rather than three ring E carbons as observed for **4-2** (see Section **4.4**). This observation was consistent with the HMBC correlation pattern exhibited by 22-hydroxyhopanoids (see Chapter Two and Chapter Three).

Table 5-2. ^{13}C and ^{1}H NMR signals (δ ppm in $CDCl_3$) observed for 21α-H-hopan-22-ol (**5-4**), 22-hydroxyflavicano-25,3β-lactone (**5-3**) and 22α-hydroxystictano-25,3β-lactone (**4-2**).

atom	21α-H-hopan-22-ol (5-4) *			22-hydroxyflavicano-25,3β-lactone (5-3)			22α-hydroxystictano-25,3β-lactone (4-2)		
	^{13}C	$^{1}H_\alpha$	$^{1}H_\beta$	^{13}C	$^{1}H_\alpha$	$^{1}H_\beta$	^{13}C	$^{1}H_\alpha$	$^{1}H_\beta$
1	40.31 t	0.77	1.44	24.0 t	1.53 d	1.30 t	24.0 t	1.53 d	1.29 d
2	18.69 t	1.37	1.55	20.2 t	~1.97 q (overlapped)		20.3 t	~1.98 q (overlapped)	
3	42.10 d	1.13	1.35	82.5 d	4.03 d		82.5 d	4.03 d	
4	33.25 s			38.3 s			38.3 s		
5	56.11 d	0.72		46.9 d	1.63 d		46.8 d	1.63 d	
6	18.69 t	1.47	1.34	25.8 t	1.87 t	1.63 q	25.8 t	1.86 ddd	1.63 q
7	33.25 t	1.21	1.46	33.2 t	0.94 t	1.98 d	32.7 t	0.97 d	1.98 d
8	41.87 s			40.2 s			40.4 s		
9	50.42 d	1.25		33.7 d	2.58 dd		33.5 d	2.58 dd	
10	37.39 s			45.1 s			45.0 s		
11	20.91 t	1.51	1.32	21.8 t[a]	1.47 d	1.02 d	20.9 t	1.55 t	1.46 d
12	23.80 t	1.45	1.38	23.5 t[a]	1.39 d	1.64 t	21.8 t	1.47 d	1.03 t
13	48.56 d	1.41		49.1 d	1.36 d		49.1 d	1.28 d	
14	41.72 s			42.7 s			42.3 s		
15	32.67 t	1.18	1.40	32.8 t	1.32 t	1.37 d	31.7 t	~1.37 (overlapped)	
16	23.21 t	1.38	1.77	23.0 t	1.79 d	1.38 q	19.3 t	1.75 dd	1.23 q
17	52.07 d	0.98		52.4 d	1.00 t		48.6 d	1.05 t	
18	44.90 s			45.2 s			38.6 s		
19	39.50 t	1.45	0.95	39.4 t	1.47 t	0.94 q	35.0 t	1.46 d	1.03 t
20	24.82 t	1.74	1.31	24.9 t	1.74 t	1.31 q	34.9 t	1.49 t	1.26 d
21	51.05 d	1.74		51.0 d	1.75 d		35.8 s		
22	73.62 s			73.6 s			76.5 d	3.17 d	
23	33.41 q	0.848		26.5 q	1.03 s		26.5 q	1.03 s	
24	21.60 q	0.793		20.3 q	0.87 s		20.3 q	0.87 s	
25	15.88 q	0.820		178.3 s			178.3 s		
26	16.73 q	0.977		22.4 q	1.11 s		22.2 q	1.11 s	
27	16.70 q	0.948		17.1 q	0.98 s		17.2 q	1.01 s	
28	15.37 q	0.693 d (*J*= 0.6Hz)		15.3 q	0.71 d (*J* = 0.9 Hz)		13.6 q	0.76 s	
29	29.45 q	1.184		29.6 q	1.18 s		29.9 q	0.87 s	
30	26.49 q	1.190		26.6 q	1.19 s		18.6 q	0.99 s	

* assignments reported by Ageta *et al.* (1993)

5.3.2.2 ^{13}C and DEPT135 NMR Spectra of 22-Hydroxyflavicano-25,3β-lactone (5-3)

The ^{13}C NMR spectrum of **5-3** exhibited a total of thirty signal resonances, which were identified by a DEPT135 NMR spectrum as arising from seven quartet (CH_3), ten

triplet (CH_2), six doublet (CH), and seven singlet (C) carbons. The ^{13}C NMR spectrum of **5-3** included signals attributable to a lactone system (178.3 ppm, -CHOC̲O-; 82.5 ppm, -C̲HOCO-) and a quaternary oxygenated carbon (73.6 ppm). The ^{13}C and DEPT135 NMR spectra were consistent with the molecular formula of **5-3** being $C_{30}H_{48}O_3$ (456 daltons) (see Section **5.3.1**).

The downfield signals at 178.3 ppm and 82.5 ppm were consistent with the presence of a lactone group and a hydroxyl group, respectively, and readily assigned to C-25 (a carbonyl carbon) and C-3 (an oxygenated carbon). Other ring A/B carbon resonances corresponded closely to those observed for **4-2** (see Table 5-2), while most signals attributable to rings C, D and E resembled those observed for **5-4** since there was an antipodal relationship between **5-3** and **5-4** (see Figure 5-1)

Consistent with the presence of a five-membered ring E system in **5-3**, the C-16 (23.0 ppm), C-17 (52.4 ppm), C-18 (45.2 ppm), C-20 (24.9 ppm), C-21 (51.0 ppm) and C-28 (15.3 ppm) resonances of **5-3** differed significantly from those observed for **4-2** (see Table 5-2).

The downfield quaternary carbon signal which appeared at 73.6 ppm was assigned to the oxygenated C-22 atom of the {-$C(CH_3)_2OH$} side chain. Comparisons with the chemical shifts determined for the C-22, C-28, C-29 and C-30 signals of 22-hydroxyhopan-7-one (**2-1**) (see Table 2-2, Chapter Two) indicated the {-$C(CH_3)_2OH$} side chain of the new flavicane (**5-3**) to be α-oriented. In particular the C-29 and C-30 resonances of 22-hydroxyhopan-7-one (**2-1**) occurred at 29.0 and 30.7 ppm respectively, whereas the C-29 and C-30 resonances of the new flavicane (**5-3**) occurred at 29.4 and 26.6 ppm respectively. It should be noted that rings D and E of 21α-H-hopane and flavicane triterpenes are antipodally related (see Figure 5-1), thus the chemical shifts of a 21α-oriented group in a flavicanoid should be compared with those of a 21β-oriented group in a 21α-H-hopanoid. The C-22, C-28, C-29 and C-30 resonances of 21α-H-hopan-22-ol (**5-4**) (73.62, 15.37, 29.45 and 26.49 ppm respectively) reported by Ageta *et al.* (1993, 1994) correspond to those observed for the new flavicane (**5-3**) (see Table 5-2).

5.3.2.3 HMBC and HSQC Spectra of 22-Hydroxyflavicano-25,3β-lactone (5-3)

Correlations observed in the HMBC and HSQC spectra facilitated the complete assignment of the ^{13}C and ^{1}H NMR signals of **5-3**. Selected HMBC correlations are presented in Table 5-3.

Table 5-3. ^{1}J, ^{2}J and ^{3}J heteronuclear ^{1}H-^{13}C correlations (δ ppm in $CDCl_3$) observed for 22-hydroxyflavicano-25,3β-lactone (**5-3**).

^{1}H signal	^{1}J correlated ^{13}C signal	^{2}J and ^{3}J correlated ^{13}C signals
1.03 s (4α-Me)	26.5 (C-23)	82.5 (C-3), 46.9 (C-5), 38.3 (C-4), 20.3 (C-24)
0.87 s (4β-Me)	20.3 (C-24)	82.5 (C-3), 46.9 (C-5), 38.3 (C-4), 26.5 (C-23)
1.11 s (8α-Me)	22.4 (C-26)	42.7 (C-14), 40.2 (C-8), 33.7 (C-9), 33.2 (C-7)
0.98 s (14β-Me)	17.2 (C-27)	49.1 (C-13), 42.7 (C-14), 40.2 (C-8), 32.8 (C-15)
0.71 s (18β-Me)	15.3 (C-28)	52.4 (C-17), 49.1 (C-13), 45.1 (C-18), 39.4 (C-19)
1.18 s (22a-Me)	29.6 (C-29)	73.6 (C-22), 51.0 (C-21), 26.5 (C-30)
1.19 s (22b-Me)	26.5 (C-30)	73.6 (C-22), 51.0 (C-21), 29.6 (C-29)
4.03 d (H-3α)	82.5 (C-3)	178.3 (C-25), 46.9 (C-5), 38.3 (C-4), 26.5 (C-23) 20.3 (C-24), 20.2 (C-2)
2.58 dd (H-9β)	33.7 (C-9)	178.3 (C-25), 45.1 (C-10), 42.7 (C-14), 40.2 (C-8) 25.8 (C-6), 23.5 (C-11)
1.75 d (H-21β)	51.0 (C-21)	73.6 (C-22), 52.4 (C-17), 29.6 (C-29), 26.5 (C-30), 23.0 (C-20)
1.63 d (H-5α)	46.9 (C-5)	45.1 (C-10), 38.3 (C-4), 33.2 (C-7), 26.5 (C-23) 25.8 (C-6), 20.3 (C-24)

Methyl group assignments

Assignments for the seven methyl groups of **5-3** were readily determined by comparison with those observed for **4-2** and **5-4** (see Table 5-2), and by analyses of HMBC and HSQC spectral data. Selected HMBC correlations (see Figure 5-4) observed for the methyl groups of **5-3** are depicted in Figure 5-3.

The ^{2}J HMBC correlations exhibited by the 4α- and 4β-methyl group protons of **5-3** corresponded closely with those observed for **4-2**, and were fully consistent with the presence of a ring A lactone group. The methyl group signals which appeared at 1.11, 0.98 and 0.71 ppm were assigned to 8α-, 14β- and 18β-methyl groups respectively by ^{2}J HMBC correlations to C-8 (40.2 ppm), C-14 (42.7 ppm) and C-18 (45.2 ppm)

quaternary carbons, respectively, and by the other ^3J HMBC correlations presented in Table 5-3. The modest upfield shift exhibited by the 18β-methyl group (0.71 ppm) of **5-3**, compared to the corresponding methyl group of **4-2** (0.76 ppm), was consistent with the α-orientation of the side-chain at C-21.

Methine proton assignments

The assignments of H-3α (4.03 ppm) and H-9β (2.58 ppm) were easily achieved by their HSQC correlations to the carbon signals occurred at 82.5 and 33.7 ppm respectively, while the HMBC correlations exhibited by both confirmed the above assignments (see Table 5-3). The four remaining methine protons of **5-3** were readily identified from a combination of HMBC (see Table 5-3) and HSQC spectral data (see Table 5-2).

Methylene proton assignments

The resonances of the ring A and B methylene protons of **5-3** were comparable to those determined for **4-2** while the resonances of the ring D and E methylene protons can be compared with those determined for **5-4**, since there is an antipodal relationship between the respective rings of **5-3** and **5-4** (see Figure 5-1 and Table 5-2).

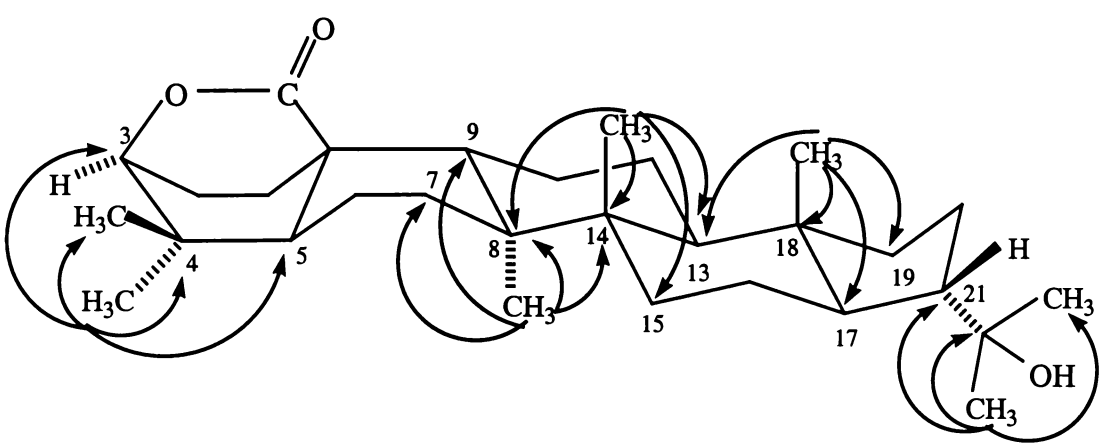

Figure 5-3. Selected HMBC correlations observed for the methyl groups of 22-hydroxyflavicano-25,3β-lactone (**5-3**).

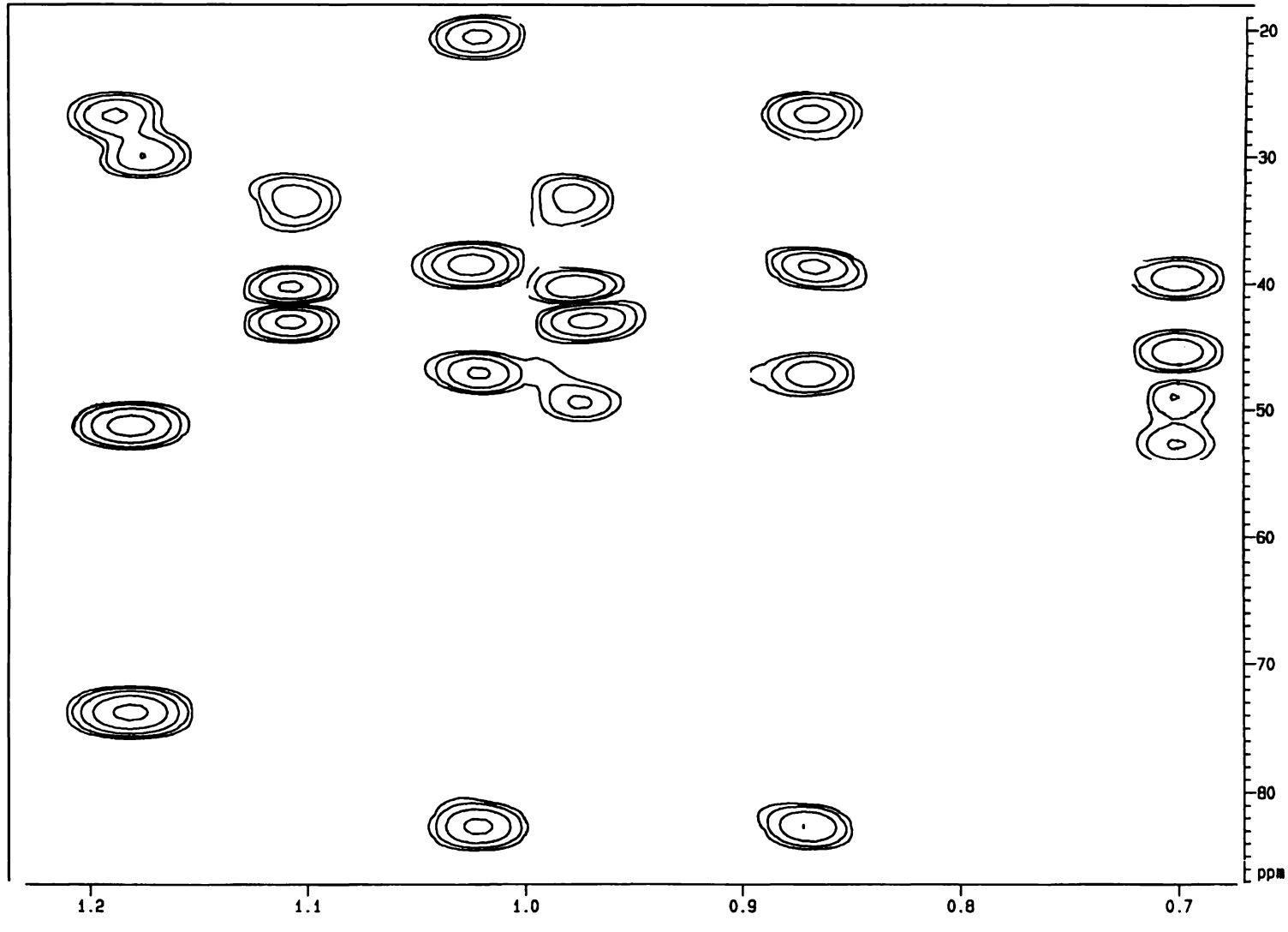

Figure 5-4. Selected HMBC correlations observed for the methyl groups of 22-hydroxyflavicano-25,3β-lactone (**5-3**).

5.3.2.4 NOE Data and Molecular Modelling Analyses of 22-Hydroxyflavicano-25,3β-lactone (5-3)

Structurally significant NOE responses observed for the methyl groups of **5-3** in NOE-difference experiments are presented in Table 5-4 and depicted in Figure 5-5.

Table 5-4. NOE effects (δ ppm in $CDCl_3$) observed for 22-hydroxyflavicano-25,3β-lactone (**5-3**).

irradiated ^{1}H signals	enhanced ^{1}H signals
1.03 s (4α-Me)	0.87 s (4α-Me), 4.03 d (H-3α), ~1.97 (H-2α/β), 1.63 d (H-5α)
0.87 s (4β-Me)	1.03 s (4α-Me), 4.03 d (H-3α)
1.11 s (8α-Me)	1.87 t (H-6α), 1.63 d (H-5α), 1.36 d (H-13α), 1.32 t /1.37 d (H-15α/β)
0.98 s (14β-Me)	0.71 d (18β-Me), 2.58 dd (H-9β), 1.64 t (H-12β)
0.71 d (18β-Me)	0.98 s (14β-Me), 1.75 d (H-21β), 1.64 t (H-12β), 1.47 t (H-19β), 1.38 q (H-16β)
1.18 s (22a-Me)	1.19 s (22b-Me), 1.75 d (H-21β), 1.38 q (H-20α), 1.00 t (H-17α)
1.19 s (22b-Me)	1.18 s (22a-Me), 1.75 d (H-21β), 1.38 q (H-20α), 1.00 t (H-17α)
2.58 dd (H-9β)	0.98 s (14β-Me), 1.98 d (H-7β), 1.63 q (H-6β), 1.02 d (H-11β)
4.03 d (H-3α)	1.03 s (4α- Me), 0.87 s (4α-Me), ~1.97 (H-2α/β)

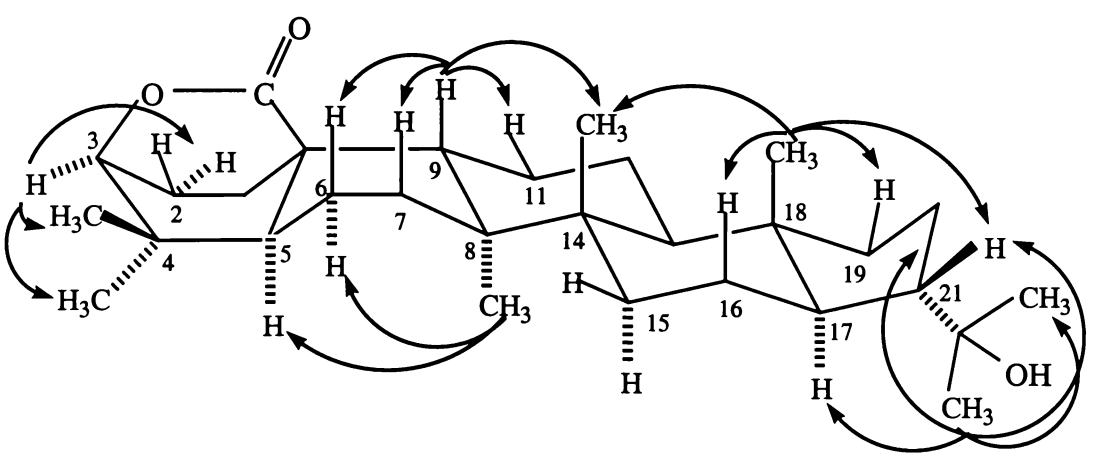

Figure 5-5. Selected NOE's observed for 22-hydroxyflavican-25,3β-lactone (**5-3**).

Irradiation of H-3α (4.03 ppm) enhanced H-2α/β (~1.98 ppm), and the 4α-methyl (1.03 ppm) and 4β-methyl (0.87 ppm) groups. Irradiation of H-9β (2.58 ppm) enhanced H-7β (1.98 ppm), H-6β (1.63 ppm), H-11β (1.02 ppm) and the 14β-methyl group (ie H-27) (0.98 ppm), while irradiation of the 18β-methyl group (ie H-28) (0.71 ppm) enhanced the 14β-methyl group (ie H-27) (0.98 ppm), H-12β (1.64 ppm), H-19β (1.47 ppm), H-16β (1.38 ppm) and H-21β (1.75 ppm). These observations showed that H-21β was β-oriented.

Figure 5-6. MM2 modelled structure of 22-hydroxyflavicano-25,3β-lactone (**5-3**).

Chapter Six

Experimental

6.1 General Experimental Methods

6.1.1 Chromatographic Methods

Gas Chromatography-Mass Spectrometry (GC/MS)

GC/MS was performed using a 25 m × 0.22 mm id × 0.3 μm film thickness HP-1 (methyl-silicone gum) capillary column installed in a Hewlett Packard 5980A gas chromatograph interfaced to an HP5970B mass-selective detector, operated in total ion chromatogram (TIC) mode (*m/z* 40 to 550). GC/MS analyses were typically temperature programmed from 200°C to 290°C (15 min. hold) at 15°C /min.

Thin Layer Chromatography (TLC)

TLC analyses were conducted on aluminum sheets coated with silica gel 60 F_{254} (Merck Art.5554). Plates were developed with mixtures of diethyl ether and light petroleum. Compounds were detected by spraying the developed plate with a 10% (w/v) ethanolic solution of *dodeca*-molybdophosphoric acid, and charring in an oven (*ca.* 100°C) for several minutes.

Preparative Layer Chromatography (PLC)

Preparative layer chromatography was conducted on silica gel $PF_{254+366}$ (Merck) layers coated on glass plates (40 × 20 × 0.4 cm). Samples were typically applied on to the

plates as concentrated chloroform solutions using a 2 mL syringe with a fine wool-brush attached to the tip of a shortened needle. The plates were developed by the ascending method using mixtures of hexane and diethyl ether, or benzene and hexane as the developing solvent, depending on the polarity of the compounds to be separated. Bands from the plates were scrapped from the plates and packed into the glass columns and eluted with diethyl ether.

Radial Preparative Layer Chromatography

Radial preparative layer chromatography was performed using a Chromatotron 7924T and a 22.5 cm diameter glass plate coated with 2 mm of silica gel $PF_{254+366}$ (Merck). Plates were activated overnight in an oven 60~80°C prior to use.

Column Chromatography

Column chromatography was performed on aluminum oxide (alumina) (BDH, Brockman Grade II), using combinations of light petroleum and diethyl ether as eluents, depending on the polarity of the compounds to be separated.

Column Chromatography with Silver Nitrate Impregnated Alumina

Silver nitrate impregnated aluminum oxide was prepared by dissolving silver nitrate (20 g) in water (*ca.* 15~20 mL), followed by the addition of methanol (150 mL) and aluminum oxide (200 g). After the removal of methanol and water by using a rotary evaporator and a flask covered with aluminum foil to exclude light. Silver nitrate impregnated aluminum oxide was activated overnight at 130°C.

6.1.2 Nuclear Magnetic Resonance (NMR) Experiments

One- and two-dimensional ^{1}H and ^{13}C NMR spectra were determined at 27°C using a Bruker AC-300 NMR spectrometer equipped with a standard 5 mm probe-head operating at 300.13 MHz for ^{1}H and 75.45 MHz for ^{13}C, or at 30°C using a Bruker DXR–400 NMR spectrometer fitted with a 5 mm inverse probe-head operating at

400.13 MHz for ^{1}H and 100.62 MHz for ^{13}C. Unless otherwise stated chemical shifts were obtained in $CDCl_3$ solutions and reported relative to internal $CDCl_3$ (δ 7.26 ppm for ^{1}H, and δ 77.06 ppm for ^{13}C).

Methylene, methine and methyl carbon resonances, designated as t (triplet), d (doublet) and q (quartet) carbons respectively, were identified using the DEPT135 sequence. Quaternary carbons (s, singlet carbons) were suppressed in DEPT135 NMR spectra.

Two-dimensional COSY, long-range COSY (LRCOSY), double quantum filtered COSY (DQFCOSY) and inverse mode heteronuclear multiple-bond correlated (HMBC) spectra were determined in absolute value mode. NOESY, ROESY, and ^{1}J ^{13}C-^{1}H correlated inverse mode HMQC (or HSQC) spectra were determined in phase-sensitive mode. Typical NMR data acquisition and processing conditions are given below.

^{1}H NMR Spectra

400 MHz ^{1}H NMR spectra were typically acquired using the following conditions: SW (sweep width) = 5593 Hz (14 ppm), 90° pulse, SI (size of real spectrum) = 32 K, TD (Time Domain points) = 32 K, D1 (relaxation delay) = 1.0 s, Acq (acquisition time) = 2.7 s, LB (line broadening factor) = 0.

NOE-difference Spectra

NOE-difference experiments were performed with SI = TD = 16 K, SW = 5593 Hz, LB = 0.5 Hz, D1 = 1 s, an irradiation power level (PI14) of 85 to 92 db (for multiplets and methyl groups respectively), an irradiation time of 3.2 s, and sequential irradiation of each line of selected signals, or multiplets, repeated cycles of the complete set of NOE experiments, followed by subtraction of a control FID from the FID determined for an irradiated signal, and Fourier transformation of the resulting difference FID.

^{13}C NMR Spectra

100 MHz ^{13}C NMR spectra were typically acquired using the following conditions: SW = 24691 Hz, 70° pulse, SI = TD = 32 K, AQ= 1.34 s, D1 = 1.0 s and Fourier transformed with LB = 2.

DEPT135 Spectra

100 MHz DEPT135 NMR spectra were typically acquired using the following conditions: SW = 24691 Hz, 70° pulse, SI = TD = 32 K, AQ= 1.34 s, D1 = 1.0 s, D2 =1/2*J* = 3.8 ms and Fourier transformed with LB = 2.

COSY Spectra

400 MHz COSY spectra were typically acquired using the following conditions: SW1 = SW2 = 2688 Hz, SI1 = SI2 = 1 K, TD1 = 256, TD2 = 1 K, AQ= 0.19 s, D1 = 1.0 s., and processed with MC1 = QF, SSB1 = SSB2 = 0, WDW1 = WDW2 = SINE.

HMBC Spectra

Gradient selected inverse mode 400 MHz HMBC spectra were typically acquired using the following conditions: SW1 = 19118 Hz, SW2 = 2723 Hz, SI1 = SI2 = 1 K, TD1 = 160, TD2 = 1 K, AQ = 0.18 s., D1 = 1 s., D2 = 1/2*J* =3.8 ms, D6 (mixing time) = 80 ms, and processed with MC2 = QF, SSB1 = SSB2 = 0, WDW1 = WDW2 = SINE.

HSQC and HMQC Spectra

Gradient selected inverse mode 400 MHz HSQC or HMQC spectra were typically acquired using the following conditions: SW1 = 15092 Hz, SW2 = 2723 Hz, SI1 = SI2 = 1 K, TD1 = 400, TD2 = 1 K, Acq = 0.18 s, D1 = 1 s, D2 = 1/2*J* = 3.8 ms, and processed with MC2 = TPPI, SSB1 = SSB2 = 2, WDW1 = WDW2 = QSINE.

NOESY Spectra

Phase sensitive 400 MHz NOESY spectra were typically acquired using the following conditions: SW1 = SW2 = 2874 Hz, SI1 = SI2 = 1 K, TD1 = 400, TD2 = 1 K, AQ = 0.178 s, D1 = 1.0 s, D9 (mixing time) = 0.7 s, and processed with MC2 = TPPI, SSB1 = SSB2 = 2, WDW1 = WDW2 = QSINE.

ROSEY Spectra

400 MHz ROESY spectra were typically acquired using the following conditions: SW1 = SW2 = 5594 Hz (with the spectral window centred *ca.* 1 ppm upfield, or downfield of signals of interest), SI1 = SI2 = 1 K, TD1 = 400 (or 512), TD2 = 2 K, AQ = 0.18 s, D1 = 1.0 s, P15 (spinlock time) = 250 ms, with PL1 =3 db and processed with MC2 = TPPI, SSB1 = SSB2 = 2 and WDW1 = WDW2 = QSINE.

6.1.3 Photochemical Reactions of Triterpenoids

Photochemical reactions were carried out using a Hanovia 125 W medium pressure mercury lamp at room temperature and a Pyrex tube, or a quartz tube, as the photochemical reaction chamber. The progress of photochemical reactions was monitored by GC/MS analyses of subsamples taken from the reaction chamber (tube). Reactions were continued, either until no starting material remained, or until no significant reaction progress was observed. Anhydrous benzene, benzene-methanol, or benzene-isopropanol was used as the solvent for photochemical reactions. Preliminary experiments were also performed using 22-hydroxyhopan-7-one (**2-1**) and tetrahydrofuran (THF) and dioxane as the solvent, however yields were lower, and reaction times were longer, than was the case for benzene.

6.1.4 Hydrogenation Procedure

Hydrogenation reactions were carried out at 50~60 psi using a series 3910 Parr hydrogenator (shaker-type) and a thick walled 250 mL glass. Compounds to be hydrogenated were dissolved in ethyl acetate, and shaken in a hydrogen atmosphere in the presence of platinum or palladium catalysts.

6.1.5 Melting Point Determinations

Melting points were determined on a Reichert Thermopan melting-point instrument or on an Olympus model ST microscope.

6.1.6 Work-up Procedures

Unless otherwise stated, the term " work-up" refers to the following steps:

- dilution of the reaction mixture with approximately five volumes of water.
- extraction with two portions of chloroform.
- filtration of the chloroform extracts through an alumina column to remove any residual water, trace acid and other inorganic residues
- rotary evaporation to remove solvent(s) using a Buchi RE111 rotovap.

6.1.7 Molecular Modelling

Molecular modelling investigations were carried out using MacroModel (version 4.5) (August 1994, Department of Chemistry, Columbia University, New York, USA) and Chem3D plus (version 3.5) software (CambridgeSoft Corporation, Cambridge, Massachusetts, USA) and MM2 parameter sets, running on Macintosh computers. Global minima was recognised using MacroModel software, and subsequently atom coordinates and graphical representations were refined using Chem3D plus software.

6.2 Experimental: Chapter Two

6.2.1 Preparation of 22-Hydroxyhopan-7-one and Derivatives

Extraction of *Pseudocyphellaria homeophylla*

The dry, finely ground lichen material (854 g) was extracted with light petroleum in a Soxhlet apparatus for 72 h. Evaporation of the solvent afforded a mixture of extractives (37.7 g) which was shown by TLC analysis to consist mainly of 7β-acetoxyhopan-22-ol (**2-4**) and hopane-15α,22-diol (**3-4**).

Separation of 7β-Acetoxyhopan-22-ol (2-4) and Hopane-15α,22-diol (3-4)

Separation of the extract (19.5 g) was performed by column chromatography on alumina (500 g). Elution with light petroleum:diethyl ether (2:1) afforded 7β-acetoxyhopan-22-ol (**2-4**) (9.8 g), m.p. 246-247°C (lit. m.p. 247-248°C, Corbett & Young, 1966a). Elution with diethyl ether gave hopane-15α,22-diol (**3-4**) (6.6 g), m.p. 247-248°C (lit. m.p. 249°C, Corbett & Young, 1966b). Both of these compounds exhibited ^{1}H NMR spectral data identical to that reported by Corbett & Young (1966a, 1966b).

Reduction of 7β-Acetoxyhopan-22-ol (2-4)

Lithium aluminum hydride (LAH) (7 g) was carefully added to a solution of 7β-acetoxyhopan-22-ol (**2-4**) (9.8 g) in dry diethyl ether (50 mL). A volume of tetrahydrofuran (THF), sufficient to dissolve all of the starting material (*ca.* 20 drops) was also added. The solution was refluxed until TLC analyses showed that the reaction was complete (*ca.* 6 h). Excess LAH was destroyed by the careful addition of water *via* the condenser, until the resulting vigorous reaction ceased and a grey precipitate was formed. Hydrochloric acid (2 M) was added, with gently shaking, until the precipitate dissolved, and the mixture was worked-up in the usual way to afford hopane-7β,22-diol (**2-5**) (6.1 g), m.p. 225-258°C (lit. m.p. 229°C, Corbett & Young, 1966a); ^{1}H NMR (δ ppm, $CDCl_3$): 0.77 (3H, s, H-24), 0.81 (3×3H, s, H-23, H-25 and H-28), 0.88 (3H, s, H-26), 1.00, 1.05 (3H, s, H-27), 1.18 (3H, s, H-29), 1.20 (3H, s, H-30), 3.90 (1H, dd, H-7α). This data corresponded to that reported for this compound by Corbett & Young (1966a).

Preparation of 22-Hydroxyhopan-7-one (2-1)

Hopane-7β,22-diol (**2-5**) (5.95 g) was dissolved in dry pyridine (120 mL) and chromium trioxide (3 g) was added slowly with stirring. The reaction mixture was stirred at room temperature for 24 h, after which it was poured into water (700 mL) and extracted with chloroform (2×150 mL). The combined chloroform extracts were washed with 1M hydrochloric acid (30 mL), and dried over anhydrous sodium sulphate.

Removal of solvent using a rotary evaporator afforded 22-hydroxyhopan-7-one (**2-1**) (5.33 g), m.p. 254-255°C (lit. m.p. 256°C, Corbett & Young, 1966a); ^{1}H NMR (δ ppm, $CDCl_3$): 0.72 (3H, s, H-28), 0.77 (3H, s, H-24), 0.80 (3H, s, H-23), 0.96 (3H, s, H-25), 1.01 (3H, s, H-27), 1.14 (3H, s, H-29), 1.16 (3H, s, H-26), 1.18 (3H, s, H-30); ^{13}C NMR (δ ppm, $CDCl_3$): 15.6 (C-25), 15.8 (C-26), 16.0 (C-28), 18.4 (C-2), 19.8 (C-27), 20.6 (C-11), 20.7 (C-24), 22.2 (C-16), 24.6 (C-12), 26.2 (C-20), 29.0 (C-29), 30.7 (C-30), 32.5 (C-23), 33.3 (C-4), 35.7 (C-15), 37.5 (C-10), 37.8 (C-6), 40.3 (C-1), 41.3 (C-19), 41.6 (C-3), 42.5 (C-14), 44.5 (C-18), 51.1 (C-21), 51.4 (C-13), 52.9 (C-9), 53.9 (C-5), 58.3 (C-8), 54.0 (C-17), 73.6 (C-22), 215.2 (C-7).

Preparation of Hop-22(29)-en-7-one (2-3)

A solution of 22-hydroxyhopan-7-one (**2-1**) (200 mg) in pyridine (20 mL) was stirred with phosphorous oxychloride (1.3 mL) for 24 h at room temperature and worked-up in the usual way to afford a mixture which consisted mainly of hop-21-en-7-one and hop-22(29)-en-7-one (**2-3**). The separation of the mixture using a silver nitrate impregnated alumina column (20 g) and mixtures of light petroleum and diethyl ether as eluents, afforded hop-21-en-7-one (89 mg) (first eluting component) and hop-22(29)-en-7-one (**2-3**) (64 mg) (second eluting component).

Hop-21-en-7-one, had m.p.197-199°C (lit. m.p.198-200°C, Corbett & Young, 1966a;); ^{13}C NMR (δ ppm, $CDCl_3$): 14.6 (C-28), 15.7 (C-25), 15.7 (C-27), 18.4 (C-2), 19.4 (C-26), 19.4 (C-29), 20.6 (C-11), 20.9 (C-24), 22.6 (C-30), 23.5 (C-16), 24.1 (C-12), 28.0 (C-20), 32.6 (C-23), 33.3 (C-4), 34.1 (C-15), 37.5 (C-10), 37.8 (C-6), 39.1 (C-19), 40.3 (C-1), 41.6 (C-3), 42.1 (C-14), 44.5 (C-18), 49.7 (C-13), 52.9 (C-5), 53.9 (C-9), 56.0 (C-17), 58.2 (C-8), 120.6 (C-22), 135.5 (C-21), 215.3 (C-7); MS (70 eV): 424 (M^+, $C_{30}H_{48}O$) (42%), 409 (19), 381 (100), 355 (79), 234 (13), 220 (37), 205 (21), 189 (66), 161 (26), 121 (63), 81 (37), 55 (45).

Hop-22(29)-en-7-one (**2-3**), had m.p.: 200~201°C (lit. m.p. 201-202°C, Smith, 1968); ^{1}H NMR (δ ppm, $CDCl_3$):): 0.76 (3H, s, H-24), 0.81 (3H, s, H-23), 0.96 (3H, s, H-25), 1.02 (3H, s, H-28), 1.05 (3H, s, H-27), 1.20 (3H, s, H-26), 1.75 (3H, s, H-30), 4.78 (2H, d, J = 0.80 Hz, H-29); ^{13}C NMR (δ ppm, $CDCl_3$) 15.7 (C-27), 15.8 (C-25), 15.9 (C-28),

18.4 (C-2), 19.4 (C-26), 20.7 (C-11), 20.9 (C-24), 22.0 (C-16), 24.5(C-12), 25.1 (C-30), 26.9 (C-20), 32.6 (C-231), 33.4 (C-4), 34.9 (C-15), 37.6 (C-10), 37.9 (C-6), 40.3 (C-1), 41.6 (C-19), 41.9 (C-3), 42.7 (C-14), 45.3 (C-18), 46.5 (C-21), 51.0 (C-13), 52.9 (C-5), 53.9 (C-9), 55.0 (C-17), 58.3 (C-8), 110.0 (C-29), 148.5 (C-22), 215.3 (C-7). These ^{13}C signal assignments corresponded to those reported by Bird (1984); MS (70 eV): 424 (M^+, $C_{30}H_{48}O$) (26%), 355 (8), 313 (26), 234 (21), 220 (92), 205 (32), 189 (100), 161(18), 109 (42), 81 (39), 55 (37).

Preparation of 7,8-Secohopane-7,22-diol (2-6)

A solution of methyl 22-hydroxy-7,8-secohopan-7-oate (**2-2**) (20 mg) in dry tetrahydrofuran (THF) (50 mL) was refluxed with LAH (250 mg) (carefully added over 10 min *via* the condenser) for 3 h.. Work-up and purification of the product by radial PLC with mixtures of light petroleum and diethyl ether as eluents, afforded 7,8-secohopane-7,22-diol (**2-6**) (16 mg) as an oil; ^1H NMR (δ ppm, $CDCl_3$): 0.74 (3H, s, H-28), 0.83 (3H, d, J = 6.9 Hz, H-26); 0.85 (3H, s, H-23), 0.87 (3H, s, H-25), 0.94 (3H, s, H-24), 1.02 (3H, s, H-27), 1.17 (3H, s, 22a-Me), 1.21 (3H, s, 22b-Me), 3.57 (2H, t, J = 8.0 Hz, 7-C$\underline{H_2}$OH); ^{13}C NMR (δ ppm, $CDCl_3$): 10.7 (C-26), 16.2 (C-28), 17.4 (C-25), 18.6 (C-2), 21.9 (C-11), 22.1 (C-16), 22.6 (C-24), 24.9 (C-12), 25.3 (C-27), 26.6 (C-20), 28.8 (C-29), 30.8 (C-30), 31.6 (C-6), 34.1 (C-1), 34.6 (C-23), 35.1 (C-4), 39.1 (C-15), 39.3 (C-14), 39.6 (C-9), 40.0 (C-10), 40.7 (C-19), 41.9 (C-3), 44.1 (C-18), 44.2 (C-8), 46.6 (C-5), 49.8 (C-13), 51.0 (C-21), 54.7 (C-17), 65.8 (C-7), 74.0 (C-22), ; MS (70 eV): 446 (M^+, $C_{30}H_{54}O_2$, not seen), 428 (4 %), 413 (10), 385 (6), 359 (9), 317 (5), 259 (25), 217 (20), 169 (21), 151 (35), 123 (23), 121 (38.5), 69 (100), 59 (11). Found: *m/z* 428.4040; $C_{30}H_{52}O$ (M^+-H_2O) requires *m/z* 428.4018.

6.2.2 Photochemical Reactions of 22-Hydroxyhopan-7-one and Hop-22(29)-en-7-one

Photolysis of 22-Hydroxyhopan-7-one (2-1) in Benzene-Methanol

A solution of 22-hydroxyhopan-7-one (**2-1**) (80 mg) in dry benzene-methanol (1:1, 20 mL) was irradiated by using a Hanovia 125 W medium pressure mercury lamp at

room temperature. The progress of the reaction was monitored by GC/MS analyses of subsamples taken from the reaction mixture. The reaction was continued until no starting material remained (4 h). Removal of the solvent under reduced pressure afforded a material which when separated by PLC on silica gel with light petroleum:diethyl ether (1:1) as eluent gave methyl 22-hydroxy-7,8-secohopan-7-oate (**2-2**) (35 mg) as a gum, ^{1}H NMR (δ ppm, $CDCl_3$): 0.72 (3H, s, H-28), 0.84 (3H, d, J = 6.9 Hz, H-26), 0.85 (3H, s, H-23), 0.87 (3H, s, H-25), 0.91 (3H,s, H-24), 0.94 (3H, s, H-27), 1.18 (3H, s, 22a-Me), 1.21 (3H, s, 22b-Me), 3.70 (3H, s, 7-COOC$\underline{H}_3$); ^{13}C NMR (δ ppm, $CDCl_3$): 10.8 (C-26), 16.2 (C-28), 17.8 (C-25), 18.6 (C-2), 22.1 (C-11), 22.2 (C-16), 22.8 (C-24), 25.0 (C-12), 25.2 (C-27), 26.6 (C-20), 28.9 (C-29), 30.9 (C-30), 32.6 (C-6), 34.0 (C-23), 34.2 (C-1), 35.1 (C-4), 39.2 (C-15), 39.3 (C-14), 40.0 (C-10), 40.7 (C-9), 40.8 (C-19), 41.7 (C-3), 44.1 (C-8), 44.1 (C-18), 46.5 (C-5), 49.8 (C-13), 51.1 (C-21), 51.6 (7-COO$\underline{C}H_3$), 54.7 (C-17), 74.0 (C-22), 175.5 (C-7); MS (70 eV): 474 (M^+, $C_{31}H_{54}O_3$, not seen), 456 (37%), 441 (11), 413 (39), 387 (8), 345 (21), 259 (32), 197 (100), 123 (84), 121(66), 69 (45), 59 (34). Found: *m/z* 456.3983; $C_{31}H_{52}O_2$ (M^+-H_2O) requires *m/z* 456.3967.

Photolysis of 22-Hydroxyhopan-7-one (2-1) in Benzene

Photolysis of 22-hydroxyhopan-7-one (**2-1**) (60 mg) in benzene (20 mL) for 9 h, and again for 16 h, afforded product material which was shown by GC/MS analyses to be comprised mainly of starting material (**2-1**), two minor products (products 1 and 2), and a number of other components believed to be dehydrated analogues of the starting material (**2-1**) (see Section **2.3.1**). Because of the low yield of photolysed products, and the difficulties experienced when attempting to separate the product mixture, efforts to isolate the proposed products were abandoned.

Photolysis of 22-Hydroxyhopan-7-one (2-1) in Benzene-Isopropanol

A solution of 22-hydroxyhopan-7-one (**2-1**) (60 mg) in benzene-isopropanol (1:1, 20 mL) was photolysed for 8 h. Work-up using aqueous $NaHCO_3$ rather than water (in order to prevent the possible dehydration of the photochemical product in the presence of trace acids in solvents used during the usual work-up procedure) gave product

material which was purified using radial PLC on silica gel with light petroleum:diethyl ether (3:2) to afford isopropyl 22-hydroxy-7,8-secohopan-7-oate (**2-8**) (12 mg), m.p.133-135°C; ^{1}H NMR (δ ppm,$CDCl_3$): 0.72 (3H, s, H-28), 0.84 (3H, s, H-25), 0.84 (3H, d, *J* = 6.9 Hz, H-26), 0.85 (3H, s, H-23), 0.93 (3H, s, H-24), 0.97 (3H, s, H-27), 1.18 (3H, s, 22a-Me), 1.21 (3H, s, 22b-Me), 1.23/1.25 {3H/3H, d, *J* = 6.3 Hz, 7-COOCH($C\underline{H}_3$)$_2$}, 5.00 {1H, m, 7-COO$C\underline{H}$(CH_3)$_2$}; ^{13}C NMR (δ ppm, $CDCl_3$): 10.7 (C-26), 16.2 (C-28), 17.7 (C-25), 18.6 (C-2), 21.9 {7-COOCH($\underline{C}H_3$)$_2$}, 22.2 (C-16), 22.3 (C-11), 22.7 (C-24), 25.1 (C-12), 25.3 (C-27), 26.6 (C-20), 28.9 (C-29), 30.9 (C-30), 33.4 (C-6), 33.9 (C-23), 34.2 (C-1), 35.1 (C-4), 39.1 (C-15), 39.3 (C-14), 39.8 (C-10), 40.5 (C-9), 40.7 (C-19), 41.7 (C-3), 44.1 (C-8), 44.1 (C-18), 46.1 (C-5), 49.8 (C-13), 51.1 (C-21), 54.7 (C-17), 67.6 {7-COO$\underline{C}$H(CH_3)$_2$}, 74.0 (C-22), 174.5 (C-7); ^{1}H NMR (δ ppm, C_6D_5N): 0.90 (3H, s, H-25), 0.90 (3H, d, *J* = 6.9 Hz, H-26), 0.95 (3H, s, H-23), 0.96 (3H, s, H-28), 1.00 (3H, s, H-24), 1.12 (3H, s, H-27), 1.25/1.27 {3H/3H, d, *J* = 6.3 Hz, 7-COOCH($C\underline{H}_3$)$_2$}, 1.36 (3H, s, 22a-Me), 1.43 (3H, s, 22b-Me), 5.15 {1H, m, 7-COO$C\underline{H}$(CH_3)$_2$}; ^{13}C NMR (δ ppm, C_5D_5N): 11.0 (C-26), 16.5 (C-28), 17.9 (C-25), 18.9 (C-2), 22.0 {7-COOCH($\underline{C}H_3$)$_2$}, 22.6 (C-16), 22.7 (C-11), 22.8 (C-24), 25.5 (C-12), 25.7 (C-27), 27.0 (C-20), 30.0 (C-29), 31.5 (C-30), 33.6 (C-6), 34.1 (C-23), 34.5 (C-1), 35.2 (C-4), 39.5 (C-15), 39.7 (C-10), 40.1 (C-14), 40.8 (C-9), 41.3 (C-19), 42.0 (C-3), 44.5 (C-8), 44.5 (C-18), 46.4 (C-5), 50.2 (C-13), 51.5 (C-21), 55.4 (C-17), 67.7 {7-COO$\underline{C}$H(CH_3)$_2$}, 72.5 (C-22), 174.4 (C-7); MS (70 eV): 502 (M^+, $C_{33}H_{58}O_3$, not seen), 484 (22%), 441 (17), 415 (4), 373 (17), 281 (4), 259 (22), 225 (26), 183 (100), 123 (65), 69 (48), 59 (30).

Photolysis of Hop-22(29)-en-7-one (2-3) in Benzene-Methanol

Photolysis of hop-22(29)-en-7-one (**2-3**) (50 mg) in dry benzene-methanol (1:1, 20 ml), followed by purification of the product by radial PLC on silica gel using mixtures of light petroleum and diethyl ether as eluents, afforded methyl 7,8-secohop-22(29)-en-7-oate (**2-9**) (14 mg) as an oil, ^{1}H NMR (δ ppm, $CDCl_3$): 0.67 (3H, d, *J* = 0.53 Hz, H-28), 0.83 (3H, d, *J* = 7.0 Hz, H-26), 0.85 (3H, s, H-25), 0.86 (3H. s, H-23), 0.90 (3H, s, H-24), 0.91 (3H, s, H-27), 1.76 (3H, s, H-30), 4.77 (2H, d, *J* = 0.84 Hz, H-29), 3.70 (3H, s, 7-$COOCH_3$); ^{13}C NMR (δ ppm, $CDCl_3$): 10.7 (C-26), 16.1 (C-28), 17.7 (C-25), 18.6 (C-2), 21.9 (C-16), 22.1 (C-11), 22.7 (C-24), 24.7 (C-12), 24.8 (C-27),

25.0 (C-30), 27.4 (C-20), 32.6 (C-6), 34.0 (C-23), 34.2 (C-1), 35.0 (C-4), 38.4 (C-15), 39.4 (C-14), 40.0 (C-10), 40.7 (C-9), 41.3 (C-19), 41.7 (C-3), 44.1 (C-8), 44.8 (C-18), 46.4 (C-21), 46.5 (C-5), 49.4 (C-13), 51.5 (7-COO$\underline{C}H_3$), 55.6 (C-17), 110.1 (C-29), 148.7 (C-22), 175.4 (C-7); MS (70 eV): 456 (M^+, $C_{31}H_{52}O_2$) (10 %,) 387 (3), 345 (29), 259 (34), 198 (21), 197 (100), 123 (89), 69 (58). Found: *m/z* 456.4004; $C_{31}H_{52}O_2$ (M^+-H_2O) requires *m/z* 456.3967.

6.3 Experimental: Chapter Three

6.3.1 Preparation of 22-Hydroxyhopan-15-one and Its Derivatives

Preparation of 22-Hydroxyhopan-15-one (3-1)

Chromium trioxide (5 g) was added slowly with stirring into a solution of hopane-15α,22-diol (**3-4**) (3.25 g) dissolved in anhydrous pyridine (60 mL). The solution was stirred at room temperature for 24 h, and worked-up in the usual way to afford 22-hydroxyhopan-15-one (**3-1**) (3.09 g), m.p. 278-280°C (lit. m.p. 279-280°C, Corbett & Young, 1966b); ^{1}H NMR (δ ppm, $CDCl_3$): 0.75 (3H, s, H-24), 0.77 (3H, s, H-25), 0.80 (3H, s, H-23), 0.91 (3H, s, H-28), 1.00 (3H, s, H-26), 1.12 (3H, s, H-29), 1.14 (3H, s, H-27), 1.16 (3H, s, H-30); ^{13}C NMR (δ ppm, $CDCl_3$): 15.5 (C-27), 15.9 (C-25), 16.0 (C-28), 18.8 (C-2), 18.8 (C-6), 19.4 (C-26), 21.4 (C-11), 21.6 (C-24), 24.0 (C-12), 26.9 (C-20), 29.1 (C-29), 31.1 (C-30), 33.2 (C-4), 33.4 (C-23), 34.3 (C-7), 38.2 (C-10), 40.4 (C-1), 40.8 (C-19), 41.3 (C-16), 42.0 (C-3), 43.1 (C-8), 44.1 (C-18), 50.1 (C-21), 50.6 (C-13), 51.0 (C-17), 51.8 (C-9), 56.4 (C-5), 57.2 (C-14), 73.3 (C-22), 214.8 (C-15),

Preparation of Hop-21-en-15-one (3-8) and Hop-22(29)-en-15-one (3-9)

A solution of 22-hydroxyhopan-15-one (**3-1**) (2 g) in anhydrous pyridine (100 mL) was stirred with phosphorous oxychloride ($POCl_3$) (5 mL) for overnight at room temperature, and worked-up in the usual way to afford a mixture which mainly consisted of hop-21-en-15-one (**3-8**) and hop-22(29)-en-15-one (**3-9**). The separation of the mixture was performed using a silver nitrate impregnated alumina column (50 g)

and mixtures of light petroleum and diethyl ether as eluents. Elution with light petroleum:diethyl ether (20:1~10:1) afforded hop-21-en-15-one (**3-8**) (0.95 g), and further elution with light petroleum:diethyl ether (5:1) gave hop-22(29)-en-15-one (**3-9**) (0.58 g).

Hop-21-en-15-one (**3-8**), had m.p. 219-221°C (lit. m.p. 220°C, Smith, 1968); ^{1}H NMR (δ ppm, $CDCl_3$): 0.80 (3H, s, H-24), 0.82 (3H, s, H-25), 0.85 (3H, s, H-23), 0.87 (3H, s, H-28), 1.06 (3H, s, H-26), 1.22 (3H, s, H-27), 1.58 (3H, s, 22b-Me), 1.66 (3H, s, 22a-Me); ^{13}C NMR (δ ppm, $CDCl_3$): 14.5 (C-28), 15.7 (C-27), 15.9 (C-25), 18.8 (C-2), 18.8 (C-6), 19.4 (C-29), 19.5 (C-26), 21.4 (C-11), 21.6 (C-24), 22.9 (C-30), 23.4 (C-12), 28.8 (C-20), 33.3 (C-4), 33.4 (C-23), 34.3 (C-7), 38.2 (C-10), 38.6 (C-19), 40.5 (C-1), 42.0 (C-3), 42.8 (C-16), 43.1 (C-8), 44.3 (C-18), 48.8 (C-13), 51.8 (C-9), 53.5 (C-17), 56.5 (C-5), 56.7 (C-14), 122.4 (C-22), 133.4 (C-21), 215.4 (C-15); MS (70 eV): *m/z* 424 (M^+, $C_{30}H_{48}O$) (69%), 409 (31), 381 (14), 355 (8), 342 (16), 281 (14), 271 (14), 231 (47), 218 (17), 207 (25), 205 (20), 204 (27), 203 (100), 191 (80), 149 (16), 121 (52), 95 (44), 81 (52), 69 (53).

Hop-22(29)-en-15-one (**3-9**) had m.p. 202-205°C (lit. m.p. 206°C, Smith, 1968); ^{1}H NMR (δ ppm, $CDCl_3$): 0.79 (3H, s, H-24), 0.81 (3H, d, J = 0.6 Hz, H-25), 0.84 (3H, s, H-23), 0.92 (3H, d, J = 0.8 Hz, H-28), 1.04 (3H, s, H-26), 1.17 (3H, s, H-27), 1.71 (3H, s, H-30), 4.80 (1H, br s, H-29b), 4.86 (1H, br s, H-29a); ^{13}C NMR (δ ppm, $CDCl_3$): 15.4 (C-27), 15.9 (C-25), 15.9 (C-28), 18.8 (C-2), 18.8 (C-6), 19.3 (C-26), 21.4 (C-11), 21.6 (C-24), 23.9 (C-12), 25.0 (C-30), 27.8 (C-20), 33.3 (C-4), 33.4 (C-23), 34.2 (C-7), 38.2 (C-10), 40.4 (C-1), 40.8 (C-19), 41.4(C-16), 42.0 (C-3), 43.0 (C-8), 44.7 (C-18), 45.5 (C-21), 50.3 (C-13), 51.8 (C-9), 52.0 (C-17), 56.4 (C-5), 56.5 (C-14), 111.5 (C-29), 146.8 (C-22), 215.4 (C-15); MS (70 eV): *m/z* 424 (M^+, $C_{30}H_{48}O$) (72%), 409 (14), 400 (5), 357 (3), 342 (3), 283 (3), 271 (12.5), 231 (67), 218 (23), 205 (19), 204 (12.5), 203 (28), 191 (100), 149 (19), 123 (55), 95 (47), 81 (53), 69 (47).

Hydrogenation of Hop-21-en-15-one (3-8)

A solution of hop-21-en-15-one (**3-8**) (300 mg) in ethyl acetate (150 mL) was hydrogenated over Adam's catalyst (after it had been reduced to Pt) for 6 days under 60

psi. Filtration of the catalyst and removal of the solvent under reduced pressure afforded the corresponding hydrogenation product 21α-H-hopan-15-one (**3-11**) (252 mg), m.p. 202-204°C (lit. m.p. 204~206°C, Smith, 1968); ^{1}H NMR (δ ppm, $CDCl_3$): 0.79 (3H, s, H-24), 0.79 (3H, d, *J* = 6.6 Hz, 22a-Me), 0.82 (3H, d, *J* = 0.8 Hz, H-25), 0.85 (3H, s, H-23), 0.86 (3H, d, *J* = 1.1 Hz, H-28), 0.88 (3H, d, *J* = 6.6 Hz, 22b-Me), 1.06 (3H, s, H-26), 1.19 (3H, s, H-27), 2.20 (1H, dd, *J* = 19.3, 4.5 Hz, H-16β), 2.46 (1H, t, *J* = 19.5 Hz, H-16α); ^{13}C NMR (δ ppm, $CDCl_3$): 15.1 (C-28), 15.5 (C-27), 16.0 (C-25), 17.8 (C-29), 18.8 (C-2), 18.8 (C-6), 19.4 (C-26), 21.4 (C-11), 21.6 (C-24), 22.0 (C-30), 23.4 (C-20), 23.7 (C-12), 29.0 (C-22), 33.3 (C-4), 33.4 (C-23), 34.3 (C-7), 38.2 (C-10), 39.3 (C-19), 40.5 (C-1), 41.2 (C-16), 42.0 (C-3), 43.1 (C-8), 44.3 (C-18), 45.9 (C-21), 49.7 (C-13), 51.9 (C-9), 51.2 (C-17), 56.5 (C-5), 57.2 (C-14), 215.2 (C-15); MS (70 eV): *m/z* 426 (M^+, $C_{30}H_{50}O$) (49 %), 411 (11), 383 (11), 273 (14), 234 (35), 233 (75), 220 (38), 207 (27), 206 (27), 205 (21), 191 (100), 189 (6), 177 (8), 163 (13), 149 (10), 137 (16), 123 (48), 109 (25), 95 (46), 81 (59), 69 (54).

Hydrogenation of Hop-22(29)-en-15-one (3-9)

A solution of hop-22(29)-en-15-one (**3-9**) (300 mg) in ethyl acetate (150 mL) was hydrogenated over Adam's catalyst for 2 h under 60 psi. Filtration of the catalyst and removal of the solvent under reduced pressure afforded the corresponding hydrogenation product hopan-15-one (**3-10**) (286 mg), m.p. 240-241°C (lit. m.p. 242°C, Corbett and Young, 1966b); ^{1}H NMR (δ ppm, $CDCl_3$): 0.79 (3H, s, H-24), 0.82 (3H, d, *J* = 0.5 Hz, H-25), 0.84 (3H, d, *J* = 6.4 Hz, 22a-Me), 0.85 (3H, s, H-23), 0.88 (3H, d, *J* = 6.4 Hz, 22b-Me), 0.92 (3H, d, *J* = 0.9 Hz, H-28), 1.04 (3H, s, H-26), 1.20 (3H, s, H-27), 2.39 (1H, dd, *J* = 16.8, 2.7 Hz, H-16β), 2.74 (1H, dd, *J* = 15.6, 14.1 Hz, H-16α); ^{13}C NMR (δ ppm, $CDCl_3$): 15.5 (C-27), 15.6 (C-28), 16.0 (C-25), 18.8 (C-2), 18.8 (C-6), 19.1 (C-26), 21.4 (C-11), 21.6 (C-24), 22.5 (C-29), 23.7 (C-30), 23.9 (C-12), 28.0 (C-20), 31.3 (C-22), 33.3 (C-4), 33.4 (C-23), 34.2 (C-7), 38.2 (C-10), 40.5 (C-1), 41.1 (C-19), 41.8 (C-16), 42.1 (C-3), 42.9 (C-8), 44.3 (C-18), 47.0 (C-21), 50.1 (C-13), 51.9 (C-9), 52.0 (C-17), 56.5 (C-5), 56.9 (C-14), 215.4 (C-15); MS (70 eV): *m/z* 426 (M^+, $C_{30}H_{50}O$) (28%), 411 (8), 383 (16), 273 (9), 234 (34), 233 (81), 220 (41), 207 (23), 206 (50), 205 (25), 191 (100), 189 (8), 177 (6), 163 (9), 149 (5), 137 (9), 123 (20), 109 (13), 95 (28), 81 (38), 69 (38).

6.3.2 Photolysis of 22-Hydroxyhopan-15-one (3-1) and Its Derivatives

Photolysis of 22-Hydroxyhopan-15-one (3-1) in Benzene-Methanol

A solution of 22-hydroxyhopan-15-one (**3-1**) (60 mg) in dry benzene-methanol (1:1, 20 mL) was irradiated using a Hanovia 125 W medium pressure mercury lamp at room temperature for 8 h. Evaporation of the solvent afforded a product mixture which contained three or four compounds by TLC analyses (1:1, H-E). Separation on the product mixture using PLC on silica gel with mixtures of light petroleum and diethyl ether as eluents afforded 14,15-seco-15,22-*O*-*abeo*hop-14(27)-en-15α-ol (**3-3**) (m.p.168-170°C) (27 mg) and 14,15-seco-15,22-*O*-*abeo*hop-14(27)-en-15-one (**3-5**) (m.p.174-178°C) (14 mg).

14,15-Seco-15,22-*O*-*abeo*hop-14(27)-en-15α-ol (**3-3**) had ^{1}H NMR (δ ppm, $CDCl_3$): 0.83 (3H, s, H-24), 0.86 (3H, d, *J* = 0.8 Hz, H-25), 0.87 (3H, s, H-23), 0.98 (3H, s, H-28), 1.00 (3H, s, H-26), 1.18 (3H, s, 22α-Me), 1.24 (3H, s, 22β-Me), 1.94 (1H, dddd, *J* = 12.2, 3.2, 3.2, 3.2 Hz, H-12β), 2.12 (1H, dd, *J* = 12.4, 2.3 Hz, H-13β), 2.66 (1H, ddd, *J* = 13.1, 5.1, 5.1 Hz, H-17β), 4.56 (1H, d, *J* = 1.4 Hz, H-27b), 4.83 (1H, br s, H-27a).; ^{13}C NMR (δ ppm, $CDCl_3$): 16.2 (C-25), 17.9 (C-28), 18.7 (C-2), 19.2 (C-6), 21.6 (C-24), 22.3 (C-26), 22.4 (C-11), 23.0 (C-12), 26.6 (C-29), 28.5 (C-30), 30.8 (C-20), 32.1 (C-16), 33.4 (C-4), 33.5 (C-23), 38.4 (C-10), 39.2 (C-7), 39.2 (C-19), 39.6 (C-17), 40.0 (C-1), 41.7 (C-8), 42.2 (C-3), 46.3 (C-21), 46.5 (C-18), 47.4 (C-13), 57.0 (C-5), 60.2 (C-9), 74.7 (C-22), 91.7 (C-15), 102.7 (C-27), 161.5 (C-14); MS (70 eV): *m/z* 442 (M^+, $C_{30}H_{50}O_2$, not seen), 424 (0.3 %), 409 (1.3), 259 (0.2), 245 (0.4), 203 (1.1), 191 (0.4), 177 (2), 164 (100), 149 (4), 121 (22), 108 (11), 95 (17), 81 (18), 69 (23), 55 (26). Found: *m/z* 164.1225; $C_{11}H_{16}O$ (base peak) requires *m/z* 164.1201. HRMS data could not be obtained for the M^+ ion.

14,15-Seco-15,22-*O*-*abeo*hop-14(27)-en-15-one (**3-5**) had ^{1}H NMR (δ ppm, $CDCl_3$): 0.82 (3H, s, H-24), 0.85 (3H, s, H-25), 0.86 (3H, s, H-23), 1.01 (3H, s, H-26), 1.03 (3H, s, H-28), 1.35 (3H, s, 22α-Me), 1.39 (3H, s, 22β-Me), 2.81 (1H, dd, *J* = 16.5, 7.9 Hz, H-17β), 2.41 (1H, dd, *J* = 17.7, 7.5 Hz, H-16α), 2.50 (1H, dd, *J* = 17.7, 9.1 Hz, H-16β), 4.45 (1H, d, *J* = 1.0 Hz, H-27b), 4.82 (1H, br s, H-27a); ^{13}C NMR (δ ppm, $CDCl_3$):

16.2 (C-25), 18.6 (C-28), 18.7 (C-2), 19.1 (C-6), 21.6 (C-24), 22.2 (C-11), 22.3 (C-26), 24.3 (C-12), 27.6 (C-29), 29.1 (C-30), 29.4 (C-16), 30.9 (C-20), 33.3 (C-4), 33.4 (C-23), 38.3 (C-10), 39.0 (C-17), 39.2 (C-7), 40.0 (C-1), 40.0 (C-19), 41.7 (C-8), 42.1 (C-3), 46.7 (C-21), 47.5 (C-18), 48.6 (C-13), 56.9 (C-5), 59.8 (C-9), 81.9 (C-22), 102.8 (C-27), 161.0 (C-14), 172.9 (C-15); MS (70 eV): *m/z* 440 (M^+, $C_{30}H_{48}O_2$, not seen), 425 (0.5 %), 409 (2), 259 (11), 245 (13.4), 217 (10), 191 (7), 181 (100), 180 (88), 177 (6), 163 (7), 149 (6), 121 (33), 108 (9), 95 (31), 81 (72), 69 (53), 55 (42). Found: *m/z* 181.1251; $C_{11}H_{17}O_2$ (base peak) requires *m/z* 181.1229. HRMS data could not be obtained for the M^+ ion.

Preparation of 15α-Acetoxy-14,15-seco-15,22-*O*-*abeo*hop-14(27)-ene (3-7)

A solution of 14,15-seco-15,22-*O*-*abeo*hop-14(27)-en-15α-ol (**3-3**) (20 mg) in pyridine (1 mL) and acetic anhydride (1 mL) was left to stand for overnight at room temperature. Work-up in the usual way afforded 15α-acetoxy-14,15-seco-15,22-*O*-*abeo*hop-14(27)-ene (**3-7**) (21.5 mg), ^{1}H NMR (δ ppm, $CDCl_3$): 0.83 (3H, s, H-24), 0.86 (3H, s, H-25), 0.87 (3H, s, H-23), 0.98 (3H, s, H-28), 1.00 (3H, s, H-26), 1.19 (3H, s, H-30), 1.30 (3H, s, H-29), 2.13 (1H, d, *J* = 10.0 Hz, H-13β), 2.74 (1H, ddd, *J* = 13.5, 5.3, 5.3 Hz, H-17β), 4.54 (1H, br s, H-27a), 4.83 (1H, br s, H-27b), 5.91 (1H, dd, *J* = 10.3, 2.4 Hz, H-15β); ^{13}C NMR (δ ppm, $CDCl_3$): 16.2 (C-25), 18.0 (C-28), 18.8 (C-2), 19.2 (C-6), 21.5 (C-24), 21.6 (15-COO<u>C</u>H$_3$), 22.3 (C-26), 22.4 (C-11), 23.0 (C-12), 26.3 (C-29), 28.3 (C-30), 29.0 (C-16), 30.7 (C-20), 33.4 (C-4), 33.5 (C-23), 38.4 (C-10), 39.2 (C-7), 39.2 (C-19), 39.6 (C-17), 40.0 (C-1), 41.7 (C-8), 42.2 (C-3), 46.3 (C-21), 47.4 (C-18), 47.5 (C-13), 57.0 (C-5), 60.2 (C-9), 75.7 (C-22), 91.9 (C-15), 102.9 (C-27), 161.3 (C-14), 169.7 (15-<u>C</u>OOCH$_3$); MS (70 eV): *m/z* 484 (M^+, $C_{32}H_{52}O_2$, not seen), 424 (0.2 %), 409 (1), 259 (0.2), 245 (0.4), 191 (0.6), 177 (2), 164 (100), 149 (5), 121 (23), 108 (12), 95 (17), 81 (18), 69 (25), 55 (27). Found: *m/z* 164.1238; $C_{11}H_{16}O$ (base peak) requires *m/z* 164.1201. HRMS data could not be obtained for the M^+ ion.

Photolysis of 22-Hydroxyhopan-15-one (3-1) in Benzene-Isopropanol

Repetition of the photolysis reaction described above on 22-hydroxyhopan-15-one (**3-1**) (60 mg) in dry benzene-isopropanol (1:1, 20 mL) afforded a mixture product. The isolation using radial PLC on silica gel with mixtures of light petroleum and diethyl ether as eluents gave one major product 14,15-seco-15,22-*O*-*abeo*hop-14(27)-en-15α-ol (**3-3**) (m.p.168-170°C) (20 mg) and one minor product 14,15-seco-15,22-*O*-*abeo*hopa-14(27),15-diene (**3-6**) (m.p.144-147°C) (12 mg).

14,15-Seco-15,22-*O*-*abeo*hopa-14(27),15-diene (**3-6**), had ^{1}H NMR (δ ppm, $CDCl_3$): 0.83 (3H, s, H-24), 0.86 (3H, s, H-25), 0.87 (3H, s, H-23), 1.02 (3H, s, H-26), 1.06 (3H, s, H-28), 1.20 (3H, s, 22α-Me), 1.21 (3H, s, 22β-Me), 1.94 (1H, dddd, J = 12.2, 3.3, 3.3, 3.3 Hz, H-12β), 1.84 (1H, m, H-21β), 2.12 (1H, dd, J = 12.5, 2.7 Hz, H-13β), 2.76 (1H, br d, J = 7.3 Hz, H-17β), 4.59 (1H, br s, H-27b), 4.59 (1H, m, H-16), 4.82 (1H, br s, H-27a), 6.19 (1H, dd, J = 6.5, 2.0 Hz, H-15); ^{13}C NMR (δ ppm, $CDCl_3$): 16.2 (C-25), 18.8 (C-2), 19.2 (C-6), 19.8 (C-28), 21.6 (C-24), 22.2 (C-11), 22.3 (C-26), 24.2 (C-12), 25.4 (C-29), 27.5 (C-30), 30.7 (C-20), 33.4 (C-4), 33.5 (C-23), 38.3 (C-10), 39.4 (C-7), 39.6 (C-17), 40.1 (C-1), 41.6 (C-8), 41.6 (C-19), 42.2 (C-3), 46.5 (C-18), 48.0 (C-21), 48.9 (C-13), 56.9 (C-5), 59.8 (C-9), 74.9 (C-22), 101.6 (C-16), 102.8 (C-27), 140.8 (C-15), 161.3 (C-14); MS (70 eV): *m/z* 424 (M^+, $C_{30}H_{48}O$) (0.2 %), 409 (0.8), 259 (0.2), 245 (0.3), 203 (1.0), 191 (0.5), 177 (3.0), 164 (100), 149 (6), 121 (30), 108 (14), 95 (21), 81 (22), 69 (29), 55 (31). HRMS data could not be obtained for the M^+ ion.

Photolysis of 22-Hydroxyhopan-15-one (3-1) in Benzene

Repetition of the above reaction on 22-hydroxyhopan-15-one (**3-1**) (60 mg) in dry benzene (20 mL) afforded a product mixture. The separation using radial PLC on silica gel with mixtures of light petroleum and diethyl ether as eluents gave 14,15-seco-15,22-*O*-*abeo*hop-14(27)-en-15α-ol (**3-3**) (m.p.168-170°C) (29 mg) and 14,15-seco-15,22-*O*-*abeo*hopa-14(27),15-diene (**3-6**) (m.p.144-147°C) (17 mg).

Photolysis of Hop-21-en-15-one (3-8) in Benzene-Methanol

Photolysis of hop-21-en-15-one (**3-8**) (60 mg) in dry benzene-methanol (1:1, 20 mL) afforded a product mixture. The separation using radial PLC on silica gel with benzene and light petroleum gave one fraction, which consisted of starting material hop-21-en-15-one (**3-8**) and the product 14,15-secohopa-14(27),21-dien-15-al (**3-12**), ^{1}H NMR (δ ppm, $CDCl_3$): 0.82 (3H, s, H-24), 0.84 (3H, s, H-25), 0.85 (3H, s, H-26), 0.86 (3H, s, H-23), 0.98 (3H, s, H-28), 1.54 (3H, s, H-29), 1.56 (3H, s, H-30), 2.21 (1H, ddd, J = 12.8, 7.3, 2.7 Hz, H-16α), 2.57 (1H, ddd, J = 12.8, 7.3, 2.7 Hz, H-16β), 3.75 (1H, t, J = 7.5 Hz, H-17β), 4.75 (1H, br s, H-27), 4.87 (1H, br s, H-27), 9.76 (1H, t, J = 2.6 Hz, 15-CHO); ^{13}C NMR (δ ppm, $CDCl_3$): 16.1 (C-25), 17.8 (C-28), 18.7 (C-2), 19.1 (C-6), 20.7 (C-29), 21.3 (C-30), 21.4 (C-26), 21.6 (C-24), 22.4 (C-11), 25.8 (C-12), 30.6 (C-20), 33.3 (C-4), 33.5 (C-23), 35.7 (C-19), 38.3 (C-10), 39.2 (C-7), 40.0 (C-1), 41.9 (C-8), 41.9 (C-13), 42.1 (C-3), 43.0 (C-17), 46.1 (C-16), 46.7 (C-18), 57.0 (C-5), 60.2 (C-9), 102.9 (C-27), 123.5 (C-22), 138.2 (C-21), 161.0 (C-14), 203.6 (C-15), MS (70 eV): *m/z*: 424 (M^+, $C_{30}H_{48}O$) (11%), 409 (30), 381 (3), 355 (2), 281 (2), 259 (5), 245 (6), 191 (14), 164 (100), 147 (22), 136 (36), 121 (97), 95 (37.5), 81 (30), 69 (28). HRMS data could not be obtained for this compound.

Photolysis of Hop-22(29)-en-15-one (3-9) in Benzene-Methanol

Repetition of the above reaction on hop-22(29)-en-15-one (**3-9**) (60 mg) in dry benzene-methanol (1:1, 20 mL) gave a complicated product mixture, which was not worth doing further separation.

Photolysis of Hopan-15-one (3-10) in Benzene-Methanol

Repetition of the above reaction on hopan-15-one (**3-10**) (60 mg) in dry benzene-methanol (1:1, 20 mL) gave a product mixture. The separation using radial PLC on silica gel with mixtures of light petroleum and diethyl ether as eluents afforded 14,15-seco-15,22-*abeo*hop-14(27)-en-15α-ol (**3-13**) (19 mg) and 14,15-seco-15,22-*abeo*hop-14(27)-en-15β-ol (**3-14**) (12 mg).

14,15-Seco-15,22-*abeo*hop-14(27)-en-15α-ol (**3-13**), had m.p.196-198°C; ^{1}H NMR (δ ppm, $CDCl_3$): 0.83 (3H, s, H-24), 0.86 (3H, s, H-23), 0.86 (3H, s, H-25), 0.92 (3H, s, H-30), 0.94 (3H, s, H-29), 1.01 (3H, s, H-28), 1.02 (3H, s, H-26), 1.90 (1H, dddd, *J* = 12.3, 3.4, 3.4, 3.4 Hz, H-12β), 2.37 (1H, dd, *J* = 18.1, 9.4 Hz, H-17β), 3.70 (1H, t, *J* = 6.1 Hz, H-15β), 4.51 (1H, br s, H-27b), 4.76 (1H, br s, H-27a); ^{13}C NMR (δ ppm, $CDCl_3$): 16.2 (C-25), 18.6 (C-29), 18.8 (C-2), 18.9 (C-28), 19.2 (C-6), 21.6 (C-24), 22.0 (C-11), 22.3 (C-26), 26.0 (C-20), 29.3 (C-30), 31.0 (C-12), 33.4 (C-4), 33.5 (C-23), 35.6 (C-16), 38.3 (C-10), 39.5 (C-7), 40.1 (C-1), 41.4 (C-8), 42.2 (C-3), 43.1 (C-22), 45.0 (C-19), 46.0 (C-18), 47.5 (C-17), 51.1 (C-13), 55.6 (C-21), 56.9 (C-5), 59.4 (C-9), 161.6 (C-14), 82.8 (C-15), 102.6 (C-27); MS (70 eV): *m/z* 426 (M^+, $C_{30}H_{50}O$) (2%), 411(2), 260 (5), 245 (5), 217 (3), 167 (11), 166 (23), 165 (13), 149 (86), 148 (25), 133 (36), 123 (47), 121 (33), 107 (69), 95 (100), 81 (59), 69 (73). Found: *m/z* 426.3844 (M^+); $C_{30}H_{50}O$ requires *m/z* 426.3862.

14,15-Seco-15,22-*abeo*hop-14(27)-en-15β-ol (**3-14**), had m.p. 205-208°C; ^{1}H NMR (δ ppm, $CDCl_3$): 0.83 (3H, s, H-24), 0.86 (3H, s, H-23), 0.86 (3H, s, H-25), 0.87 (3H, s, H-30), 0.96 (3H, s, H-28), 0.97 (3H, s, H-29), 1.02 (3H, s, H-26), 1.87 (1H, dddd, *J* = 12.1, 3.4, 3.4, 3.4 Hz, H-12β), 2.37 (1H, ddd, *J* = 10.9, 10.9 and 3.5 Hz, H-17β), 3.81, dd (*J* = 9.6, 7.6 Hz, H-15α), 4.48 (1H, d, *J* = 1 Hz, H-27b), 4.74 (1H, s, H-27a); ^{13}C NMR (δ ppm, $CDCl_3$): 16.2 (C-25), 21.9 (C-29), 18.8 (C-2), 18.5 (C-28), 19.1 (C-6), 21.6 (C-24), 21.9 (C-11), 22.4 (C-26), 27.0 (C-20), 22.7 (C-30), 31.0 (C-12), 33.4 (C-4), 33.5 (C-23), 35.4 (C-16), 38.2 (C-10), 39.6 (C-7), 40.1(C-1), 41.3 (C-8), 42.2 (C-3), 42.3 (C-22), 45.4(C-19), 45.3(C-18), 46.5 (C-17), 52.4 (C-13), 56.3 (C-21), 56.8 (C-5), 59.2 (C-9), 102.7 (C-27), 161.5 (C-14), 79.5 (C-15); MS (70 eV): *m/z*: 426 (M^+, $C_{30}H_{50}O$) (2%), 413 (2), 260 (5), 245 (6), 217 (5), 166 (33), 165 (14), 149 (17), 148 (23), 133 (38), 123 (70), 121 (23), 107 (28), 95 (100), 81 (30), 79 (30), 69 (52). Found: *m/z* 426.3890 (M^+); $C_{30}H_{50}O$ requires *m/z* 426.3862.

Photolysis of 21α-H-Hopan-15-one (3-11) in Benzene-Methanol

Repetition of the above reaction on 21α-H-hopan-15-one (**3-11**) (50 mg) in dry benzene-methanol (1:1, 20 mL) gave a product mixture. The separation using radial PLC on silica gel with mixtures of benzene and light petroleum as eluents afforded

mixtures of the two secoesters, methyl 14α,21α-H-14,15-secohopan-15-oate (**3-15**) (secoester 1) and methyl 21α-H-14,15-secohopan-15-oate (**3-16**) (secoester 2). Earlier eluting fractions (eg fraction 8) contained a greater level of secoester 2 (**3-16**) while later eluting fractions (eg fraction 10) contained a greater level of secoester 1 (**3-15**).

Methyl 14α,21α-H-14,15-secohopan-15-oate (**3-15**) (secoester 1), had ^{1}H NMR (δ ppm, $CDCl_3$): 0.78 (3H, d, *J* = 0.64 Hz, H-26), 0.79 (3H, s, H-24), 0.80 (3H, s, H-25), 0.81 (3H, d, *J* = 6.8 Hz, 22a-Me), 0.84 (3H, s, H-23), 0.85 (3H, s, H-28), 0.85 (3H, d, *J* = 6.8 Hz, 22b-Me), 0.89 (3H, d, *J* = 6.8 Hz, H-27), 2.00 (1H, dd, *J* = 13.8, 3.6 Hz, H-16β), 2.20 (1H, m, *J* = 6.9, 6.9, 3.2 Hz, H-17β), 2.39 (1H, dd, *J* = 13.7, 3.5 Hz, H-16α), 3.63 (3H, s, 15-$COOCH_3$); ^{13}C NMR (δ ppm, $CDCl_3$): 14.0 (C-27), 14.6 (C-26), 16.3 (C-25), 17.7 (C-29), 18.8 (C-2), 19.1 (C-6), 21.1 (C-28), 21.2 (C-11), 21.5 (C-24), 22.5 (C-30), 23.7 (C-20), 28.5 (C-12), 30.7 (C-22), 33.3 (C-4), 33.4 (C-23), 34.8 (C-19), 36.9 (C-16), 37.6 (C-10), 38.5 (C-8), 40.0 (C-1), 41.6(C-7), 42.2 (C-3), 42.9 (C-13), 45.1 (C-17), 47.2 (C-18), 47,8 (C-14), 51.3 (C-21), 56.4 (C-5), 59.9 (C-9), 174.7 (C-15); MS (70 eV): *m/z* 458 (M^+, $C_{31}H_{54}O_2$) (3 %), 443 (5), 427 (2), 409 (2), 261 (33), 197 (100), 191 (38), 177 (9), 165 (20), 153 (13), 137 (48), 123 (88), 109 (33), 95 (45), 81 (39), 69 (52). Found: *m/z* 458.4092 (M^+); $C_{31}H_{54}O_2$ requires *m/z* 458.4124.

Methyl 21α-H-14,15-secohopan-15-oate (**3-16**) (secoester 2), had ^{1}H NMR (δ ppm, $CDCl_3$): 0.76 (3H, s, H-28), 0.78 (3H, s, H-25), 0.79 (3H, d, *J* = 6.8 Hz, H-27), 0.80 (3H, s, H-24), 0.80 (3H, d, *J* = 6.8 Hz, 22a-Me), 0.85 (3H, s, H-23), 0.88 (3H, d, *J* = 6.8 Hz, 22b-Me), 0.97 (3H, s, H-26), 3.66 (3H, s, 15-$COOCH_3$); ^{13}C NMR (δ ppm, $CDCl_3$): 9.9 (C-27), 16.1 (C-25), 16.1 (C-29), 18.8 (C-2), 18.9 (C-6), 20.5 (C-28), 21.7 (C-24), 21.8 (C-11), 21.8 (C-20), 22.6 (C-30), 23.5 (C-12), 24.5 (C-26), 33.4 (C-4), 33.5 (C-23), 33.7 (C-19), 35.0 (C-16), 37.3 (C-10), 38.0 (C-7), 38.6 (C-8), 38.7 (C-22), 40.1 (C-1), 40.1 (C-13), 42.3 (C-3), 44.4 (C-14), 45.1 (C-17), 46.4 (C-18), 48.1 (C-21), 50.4 (C-9), 57.0 (C-5), 175.0 (C-15); MS (70 eV): *m/z* 458 (M^+, $C_{31}H_{54}O_2$) (2 %), 443 (5), 427 (2), 409 (2), 261 (34), 197 (86), 191 (34), 177 (8), 165 (30), 153 (28), 137 (52), 123 (100), 109 (33), 95 (50), 81 (61), 69 (58). Found: *m/z* 458.4164 (M^+); $C_{31}H_{54}O_2$ requires *m/z* 458.4124.

6.4 Experimental: Chapter Four

6.4.1 Isolation of New Stictane Triterpenes from *Pseudophellaria colensoi*

Extraction of *Pseudocyphellaria colensoi*

The dry, finely ground lichen material (369 g) was extracted with light petroleum (4 L) in a Soxhlet apparatus for 96 h. Filtration of the brownish-orange pigments followed by fractional concentration of the filtrate yielded a crude orange-green coloured extract (15.2 g) which contained mainly triterpenoids. TLC analysis with hexane and diethyl ether (1:1) showed the presence of five major stictane triterpenes and some other (minor) unknown compounds, possibly also stictane triterpenes.

Column Chromatography of the Extract

The extract (15.2 g) was chromatographed on a column of 500 g alumina and eluted with light petroleum and diethyl ether with increasing ratio of diethyl ether in the eluent. Fourteen fractions were collected. TLC and GC/MS analyses showed the presence in the some of the fractions of 2α,3β,22α-triacetoxystictane (**4-3**), 22α-hydroxystictan-3-one (**4-8**), 2α,3β-diacetoxystictan-22α-ol (**4-4**), 2α-acetoxystictane-3β,22α-diol (**4-5**), 3β-acetoxystictane-2α,22α-diol (**4-6**) and stictane-3β,22α-diol (**4-7**). Compounds of uncertain structure were detected in fractions 6, 8 and 10.

6.4.3 Isolation of Minor Stictane Triterpenes

22α-Hydroxystictano-25,3β-lactone (4-2)

Separation of fraction 6 (30 mg) was performed using radial PLC on silica gel. Elution with hexane and mixtures of hexane and diethyl ether, through to diethyl ether, afforded 22α-hydroxystictano-25,3β-lactone (**4-2**) (8 mg), a glassy solid (lit. m.p. 320-324°C, Wilkins *et al.*, 1989), ^{1}H NMR (δ ppm, $CDCl_3$): 0.76 (3H, s, H-28), 0.87 (2×3H, s, H-24 and H-30), 0.99 (3H, s, H-29), 1.01 (3H, s, H-27), 1.03 (3H, s, H-23), 1.11 (3H, s, H-26), 1.75 (1H, dd, J =10.9, 3.1 Hz, H-16α), 1.86 (1H, ddd, J = 9.5, 9.5 and 3.5 Hz, H-6α), 2.58 (1H, dd, J = 12.3, 3.3 Hz, H-9β), 3.17 (1H, d, J = 11 Hz, H-22β), 4.03

(1H, d, J = 4.6 Hz, H-3α); ^{13}C NMR (δ ppm, $CDCl_3$): 13.6 (C-28), 17.2 (C-27), 18.6 (C-29), 19.3 (C-16), 20.3 (C-6), 20.3 (C-24), 20.9 (C-11), 21.8 (C-12), 22.2 (C-26), 24.0 (C-1), 25.8 (C-2), 26.5 (C-23), 29.9 (C-30), 31.7 (C-15), 32.7 (C-7), 33.5 (C-9), 34.9 (C-20), 35.0 (C-19), 35.8 (C-21), 38.3 (C-4), 38.6 (C-18), 40.4 (C-8), 42.3 (C-14), 45.0 (C-10), 46.8 (C-5), 48.6 (C-17), 49.1 (C-13), 76.5 (C-22), 82.5 (C-3), 178.3 (C-25); MS (70 eV): *m/z* 456 (M^+ = 456.36, $C_{30}H_{48}O_3$) (11%), 438 (79), 423 (38), 395 (45), 369 (36), 329 (6.25), 221 (19), 207 (22), 205 (19), 204 (19), 203 (17), 201 (8), 191 (64), 190 (44), 189 (100), 188 (6), 187 (27), 109 (47), 69 (89), 43 (89).

Hydrolysis of Fraction 8

A solution of the fraction 8 (30 mg) [which consisted mainly of 2α,3β,22α-triacetoxystictane (**4-3**) and the new triacetate (**4-1**)], in 5% ethanolic potassium hydroxide (20 mL) was stirred for 72 h at room temperature. TLC analyses showed that these conditions hydrolysed triacetate (**4-3**), but not (**4-1**). Work-up in the usual way afforded a mixture of 22α-acetoxystictane-2α,3β-diol (**4-9**) and the new triacetate (**4-1**) which were separated using radial PLC on silica gel. Elution with hexane and mixtures of hexane and diethyl ether through to diethyl ether afforded fractions which contained 3β,6α,22α-triacetoxystictane (**4-1**) (8 mg). Further elution with diethyl ether gave 22α-acetoxystictane-2α,3β-diol (**4-9**) (11 mg).

3β,6α,22α-Triacetoxystictane (**4-1**), a glassy solid which could not be induced to crystallise, had ^{1}H NMR (δ ppm, $CDCl_3$): 0.81 (3H, s, H-28), 0.85 (3H, s, 22α-Me), 0.93 (3H, s, 22β-Me), 0.94 (2×3H, s, H-24 and H-27), 1.03 (3H, s, H-23), 1.04 (3H, s, H-25), 1.21 (3H, s, H-26), 2.03 (3H, s, C-6-OCOC$\underline{H}_3$), 2.05 (2×3H, s, C-3-OCOC$\underline{H}_3$ and C-22-OCOC$\underline{H}_3$), 2.18 (1H, dd, J = 13.9, 6.4 Hz, H-7β), 1.92 (1H, d, J = 10.8 Hz, H-5α); 4.48 (1H, dd, J = 11.7, 5.1 Hz, H-3α), 4.68 (1H, d, J = 10.9 Hz, H22β), 5.11 (1H, m, J = 10.8, 8.2, 6.4 Hz, H-6β); ^{13}C NMR (δ ppm, $CDCl_3$): 13.5 (C-28), 17.1 (C-27), 17.7 (C-24), 19.6 (C-30), 19.7(C-16), 21.0 ($\underline{C}H_3$COO-C-22), 21.3 ($\underline{C}H_3$COO-C-3), 21.6 (C-12), 21.7 (C-26), 21.9 ($\underline{C}H_3$COO-C-6), 22.9 (C-11), 24.5 (C-25), 24.9 (C-2), 29.5 (C-29), 31.0 (C-23), 31.7 (C-15), 33.0 (C-1), 34.9 (C-20), 35.0 (C-19), 35.3 (C-21), 38.3 (C-4), 38.4 (C-10), 38.8 (C-18), 41.3 (C-7), 42.5 (C-8), 42.5 (C-14), 46.7

(C-9), 46.7 (C-17), 48.5 (C-13), 50.9 (C-5), 71.4 (C-6), 78.4 (C-22), 80.7 (C-3), 170.4 ($CH_3\underline{C}OO$-C-6), 171.1 ($CH_3\underline{C}OO$-C-3), 171.1 ($CH_3\underline{C}OO$-C-22); MS (70 eV): *m/z* 586 (M^+, $C_{36}H_{58}O_6$) (1%), 526 (4), 511(46), 483 (4), 466 (27), 451(13), 424 (6); 406 (10), 203 (19), 189 (71), 187 (80), 43 (100). Found: *m/z* 526.4050 (M^+-HOAc); $C_{34}H_{54}O_4$ requires *m/z* 526.4022. HRMS data could not be obtained for the M^+ ion.

Preparation of 3β,22α-Diacetoxystictane (4-10)

A solution of stictane-3β,22α-diol (**4-7**) (30 mg) in pyridine (1 mL) with acetic anhydride (1 mL) was left to stand for overnight, and work-up in the usual way afforded the expected acetate product (**4-10**), ^{1}H NMR (δ ppm, $CDCl_3$): 0.81 (3H, s, H-28), 0.85 (2×3H, s, H-24 and 22α-Me), 0.86 (3H, s, H-23), 0.89 (3H, s, H-27), 0.93 (2×3H, s, H-25 and 22β-Me), 1.14 (3H, s, H-26), 2.04 (3H, s, $C\underline{H}_3COO$-C-3), 2.06 (3H, s, $C\underline{H}_3COO$-C-22), 4.49 (1H, d, *J* = 10.6, 5.2 Hz, H-3α), 4.69 (1H, d, *J* = 10.7 Hz, H-22β); ^{13}C NMR (δ ppm, $CDCl_3$): 13.5 (C-28), 17.2 (C-24), 17.2 (C-27), 18.9 (C-6), 19.7 (C-16), 19.7 (C-30), 21.0 ($\underline{C}H_3COO$-C-22), 21.3 ($\underline{C}H_3COO$-C-3), 21.6 (C-12), 22.6 (C-11), 22.6 (C-26), 22.8 (C-25), 25.4 (C-2), 29.0 (C-23), 29.5 (C-29), 31.7 (C-15), 32.9 (C-1), 34.4 (C-7), 34.9 (C-19), 34.9 (C-20), 35.3 (C-21), 36.8 (C-10), 38.3 (C-4), 38.8 (C-18), 41.8 (C-8), 42.6 (C-14), 45.9 (C-9), 46.6 (C-17), 48.1 (C-5), 48.8 (C-13), 78.6 (C-22), 81.2 (C-3), 171.1 ($CH_3\underline{C}OO$-C-3), 171.2 ($CH_3\underline{C}OO$-C-22); MS (70 eV): 528 (M^+, $C_{34}H_{56}O_4$) (5 %), 468 (44), 453 (58), 425 (7), 408 (23), 393 (11), 365 (5), 317 (11), 289 (3), 276 (3), 272 (5), 259 (5), 249 (8), 229 (11), 216 (8), 205 (16), 204 (22), 203 (22), 191 (38), 189 (95), 187 (28), 43 (100).

6.5 Experimental: Chapter Five

6.5.1 Isolation of a New Flavicane Triterpene

22-Hydroxyflavicano-25,3β-lactone (5-3)

Separation of fraction 10 (30 mg) was performed using radial PLC on silica gel. Elution with hexane and mixtures of hexane and diethyl ether through to diethyl ether afforded 22-hydroxyflavicano-25,3β-lactone (**5-3**) (6 mg), a glassy solid, had ^{1}H NMR

(δ ppm, $CDCl_3$): 0.71 (3H, d, J = 0.9 Hz, H-28); 0.87 (3H, s, H-24); 0.98 (3H, s, H-27); 1.03 (3H, s, H-23); 1.11 (3H, s, H-26); 1.18 (3H, s, 22a-Me); 1.19 (3H, s, 22b-Me); 2.58 (1H, dd, J = 12.4, 3.5 Hz, H-9β); 4.03 (1H, d, J = 4.6 Hz, H-3α); ^{13}C NMR (δ ppm, $CDCl_3$): 15.3 (C-28), 17.1 (C-27), 20.2 (C-6), 20.3 (C-24), 21.8 (C-11), 22.4 (C-26), 23.0 (C-20), 23.5 (C-12), 24.0 (C-1), 24.9 (C-16), 25.8 (C-2), 26.5 (C-23), 26.6 (C-29), 29.6 (C-30), 32.8 (C-15), 33.2 (C-7), 33.7 (C-9), 38.3 (C-4), 39.4 (C-19), 40.2 (C-8), 42.7 (C-14), 45.1(C-10), 45.2 (C-18), 46.9 (C-5), 49.1 (C-13), 51.0 (C-21), 52.4 (C-17), 73.6 (C-22), 82.5 (C-3), 178.3 (C-25); MS (70 eV): *m/z* 456 (M^+, $C_{30}H_{48}O_3$, not seen), 438 (14%), 423 (3), 395 (3), 369 (6), 247 (5), 205 (5), 204 (5), 203 (8), 191 (30), 190 (27), 189 (100), 187 (11), 149 (23), 59 (84). Found: *m/z* 438.3480 (M^+-H_2O); $C_{30}H_{46}O_2$ requires *m/z* 438.3498. HRMS data could not be obtained for the M^+ ion.

References

Ageta, H., Shiojima, K., Suzuki, H. & Nakamura, S. (**1993**). NMR Spectra of Triterpenoids. I. Conformation of the Side Chain of Hopane and Isohopane, and Their Derivatives. *Chem. Pharm. Bull.*, **41**, 1939-1943.

Ageta, H., Shiojima, K., Arai, Y., Suzuki, H. & Kiyotani, T. (**1994**). NMR Spectra of Triterpenoids. II. Hopanes and Migrated Hopanes. *Chem. Pharm. Bull.*, **42**, 39-44.

Aoyagi, R., Tsuyuki, T. & Takahashi, T. (**1970**). Photochemical Interconversion between Norfriedelin and 5α-Vinyl-10β-formylmethyl-des-A-friedelin. *Bull. Chem. Soc. Japan*, **43**, 3967-3972.

Aoyagi, R., Tsuyuki, T., Takai, M., Takahashi, T., Kohen, F. & Stevenson, R. (**1973**). Mechanism of Formation of Unusual Photodegradation Products from Friedelin. *Tetrahedron*, **29**, 4331-4340.

Arigoni, D., Barton, D. H. R., Bernasconi, R., Djerassi, C., Mills, J. S. & Wolff, R. (**1959**). The Constitutions of Dammarenolic and Nyctanthic Acids. *Proc. Chem. Soc.*, 306-307.

Back, K. W. & Chappell, J. (**1996**). Identifying Functional Domains within Terpene Cyclises using a Domain-swapping Strategy. *Proc. Nat. Acad. Sci. USA*, **93,** 6841-6845.

Ballarindenti, A., Cocucci, S. M., & Digirolamo, F. (**1998**). Environmental Pollution and Forest Stress – A Multidisciplinary Approach Study on Alpine Forest Ecosystems. *Chemosphere*, **36**, 1049-1054.

Bamford, C. H. & Norrish, R. G. W. (**1938**). Primary Photochemical Reactions. Part X. The Photolysis of Cyclic Ketones in the Gas Phase. *J. Chem. Soc.*, 1521-1531.

Bird, P. W. (**1984**). A Spectral and Synthetic Investigation of Some Natural Products. M.Sc. thesis, The University of Waikato, Hamilton, New Zealand.

Bladon, P., McMeekin, W. & Williams, I. A. (**1963**). Steroids Derived from Hecoginin. Part III. The Photochemistry of Hecogenin Acetate. *J. Chem. Soc.*, 5727-5737.

Breitmaier, E. & Voelter, W. (**1987**). Carbon-13 NMR Spectroscopy: High Resolution Methods and Applications in Organic Chemistry and Biochemistry. 3rd edition, Weinheim; New York, USA.

Burton, J. F. & Cain, B. F. (**1959**). Pathology–Anti-leukaemic Activity of Polyporic Acid. *Nature*, **184**, 1326.

Cain, B. F. (**1961**). Potential Anti-tumour Agents. Part I. Polyporic Acid Series. *J. Chem. Soc.*, 936-940.

Chambers, R. J. & Marples, B. A. (**1972**). Photolysis of Steroidal β,γ-Epoxyketones. *J. C. S. Chem. Comm.*, 1122-1123.

Chin, W. J., Corbett, R. E., Heng, C. K. & Wilkins, A. L. (**1973**). Lichens and Fungi. Part XI. Isolation and Structural Elucidation of a New Group Triterpenes from *Sticta coronata, S. colensoi and S. flavicans. J. Chem. Soc. Perkin Trans. I*, 1437-1446.

Ciamician, G. & Silber, P. (**1907**). *Ber.*, **40**, 2419.

Corbett, R. E. & Young, H. (**1966a**). Lichens and Fungi. Part II. Isolation and Structural Elucidation of 7β-Acetoxyhopan-22-ol from *Sticta billardierii* Del. *J. Chem. Soc. (C)*, 1556-1563.

Corbett, R. E. & Young, H. (**1966b**). Lichens and Fungi. Part III. Isolation and Structural Elucidation of 15α,22-Dihydroxyhopane from *Sticta billardierii* Del. *J. Chem. Soc. (C)*, 1564-1567.

Corbett, R. E. & Cumming, S. D. (**1971**). Lichens and Fingi. Part VII. Extractives from the Lichens *Sticta mougeotiana* var. *dissecta* Del. *J. Chem. Soc. (C)*, 955-960.

Corbett, R. E., Cong, A. N. T., Holland, P. T. & Wilkins, A. L. (**1987**). Lichens and Fungi. XVIII. Extractives from *Pseudocyphellaria rubella. Aust. J. Chem.*, **40**, 461-468.

Corbett, R. E. & Wilkins, A. L. (**1976a**). Lichens and Fungi. Part XII. Dehydration and Isomerisation of Stictane Triterpenoids. *J. Chem. Soc. Perkin Trans. I*, 857-863.

Corbett, R. E. & Wilkins, A. L. (**1976b**). Lichens and Fungi. Part XIII. Comparison of the Nuclear Magnetic Resonance and Mass Spectra of 17,21-Secohopane and 17,21-Secoflavicane Derivatives. *J. Chem. Soc. Perkin Trans. I,* 1316-1320.

Corbett, R. E., Heng, C. K. & Wilkins, A. L. (**1976c**). Lichens and Fungi. Part XIV. A Revised Structure for Retigerane Triterpenoids. *Aust. J. Chem.* **29**, 2567-2570.

Corbett, R. E. & Wilkins, A. L. (**1977**). Lichens and Fungi. Part XV. Revised Structures of Hopane Triterpenoids Isolated from the Lichen *Pseudocyphellaria mougeotiana. Aust. J. Chem.*, **30**, 2329-2332.

Corbett, R. E., Simpson, J., Goh, E. M., Nicholson, B. K., Wilkins, A. L. & Robinson, W. T. (**1982**). Lichens and Fungi. Part 16. The Crystal and Molecular Structures of Stictane-3β,22α-diol and 22α-Hydroxy-3,4-secostictan-3-oic acid. *J. Chem. Soc. Perkin Trans. II*, 1339-1343.

Corbett, R. E., Cong, A. N. T., Wilkins, A. L. & Thomson, R. A. (**1985**). Lichens and Fungi. Part 17. The Synthesis and Absolute Configuration at C-20 of the (R)-and (S)-Epimers of Some 29-Substituted Lupane Derivatives and the Crystal Structure of (20R)-3β-Acetoxylupan-29-ol. *J. Chem. Soc. Perkin Trans. I*, 2051-2056.

Corbett, R. E., Cong, A. N. T. & Holland, P. T. (**1987**). Lichens and Fungi. XVIII Extractives from *Pseudocyphellaria rubella. Aust. J. Chem.,* **40**, 461-468.

Cowan, D. O. & Drisko, R. L. (**1976**). Elements of Organic Photochemistry. Plenum Press, New York, USA.

DePuy, C. H. & Chapman, O. L. (**1972**). Molecular Reactions and Photochemistry. Prentice-Hall, Englewood Cliffs, N. J. USA.

Dreyer, D. L, & Rigod, J. F. (**1974**). Citrus Bitter Principles. XII. Photochemistry of Limonin. *J. Org. Chem.*, **39**, 263-265.

Elix, J. A., Whitton, A. A. & Sargent, M. V. (**1984**). Recent Progress in the Chemistry of Lichen Substances. *Prog. Chem. Org. Nat. Prod.*, **45**, 103-234.

Elix, J. A., Wilkins, A. L. & Wardlaw, J. H. (**1987**). Five New Fully Substituted Depsides from the Lichen *Pseudocyphellaria pickeringii*. *Aust. J. Chem.*, **40**, 2023-2029.

Galloway, J. D. (**1985**). Flora of New Zealand Lichens. P. D. Hasselberg, Government Printer, Wellington, New Zealand.

Goh, E. M. (**1981**). Structural and Synthetic Studies of Some Natural Products. D.Phil. thesis, The University of Waikato, Hamilton, New Zealand.

Goh, E. M., Holland, P. T. & Wilkins, A. L. (**1978**). Structural Elucidation of a New Group of Secostictane Triterpenoids. *J. Chem. Soc. Perkin Trans. I*, 1560-1564.

Gonzalea, A. G., Martin, J. D. & Perez, C. (**1974**). Three New Triterpenoids from *Xanthoria resendei*. *Phytochemistry*, **13**, 1547-1549.

Gonzaleztejero, M. R., Martinezlirola, M. J., Casaresporcel, M. & Moleromesa, J. (**1995**). Three lichens used in popular medicine in eastern Andalucia (Spain). *Economic Botany*, **49**, 96-98.

Hirota, H., Tsuyuki, T., Tanahashi, Y. & Takahashi, T. (**1974**). Photochemical Reactions of Lupan-3-one. *Bull. Chem. Soc. Japan*, **49**, 2283-2286.

Horspool, W. M. (**1976**). Aspects of Organic Photochemistry. Academic Press, London, England.

Horspool, W. M. (**1994**). Photolysis of Carbonyl Compounds. *Photochemistry*. **25**, 67-100.

Huneck, S & Yoshimura, I. (**1996**). Identification of Lichen Substances. Springer, Berlin, Germany.

Hunter, D. W. F. (**1993**). Photolytic, Spectroscopic and Computational Investigations of Some Triterpenes. M.Sc. thesis, The University of Waikato, Hamilton, New Zealand.

Kohen, F. & Stevenson, R. (**1966**). Photodecarbonylation of Friedelin. *Chem. and Ind. (London),* 1844-1845.

Kohen, F., Samson, A. S. & Stevenson, R. (**1969**). Friedelin and Related Compounds. X. Products from Ultraviolet Irradiation of Friedelin. *J. Org. Chem.*, **34**, 1355-1358.

Lamola, A.A. & Turro, N.J. (**1969**). Energy Transfer and Organic Photochemistry. Interscience Publishers, New York, USA.

Malcolm, W. M. & Galloway, J. D. (**1997**). New Zealand Lichens Checklist. Museum of New Zealand Te Papa Tongarewa, Wellington, New Zealand.

Marcano, V., Rodriguez-Alcocer, V. & Mendez, A. M. (**1999**). Occurrence of Usnic Acid in *Usnea laevis* Nylander (lichenized ascomycetes) from the Venezuelan Andes. *J. Ethnopharmacol.*, **66**, 343-346.

Nakanishi, K., Goto, T., Ito, S., Natori, S. & Nozoe, S. (**1975**). Natural Products Chemistry. Vol. 2, Academic Press, New York, USA.

Okogun, J. I., Duddeck, H., Habermehl, G., Krebs, H. C., Toth, G & Simon, A. (**1998**). Constitution, Stereochemistry and Conformational Behaviour of the Photoreaction Product of 7-Deacetoxy-7-oxokhivorin. *Mag. Res. Chem.*, **36**, 371-375.

Quannes, C. & Beugelmans, R. (**1972**). Photochemical Reactions. XVII. Open A-Ring Tetracyclic Triterpenes in the Cyclolaudane Series. *Bull. Soc. Chim. France.* **11**, 4275-4279.

Purvis, O. W., Elix, J. A., Broomhead, J. A. & Jones, G. C. (**1987**). The Occurrence of Copper-Norstictic Acid in Lichens from Cupriferous Substrata. *Lichenologist*, **19**, 193.

Purvis, O. W., Elix, J. A. & Gaul, K. L. (**1990**). The Occurrence of Copper-Psoromic Acid in Lichens from Cupriferous Substrata. *Lichenologist*, **22**, 345.

Rao, P. S. & Seshadri, T. R. (**1968**). Chemical Investigation of Indian Lichens. XXIX. Structural Studies of Retigeradiol. *Indian J. Chem.*, **6**, 398-400.

Ronaldson, K. J. & Wilkins, A. L. (**1978**) The Structure of Amphistictinic Acid, a Triterpenoid Constituent of the Lichen *Pseudocyphellaria amphisticta*, *Aust. J. Chem.*, **31**, 215-219.

Sanders J. K. M. & Hunter B. K. (**1993**). Modern NMR Spectroscopy–A Guide for Chemists. Oxford University Press, Oxford, England.

Schimdt, J. & Huneck, S. (**1979**). Mass Spectroscopy of Natural Products VI–Localization of Functional Groups in the Hopane Skeleton. *Organic Mass Spectrometry*, **14**, 656-662.

Smith, R. A. J. (**1968**). D.Phil. thesis, The University of Otago, Dunedin, New Zealand.

Smriga, M. & Saito, H. (**2000**). Effect of Selected Thallophytic Glucans on Learning Behaviour and Short-term Potentiation. *Phytotherapy Research*, **14**, 153-155.

Stevens, G. N. (**1998**). Endangered Species Programme Report, Section 2 – Lichens. Environment Australia, PO Box 636, Canberra, ACT2601, Australia.

Stevenson, R., Tsuyuki, T., Aoyagi, R., & Takahashi, T. (**1971**). Friedelin and Related Compounds. Part XI. Identification of a Saturated Nor-Aldehyde from Ultraviolet Irradiation of Friedelin. *Bull. Chem. Soc. Japan*, **44**, 2567.

Takai, M, Aoyagi, R., Yamada, S., Tsuyuki, T. & Takahashi, T. (**1970**). An Unusual Photochemical Reaction of Friedelin. *Bull. Chem. Soc. Japan*, **43**, 972.

Walker, J. L. & Lintott, E. A. (**1997**). A Phytochemical Register of New Zealand Lichens. *N. Z. J. Bot.*, **35**, 369-384.

Wilkins, A. L. (**1977a**). The Structure of a Triterpenoid Ketol from *Cetraria nivalis*. *Phytochemistry*, **16**, 608-609.

Wilkins, A. L. (**1977b**). Durvillonol and Duvilldiol: Structure and Occurrence. *Phytochemistry*, **16**, 2031-2032.

Wilkins, A. L. & James, P. W. (**1979**). The Chemistry of *Pseudocyphellaria impressa* S. Lat. In New Zealand. *Lichenologist*, **11**, 271-281.

Wilkins, A. L. (**1980**). Nephrin; Structure and Occurrence in *Nephroma* Species. *Phytochemistry*, **19**, 696-697.

Wilkins, A. L., Jager, P. M. & Bird, W. (**1987a**). Carbon-13 NMR Study of Some Triterpene Hydrocarbons of the Hopane Group. *Mag. Res. Chem.*, **25**, 503-507.

Wilkins, A. L., Ronaldson, K. J., Jager, P. M. & Bird, W. (**1987b**). A ^{13}C NMR Study of Some Oxygenated Hopane Triterpenes. *Aust. J. Chem.*, **40**, 1713-1721.

Wilkins, A. L. & Goh, E. M. (**1988**). The X-Ray Crystal Structure and Photochemistry of 22α-Hydroxystictan-3-one; a Triterpenoid Keto Alcohol from *Pseudocyphellaria* Species. *Aust. J. Chem.*, **41**, 143-150.

Wilkins, A. L., Bremer, J., Ralph, J., Holland, P. T., Ronaldson, K. J., Jager, P. M. & Bird, W. (**1989a**). A One- and Two-Dimensional ^{13}C and ^{1}H N.M.R. Study of Some Triterpenes of the Hopane, Stictane and Flavicene Groups. *Aust. J. Chem.*, **42**, 243-257.

Wilkins, A. L., Elix, J. A., Gonzalez, A. G. & Perez, C. (**1989b**). A One- and Two-Dimensional ^{1}H and ^{13}C N.M.R. Study of Some Fernene Triterpenoids. *Aust. J. Chem.*, **42**, 1185-1189.

Wilkins, A. L., Elix, J. A., Gaul, K. L. & Moberg, R. (**1989c**). New Hopane Triterpenoids from Lichens in the Family *Physiaceae*. *Aust. J. Chem.*, **42**, 1415-1422.

Wilkins, A. L. & Elix, J. A. (**1990**). New Fernene Triterpenes from the Lichen *Pseudocyphellaria aurata*. *Aust. J. Chem.*, **43**, 623-627.

Yosioka, I., Yamaki, M. & Kitagawa, I. (**1966**). On the Triterpenic Constituents of a Lichen, *Parmelia entotheiochroa* Hue; Zeorin, Leucotylin, Leucotylic Acid, and Five New Related Compounds. *Chem. Pharm. Bull.*, **14**, 804-807.

Zhao, T. (**1983**). Proton Nuclear Magnetic Resonance. Beijing University Press, Beijing, China.